DR# 0423-5

Energy

FOSSIL

HYDRODYNAMICS OF FISCHER-TROPSCH SYNTHESIS IN SLURRY BUBBLE COLUMN REACTORS

MASTER

Final Report

By
Dragomir B. Bukur
James G. Daly
Snehal A. Patel
Matheo L. Raphael
Gary B. Tatterson

June 1987

DISCLAIMER

DISCLAIMER

This report was prepared as an account of work sponsored by an agency of the United States Government. Neither the United States Government nor any agency Thereof, nor any of their employees, makes any warranty, express or implied, or assumes any legal liability or responsibility for the accuracy, completeness, or usefulness of any information, apparatus, product, or process disclosed, or represents that its use would not infringe privately owned rights. Reference herein to any specific commercial product, process, or service by trade name, trademark, manufacturer, or otherwise does not necessarily constitute or imply its endorsement, recommendation, or favoring by the United States Government or any agency thereof. The views and opinions of authors expressed herein do not necessarily state or reflect those of the United States Government or any agency thereof.

DISCLAIMER

Portions of this document may be illegible in electronic image products. Images are produced from the best available original document.

HYDRODYNAMICS OF FISCHER-TROPSCH SYNTHESIS

IN SLURRY BUBBLE COLUMN REACTORS

FINAL REPORT

DRAGOMIR B. BUKUR, JAMES G. DALY, SNEHAL A. PATEL,

MATHEO L. RAPHAEL, AND GARY B. TATTERSON*

TEXAS A&M UNIVERSITY

DEPARTMENT OF CHEMICAL ENGINEERING AND

*DEPARTMENT OF MECHANICAL ENGINEERING

COLLEGE STATION, TEXAS 77843

JUNE 1987

TABLE OF CONTENTS

TABLE OF CONTENTS (contd.)

TABLE OF CONTENTS (contd.)

LIST OF TABLES

LIST OF FIGURES

LIST OF FIGURES (contd.)

ABSTRACT

This report describes studies on hydrodynamics of bubble columns for Fischer-Tropsch synthesis under a DOE Contract No. DE-AC22-84PC70027.

These studies were carried out in columns of 0.051 m and 0.229 m in diameter and 3 m tall to determine effects of operating conditions (temperature and gas flow rate), distributor type (sintered metal plate and single and multi-hole perforated plates) and liquid media (paraffin and reactor waxes) on gas hold-up and bubble size distribution. In experiments with the Fischer-Tropsch (F-T) derived paraffin wax (FT-300) for temperatures between 230°C and 280°C there is a range of gas velocities (transition region) where two values of gas hold-up (i.e. two flow regimes) are possible. Higher hold-ups were accompanied by the presence of foam ("foamy" regime) whereas lower values were obtained in the absence of foam ("slug flow" in the 0.051 m column, or "churn-turbulent" flow regime in the 0.229 m column). This type of behavior has been observed for the first time in a system with molten paraffin wax as the liquid medium. Several factors which have significant effect on foaming characteristics of this system were identified. Reactor waxes have much smaller tendency to foam and produce lower hold-ups due to the presence of larger bubbles.

Bubble size distribution and Sauter mean bubble diameters were determined by photographic method and by dynamic gas disengagement method. Significant differences in Sauter mean bubble diameters were obtained in experiments with different waxes, even though the gas hold-up values were similar.

Finally, new correlations for prediction of the gas hold-up and the specific gas-liquid interfacial area were developed on the basis of results obtained in the present study.

I. OBJECTIVE AND SCOPE OF WORK

The objective and scope of work given here are based on the original Statement of Work of the contract.

The overall objective of this contract is to determine effects of column geometry, distributor design, operating conditions (temperature and gas flow rate), and oxygenated compounds on hydrodynamics of slurry bubble column reactors for Fischer-Tropsch synthesis, using a hard paraffin wax as the liquid medium. To accomplish these objectives, the following specific tasks will be undertaken.

Task 1 - Project Work Plan

The objective of this task is to establish a detailed project work plan covering the entire period of performance of the contract, including estimated costs and manhours expended by month for each task.

Task 2 - Bubble Column Reactor Design/Construction

Two bubble columns made of borosilicate glass of approximately 2" (0.05 m) and 9" (0.23 m) in diameter and 10 ft (3 m) tall will be designed and assembled for measurement of the gas hold-up and the bubble size distribution. After the design, procurement of equipment and instrumentation, and construction of the unit is completed, a shakedown of test facilities will be made to verify achievement of planned operating conditions. During this period instruments will be calibrated.

Task 3 - Process Variable Studies

The objective of this task is to determine the effect of various system variables (e.g. gas flow rate, temperature, and addition of minor amounts of oxygenated compounds) on hydrodynamic properties using the two bubble columns (2" and 9" ID) and different types of distributors. All

experiments will be conducted using nitrogen at atmospheric pressure. It is planned to determine the following hydrodynamic characteristics: gas hold-up, flow regime characterization, bubble size distribution, and the gas-liquid interfacial area.

Task 4 - Correlation Development and Data Reduction

Correlations based on our experimental data for prediction of average gas hold-up and the gas-liquid interfacial area will be developed.

II. SUMMARY

A. Background

Fischer-Tropsch (F-T) synthesis reaction represents an important route for indirect coal liquefaction. It was utilized on a large scale during World War II for production of motor fuels in Germany. At the present time commerical size units are in operation only at Sasol in South Africa. Fixed bed (Germany and Sasol) and entrained bed (Sasol) type of reactors have been used for conversion of synthesis gas into hydrocarbon products.

Slurry phase F-T processing is considered a potentially economic method to convert coal derived synthesis gas into liquid fuels. Largely due to its relatively simple reactor design, improved thermal efficiency, and ability to process CO-rich synthesis gas, the slurry process has several potential advantages over conventional vapor phase processes.

The scale-up of slurry bubble columns is subject to uncertainty due to the fact that important hydrodynamic parameters change with the scale. Thus the results obtained in small diameter units cannot be directly translated to a large diameter reactor. The successful reactor scale-up for the slurry phase Fischer-Tropsch process was achieved in Germany in the 50's (e.g. Kolbel et al., 1955; Kolbel and Ralek, 1980). The demonstration plant unit (1.55 m in diameter and a height of 8.6 m) was constructed by Rheinpreussen-Koppers and it operated successfully over a long period of time. This successful operation came as a result of significant development effort, the details of which have not been published. Subsequent studies were done on a smaller scale, and have not been successful in reproducing reported Kolbel's data on catalyst activity and product selectivity.

3

In the majority of previous studies of slurry F-T synthesis rather small bubble column reactors were employed (less than 0.10 m in diameter). According to Deckwer et al. (1980) and Shah et al. (1982), under these conditions the reactors were operating in either the homogeneous (ideal bubbly) flow regime or the slug flow regime. On the other hand, commerical size bubble column reactors are expected to operate in the heterogeneous (churn-turbulent) flow regime. The specific gas-liquid interfacial area, as well as the gas and the liquid phase mixing are different in different flow regimes. These parameters have significant effect on the secondary reactions and consequently product selectivities obtained in different flow regimes may differ significantly. Construction and operating costs for a large diameter bubble column reactor are expected to be very high. Before this is done further work is required which will provide a rational basis for the reactor design and scale-up.

The present work on hydrodynamics of bubble columns for F-T synthesis was initiated in September 1984, under DOE Contract No. DE-AC22-84PC70027. The objectives of this study were to determine the effect of bubble column diameter (0.051 m and 0.229 m), distributor type (sintered metal plate, single and multiple hole orifice plate), operating conditions (gas velocity and temperature), and oxygenated compounds on gas hold-up and bubble size distribution using molten paraffin wax as the liquid medium.

B. Results

Two glass (0.051 and 0.229 m in diameter, 3m in height) and two stainless steel columns of similar dimensions (0.051 m and 0.241 m in diameter, 3 m tall) were employed in this study. The glass columns were used for measurement of the average gas hold-up and bubble size distribution,

whereas the stainless steel columns were used for measurement of axial gas hold-up distribution. The construction work and fabrication of auxilliary vessels for all columns were completed in May 1985. The shakedown run with the small glass column was made in May 1985, and for the other three columns in June 1985. All columns were operated in a batch mode with respect to a liquid medium.

Flow regimes in the two glass columns were determined from visual observations of the flow field which were also recorded with a video camera. The homogeneous (ideal bubbly) regime, characterized by nearly uniform bubble size distribution, was observed in the small column at the gas velocity of 0.01 m/s. At velocities of 0.02 and 0.03 m/s slugs start appearing in the upper part of the column, and the flow may be characterized as a transition between the homogeneous and slug flow regimes. At higher gas velocity the slug flow regime prevails. However, even in the slug flow regime a large number of small bubbles was still present in experiments with Fischer-Tropsch derived paraffin waxes and their specific gas-liquid interfacial area is much greater than that in air-water system in the presence of slugs. Foaming, accompanied with hold-up values up to 75%, was often observed at lower gas velocities with all types of distributors (sintered metal plate - SMP, and orifice plate), and this type of operation is referred to as the "foamy" regime. Slugs were also present in this flow regime at velocities greater than 0.02 m/s. The flow regime in the larger diameter column was homogeneous at 0.01 m/s, followed by transition to "churn-turbulent" flow which was complete at the gas velocity of 0.03 m/s. During runs when foam was produced, the homogeneous flow regime was followed by the "foamy" regime in the velocity

5

range 0.02-0.05 m/s. At velocities greater than 0.05 m/s the "churn-turbulent" flow was the only stable flow regime.

Results of average gas hold-up measurements revealed the following:

- For temperatures between 230°C and 280°C, there is a range of gas velocities over which two values of gas hold-up are possible with FT-300 wax. The higher gas hold-ups are accompanied by the presence of foam ("foamy" regime). In the absence of foam, "slug flow" prevails in the 0.051 m ID column, whereas flow in the 0.229 m ID column is in the "churn-turbulent" regime. The start-up procedure determines which flow regime will be attained, with increasing order of gas velocities favoring the "foamy" regime. A transition from the "foamy" to the "slug flow" or "churn-turbulent" regime occurs when u_g exceeds a certain critical value, and the transition to the "foamy" regime occurs when u_g drops below a certain critical value. Since the two critical velocities are different, a hysteresis loop is created. In a system with molten paraffin wax as the liquid medium this type of behavior has been observed for the first time.

- Gas hold-up increases with temperature, and this increase is more significant in the presence of foam. As the temperature decreases the liquid viscosity increases which promotes bubble coalescence and produces lower hold-ups.

- In the absence of foam the column diameter (0.051 m and 0.229 m) had rather small effect on gas hold-up in experiments with a paraffin wax (trade name FT-300) and raw wax from Sasol's Arge reactor using 1.85 mm hole orifice distributors. However, in experiments with smaller

6

hole orifices (1 mm hole orifice in the 0.051 m column and 19 x 1 mm perforated plate in the 0.229 m column) with FT-300 wax higher hold-ups were obtained in the smaller column both in the presence and in the absence of foam.

- Distributor type did not have a significant effect on the gas hold-up in both columns in the absence of foaming. In the "foamy" regime the SMP distributor gave the highest hold-up values, whereas orifice distributors produced lower hold-ups. In the smaller diameter column higher hold-ups (more foam) were obtained with smaller orifices, but such effect was not observed in the 0.229 m ID column.

- The addition of small amounts (up to 10% by weight) of oxygenated species (1-octadecanol and octadecanoic acid) to FT-300 wax delayed foam break-up to higher gas velocities, but did not have a significant effect on the gas hold-up.

- Hydrodynamic behavior of four reactor waxes (Sasol's Arge wax, and three composite waxes produced during runs in Mobil's pilot plant bubble column reactor—Unit CT-256) was evaluated in the 0.051 m ID glass column. It was found that these waxes have a very small tendency to foam (only at 0.01 m/s with a 40 μm SMP) and thus do not exhibit hysterisis behavior observed with FT-300 paraffin wax. Distributor type (SMP and orifice plate) and temperature (200 and 265°C) had rather small effect on hold-up values. Hold-ups obtained with reactor waxes are similar to those obtained with FT-300 wax in the absence of foam.

Axial gas hold-up measurements were made in the two stainless steel columns with FT-300 wax, and in the 0.241 m ID column with Sasol's wax.

7

The hold-up profiles along the height of the column were found to be dependent on the flow regime. In the presence of foam the gas hold-ups near the top of dispersion were significantly higher than those in the lower portion of the column. In the absence of foam, the increase in hold-up with column height was only marginal. An increase in gas velocity shifts the axial gas hold-up profile upwards (towards higher values) irrespective of whether the foam was present or not.

Bubble size distribution and Sauter bubble diameter were determined by photographic method and by dynamic gas disengagement (DGD) technique. Photographs of bubbles near the wall were taken in the two glass columns, and near the center of the 0.241 m in diameter stainless steel (SS) column through a specially designed viewing port. The major findings from photographic measurements of bubble size distribution with FT-300 wax are:

- The Sauter mean bubble diameter (d_s) decreases with an increase in height above the distributor. The extent of this decrease depends on the flow regime, with more significant decreases in cases where foam is present.

- The value of d_s appears to be fairly constant with changes in superficial gas velocity in the 0.051 m ID column, however in the large columns (0.229 m ID glass and 0.241 m ID SS), it decreases marginally with an increase in superficial gas velocity.

- The 40 μm SMP distributor produced significantly smaller bubbles ($d_s \approx$ 0.5-0.7 mm at 265°C) compared to the 1.85 mm orifice plate distributor ($d_s = 1.2$-2.2 mm under similar conditions). However, d_s in the 0.229 m and 0.241 m columns, with improvements in the technique (significantly larger bubble count), were around 0.5 mm at the wall

and around 0.8 mm near the center (for velocities greater than 0.5 m/s). The change of Sauter diameter with radial position is as expected, since large bubbles rise preferentially near the center of the column, while small bubbles concentrate near the wall.

Photographic measurements could not be made with reactor waxes due to their dark color, but the Sauter diameters for these waxes, as well as for FT-300 wax, were estimated using the DGD technique. The highlights of these investigations are:

- Column diameter and orifice hole diameter did not have a significant effect on the d_s value for FT-300 wax.

- The presence of foam had a strong effect on d_s values. At 265°C the Sauter mean diameter for FT-300 wax was approximately 0.5 mm which is the same as obtained with photographic method.

- Temperature had a significant effect on the Sauter mean bubble diameter (d_s), with values at 200°C being significantly larger than values at 265°C for all wax types, despite relatively small differences between hold-up values at the two temperatures.

- Wax type had a significant effect on d_s values, with the smallest bubbles being produced by FT-300 wax and the largest by Mobil reactor wax. The trends were similar at both 200°C and at 265°C. At 265°C Sauter mean diameters for FT-300 wax were around 0.8 mm for superficial gas velocities greater than 0.05 m/s; while those for Sasol reactor wax approached 2 mm and Mobil reactor wax gave values around 4 to 5 mm.

In general, a good agreement was obtained for Sauter bubble diameters estimated from these two methods. The important conclusion from the

present study is that similar gas hold-ups do not necessarily imply similar bubble size distributions. Significant differences in Sauter bubble diameters were obtained in experiments with different waxes at a given temperature or with a given wax at two temperatures (200 and 265°C), even though the hold-up values were similar.

Finally, based on our measurements of gas hold-ups and Sauter mean bubble diameters, correlations for prediction of the average gas hold-up and the specific gas-liquid interfacial area were developed. Since these correlations were obtained from a large data base they are expected to be useful to those engaged in design and scale-up of bubble column reactors for Fischer-Tropsch synthesis.

III. <u>LITERATURE REVIEW</u>

There is a vast amount of literature on hydrodynamics of bubble columns with gas-liquid systems (primarily air-water or other pure liquids), and several good reviews are available (e.g. Van Landeghem, 1980; Ostergaard, 1980; Shah et al., 1982; Heijnen and Van't Riet, 1984). Hydrodynamic parameters in systems with pure liquids (non-foaming systems) are significantly different than in systems which have foaming capacity (e.g. hydrocarbon mixtures, industrial oils particularly at high temperature and pressure, oxygenated impurities in hydrocarbons, aqueous solutions of alcohols and organic acids, etc.) as shown in recent studies by Smith, D.N. et al. (1984b), O'Dowd et al. (1985) and Shah et al. (1985). This was illustrated in experiments by Quicker and Deckwer (1981) who found that pure hydrocarbons with the same viscosity, density and surface tension as Fischer-Tropsch (F-T) derived paraffin wax produce 2-3 times larger bubbles and about one half the gas hold-up produced with F-T wax. It follows that results obtained using liquids other than F-T waxes can not be used for design and scale-up of slurry bubble column reactors for Fischer-Tropsch synthesis. Thus, a detailed discussion of these systems will not be attempted here. Qualitative comparisons between results obtained in liquids other than F-T derived waxes and those obtained with F-T waxes are made in Sections V and VI of this report.

A summary of experimental conditions employed in hydrodynamic studies with F-T derived waxes as liquid media is given in Table III-I. The major findings from these studies can be briefly summarized as follows:

• There are virtually no experimental data obtained in large bubble columns at high gas velocities, i.e. under conditions of industrial

11

Table III-1. Summary of bubble-column hydrodynamic studies.

Reference	Column dc (m)	Column Hs (m)	Distributor do (mm)	Distributor no	Distributor Type[a]	Conditions ug (m/s)	Conditions wcat (%)	Conditions dcat (μm)	Conditions T (°C)	Conditions P (MPa)	Liquid[b]	Gas	Quantity Measured
Calderbank et al. (1963)	0.051	2.3-4.6^c	NA	1	SN	0-0.055	0	-	265	0.1	KW	H_2/CO	$\epsilon_{g,a}$
Farley and Ray (1964 a,b)	0.25	8.5^c	NA	1	"	0.03-0.073	13	1-3	265	0.15-1.1	"	"	ϵ_g
Zaidi et al. (1979)	0.04-0.10	0.6-1.0	0.075	-	SP	0-0.038	2-14	1	250-290	1.0	MP	CO,N_2	ϵ_g,d_s
Deckwer et al (1980)	"	"	"	-	"	0-0.04	0-16	5	143-270	0 4-1.1	"	N_2	ϵ_g,d_s
Quicker and Deckwer (1981)	0.095	1.35	1.1	19	PP	0.04	0	-	130-170	0.1	FT-300	N_2	ϵ_g,d_s
"	"	"	0.9	1	SN	"	"	-	"	"	"	"	"
Kuo et al. (1985)	0 032,0.053	0.4-1.0	0.015-0.10	-	SP	0-0.04	"	-	200-230	0.1	FT200,PW	"	ϵ_g
"	"	"	0.25-1.0	1-3	PP	0-0.05	"	-	"	0.1	"	"	"
"	0.051	0.58-7.6	0.02	-	SP	"	"	-	138-260	0.1-0.2	FT-200	"	"
"	"	"	0.5-2	1-3	PP	0-0.12	"	-	260	"	FT-200,PW	"	"
"	0.102	6-7.6	2	1	"	0-0.065	"	-	"	"	FT-200	"	"
"	"	"	1	4	"	"	"	-	"	"	FT-200,PW	"	"
"	0.026	?	0.02	-	SP	0-0.035	15	?	177	0.1-1.15	PW	H_2,N_2	"
Sanders et al. (1986)	0.05	0.5-0.9	0.2	-	"	0-0.06	0-30	?	240	1.0	FT-300,PW	H_2/CO	"
"	"	"	1.0	4	PP	?	?	NA			"		
O'Dowd et al. (1986)	0.022	NA	1	1	"	0-0.02	0	-	250,280	1.5-2.2	PW,MP	N_2	ϵ_g,d_s

[a]Distributor types: PP - Perforated Plate; SN - Single Nozzle; SP - Sintered Plate
[b]Liquid Medium: KW - Krupp Wax; MP - Molten Paraffin Wax; PW - Product Wax
[c]Expanded liquid height
NA - not available

12

importance. Most of the studies were done in bubble columns with diameters less than 0.10 m, and thus only the homogeneous (ideal bubbly) and slug flow regimes were observed.

• The value of Sauter mean bubble diameter of about 0.7 mm determined by photographic method in studies by Deckwer and co-workers (Zaidi et al., 1979; Deckwer et al., 1980; Quicker and Deckwer, 1981) is not in good agreement with that obtained in the Calderbank et al. (1963) study (~2.5 mm by light transmission method).

• There are large discrepancies in reported values of gas hold-ups obtained in various studies. They are caused by differences in wax compositions, distributor design and column geometry.

• Paraffin waxes have tendency to foam, whereas most of the raw reactor waxes do not foam (Kuo et al. 1985).

A detailed description of the effects of operating conditions, column geometry, distributor design and wax type on the average gas hold-up and bubble size distribution is given below.

A. Effect of Temperature

Deckwer et al. (1980) found a significant decrease in the gas hold-up with the increase in temperature from 180 to 240°C in the experiments in the small diameter column (0.041 m), whereas the hold-up was essentially independent of temperature in the larger diameter column (0.10 m). Contrary to this Quicker and Deckwer (1981), and Kuo et al. (1985) found that the hold-up increases with temperature.

In general, the liquid viscosity increases as the temperature decreases and higher liquid viscosity promotes bubble coalescence. Thus, one would expect that the hold-up would increase with temperature. The

13

effect of viscosity on the gas hold-up was very significant during the operation of a 0.247 m in diameter slurry bubble reactor for F-T synthesis (Farley and Ray, 1964b). During one of the runs gas hold-up dropped from 45% to 12% while the slurry viscosity increased from 2 mPa·s to over 200 mPa·s during the same period of time. This large increase in viscosity was attributed to the presence of free carbon, but it is more likely that it was caused by production of high molecular weight products (Satterfield et al., 1981).

B. Effect of Solids

The addition of solids reduces the gas hold-up (Deckwer et al., 1980; Kuo et al., 1985). This may be viewed as a viscosity effect, since the viscosity of the slurry increases with solids concentration. As stated above the hold-up is expected to decrease as the viscosity of the medium increases.

C. Effect of Pressure and Gas Type

• The system pressure in the range (0.1-1.5 MPa does not have an effect on the gas hold-up (Deckwer, et al., 1980; Kuo et al., 1985).

• Gas type (N_2 or H_2) does not have an effect on the hold-up (Kuo et al., 1985).

These results show that the density of gas has negligible effect on the gas hold-up.

D. Effect of Superficial Gas Velocity—Flow Regimes and Bubble Size
       Distribution

The majority of studies listed in Table III-1 were made in relatively small diameter columns—up to 0.10 m (except Farley and Ray, 1964a,b—up to 0.25 m) and low superficial gas velocities—up to 0.06 m/s (except Farley

and Ray, 1964b—up to 0.073 m/s, and Kuo et al., 1985—up to 0.12 m/s).

Deckwer and co-workers (Zaidi et al., 1979; Deckwer et al., 1980; Quicker and Deckwer, 1981) found that the bubble size distribution is rather uniform which characterizes the homogeneous (ideal bubbly) flow regime. Their experiments were restricted to velocities less than 0.04 m/s, due to foaming at higher velocities.

In Mobil's study (Kuo et al., 1985) it was found, in both short and long columns, that bubble coalescence takes place with all types of distributors (sintered metal plate and orifice) and that slugs start developing at velocities between 0.02 m/s and 0.03 m/s. Slugs or slug type bubbles were observed even in a 0.102 m diameter column. The bubbles produced by orifice plate distributors were nonuniform in size and larger than the ones obtained with sintered metal plate (SMP) distributors, but the average bubble size (Sauter bubble diameter) was not determined. Foaming was observed in experiments with a paraffin wax (tradename FT-200) and was more pronounced with SMP distributors, giving hold-ups as high as 75%, than with the orifice plate distributors.

In summary, the flow regimes observed in these studies with columns up to 0.10 m in diameter were: homogeneous (ideal bubbly), slug flow or the transition between these two flow regimes, and foaming regime.

Farley and Ray (1964a,b) conducted studies under reacting conditions in a fairly large bubble column reactor with a diameter of 0.247 m where the heterogeneous (or churn-turbulent) flow regime might be possible. However, they reported results for only one value of velocity (0.073 m/s). These results were described in the Section III-A. Farley and Ray (1964a) stated that foaming occurs at low gas velocities and that it can be

prevented by operating the reactor at gas velocities greater than about 0.06 m/s. In one of the experiments they found that foam break-up occurred when the velocity was increased from 0.03 m/s to 0.06 m/s, but the gas hold-up values were not reported.

Sauter mean bubble diameter was determined by Deckwer and co-workers by photographic method (Zaidi et al., 1979, Deckwer et al., 1980; Quicker and Deckwer, 1981) and by O'Dowd et al. (1986) by a hot wire anemometer. Zaidi et al. and Deckwer et al. found in experiments with a 75 μm SMP distributor that Sauter bubble diameter is approximately 0.7 mm and that it does not vary much with gas velocity (up to 0.04 m/s) and temperature (250-270°C). Quicker and Deckwer made measurements in a 0.095 m column equipped with a 0.9 mm nozzle and found that Sauter diameter decreases with velocity and is less than 1 mm for gas velocities greater than 0.01 m/s. Contrary to this, O'Dowd et al. found that Sauter bubble diameter increases with gas velocity from 3 mm to 3.9 mm, over the range of velocities (up to 0.02 m/s), for Mobil's reactor wax from run CT-256-4 (Run 4 wax). In experiments with a paraffin wax (P-22 wax from Fisher) somewhat smaller bubble sizes were measured (2.6-3.8 mm) but similar behavior to the Mobil wax with increasing velocity was observed.

Calderbank et al. (1963) reported values of the gas hold-up and the specific gas-liquid interfacial area for gas velocities up to 0.055 m/s. The interfacial area was determined by light transmission method. Sauter mean diameters estimated from these data are between 2 and 3 mm.

Discrepancies in results obtained in different studies may be attributed to differences in liquid medium employed, distributor types liquid static heights and experimental techniques.

16

E.   Effect of Column Diameter

This effect was examined by Deckwer et al. (1980) and in Mobil's study (Kuo et al., 1985).

- Deckwer et al. (1980) found that the hold-up is essentially independent of column diameter (0.041 and 0.10 m columns) for temperatures greater than 250°C.

- Kuo et al. (1985) found in experiments with FT-200 wax in short columns (2.2 m in height) that the hold-up is somewhat greater in the smaller diameter column (0.032 m) than in the larger one (0.053 m ID). This was attributed to the fact that the foam is stabilized by the walls of the narrower column.

- In studies by Kuo et al. in tall columns (0.051 and 0.102 m in diameter, 9.1 m in height) with dynamically similar orifice plate distributors (same orifice hole size and same gas velocity through the orifice) have shown no effect of column diameter with FT-200 wax, but higher hold-ups (about 30-40% in the velocity range 0.015-0.065 m/s) were obtained in the larger column in experiments with reactor waxes. (Waxes produced during Runs CT-256-7 and CT-256-8.) In the latter case, the higher hold-up in the larger column might have been due to fewer and smaller slugs.   However, this was not observed in experiments with FT-200 wax, where slugs are accompanied by a large number of small bubbles. In this case, the contribution of slugs to the gas hold-up is relatively less, and thus the column diameter did not have effect on the hold-up.

F. Effect of Static Liquid Height

The findings from different studies may be summarized as follows:

- No effect of liquid static height on the gas hold-up was found in studies by Deckwer et al. (1980) (H_s – 0.60 – 0.95 m, 75 μm SMP) and Kuo et al. (1985) with FT-200 in the 0.051 m column equipped with a 2 mm single hole orifice plate (H_s – 0.75-7.1 m).

- The gas hold-up increases as the static height decreases (Calderbank et al., 1963 with ball and cone distributor and H_s – 2.3 and 4.6 m; Kuo et al., 1985 with FT-200 wax, 20 μm SMP and H_s – 3.05-6.40 m).

- The gas hold-up increases with the liquid static height (Kuo et al., 1985 with FT-200 wax, 1 mm single orifice and 3 x 0.5 mm orifice plate distributors, and static heights of 0.6 m and 6.3 m).

These contradictory results indicate that there exists an interaction between the sparger design, the static liquid height and properties of the liquid medium. These factors affect the bubble coalescence and break-up which in turn determines the gas hold-up.

G. Effect of Distributor Type

This effect has been studied by Quicker and Deckwer (1981) and by workers at Mobil (Kuo et al., 1985).

Quicker and Deckwer (1981) obtained higher gas hold-ups with a single nozzle distributor than with a 19 x 1.1 mm perforated plate distributor, probably because of much higher jet velocity for the former distributor. Higher jet velocity (gas velocity through the orifice) implies higher kinetic energy of the fluid which produces finer bubbles and thus higher hold-ups. The hold-ups with the single nozzle distributor were even higher than those obtained by Deckwer et al. (1980) with the 75 μm SMP, which

18

contradicts results obtained in Mobil's study as well as in the present one (see Section V-B.5).

In Mobil's work it was found that:

- SMP distributors produce, in general, smaller bubbles and higher hold-ups than the orifice distributors.

- For SMP distributors, gas hold-up decreases with the increasing mean pore size which is accompanied by larger bubbles and less foam (short columns 0.032 and 0.053 m ID, 2.2 m tall).

- Distributors with small orifices (less than 0.4 mm) can give hold-ups similar to large-pore SMP distributors. Bubble size distributions, though, are different (short columns).

- Orifice-type gas distributors give similar hold-ups when the gas jet velocities through the holes are similar. However, if the orifice diameter is large enough ($\geq$ 1 mm) lower hold-ups will result at all velocities (short columns).

H.   Effect of Liquid Medium

Experiments with different waxes were conducted only in Mobil's study (Kuo et al., 1985). They found that reactor waxes give lower hold-ups than that obtained with FT-200 wax for all types of distributors (SMP and orifice plate). Also, unlike FT-200 wax most of the reactor waxes did not foam (Waxes made in runs 5, 7 and 8 did not foam, whereas the wax made during the run 4 in Mobil's pilot plant unit CT-256 produced some foam in a run with 60 μm SMP distribution at 200°C in the 0.053 m ID column). These differences in behavior of different waxes are caused to some extent by differences in their physical properties (primarily the viscosity), and

even more significantly by differences in their compositions. The presence of small amounts of surface active species is known to have a significant effect on foaming behavior and hydrodynamic parameters in gas-liquid systems. These results show that the liquid medium for hydrodynamic studies must be chosen carefully in order to obtain information useful for bubble column reactor design.

IV. TASK 2 - BUBBLE COLUMN REACTOR DESIGN/CONSTRUCTION

A. DESIGN AND SELECTION OF GAS DISTRIBUTOR

In the present study, both single hole orifice plate distributors and a sintered metal plate distributor were selected for use in the 0.051 m ID columns. The 1 mm, 1.85 mm and 4 mm orifice plate distributors, and a 40 μm sintered   metal plate distributor, were selected for our studies. These four distributors are similar to the ones used in previous   hydro-dynamic studies (see Table III-1) and/or in slurry bubble column   reactors for F-T synthesis.   The 1 mm and 1.85 mm orifice plate distributors satisfied the criterion presented by Mersmann (1978) for stable flow through an orifice as well as the criterion to prevent "weeping" at all superficial gas velocities investigated.   The 4.0 mm orifice plate satis-fied the criteria for stable flow at velocities greater than 0.024 m/s and the criterion to prevent "weeping" at velocities greater than 0.055 m/s (see Table IV-1).

For experimental studies in the 0.229 m ID and 0.241 m ID columns, perforated plate distributors (5 X 1 mm, 19 X 1 mm, and 19 X 1.85 mm) and a perforated pipe distributor (30 X 1.5 mm) were selected. The criteria presented by Mersmann were satisfied for all four distributors for all gas velocities investigated (see Table IV-1). The 5 X 1 mm perforated plate distributor was chosen because it gave jet velocities that were comparable with those in the Quicker and Deckwer (1981) study with a 0.9 mm nozzle in a 0.095 m ID column. The 19 X 1.85 mm perforated plate was chosen because it gives approximately the same orifice Weber number and the jet velocity as the 1.85 mm single hole orifice plate distributor used in the 0.051 m ID columns.   Also, in the Rheinpreussen-Koppers demonstration plant gas

21

Table IV-1. Criteria for distributor design (evaluated at $u_g=0.01$ m/s).

Criterion 1:

$$-\frac{u_j^2 d_o \rho_g}{\sigma} > 2$$

Criterion 2:

$$\frac{u_j^2}{g d_o}\left(\frac{\rho_g}{\rho_\ell - \rho_g}\right)^{5/4} \geq 0.37$$

Distributor	Criterion 1	Criterion 2
0.051 m ID column:		
1 mm	22.4	12.29
1.85 mm	3.5	0.58
4 mm	0.4[a]	0.01[b]
0.229 m ID column:		
5 X 1 mm P.Plate	326.3	203.6
19 X 1 mm P.Plate	22.6	14.1
19 X 1.85 mm P.Plate	3.9	0.65
30 X 1.5 mm P.Pipe	3.0	0.75

[a] Criterion 1 satisfied at $u_g=0.024$ m/s

[b] Criterion 2 satisfied at $u_g=0.055$ m/s

distributors with holes about 2 to 3 mm in diameter were employed (Kolbel and Ralek, 1980). We chose the 19 X 1.0 mm perforated plate distributor to study the effect of an increase in the orifice Weber number and the jet velocity (i.e. the gas velocity through the orifice) on the hydrodynamic properties. Also, this distributor is dynamically similar to the 1.0 mm single orifice plate in the 0.051 m column. The 30 X 1.5 mm perforated pipe was selected to study the effect of the distributor type and orifice diameter on the hydrodynamic properties keeping the orifice Weber number approximately the same as that for the 19 X 1.85 mm perforated plate distributor.

Mersmann (1978) presented a general criterion for stable flow through multiple orifice plates or immersion tubes with holes. For distributors with holes (d_o) smaller than the critical orifice diameter ($d_{o_{cr}}$), i.e. stable flow through the

$$d_o < d_{o_{cr}} = 2.32 \left[\frac{\sigma}{\rho_g g} \right]^{1/2} \left[\frac{\rho_g}{\rho_\ell - \rho_g} \right]^{5/8} \qquad \text{(IV-1)}$$

stable flow through the distributor is obtained when the orifice Weber number (ratio of the gas kinetic energy to the surface energy) is greater than two.

$$We_o = \frac{u_j^2 d_o \rho_g}{\sigma} \geq 2 \qquad \text{(IV-2)}$$

where the jet velocity is defined as

$$u_j = \frac{u_g d_c^2}{n d_o^2} \qquad \text{(IV-3)}$$

For perforated plates or nozzles with orifice diameters greater than

23

the critical orifice diameter (i.e. $d_o \geq d_{o_{cr}}$), "weeping" through the distributor can be prevented if the following criterion is satisfied:

$$Fr_o^2 \left[\frac{\rho_g}{\rho_\ell - \rho_g} \right]^{5/4} \geq 0.37 \qquad \text{(IV-4)}$$

where Fr_o is the orifice Froude number (ratio of the gas kinetic energy to the potential energy), and is defined as

$$Fr_o = \frac{u_i}{\sqrt{g d_o}} \qquad \text{(IV-5)}$$

The critical orifice diameter for FT-300 wax at 265°C is 1.73 mm (using physical properties presented in Table VI-1). The orifice Weber numbers and the orifice Froude numbers were calculated for the various distributors used in our studies for a superficial gas velocity of 0.01 m/s and are listed in Table IV-1.

For the perforated plates and perforated pipe distributors, the individual orifices were positioned so that the area about each opening was the same. This type of design is recommended for an even distribution of bubbles at the distributor (Richardson, 1961). The 19 holes composing the perforated plates were equally spaced in a triangular pitch, and the perforated pipe was a star shaped arrangement with six segments having five holes each (see Figures IV-1 and IV-2).

B. DESCRIPTION OF EXPERIMENTAL APPARATUS

Two bubble columns (0.051 m ID and 0.229 m ID, 3 m tall) made of borosilicate glass were assembled for measuring the average gas hold-up and bubble size distributions. Both columns were constructed in essentially the same manner, therefore, a detailed description of only the 0.051 m ID column is presented here.

24
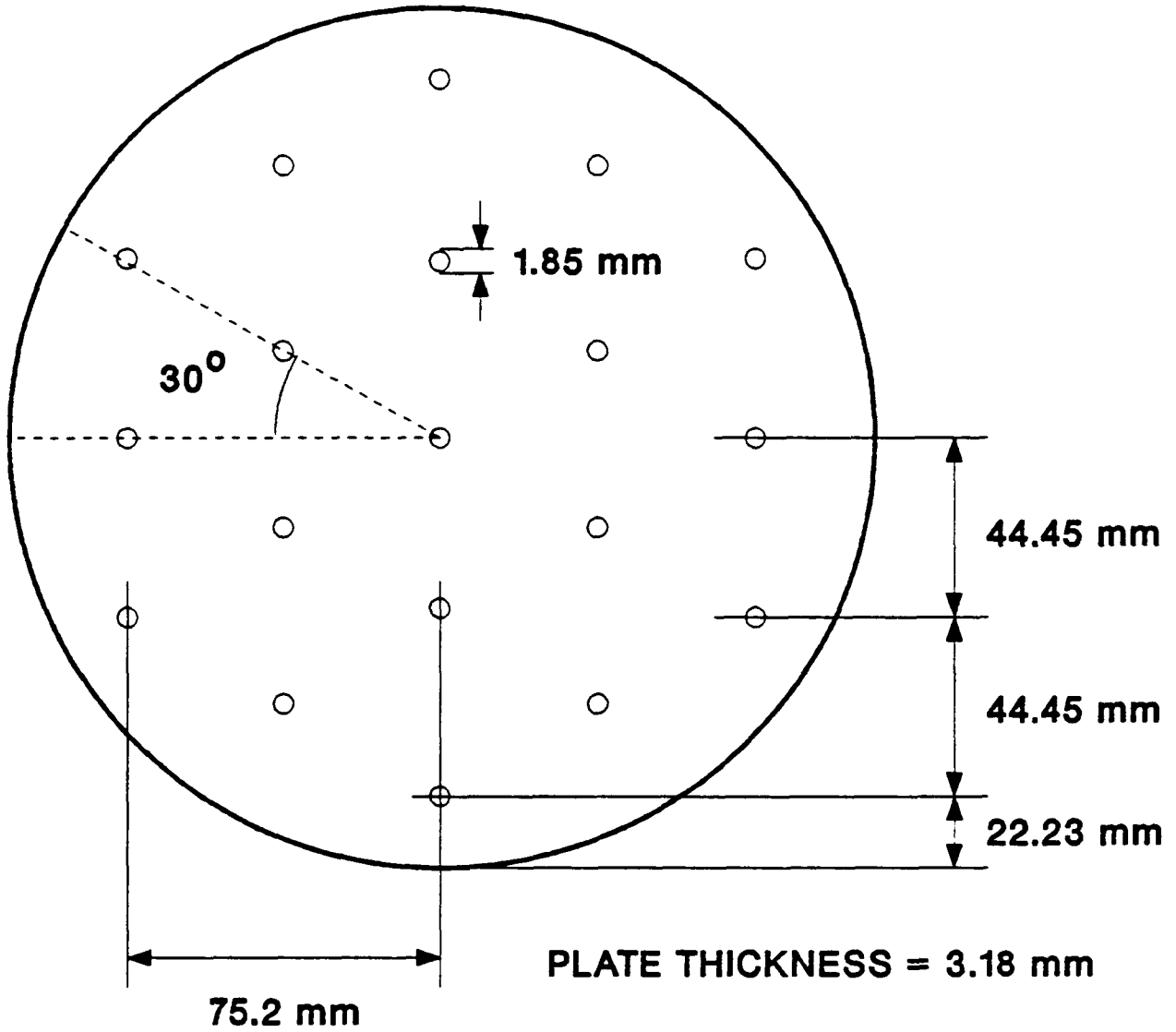
Figure IV-1. 19 X 1.85 mm perforated plate distributor

Labels within figure:
- 1.85 mm
- 30°
- 44.45 mm
- 44.45 mm
- 22.23 mm
- PLATE THICKNESS = 3.18 mm
- 75.2 mm
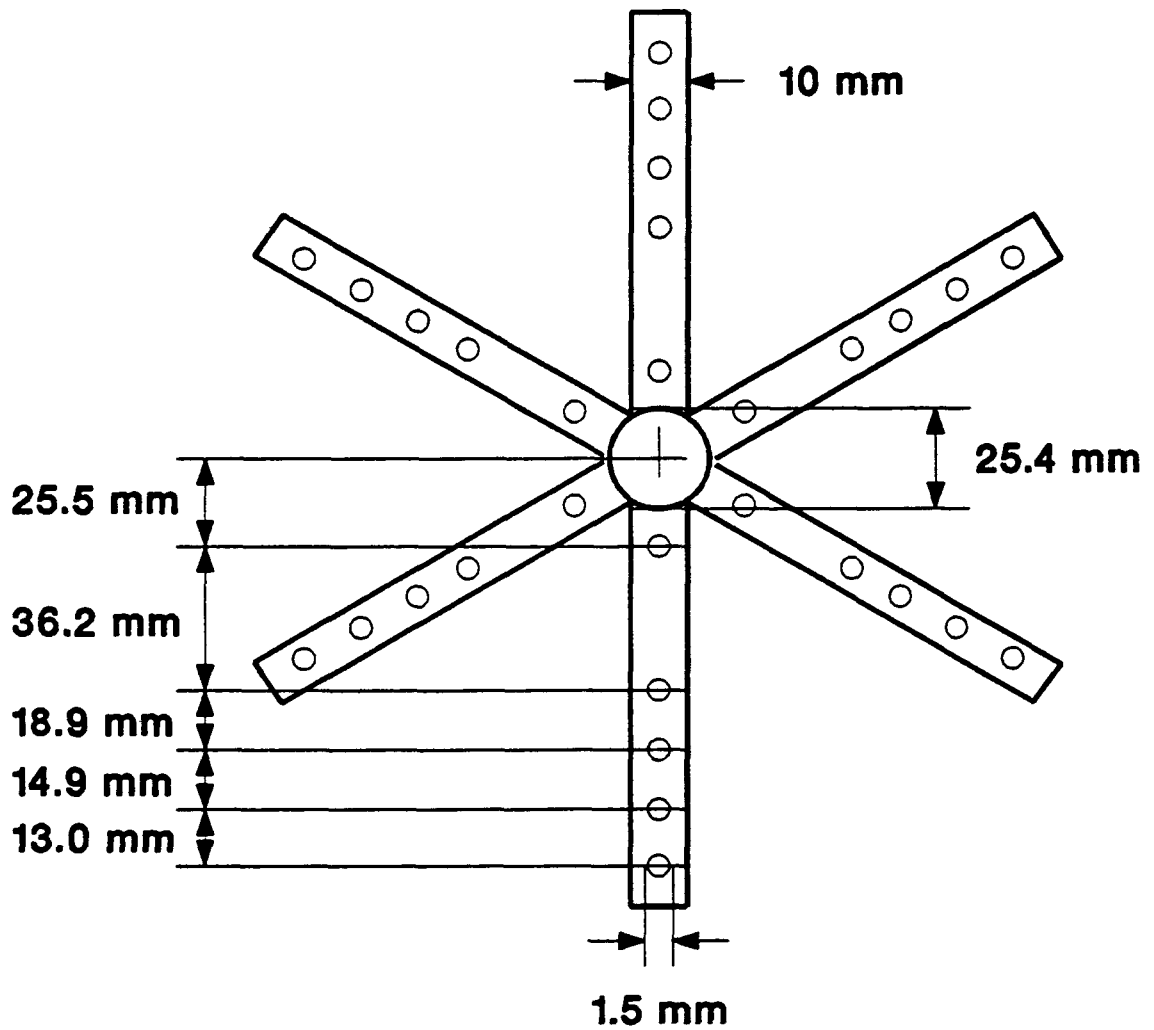
Figure IV-2. 30 X 1.5 mm perforated pipe distributor

A schematic representation of the experimental apparatus is shown in Figure IV-3. The flow rate of nitrogen from gas cylinders was measured and controlled by a mass flow meter (FC; Brooks Model 5816). For the 0.229 m ID column, a Sierra (Series 840) mass flow meter was used to measure the gas flow rate. For this column, the flow rate was controlled manually. The mass flow calibration was checked before every run using a wet test meter. The metered gas passes through a preheater (PH; electrically heated U-tube), and its temperature is monitored by two thermocouples (one located after the preheater and one just below the distributor). The thermocouples are connected to an Omega (Model 199) ten channel temperature indicator. The inlet temperature of nitrogen is manually controlled using a variable transformer. The preheated gas enters the glass bubble column (BC) through a sparger which is placed between two flanges at the bottom of the column. The column is preheated to a temperature between 150°C to 200°C using heating tapes that are wound around the column. Two Omega (Model 52) temperature controllers allow independent control of the temperature in the top and bottom halves of the bubble column. The wax in the storage tank is heated to a temperature of 150°C to 200°C before it is transported to the preheated column through a 0.013 m ID (1/2 inch) tube using a slight nitrogen overpressure. The large storage tank (0.085 m^3 capacity) was used originally for experiments in the small and large columns, however, from Run 4-1 onwards a smaller storage tank (0.009 m^3 capacity) was used for experiments in the 0.051 m ID column, while the large storage tank was used only for runs in the 0.229 m ID column.

The bubble column has four thermocouples attached to it in order to monitor its temperature. Two of these are attached to the wall of the

FIGURE IV-3

FLOW DIAGRAM OF EXPERIMENTAL APPARATUS

FC   FLOW CONTROLLER
PI   PRESSURE INDICATOR
PH   PREHEATER
TI   TEMP. INDICATOR
TIC   TEMP. CONTROLLER
BC   BUBBLE COLUMN
〜〜 ELECTRICALLY HEATED

column (upper and lower halves of the column), while the other two are placed in thermowells located along the column axis (at approximately 0.33 and 2.00 m above the distributor). During the preheating period the thermo-couples on the wall are used to control the column temperature. Once the wax is transported to the column, the column is brought to within 10 to 20°C of the desired operating temperature by gradually increasing the set point on the temperature controllers. At this point control of the column is switched to the inside thermocouples. During the entire preheating period (i.e. while wax in the column is being brought to the operating temperature) the gas flow rate is maintained at the desired start-up velo-city. The disengagement unit at the top of the column, the carry-over lines from this unit to the separator, and the separator itself are maintained at temperatures above the melting point of wax (i.e > 110°C) to prevent the solidification of any entrained liquid. The hot gases leave the separator through a 0.025 m ID (1 inch) pipe and pass through the scrubber, which is filled with a mineral spirit (varsol), before it is vented to the atmos-phere. The scrubber is used to recover components of the wax that evaporate from the column, and is maintained at approximately 75°C.

In addition to the two glass columns, two stainless steel columns (0.051 m ID and 0.241 m ID, 3 m tall) were also constructed for measuring axial hold-up. A complete description of these columns is given in Section V-C.

V. TASK 3 - PROCESS VARIABLE STUDIES

A. DESCRIPTION OF THE FLOW FIELD

The hydrodynamics of a bubble column is significantly affected by the flow regime in which the column operates. Ample evidence of this dependency is available in literature (e.g. Shah et al, 1982) and various criteria have been proposed by different researchers to differentiate the flow regimes. Deckwer et al. (1980) presented a flow regime map (Figure V-1) which qualitatively characterizes the dependence of flow regimes on the column diameter and the superficial gas velocity. At low superficial gas velocities, regardless of column diameter, the homogeneous flow regime (or the "homogeneous bubbling" regime) exists. In this flow regime, the bubbles are uniform in size and minimal interaction between neighboring bubbles occurs. Bubble coalescence and breakup occurs as the gas velocity is increased. During this process, large bubbles may appear. In columns less than 0.10 m in diameter, the large bubbles may fill the entire column diameter forming slugs; this is the "slug flow" regime. In larger diameter columns, large bubbles are formed without producing slugs. The formations of these large bubbles is associated with an increase in turbulence; this is the "churn-turbulent" regime. The shaded regions in Figure V-1 indicate the transition regions between the various flow regimes. The exact location of the boundaries associated with the transition regions will probably depend on gas distributor design, static liquid height, operating conditions and gas and liquid media.

The flow regimes described above are typically associated with nonfoaming systems. For foaming systems, Shah et al. (1985) include an additional flow regime called the foaming (or "foamy") regime. The

FIGURE V-1

BUBBLE COLUMN FLOW REGIME MAP
(adopted from Deckwer et al, 1980)
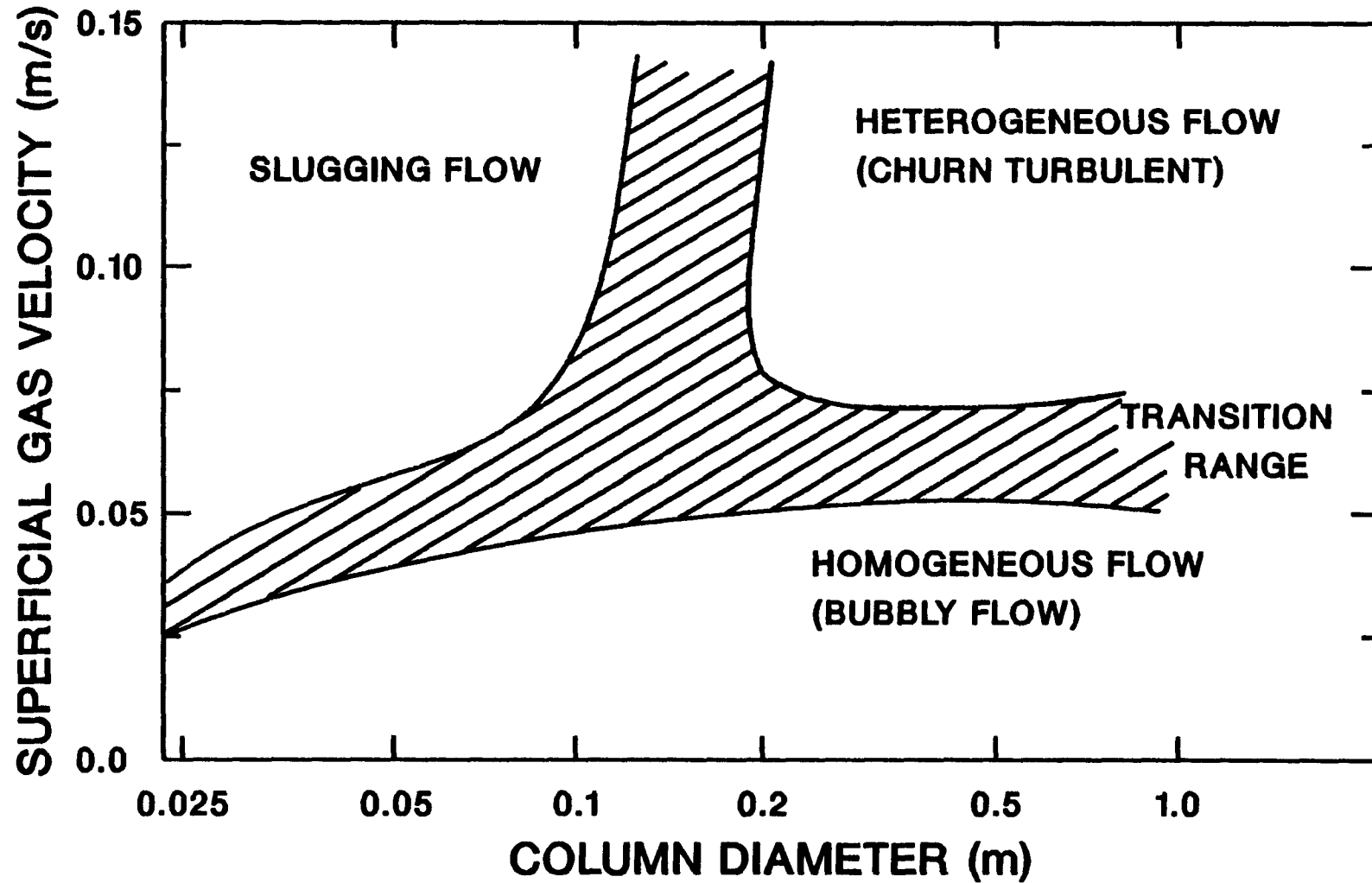
"foamy" regime overlaps the previously described regimes and is charac-
terized by the presence of a stable layer of foam on top of the dispersion.
Smith, D.N. et al. (1984b) have presented a procedure that makes it
possible to predict the transition from the "homogeneous bubbling" regime
to the "foamy" regime.

The flow fields in the 0.051 m ID and the 0.229 m ID glass columns,
for the range of conditions employed in the present study, were studied
visually, and with the aid of video tapes and photographs. Results from
experiments conducted with the paraffin waxes (FT-200 and FT-300) and with
distilled water are presented here. It was not possible to observe the flow
field with reactor waxes (Sasol's Arge reactor wax and Mobil's reactor wax)
due to the dark color of these waxes.

The major findings from these studies are:

- In the 0.051 m ID column, the "homogeneous bubbling" regime prevails
  at a superficial gas velocity of 0.01 m/s followed by a transition to
  the "slug flow" regime in the absence of foam. Whereas, in runs with
  orifice plate distributors where foam was present (e.g. with paraffin
  waxes), the "homogeneous bubbling" regime was followed by the "foamy"
  regime (for the velocity range 0.03 to 0.05 m/s in most cases), after
  which the "slug flow" regime prevails. Similar flow regimes were
  observed with the 40 μm SMP distributor, however, the "foamy" regime
  prevailed up to gas velocities of 0.09 m/s.

- In the 0.229 m ID column, the "homogeneous bubbling" regime occurs at
  gas velocities of 0.01 and 0.02 m/s followed by a transition to the
  "churn turbulent" flow regime in the absence of foam. However, in runs
  where foam was present, the "homogeneous bubbling" regime was followed

by the "foamy" regime (for the velocity range 0.03 to 0.05 m/s), after
which a transition to the "churn-turbulent" flow regime occurred.

During gas hold-up measurements in the small (0.051 m ID) and large
(0.229 m ID) glass columns, the flow field near the wall, at heights of
approximately 0.45 m, 1.2 m and 2.1 m above the distributor, was
photographed with a Canon 35 mm SLR camera and also recorded with a video
camera (Hitachi, Model GP-5AU). Based on the photographs, video tapes, and
visual observations recorded during the experiments, the following
qualitative remarks of the flow field can be made.

A.1. <u>Small Column (0.051 m ID)</u>

A.1.a. <u>Effect of Superficial Gas Velocity</u>

The effect of superficial gas velocity on bubbles produced in FT-300
wax at 265°C, using the 4.0 mm single orifice plate distributor, is
illustrated in photographs taken at a distance of approximately 1.2 m above
the distributor (Figure V-2). At a velocity of 0.02 m/s (Figure V-2a),
majority of the bubbles are distributed in two size ranges; medium size
bubbles (4-6 mm in diameter) and small bubbles (< 2 mm in diameter). Some
large bubbles are also present (30-40 mm in diameter), however, these are
not visible in Figure V-2a probably due to their tendency to remain near
the center of the column. At 0.03 m/s (Figure V-2b), the density of bubbles
increases, and a wide bubble size distribution is evident. At this
velocity, slugs start appearing at a height of 1.2 m above the distributor
(not visible in Figure V-2b). At velocities of 0.02 and 0.03 m/s the flow
regime may be characterized as the transition regime between the ideal
bubbly regime and the "slug flow" regime. At 0.04 m/s (Figure V-2c), the
density of bubbles further increases and part of a large bubble can be seen

33

FIGURE V-2

EFFECT OF SUPERFICIAL GAS VELOCITY

4.0 mm SINGLE ORIFICE DISTRIBUTOR
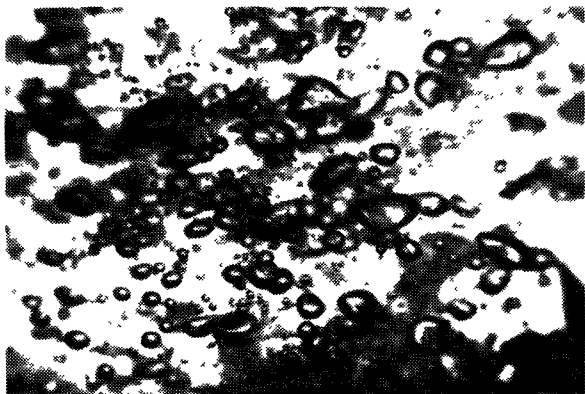
a. 0.02 m/s
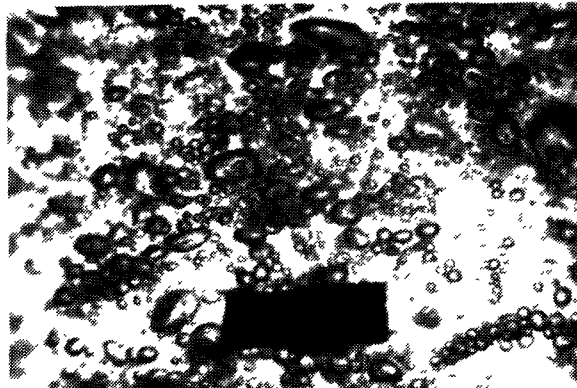
b. 0.03 m/s
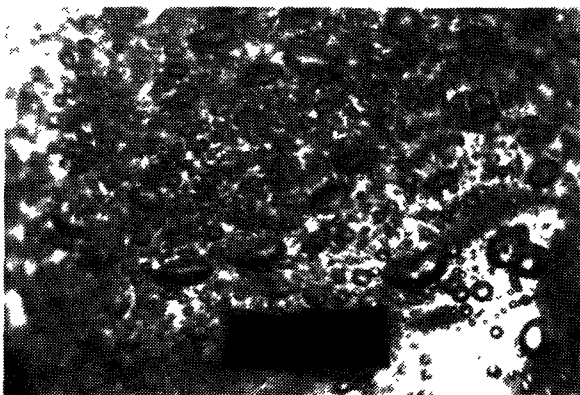
c. 0.04 m/s

d. 0.09 m/s

SCALE: |————————| 25.4 mm

HEIGHT = 1.2 m; T = 265 $^{\circ}$C; d_c = 0.051 m; FT-300 WAX

in the lower right hand side corner. At this gas velocity, the "slug flow"
regime prevails. At 0.09 m/s (Figure V-2d), slugs are easily observed.
These slugs are surrounded by fine bubbles (< 1 mm in diameter), as well as
by a few larger bubbles (3-5 mm in diameter) in diameter. Similar
observations were made when the 1.85 mm single orifice plate distributor
was used.

A.1.b. Effect of Distributor Type

The effect of distributor type at a superficial gas velocity of 0.01
m/s, using FT-300 wax as the liquid medium at a temperature of 265 °C, is
shown in Figure V-3. The bubbles produced with the 40 μm SMP distributor
are smaller and more uniform than the bubbles produced using the 4.0 mm
orifice plate. The effect of height above the distributor on bubble size
is also shown in this figure. The bubble size distribution does not change
with height for the SMP distributor (Figures V-3a and V-3c). On the other
hand, the 4.0 mm single orifice distributor produces a wide bubble size
distribution near the distributor (Figure V-3b). As the height increases
(Figure V-3d) bubble coalescence and breakup occur and two groups of
bubbles become dominant (larger bubbles 4-6 mm in diameter, and fine
bubbles less than 1 mm). The vertical black lines in Figures V-3c and V-3d
represent a portion of the thermocouple well (4.76 mm in diameter).

Figure V-4 compares the flow field obtained using the 1.85 mm orifice
plate with that obtained using the 40 μm SMP at 0.07 m/s in the slug flow
regime (foam was not present) using FT-300 wax at 265 ° C. All photographs
were taken at a height of 1.2 m above the distributor. Figures V-4a and
V-4b show slugs (only the bottom portion of a slug leaving the field of
view can be seen in Figure V-4a), accompanied by many fine bubbles (< 1 mm

FIGURE V-3

EFFECT OF DISTRIBUTOR AND
HEIGHT ABOVE THE DISTRIBUTOR

40 µm SMP

4.0 mm
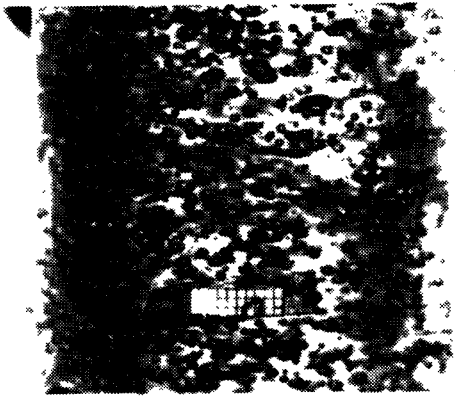
a. 0.45 m

b. 0.45 m
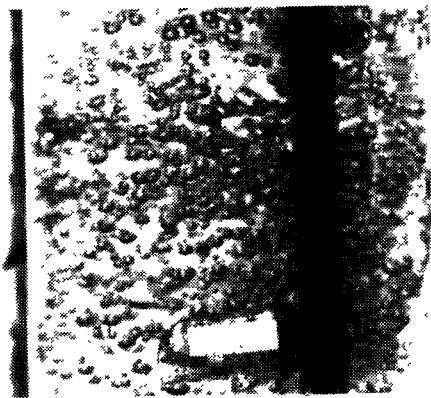
c. 2.1 m
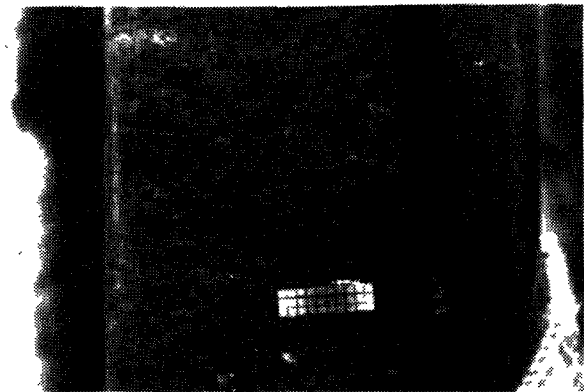
d. 2.1 m

SCALE: ⊢————⊣ 25.4 mm

$u_g = 0.01$ m/s; $T = 265$ $^{\circ}$C; $d_c = 0.051$ m; FT-300 WAX

FIGURE V-4

EFFECT OF DISTRIBUTOR

SLUG FLOW REGIME

40 μm SMP
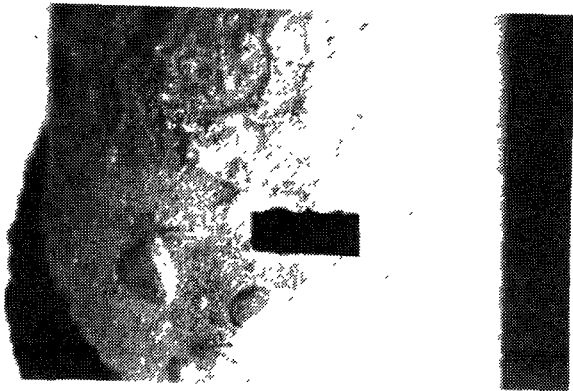
1.85 mm

a. slug present
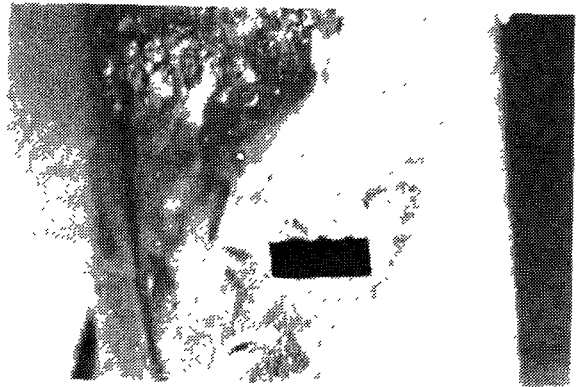
b. slug present
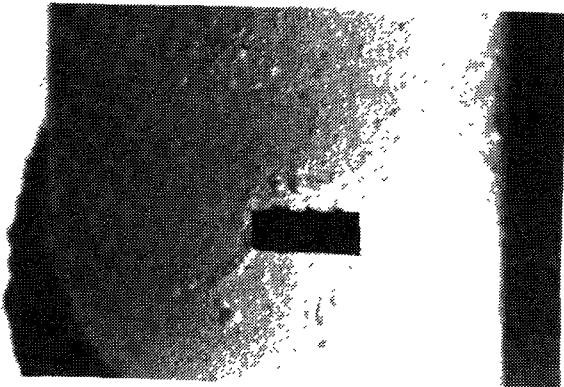
c. absence of slug
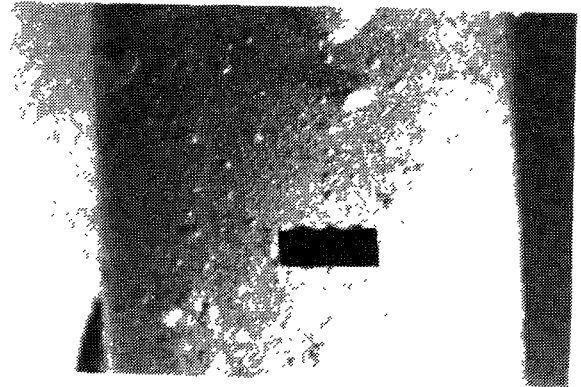
d. absence of slug

SCALE: |————| 25.4 mm

u_g = 0.07 m/s; HEIGHT = 1.2 m; T = 265 °C;
d_c = 0.051 m; FT-300 WAX

in diameter), produced when the SMP and the 1.85 mm orifice plate distributor, respectively, were used. There was no noticeable difference in the slugs formed in the two cases. Figures V-4c and V-4d are at the same height and velocity as Figures V-4a and V-4b, however, they show the flow field in the absence of slugs. Once again, there is no obvious difference in the bubbles produced by the two different distributors in the slug flow regime, when foam is not present.

Figure V-5 shows foam produced by the 40 μm SMP and the 1.85 mm orifice plate distributor at 265 °C with FT-300 wax at a velocity of 0.03 m/s. For experiments conducted with the SMP distributor in the "foamy" regime, photos were taken only at a height of 1.2 m above the distributor since foam usually filled the entire column and there was not a noticeable difference between the foam at the bottom and the top of the gas-liquid dispersion. Figure V-5a shows foam produced by the SMP distributor at a height of 1.2 m above the distributor. For experiments conducted with the 1.85 mm orifice plate distributor, foam usually appeared only at the top of the column. Figure V-5b shows foam produced by the 1.85 mm orifice plate distributor at a height of 2.1 m above the distributor. Figures V-5a and V-5b also show that the average size of bubbles produced by the two different distributors is similar and consists of bubbles less than 1 mm in diameter. The foam associated with the SMP distributor is composed of bubbles of a uniform size, whereas, foam produced with the 1.85 mm orifice plate distributor consists of a wider range of bubble sizes.

A.1.c. Effect of Height above the Distributor

Figure V-6 shows the effect of height above the distributor on bubbles formed, when the 1.85 mm orifice plate distributor was used, at velocities

FIGURE V-5

EFFECT OF DISTRIBUTOR

FOAMY REGIME

40 μm SMP
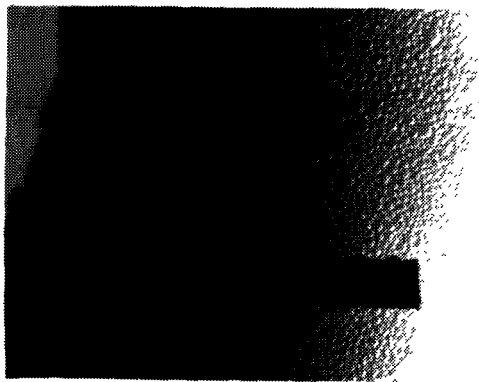
a. 1.2 m

1.85 mm
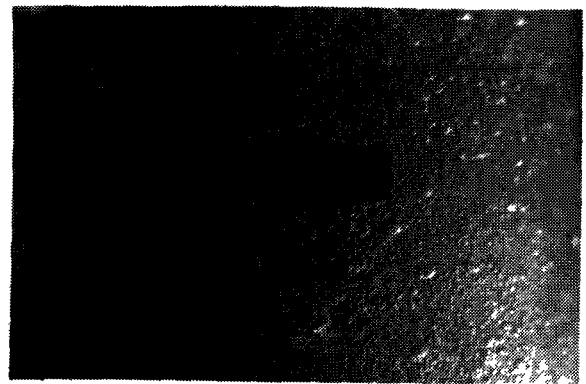
b. 2.1 m

SCALE: ⊢————⊣ 25.4 mm

$u_g = 0.03$ m/s; T = 265 ^{o}C; $d_c = 0.051$ m; FT-300 WAX

of 0.03 and 0.07 m/s, and at heights of 0.45 and 2.1 m above the distributor. All photographs were taken using FT-300 wax as the liquid medium at a temperature of 265 °C. At a velocity of 0.03 m/s there is a considerable difference in the bubbles produced near the distributor and at the top of the dispersion (Figures V-6a and V-6c, respectively). The bubble size distribution near the distributor is wide, with large bubbles (10-20 mm in diameter), intermediate size bubbles (2-8 mm in diameter), and small bubbles (< 1 mm in diameter) being present. However, at a height of 2.1 m above the distributor, the distribution is narrower, with a greater concentration of small bubbles (< 1 mm in diameter) and relatively few large bubbles. At 0.07 m/s (Figures V-6b and V-6d), there are essentially no medium size or large bubbles present at 2.1 m above the distributor (except for slugs, which are not visible in the Figure). Whereas, at a height of 0.45 m above the distributor, the bubble size distribution is significantly wider than at 2.1 m. At this height large bubbles, nearly filling the entire column cross-section, were often observed.

A.1.d. <u>Slug Frequency</u>

For majority of the experiments conducted with an orifice plate distributor, the slug frequency, regardless of liquid medium, goes through a local maximum followed by a local minimum, after which it increases gradually with gas velocity. The slug frequency was measured at approximately 0.3 m below the top of the expanded level. Figure V-7 shows the slug frequency as a function of superficial gas velocity for paraffin waxes (FT-300 and FT-200) and distilled water. Accurate measurements of the slug frequency for Sasol and Mobil reactor waxes could not be made due to the dark nature of the waxes. As can be

FIGURE V-6

EFFECT OF HEIGHT ABOVE THE DISTRIBUTOR AND SUPERFICIAL GAS VELOCITY

1.85 mm SINGLE ORIFICE DISTRIBUTOR
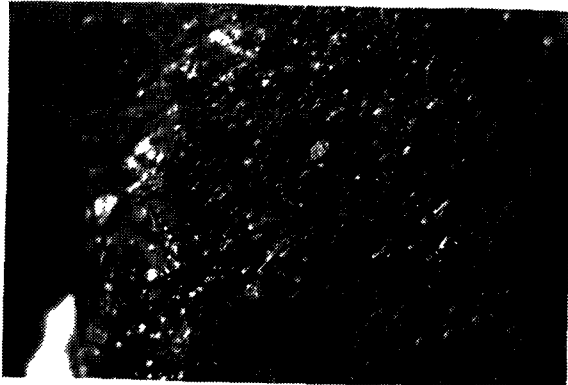
a. 0.03 m/s; 0.45 m

b. 0.07 m/s; 0.45 m
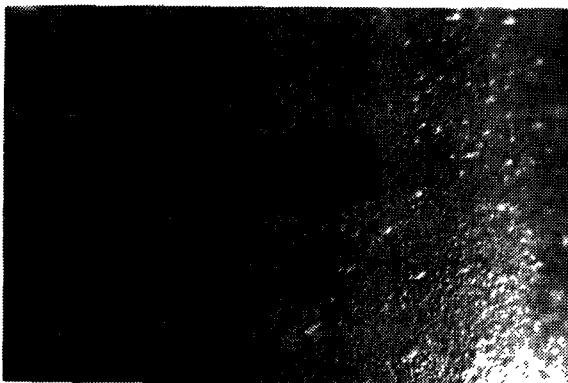
c. 0.03 m/s; 2.1 m
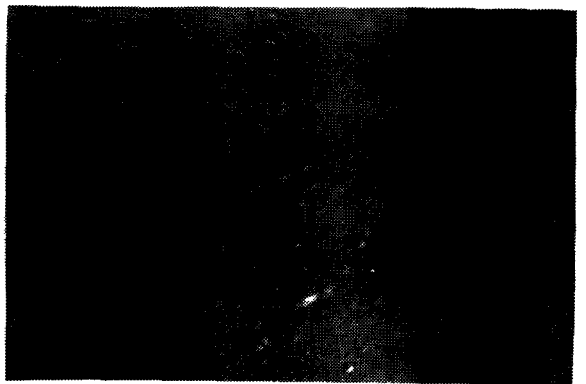
d. 0.07 m/s; 2.1 m

SCALE: ⊢————⊣ 25.4 mm; Figures a and c

SCALE: ⊢———⊣ 25.4 mm; Figures b and d

T = 265 $^\circ$C; d_c = 0.051 m; FT-300 WAX
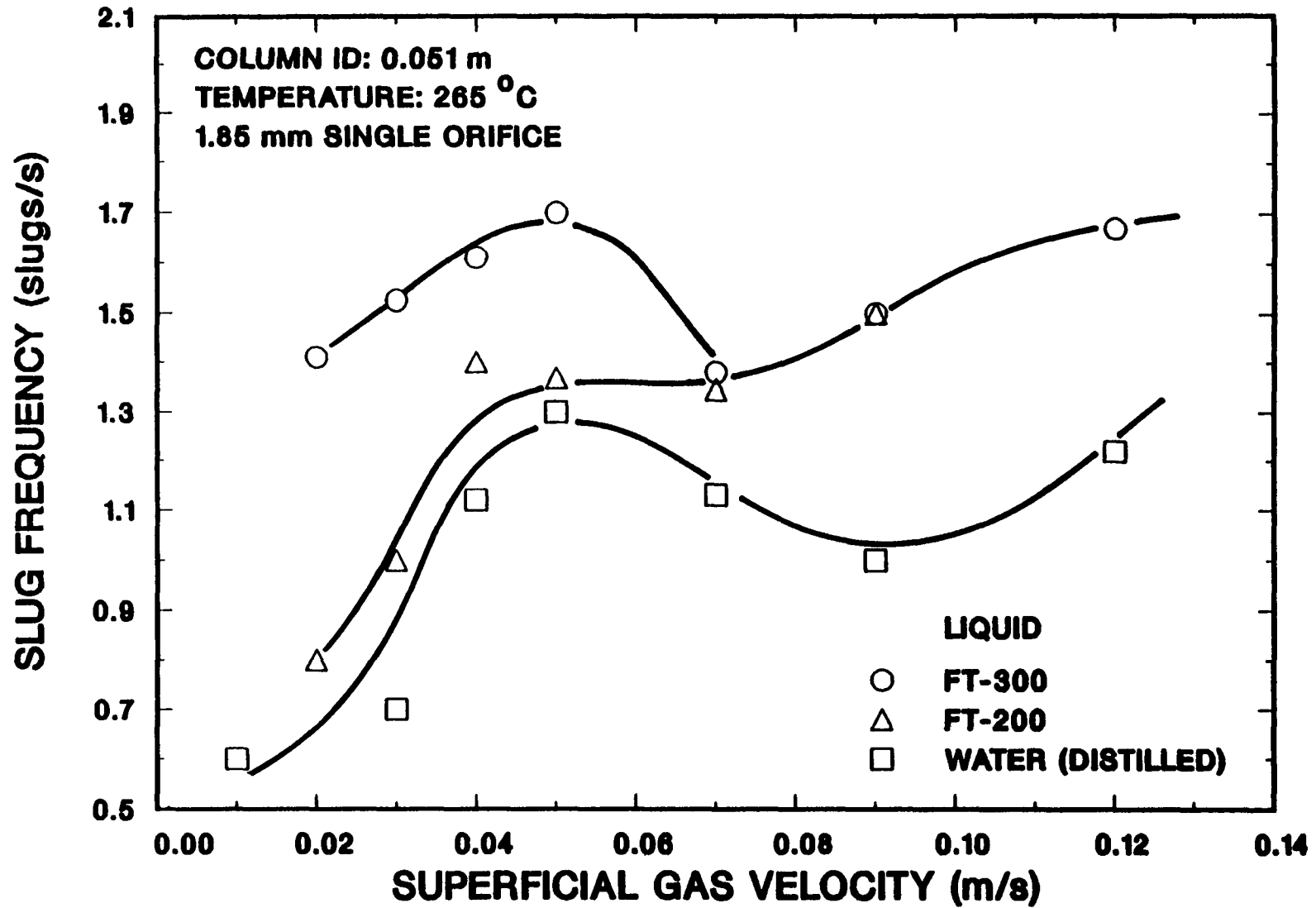
Figure V-7. Effect of superficial gas velocity and liquid medium on slug frequency (measurements made at 0.3 m below the top of the expanded level) (Run 3-2)

seen from Figure V-7, the slug frequency for each medium goes through a local maximum followed by a local minimum. Similar results were obtained by Ohki and Inoue (1970) in an air-tap water system. This type of behavior can be explained as follows. Initially, the number of slugs increases until the slug frequency reaches a maximum. At this point, the slugs begin to interact with one another, becoming longer; hence, the frequency of the observed slugs decreases. This decrease in frequency with increasing gas velocity continues till a maximum stable slug size is reached. This corresponds to the local minimum value of the slug frequency. Since slugs do not appear to grow in length beyond this point, a further increase in the gas flow rate causes the slug frequency to increase. For all three liquid mediums a maximum slug frequency occurred between 0.04 and 0.05 m/s. For FT-300 and FT-200 waxes, the minimum occurred at 0.07 m/s while with water the minimum occurred at 0.09 m/s. The slug frequencies associated with water at all velocities were less than those of either waxes. This is probably due to the fact that significantly longer slugs were formed in the experiments with water than in the experiments with wax. For velocities less than 0.07 m/s, the slug frequency of FT-200 was less than that of FT-300. This is probably due to the fact that FT-200 produces fewer large bubbles (i.e. fewer and smaller slugs); hence, the slug frequency is smaller.

Figure V-8 shows the slug frequency as a function of gas velocity for FT-300, FT-200, and water for experiments conducted with the 40 μm SMP distributor. For FT-300 and FT-200 waxes, the slug frequency increases with an increase in gas velocity and levels off (FT-300 - 2.0 slugs/s; FT-200 - 1.2 slugs/s). This is probably caused by the large

43
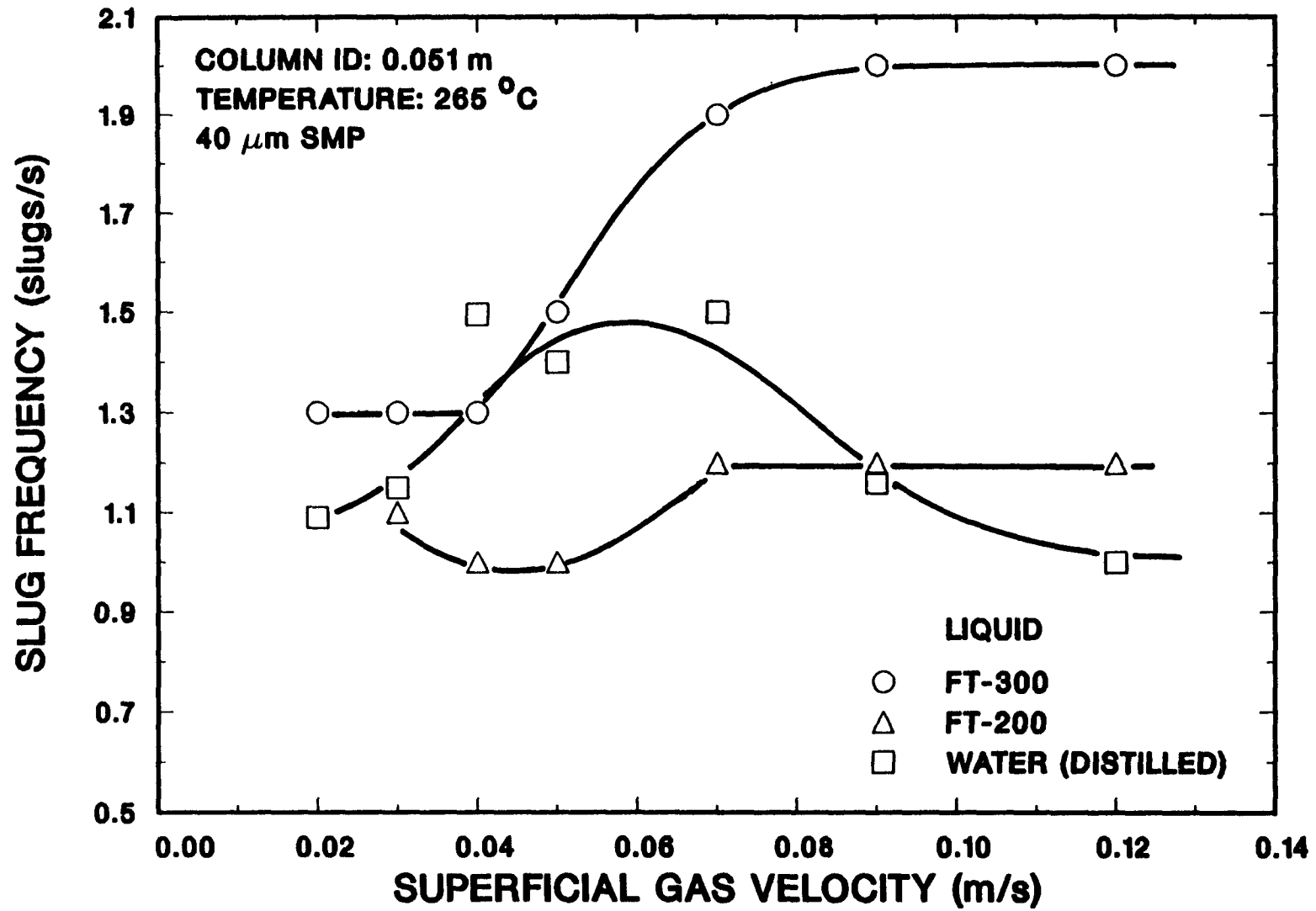
Figure V-8. Effect of superficial gas velocity and liquid medium on slug frequency (measurements made at 0.3 m below the top of the expanded level)

amounts of foam present which prevent significant bubble interaction. On the other hand, the slug frequency did go through a maximum (1.5 slugs/s) between 0.04 and 0.07 m/s for the experiment conducted with distilled water (i.e. no foam present). As seen with the 1.85 mm distributor, the slug frequency associated with FT-200 was significantly less than that of FT-300.

A.2. Large Columns (0.229-0.241 m ID)

The major difference between the flow regimes present in the 0.051 m ID column and those present in the large columns (0.229-0.241 m ID) is the absence of slugs in the latter. In the absence of foam, the "churn-turbulent" flow regime prevails in the large columns for velocities of 0.02 m/s and higher. Observations made during experiments conducted with FT-300 wax at 265°C using a 19X1.85 mm perforated plate distributor are discussed here. At a gas velocity of 0.01 m/s and a height of 0.3 m above the distributor, small bubbles (1.0 - 5.0 mm in diameter) and fine bubbles (less than 1 mm) were present. Occasionally, larger bubbles (10.0 - 20.0 mm) appeared. The fraction of fine bubbles increases with column height. As the velocity was increased, local circulation patterns are observed in the column with the small and fine bubbles moving downwards near the wall of the column. At a velocity of 0.03 m/s, large bubbles, approximately 50.0 mm in diameter, were seen bursting at the top of the dispersion. At velocities of 0.09 and 0.12 m/s the fraction of large bubbles (50.0 mm in diameter) increased, and swirling patterns were observed in the liquid. The flow regime at 0.01 m/s may be characterized as the ideal bubbly flow regime and at higher velocities as the "churn-turbulent" flow regime. During runs when foam was produced, the ideal bubbly flow regime

45

was followed by the "foamy" regime. This regime usually prevailed over the velocity range 0.02-0.05 m/s. Beyond this point a transition to the "churn-turbulent" flow regime took place. The amount of foam produced during runs in the 0.229 m ID columns was lower than that produced in the 0.051 m ID column with the orifice plate distributor.

A viewing port was constructed which enabled us to take photographs of bubbles at approximately 0.03 m from the center of the stainless steel column, at a height of 1.45 m. At a velocity of 0.01 m/s, it is expected that the bubble size at the center of the column would be approximately the same as that near the wall since the ideal bubbly regime prevails. However, at higher velocities, it is expected that larger bubbles would be present near the center of the column. Figure V-9 shows photographs obtained at 0.01 and 0.07 m/s in the large glass column (at the wall) and in the large stainless steel column (at the center). At 0.01 m/s it appears that bubbles observed at the wall are slightly larger than those observed at the center (Figures V-9a and V-9b). However, at 0.07 m/s the bubbles at the wall are smaller than those near the center (Figures V-9c and V-9d).

Since we were limited to observations at the wall of the column and at the top of the liquid level, no significant differences were seen for the other distributors employed in our study or with Sasol's Arge reactor wax. On the other hand, our experiments conducted with distilled water showed a significant increase in the fraction of large bubbles (50 mm in diameter) and essentially no bubbles less than 5 mm in diameter.

FIGURE V-9

EFFECT OF RADIAL DISTANCE

0.229 m ID Glass
height = 1.2 m
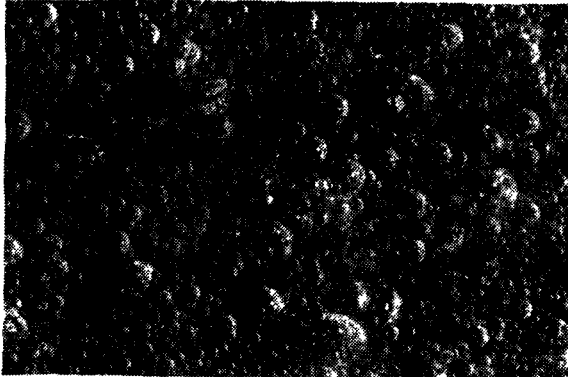
0.241 m ID SS
height = 1.45 m
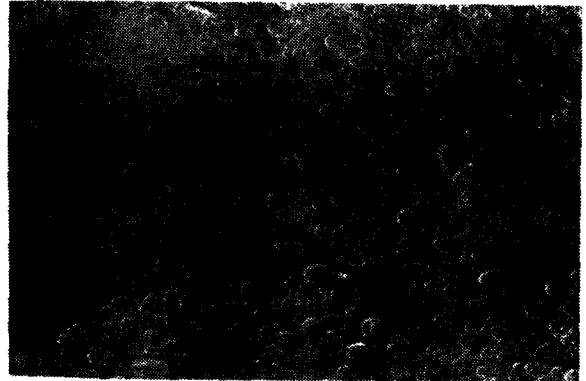
a. 0.01 m/s; at wall

b. 0.01 m/s; 0.03 m from center
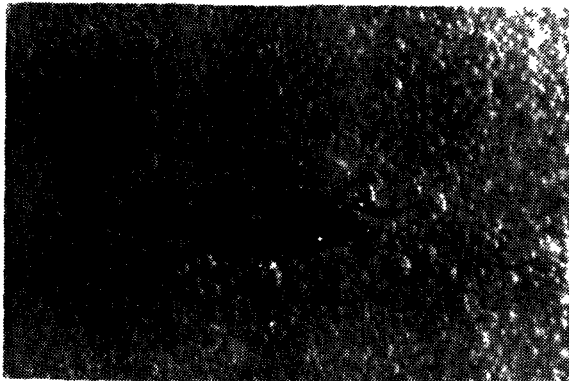
c. 0.07 m/s; at wall

d. 0.07 m/s; 0.03 m from center

SCALE: ⊢————————⊣ 25.4 mm; Figures a, b, & d

SCALE: ⊢————————————⊣ 25.4 mm; Figure c

T = 265 °C; FT-300 WAX

B. AVERAGE GAS HOLD-UP MEASUREMENTS

For a two-phase system, the average gas hold-up is defined as the volume percent of gas in the dispersion. A knowledge of the gas hold-up is necessary for reactor design, since it allows the estimation of the residence time of the gas in the reactor. The gas hold-up, together with the Sauter mean diameter, also determines the specific interfacial area available in the dispersion for mass transfer. Experiments were conducted with the FT-300 - nitrogen system in the two bubble columns (0.051 and 0.229 m ID) to measure the average gas hold-up. The effects of the various operating and design parameters on the gas hold-up were investigated. A limited number of experiments were also conducted with FT-200 wax, Sasol's Arge reactor wax, Mobil reactor wax and distilled water, to study the effect of liquid medium on the average gas hold-up.

B.1. Operating Procedure

The average gas hold-up was measured by visual observations of the expanded height of the dispersion (H) and the static liquid height (H_s), and its value was calculated from

$$\epsilon_g = \frac{H-H_s}{H} \text{ X } 100 \tag{V-1}$$

The first reading of the expanded height was made 20-30 minutes after the desired column temperature and gas flow rate were reached. These readings were repeated a minimum of three times for a given set of operating conditions, with a 20-30 minute time interval between two successive measurements to ensure that the steady state was achieved. In general, for velocities < 0.05 m/s, the readings were 30 minutes apart; whereas, for velocities greater than 0.05 m/s, the readings were 20 minutes apart. For

48

some experiments, the expanded height did not stabilize during the three measurements. In these cases, additional measurements were made until the expanded height stabilized. This was particularly necessary when foam was present at the top of the dispersion. After the last measurement for a given set of conditions the valve below the column was closed and the main flow of nitrogen stopped. The static liquid height was measured after all of the gas disengaged from the dispersion.

The static liquid height was maintained at approximately 2.0 m for majority of the experiments. For experiments conducted in the 0.051 m ID column with the 40 μm SMP distributor, static heights as low as 0.6 m were used in order to contain the foam within the column.

Several runs were made with the same batch of wax. A new batch of wax was used once the old wax began to turn yellow. APPENDIX A outlines the guidelines used for wax changes and the procedure used to clean the apparatus between runs or between wax changes. The numbering scheme employed to distinguish the different runs (see APPENDIX A) reflects the wax batch number and the run number with a given batch of wax. A summary of the different runs and operating conditions is also included in APPENDIX A.

B.2. Reproducibility and Effect of Operating Procedure

The reproducibility of average gas hold-up measurements with the FT-300 - nitrogen system is significantly affected by the operating procedure employed, and to some extent by the age of the wax or the time on stream for a given batch of wax. Experiments were conducted in the 0.051 m ID and 0.229 m ID glass columns to investigate the magnitude of these effects. The 1.85 mm and 4 mm orifice plate, and a 40 μm sintered metal plate (SMP) distributors were used in the 0.051 m ID column, whereas the 19 X 1.85 mm

perforated plate distributor was used in the 0.229 m ID column. The discussion below is based on results from 4 runs with the SMP distributor, 4 runs with the 4 mm distributor, and 12 runs with the 1.85 mm distributor conducted in the 0.051 m ID column at 265°C. In addition, 4 runs were conducted using the 19 X 1.85 mm distributor at 265°C in the 0.229 m ID column. Limited number of runs were made at 160, 200, 230 and 280°C using the various distributors in the two columns. The gas velocity in majority of the runs was in the range 0.01 to 0.12 m/s.

The major highlights of these investigations are:

- For temperatures in the range 230-280°C, there is a range of gas velocities over which two values of gas hold-up are possible with FT-300 wax for all columns and distributor types investigated. In a system with molten paraffin wax as the liquid medium this type of behavior has been observed for the first time. The higher gas hold-ups are accompanied by the presence of foam, therefore, this mode of operation is referred to as the "foamy" regime. In the absence of foam, "slug flow" prevails in the 0.051 m ID column, whereas flow in the 0.229 m ID column is in the "churn-turbulent" regime. At low gas velocities (u_g < 0.02 m/s), when foam is not present, the "homogeneous bubbling" regime prevails.

- The start-up procedure determines which flow regime will be attained, with increasing order of gas velocities favoring the "foamy" regime. A transition from the "foamy" to the "slug flow" or "churn-turbulent" regime occurs when u_g exceeds a certain critical value, and the transition to the "foamy" regime occurs when u_g drops below a certain critical value. Since the two critical velocities are different, a

50

hysteresis loop is created.

- When multiple runs, under similar conditions, are conducted with a given batch of wax, hold-up in the "foamy" regime increases with age of the wax, which might be caused by the breakdown of FT-300 wax when subjected to high temperatures for a significant length of time. Thus, foaming occurs over an extended range of velocities for older wax compared to fresh wax and there is a corresponding change in the velocity at which the transition from the "foamy" regime to the "slug-flow" or "churn-turbulent" regime occurs.

- Long term stability studies reveal large variations in hold-up with time in the "foamy" regime, and relatively low variations in the absence of foam. This causes problems with reproducibility of hold-up measurements in the presence of foam.

- Reactor waxes do not show hysteresis behavior and there is no significant effect of operating procedure.

B.2a. Effect of Start-up Procedure

Figure V-10 illustrates a typical example of hysteresis behavior with FT-300 wax at 265°C in the 0.051 m ID column using the 1.85 mm orifice plate distributor. When increasing order of gas velocities were employed (open symbols), the gas hold-up increased rapidly in the velocity range 0.01-0.03 m/s largely due to the presence of a foam layer at the top of the gas-liquid dispersion. The foam breakup, accompanied by a substantial decrease in the gas hold-up, occurred when the velocity was increased from 0.03 m/s to 0.04 m/s. This breakup may be attributed to the presence of rising slugs. Upon further increasing the gas velocity, foam was not

51
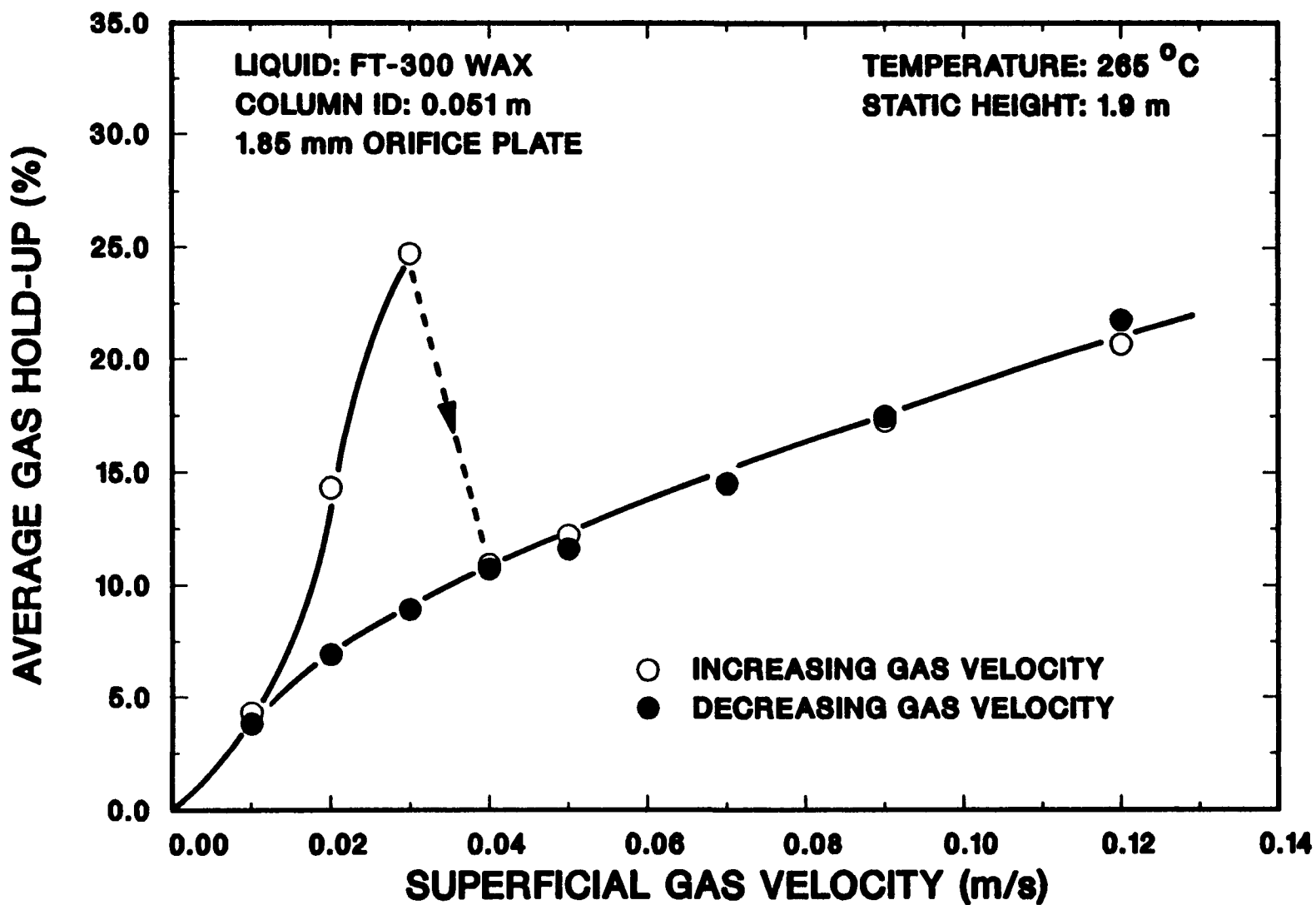
Figure V-10. Effect of start-up procedure and superficial gas velocity on gas hold-up (open symbols - Run 4-1 - indicate a start-up velocity of 0.01 m/s; solid symbols - Run 4-2 - indicate a start-up velocity of 0.12 m/s)

observed and the gas hold-up increased gradually. In a run conducted using decreasing order of velocities (solid symbols), nearly the same hold-ups (as in the run with increasing order of velocities) were obtained for velocities in the range 0.04-0.12 m/s. However, during this run foaming did not take place even at low gas velocities (0.01-0.03 m/s). In a system with molten paraffin wax as the liquid medium this type of behavior has been observed for the first time.

The mode of operation where foam is present will be referred to as the "foamy" regime. In this regime a stable layer of foam exists on the top of the liquid level, giving rise to higher hold-ups. Visual observations of the flow field show the presence of slugs or slug type bubbles at velocities greater than about 0.03 m/s. Under these conditions, if no foam is present, the mode of operation will be referred to as the "slug flow" regime. At lower gas velocities (u_g < 0.02 m/s), when foam is not present, visual observations indicate an almost uniform bubble size distribution, indicating that the flow might be in the transition or the "homogeneous bubbling" regime.

In general, all runs conducted in the temperature range 230-280°C exhibited hysteresis with respect to the hold-up values. However, the variation of gas hold-up with velocity, for runs conducted using decreasing order of velocities, was not always the same as that shown in Figure V-10. There were instances when foam also appeared in these runs and a transition from the "slug flow" to the "foamy" regime occurred. Nevertheless, the velocity at which this transition occurred was always lower than the velocity at which the transition from the "foamy" to the "slug flow" regime occurred when increasing order of velocities were employed. Figure V-11

53
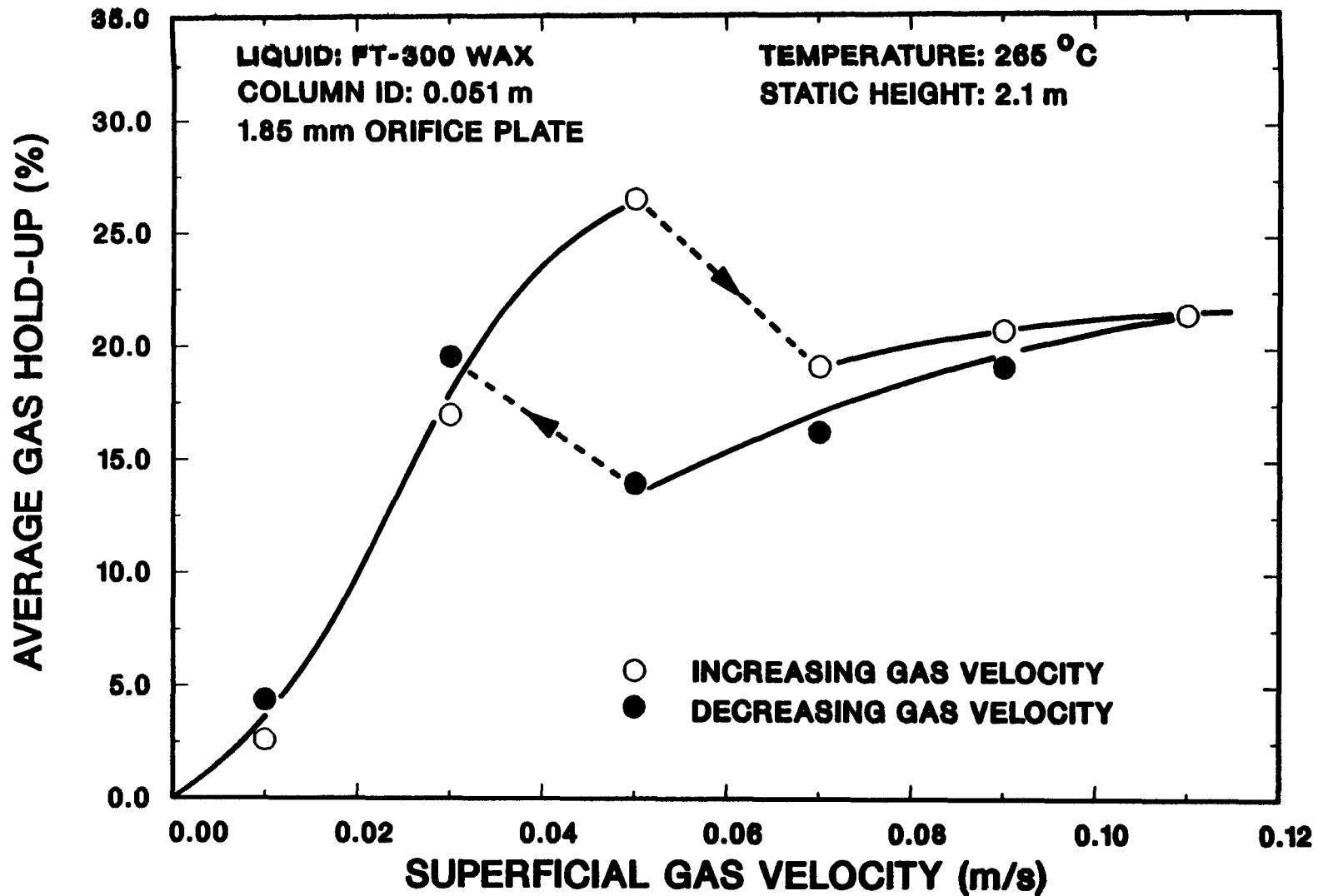
Figure V-11. Effect of operating procedure and superficial gas velocity on gas hold-up (Run 3-2)

shows an example of a run in which foam reappeared when gas velocity was changed from 0.05 m/s to 0.03 m/s, when decreasing order of velocities were used. Measurements made using the 4 mm orifice plate distributor in the 0.051 m ID column, under similar conditions, showed behavior which is qualitatively similar to that for the 1.85 mm orifice plate distributor in the temperature range 230-280°C.

Figure V-12 shows the effect of operating procedure on average gas hold-up for runs conducted using the 40 μm sintered metal plate (SMP) distributor at 265°C. When the run was conducted using increasing order of velocities (open symbols), the average gas hold-up increased rapidly in the velocity range 0.01-0.02 m/s as foam filled the entire column. The gas hold-up remained fairly constant in the velocity range 0.02-0.09 m/s; however, upon further increasing the gas velocity to 0.12 m/s the hold-up decreased significantly. This transition from the "foamy" regime to the "slug flow" regime is not complete and it is possible that a lower hold-up would be obtained at 0.12 m/s by extending the duration of run at this velocity. For the run conducted using decreasing order of velocities (solid symbols), with a start-up velocity of 0.12 m/s, foam did not appear until the gas velocity was decreased to 0.04 m/s, when a sudden increase in hold-up was observed. The hold-up values in the velocity range 0.04 m/s to 0.01 m/s are very similar to those obtained using increasing order of velocities. These results are qualitatively similar to those observed with the 1.85 mm distributor.

Figure V-13 shows results from a run conducted in the 0.229 m ID column with FT-300 wax at 265°C using a 19 X 1.85 mm perforated plate distributor. In this run increasing order of velocities were followed by
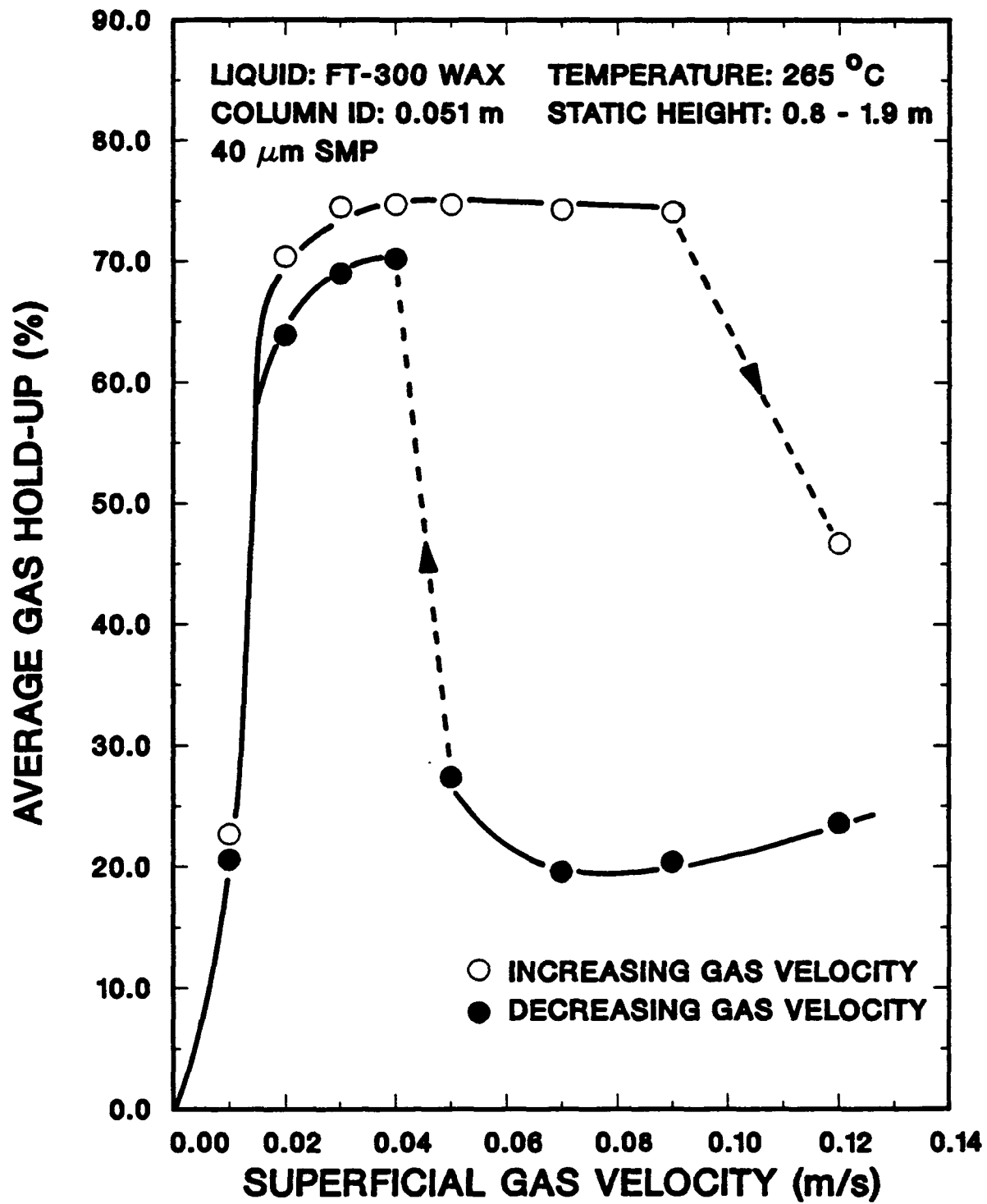
Figure V-12. Effect of start-up procedure and superficial gas velocity on gas hold-up (open symbols - Run 5-1 - indicate a start-up velocity of 0.01 m/s; solid symbols - Run 5-2 - indicate a start-up velocity of 0.12 m/s)
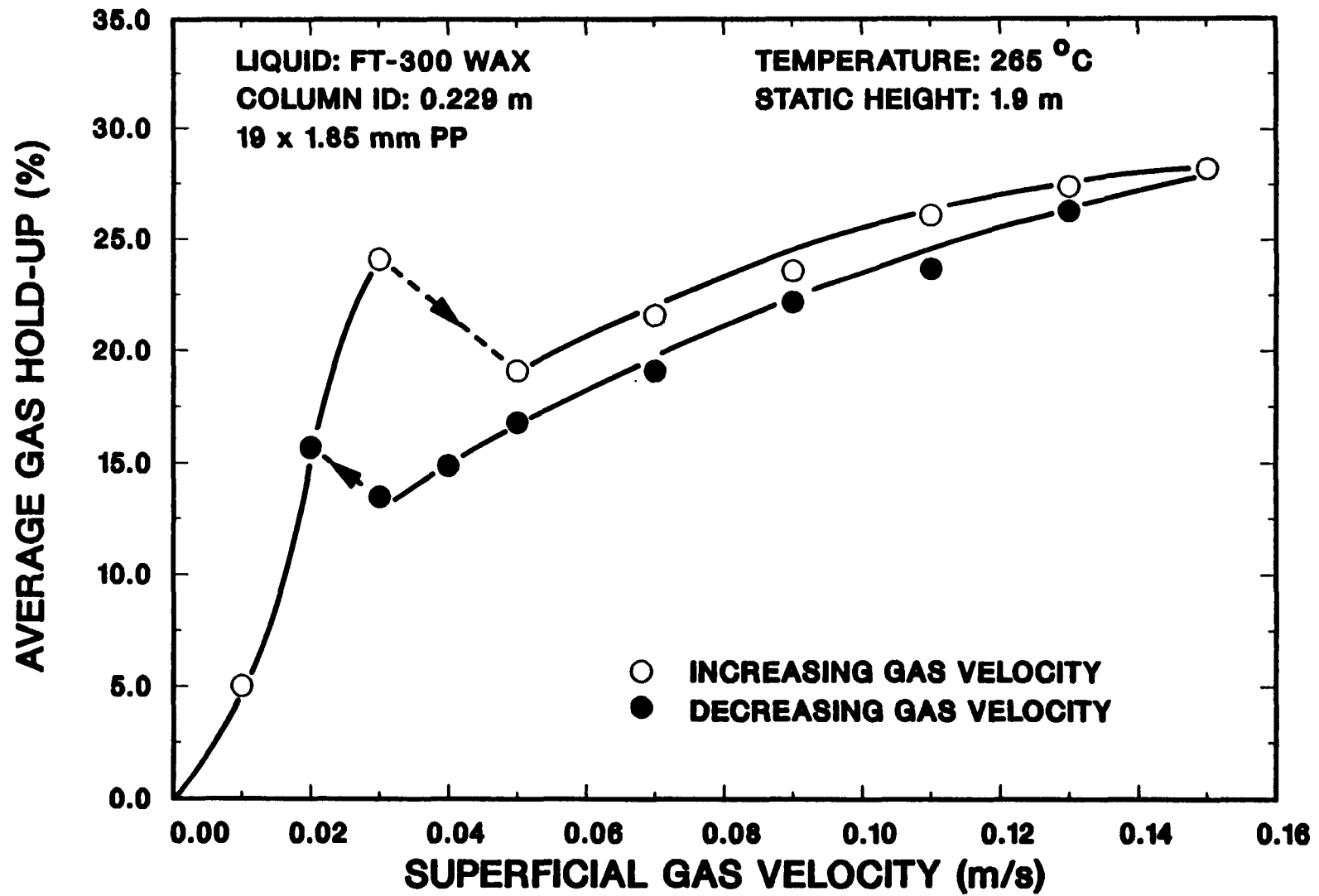
Figure V-13. Effect of operating procedure and superficial gas velocity on gas hold-up (Run 1-3)

decreasing order of velocities in the same run. These results once again illustrate the existence of two values of gas hold-up in the velocity range 0.02-0.05 m/s, with higher hold-up produced using increasing order of velocities (open symbols). The hold-up values in the absence of foam are somewhat higher for increasing order of velocities compared to decreasing order of velocities in the velocity range 0.05-0.13 m/s. These differences can be explained in terms of better mixing of the various surface active impurities into the dispersion with time elapsed, therefore, hold-up values later on in the run (when mixing is better) are lower than earlier in the run. Visual observations of the dispersion, in the absence of foam, showed intense mixing and the flow appears to be in the "churn-turbulent" flow regime. This is unlike the 0.051 m ID column, where "slug flow" exists in the absence of foam. In general, hysteresis effects were not as pronounced and reproducibility was much better in the 0.229 m ID column as compared to the 0.051 m ID column.

Studies were also conducted with reactor waxes in order to investigate the effect of operating procedure on the average gas hold-up. Results from these studies (see Section V-B.7.) show that reproducibility of hold-up values is significantly better with reactor waxes than with FT-300. Also, the operating procedure does not appear to have an effect on the average gas hold-up values and the hysteresis type of behavior was not observed.

The only known case of foam breakup in literature with a wax as the liquid medium was reported by Farley and Ray (1964a). Their studies, using the Krupp wax as the liquid medium in a 0.235 m ID reactor, showed that a transition from the "foamy" to the "churn-turbulent" regime took place within an hour of increasing the superficial gas velocity from 0.03 m/s to

0.06 m/s.

A theoretical basis for the existence of two values of the gas hold-up for a given set of operating conditions was established earlier (e.g. Wallis, p.92, 1969; Riquarts, 1979), however, experimental evidence demonstrating this type of behavior is rather scarce. In studies by Anderson and Quinn (1970) and Maruyama et al. (1981) with the air/tap water system the hysteresis type of behavior was observed. The "foamy" regime, in both studies, was obtained in experiments conducted using increasing order of velocities. A possible explanation for the breakup of foam and for the effect of start-up procedure on foaming was given by Anderson and Quinn and could be extended to explain the similar behavior of FT-300 wax. They postulated that at low gas velocities surface-active impurities, which act as coalescence promoters, diffuse gradually and accumulate at the top of the dispersion. However, once their concentration exceeds a critical level rapid coalescence takes place resulting in the formation of slugs. Once the slugs are formed at the top of the column, the impurities are dispersed back into the bulk of the liquid through intensive mixing and turbulence which accompanies slug formation. This in turn causes the slugs (large bubbles) to form at lower heights in the dispersion, thus preventing foaming. Similarly, when a run is started at a high velocity (decreasing order of velocities), the impurities are thoroughly dispersed throughout the column hampering the formation of foam even when velocities are sufficiently low. However, in some instances (e.g. the run using decreasing order of velocities in Figure V-11) the concentration gradients become steeper as the impurities begin to accumulate at the top, leading to the development of foam after some time. This theory could also be used to

offer a possible explanation for the higher hold-ups obtained in the "churn-turbulent" regime when increasing order of velocities were used compared to those obtained for decreasing order of velocities in the 0.229 m ID column (Figure V-13). Once the foam broke in this run, the impurities began to mix into the bulk of the dispersion, however, this is not an instantaneous process, and it is possible that a steady state was not reached when the increasing order of velocities were being used. Therefore hold-up values were slightly higher with increasing order of velocities (earlier in the run - shorter mixing time) compared to values with decreasing order of velocities (later in the run - longer mixing time). The better reproducibility in the 0.229 m ID column compared to the 0.051 m ID column could be attributed to the better mixing of surface active agents in the larger column.

B.2b. Effect of Wax Aging

Figures V-14 and V-15 illustrate the effect of the aging of wax on the average gas hold-up in the 0.051 m ID and the 0.229 m ID columns, respectively. In both cases, the effect of aging primarily affects hold-up values in the "foamy" regime. For the 0.051 m ID column results from three runs conducted using the same batch of wax are presented in Figure V-14. For relatively fresh wax the hold-up values (indicated by circles in Figure V-14) show no foaming for the range of superficial gas velocities employed (0.02-0.15 m/s), however, for a later run with the same batch of wax (indicated by triangles) foam appeared in the velocity range 0.02-0.03 m/s and broke as velocity was increased to 0.04 m/s. This particular run was stopped once the foam broke. A run conducted after further aging of the wax (indicated by squares) resulted in foam being produced over a relatively

60
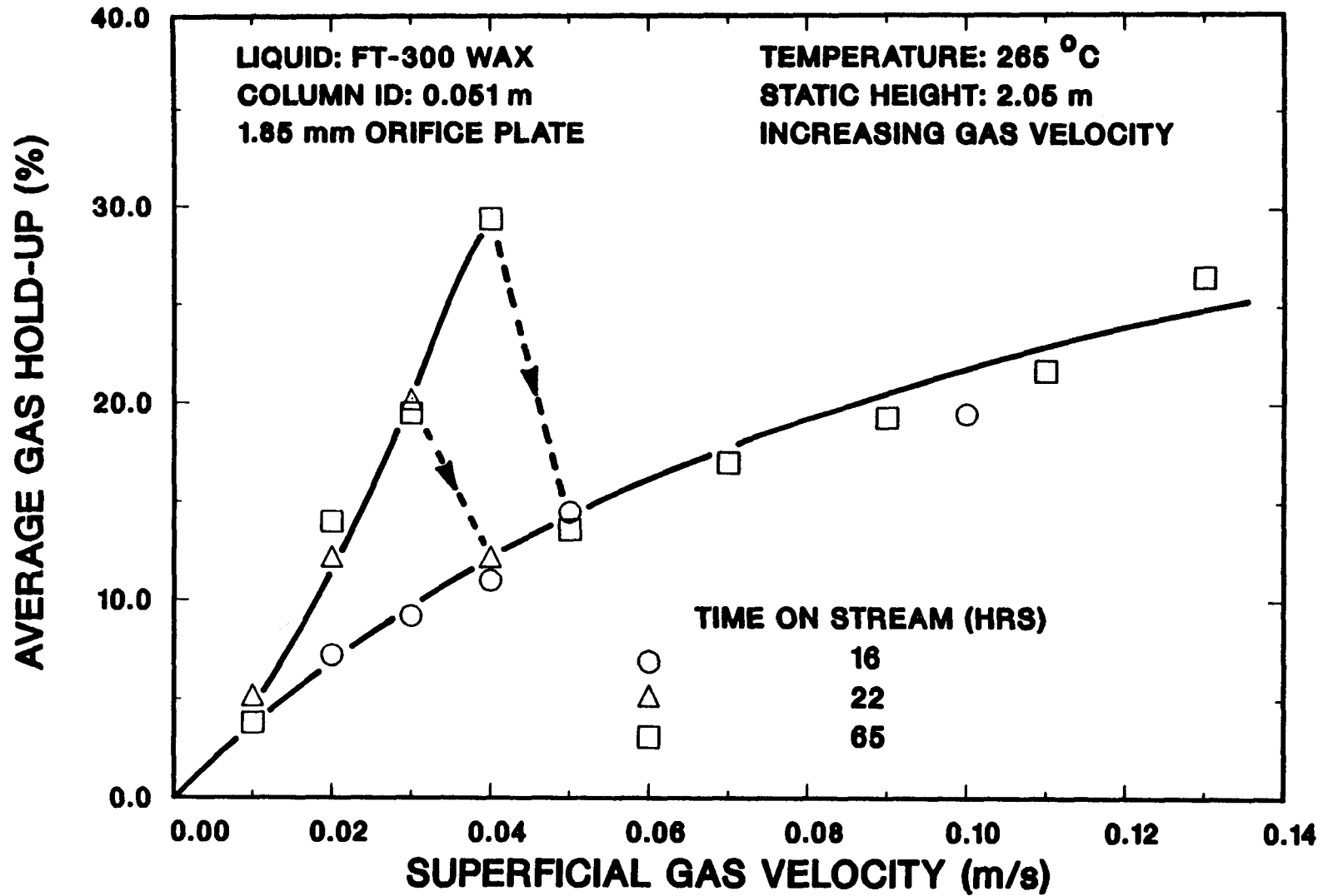
Figure V-14. Effect of wax aging on gas hold-up (O- Run 2-3; △-Run 2-4; □-Run 2-7)
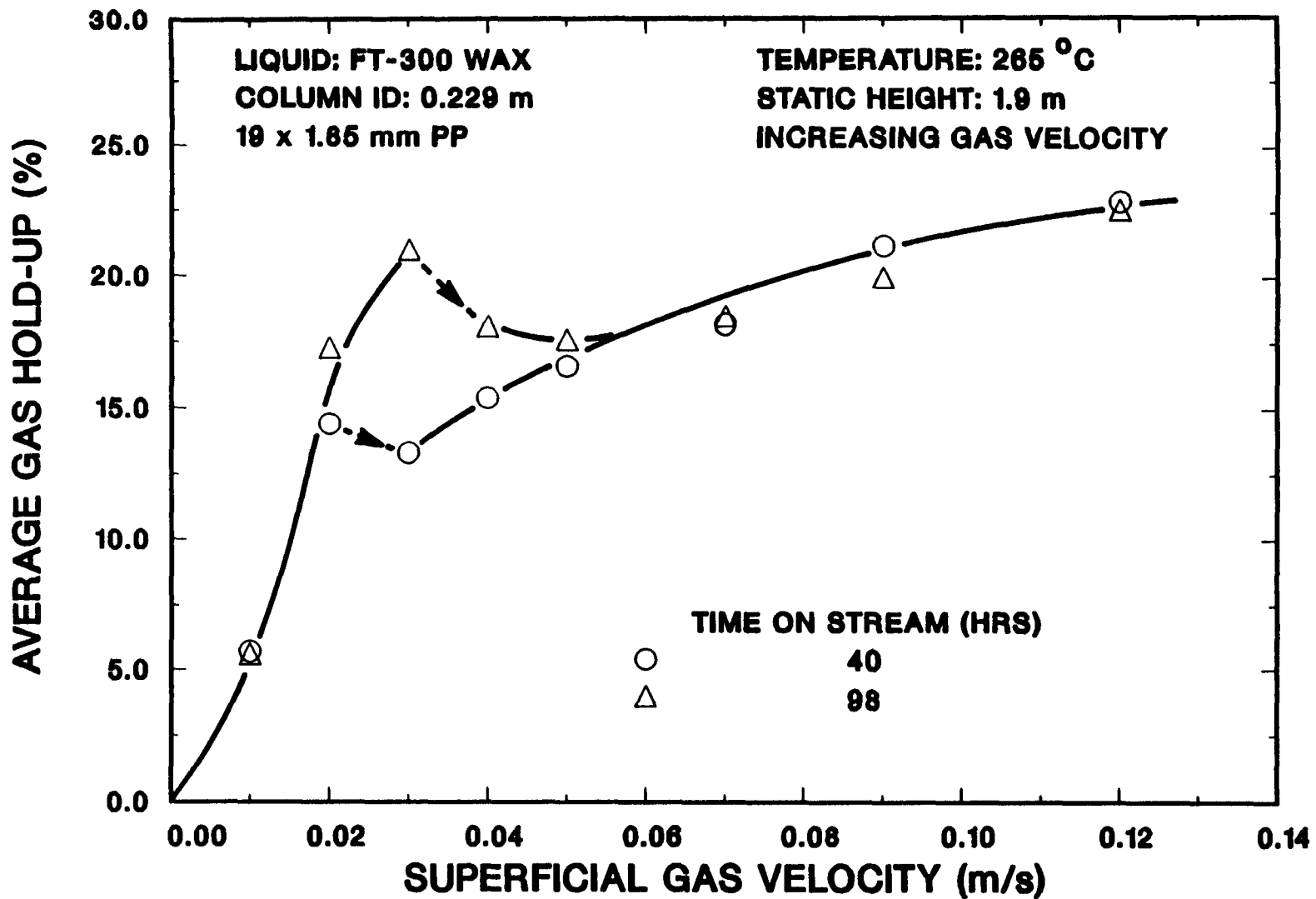
Figure V-15. Effect of wax aging on gas hold-up (O- Run 2-3; △-Run 2-8)

larger velocity range (0.02-0.04 m/s) and a corresponding delay in the breakage of foam (at 0.05 m/s compared to 0.04 m/s) was observed. The hold-up values in the absence of foam (u_g greater than 0.04 m/s) are essentially similar for the different runs. Results from two runs in the 0.229 m ID column (Figure V-15) are qualitatively similar to those from the 0.051 m ID column. The older wax once again showed foaming over a prolonged range of gas velocities, thus delaying the breakage of foam until 0.03-0.04 m/s compared to 0.02 m/s for the fresher wax. Hold-up values in the absence of foam are once again similar for the two runs. The effect of wax aging was similar for all runs irrespective of column diameter and distributor type.

B.2c. History Effects

Results from the run made in the 0.229 m ID column, presented in Figure V-13, show history effects. The consistently lower hold-up values, in the absence of foam, for decreasing order of velocities were a direct consequence of the history of the run as discussed previously. Figure V-16 compares results from two runs conducted with different operating procedures. The two runs were made one after the other with the same batch of wax, thus minimizing the effect of wax aging. When a start-up velocity of 0.01 m/s was used, hold-up values were as expected, showing a "foamy" regime followed by a transition to the "slug flow" regime (open circles). However, when an odd order of velocities was used (solid circles), with a start-up velocity of 0.09 m/s, hold-up increases as velocity is increased to 0.17 m/s (no foam was present). The gas hold-up values are consistently higher than in the previous run. Upon decreasing the velocity the same curve is followed up to 0.09 m/s, but at lower gas velocities the hold-up starts increasing and passes through a maximum at about 0.06 m/s (ϵ_g =

63
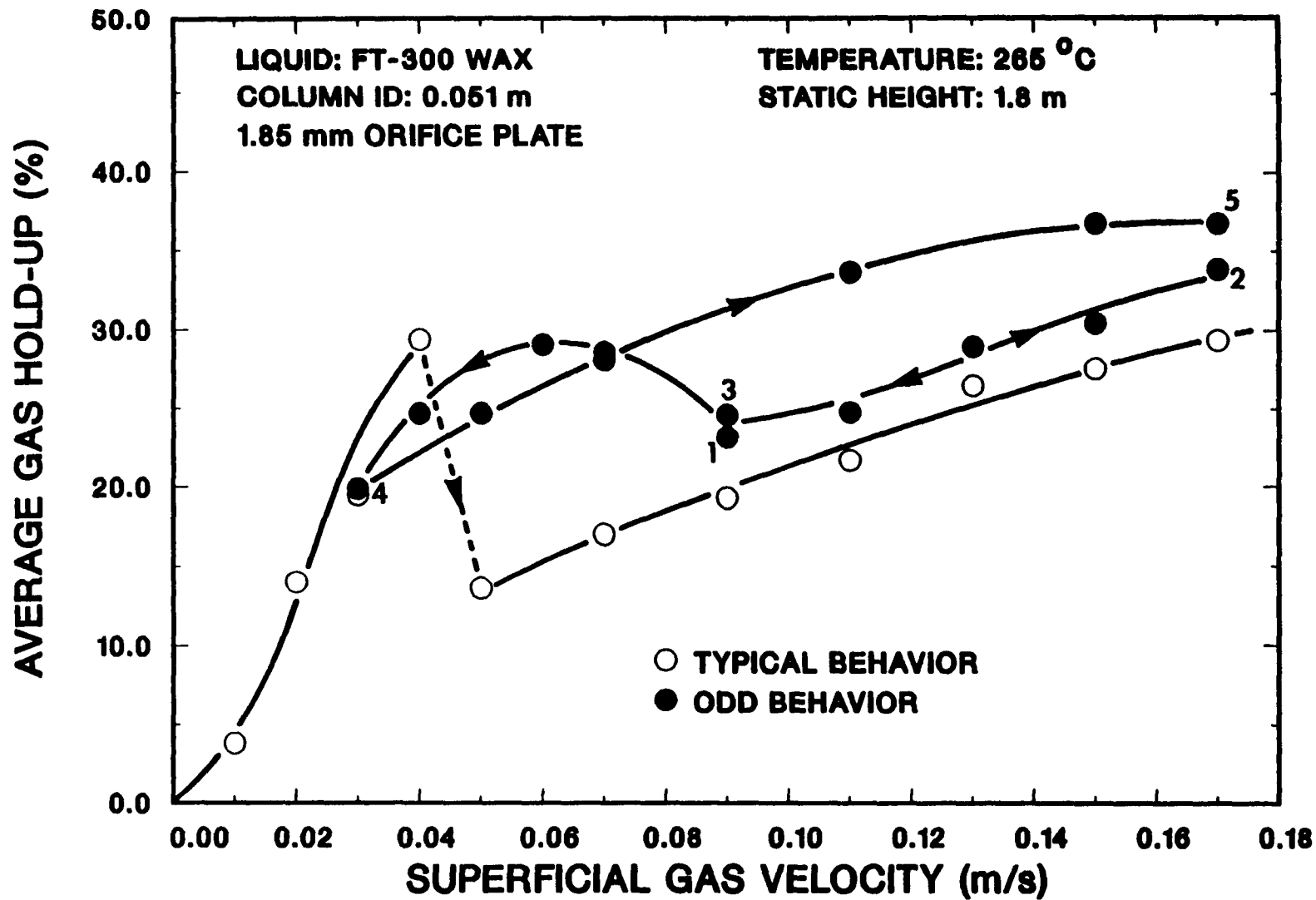
Figure V-16. Effect of run history and superficial gas velocity on gas hold-up (open symbols - Run 2-7; solid symbols - Run 2-8 - numbers on the curve indicate order of velocities employed)

29%), and then decreases, coinciding with the value from the purely increasing velocity curve at 0.03 m/s. When velocity was further increased from 0.03 to 0.17 m/s, the transition from the "foamy" to the "slug flow" regime did not take place. It appears that the history of the run, with respect to gas velocities, has an effect on hold-up values. This is not typical of the results obtained from the various runs and the reasons for this kind of behavior are not clear. This experiment illustrates the difficulties in obtaining reproducible results with a system that has a tendency to produce foam.

B.2d. Long Term Stability Studies

The long term stability runs were conducted with a run time of 4 hours per velocity using the 1.85 mm orifice plate distributor at 265°C in the 0.051 m ID column. The wax was drained to the storage tank after each velocity, therefore, it is expected that these results are independent of the operating procedure. Hold-up was measured every 15 minutes during the first hour and every 30 minutes during the subsequent 3 hours. Results from this study are presented in Figure V-17 (indicated by open circles). The vertical bars at each velocity indicate the range in which the hold-up values varied at that particular velocity. The open circles indicate an average of the eight hold-up values for each velocity. These results illustrate the large variability in hold-up values in the "foamy" regime, indicating problems with reproducibility of results in this regime. The variability in the "slug flow" regime is much smaller. These results also lend further support to the theory postulated by Anderson and Quinn. At low velocities, which are not conducive to mixing (0.01-0.04 m/s), the build-up of steep gradients of the surface active impurities occurs over a period of
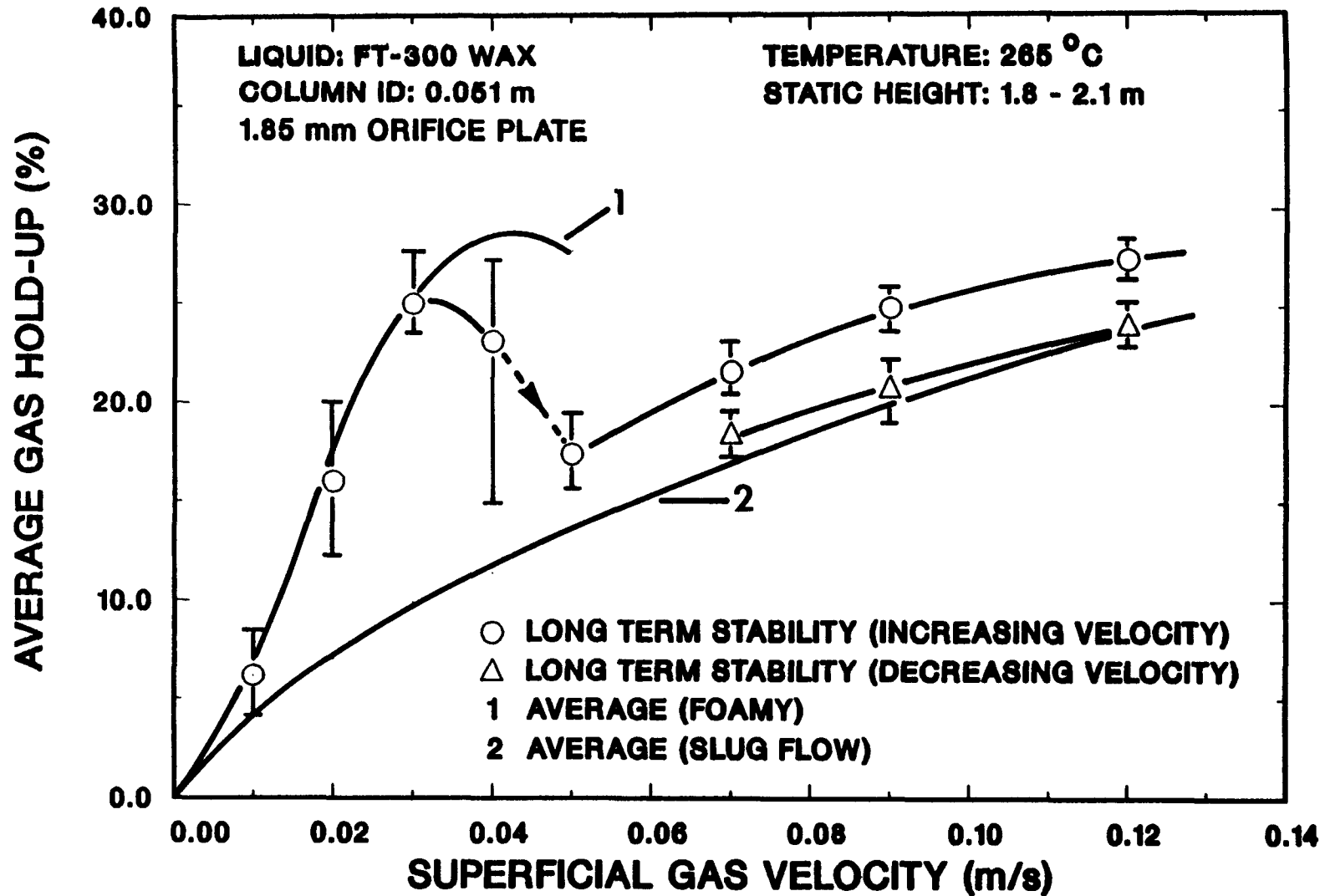
Figure V-17. Results from long term stability studies with FT-300 wax and comparison with average values from other runs (symbols - arithmetic mean of hold-ups at a given velocity; vertical bars - range in which hold-ups varied at that velocity; O - Run 6-1 - indicate a start-up velocity of 0.01 m/s; △ - Run 7-3 - indicate a start-up velocity of 0.12 m/s; curves 1 & 2 - arithmetic averages from 12 runs)

time and therefore, foaming is observed at these velocities. However, for velocities greater than 0.04 m/s, mixing is much improved and the impurities are uniformly distributed in the bulk of the liquid, preventing foaming and resulting in lower hold-up values. Therefore, even though these results are independent of start-up velocity, the behavior is similar to that observed with increasing order of velocities.

In the run discussed above, the age of wax increased with velocity, since the first set of data were obtained at 0.01 m/s (fresh wax), and velocity was progressively increased up to 0.12 m/s (oldest wax). Additional runs were therefore conducted to isolate the effect due to the aging of wax. Results from these runs are indicated by triangles in Figure V-17. The duration per velocity and the frequency of hold-up measurements were the same as in the previous run. However, for this case wax was relatively fresh at 0.12 m/s and it aged as gas velocity was progressively lowered. As expected, hold-up values for this run were substantially lower in the range of velocities investigated (0.07-0.12 m/s), lending further support to the effect of wax aging.

Figure V-17 also shows average values for gas hold-up measurements from several runs conducted at 265°C in the 0.051 m ID column using increasing/decreasing order of velocities. These values were obtained using hold-up values from a total of eight runs conducted using increasing order of velocities and a total of four runs conducted using decreasing order of velocities. The average values (curves 1 and 2) for both the "foamy" and "slug flow" regimes are presented. These results show that the "foamy" regime could be maintained only up to 0.05 m/s. Results from long-term stability runs, after accounting for wax aging, are in good agreement

with the average value curves.

The above investigations indicate that the reproducibility of hold-up values in a system which has a capacity to foam, is dependent on a complex interaction between a number of factors. Some of these factors, such as the operating procedure, can be controlled independently. Whereas, effects due to the aging of wax, and the amount of foam produced, are not as predictable. Our study shows that it is possible to eliminate foaming by using a relatively high start-up velocity.

B.3. Effect of Temperature

The effect of temperature on gas hold-up was investigated for temperatures between 160 and 280°C. Experiments were done in the 0.051 m ID and the 0.229 m ID glass columns using FT-300 wax. The 40 μm SMP and 1.85 mm orifice plate distributors were used in the 0.051 m ID column, whereas the 5 X 1 mm, 19 X 1 mm and the 19 X 1.85 mm perforated plate distributors were employed in the 0.229 m ID column. Results from these experiments can be summarized as follows:

- In the "foamy" regime, an increase in temperature is accompanied with an increase in foam, and thus higher hold-up values.

- In the absence of foam, hold-ups showed a marginal decrease with a decrease in temperature.

- It was possible to avoid foaming by operating at sufficiently low temperatures (e.g. 160°C with the 1.85 mm orifice plate distributor in the 0.051 m ID column or at 170°C with the 5 X 1 mm perforated plate distributor in the 0.229 m ID column).

Results from runs with FT-300 wax in the 0.051 m ID column using the 1.85 mm orifice plate distributor at four different operating temperatures

(160, 200, 265 and 280°C) are shown in Figure V-18. All runs were conducted using increasing order of gas velocities. These results show that the effect of temperature is significant in the presence of foam. An increase in temperature results in a corresponding increase in hold-up values, and the foam persists over an extended range of velocities at higher temperatures. The highest gas hold-ups were obtained at 280°C, whereas the lowest hold-ups were obtained at 160°C. The runs conducted at 200°C and 265°C show a substantial increase in gas hold-up as foam is produced ($u_g < 0.03$ m/s) followed by a decrease in hold-up as the transition from the "foamy" regime to the "slug flow" regime takes place. The run conducted at 280°C showed a similar increase in hold-up as foam was produced, however, the transition to the "slug flow" regime was not observed in the velocity range employed (0.01-0.09 m/s). No foam was produced during the run conducted at 160°C, therefore hold-up values were consistently lower for this run. For this run the flow regime changed from "homogeneous bubbling" to the "slug flow" regime directly. In the "slug flow" regime the effect of temperature is less pronounced, with marginally lower hold-ups obtained at lower temperatures.

Results illustrating the effect of temperature on hold-up when the 40 μm sintered metal plate distributor (SMP) was used in the 0.051 m ID column, are presented in Figure V-19. Six runs were made at 265°C, two runs at 280°C and only one run at 200°C. The data for runs conducted at 265°C were divided into two groups, based on the absence or presence of foam, and averaged (curves 1 and 2), whereas data from individual runs at 200 and 280°C are presented. With this distributor a substantial amount of

69
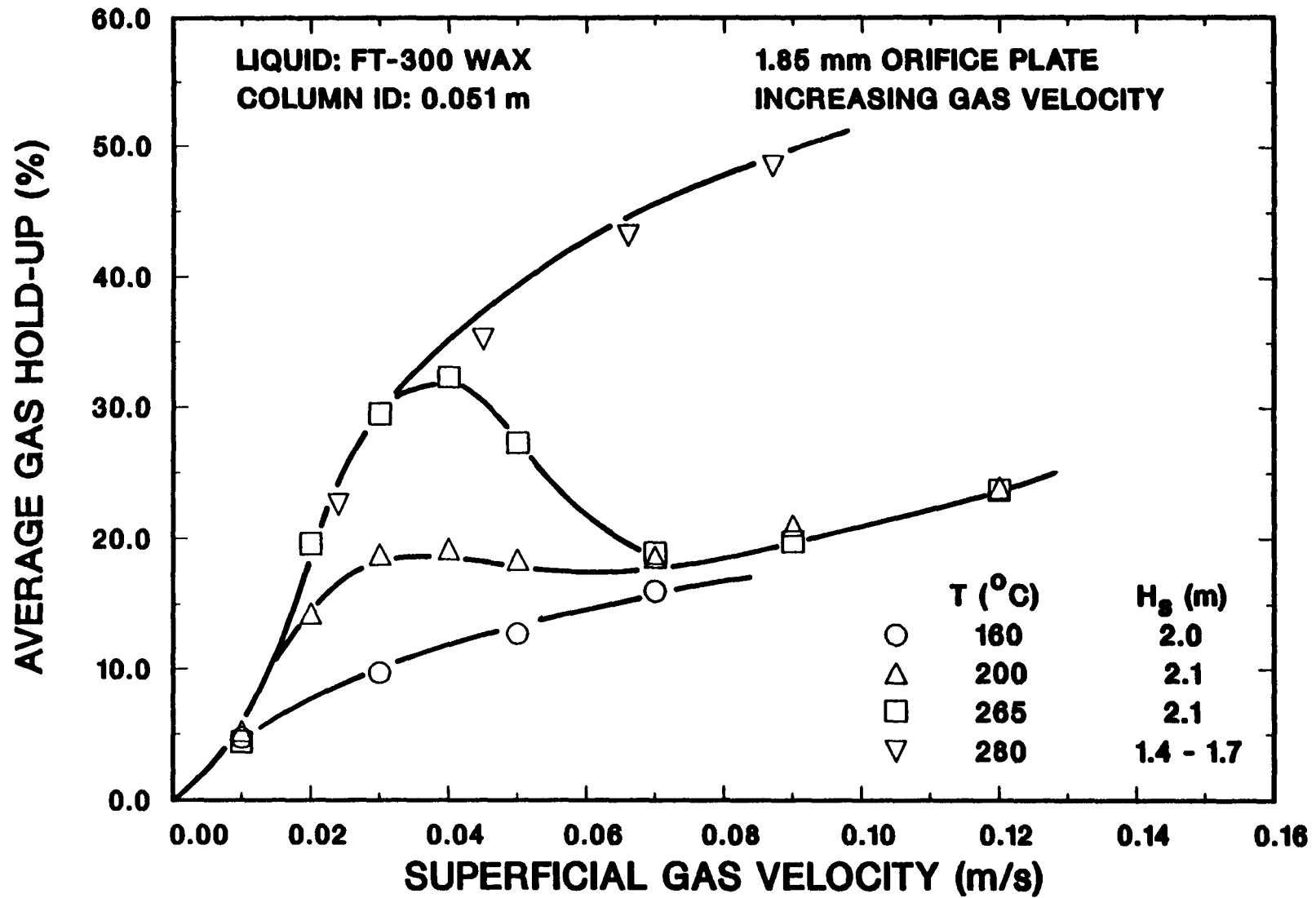
Figure V-18. Effect of operating temperature on gas hold-up (○ - Run 1-11; △ - Run 13-2; □ - Run 13-3; ▽ - Run 1-12)
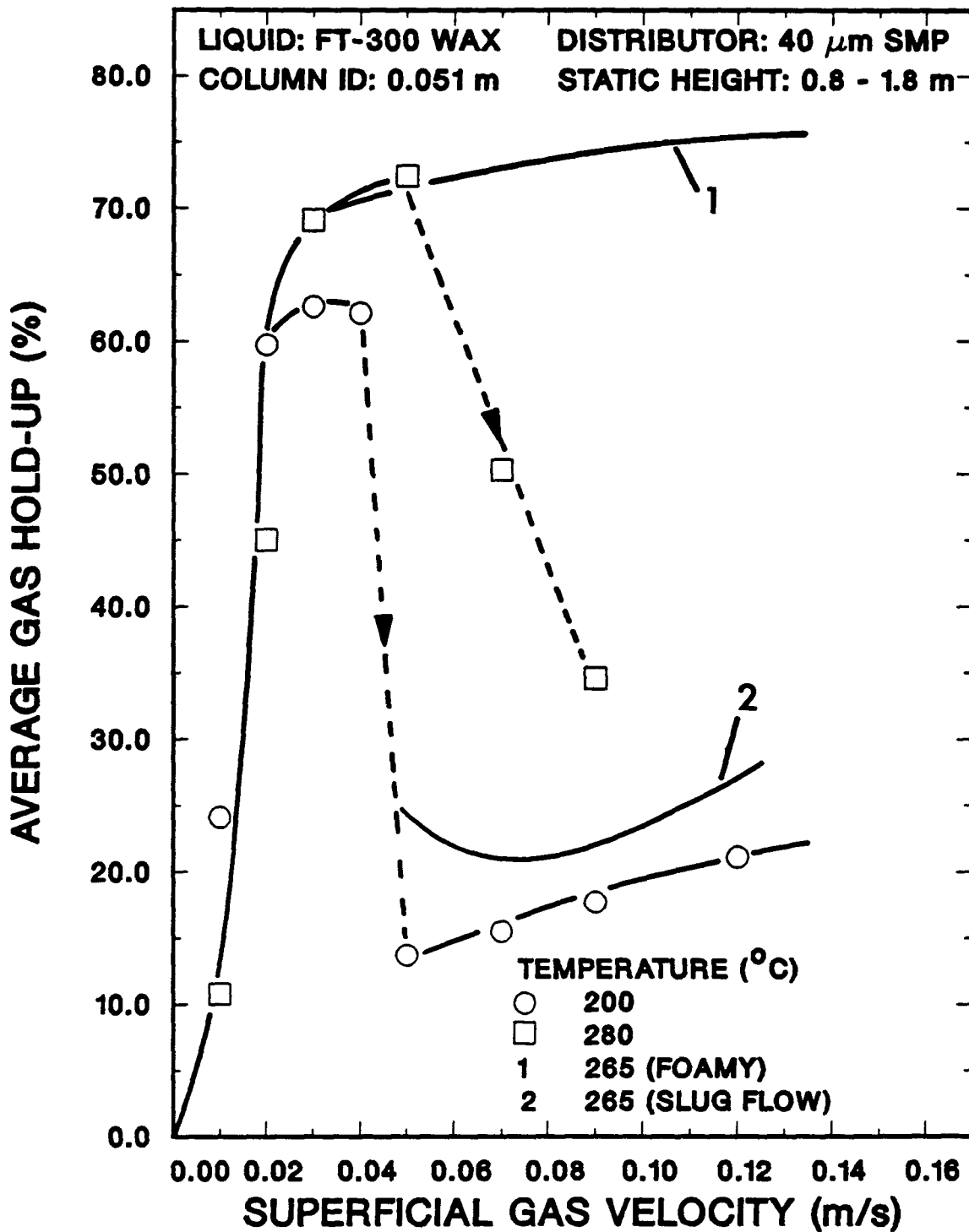
Figure V-19. Effect of operating temperature on gas hold-up (O - Run 5-3; □-Run 1b-4; curves 1 & 2 - arithmetic averages from 6 runs)

foam was produced even at 200°C. However, the transition from the "foamy" to the "slug flow" regime occurred earlier at lower temperatures compared to higher temperatures. In the "foamy" regime hold-up values at 200°C are between 5 and 10% (absolute) lower than those at 265 and 280°C. No real difference in hold-up is evident between values at 265°C and 280°C (foam occupied the entire column and hold-ups of about 70% were obtained for $U_g \geq$ 2 cm/s). Hold-up values in the "slug flow" regime show a marginal effect of temperature, with lower values obtained at 200°C compared to 265°C. The transition from the "foamy" regime to the "slug flow" regime was not complete for the run conducted at 280°C, however, it is believed that if the gas velocity was further increased, the hold-up values would eventually approach those for the runs at 265°C.

Figure V-20 shows results illustrating the effect of temperature for runs conducted in the 0.229 m ID column using the 19 X 1.85 mm perforated plate distributor. Data from a total of 7 runs at 265°C were divided into two groups (as above) and averaged. These average values (curves 1 and 2) and data from a run conducted at 200°C are presented in Figure V-20. At 265°C foam consistently broke by 0.03 m/s, while the "foamy" regime was not observed at 200°C. In the "churn-turbulent" regime, hold-up values in the velocity range 0.02-0.07 m/s were slightly higher at 265°C compared to values obtained at 200°C. This could be attributed to a high concentration of small bubbles that were still present at 265°C over this range of velocities. At gas velocities 0.07 m/s and higher, hold-up values at the two temperatures are similar, showing no effect of temperature once the "churn-turbulent" regime is well established.
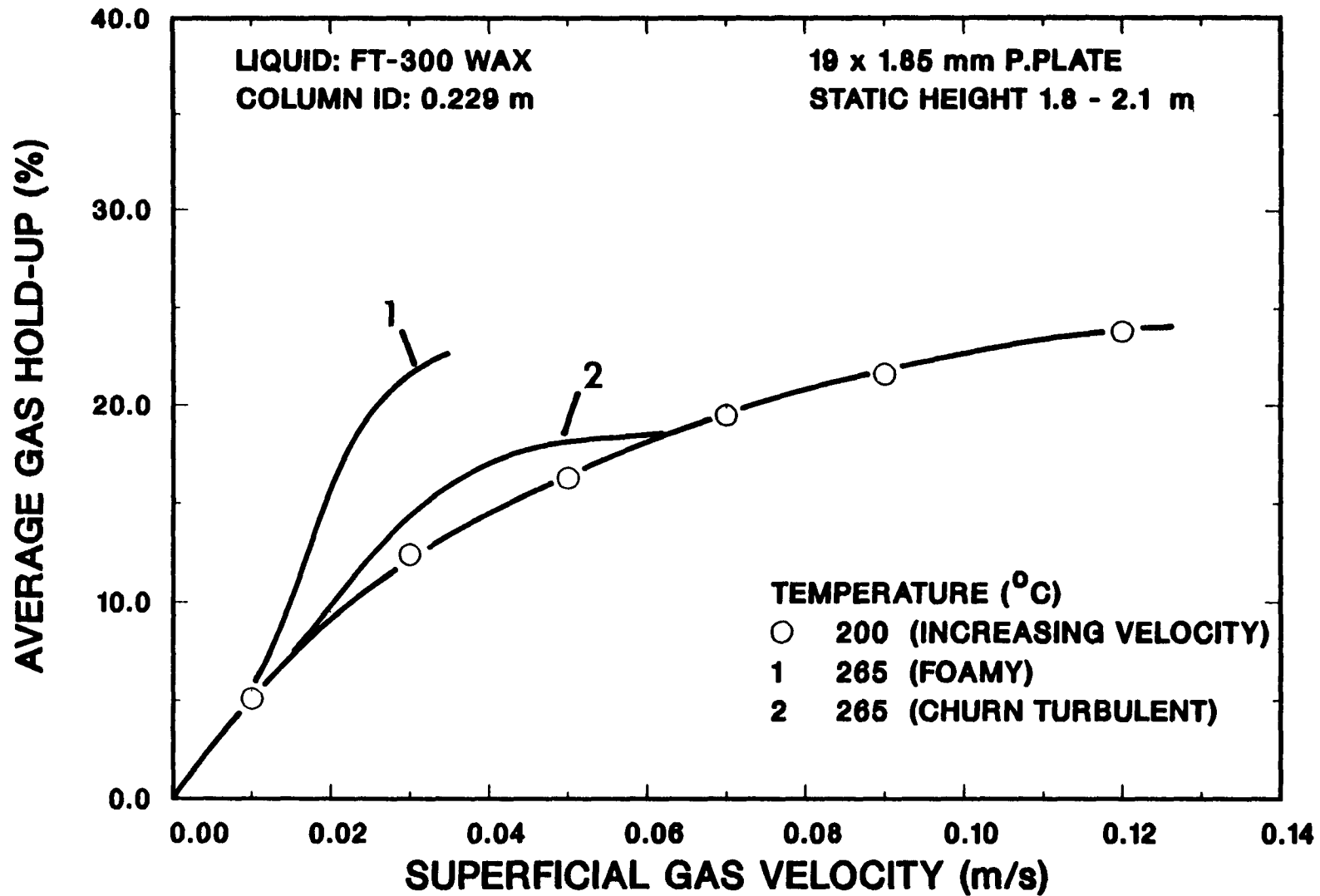
Figure V-20. Effect of operating temperature on gas hold-up (O - Run 1-1; curves 1 & 2 - arithmetic averages from 7 runs)

Experiments were also conducted in the 0.229 m ID column using the 19 X 1 mm perforated plate distributor at 200 and 265°C. The results were similar to those obtained with the 19 X 1.85 mm perforated plate distributor. No foam was produced in the run conducted at 200°C, and hold-up values for this run were slightly lower than the corresponding values obtained with the 19 X 1.85 mm distributor.

Results from experiments conducted in the 0.229 m ID column with the 5 X 1 mm perforated plate distributor are shown in Figure V-21. Runs were made at 170°C and at 265°C. Also shown in this figure are hold-up values obtained by Quicker and Deckwer (1981) at 170°C using a 0.9 mm nozzle in a 0.095 m ID column. The jet velocities with the 5 X 1 mm distributor in the present work are the same as those in the Quicker and Deckwer study.

The run conducted at 265°C showed a substantial increase in gas hold-up as the gas velocity was increased from 0.01 to 0.02 m/s. This was accompanied by the formation of a stable layer of foam at the top of the dispersion. The transition from the "foamy" regime to the "churn-turbulent" regime took place between gas velocities of 0.03 and 0.04 m/s. Thereafter hold-ups increased gradually with an increase in gas velocity. This behavior is typical for FT-300 wax at 265°C and follows trends shown with other distributors. The run conducted at 170°C did not produce any foam for the gas velocities employed (0.01-0.05 m/s). As a result, hold-ups were substantially lower than in the run at 265°C. These results are significantly different from those obtained by Quicker and Deckwer under similar conditions. Their hold-ups appear to be too high under these conditions.
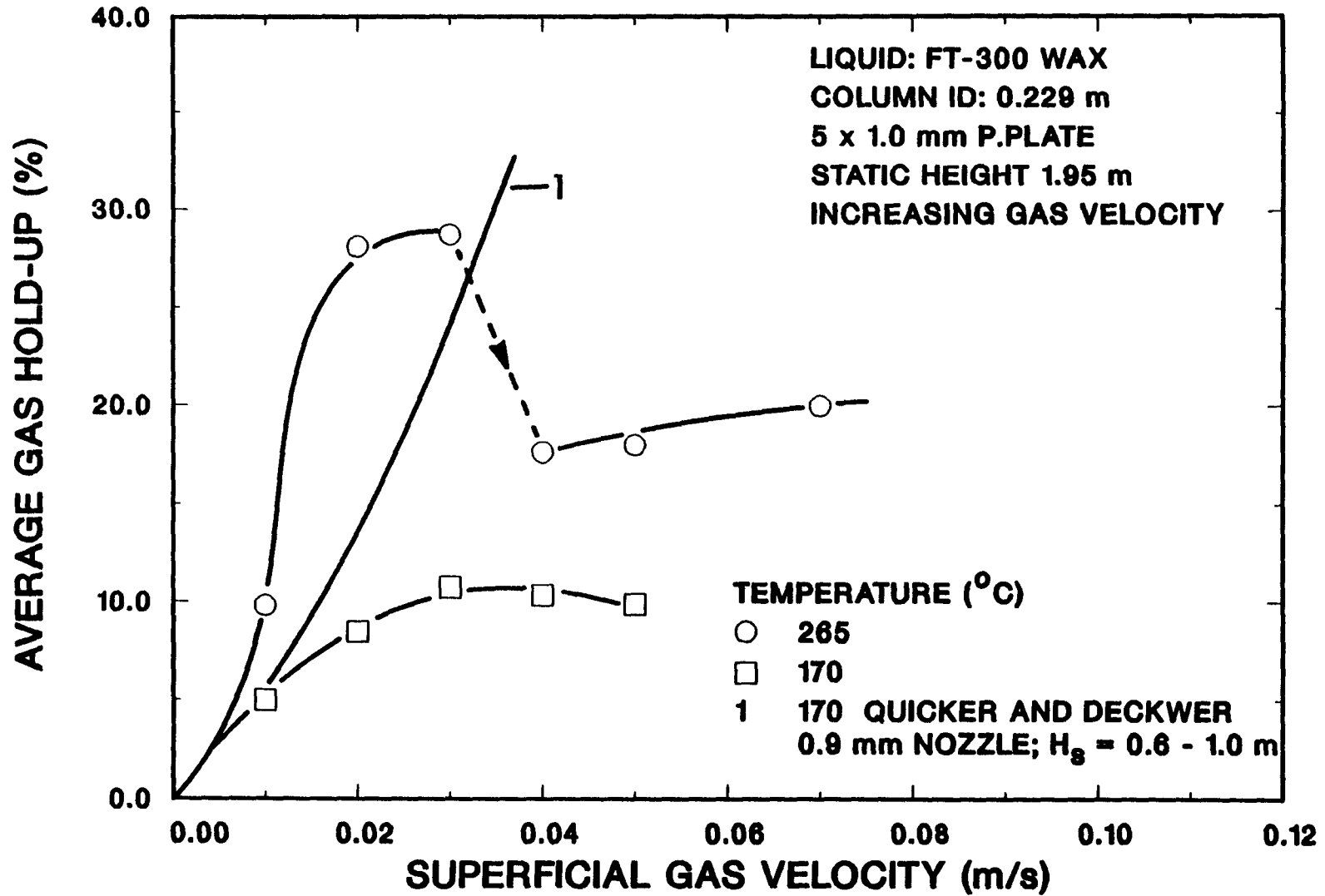
Figure V-21. Effect of operating temperature on gas hold-up and comparison with literature (◯ - Run 4-1; ☐ - Run 4-2; 1 - Quicker and Deckwer, 1981, 0.9 mm nozzle in a 0.095 m ID column)

The results presented in Figures V-18 to V-20 show that in general temperature affects the results in the "foamy" regime, however, once the transition to the "slug flow" regime (in the 0.051 m ID column) or the "churn-turbulent" regime (in the 0.229 m ID column) occurs, hold-up values do not vary much with temperature. These results also show that at sufficiently low temperatures foaming can be completely prevented. This behavior can be qualitatively explained in terms of the liquid viscosity (e.g. μ_L = 9.8 mPa.s at 160°C vs. 2.4 mPa.s at 265°C, for FT-300 wax). Bubble coalescence increases with liquid viscosity (i.e. as temperature decreases) and fine bubbles, which are precursors of foam, do not accumulate at the top of the dispersion at low temperatures.

Experiments conducted with reactor waxes (Sasol's Arge reactor wax and Mobil's reactor wax) resulted in hold-ups similar to those for FT-300 wax in the absence of foam. A marginal decrease in hold-up was observed as temperature was decreased from 265°C to 200°C, which is as expected since virtually no foam was produced in these runs (see Section V-B.7.).

Several researchers have investigated the effect of temperature using paraffin waxes as the liquid medium. The majority of these studies were conducted in the "foamy regime" and there are some discrepancies in results from these studies. Deckwer et al. (1980) found a significant decrease in hold-up as temperature was increased from 180°C to 270°C for experiments conducted in a 0.041 m ID column, while no effect of temperature was found for runs conducted in the 0.10 m ID column. Experiments conducted by Quicker and Deckwer (1981), using FT-300 wax, showed consistently higher hold-up values at 170°C compared to values at 130°C with both, a 0.9 mm nozzle and a 19 X 1.1 mm perforated plate distributor. Researchers at Mobil

(Kuo et al., 1985) used FT-200 wax as the liquid medium and found that hold-up values at 138°C were substantially lower than those at 260°C. Despite some inconsistency in results, the overall trend is that hold-up increases with an increase in temperature, in the "foamy" regime (note that all of the literature dealing with this system reports results for runs with velocities less than 0.04 m/s, i.e. in the "foamy" regime). Results from our study are in agreement with these findings.

Due to the lack of literature data, with molten wax as the liquid medium, on the effect of temperature on hold-up in the "slug flow" regime or the "churn-turbulent" regime, only a comparison with results from other systems is possible. Shah et al. (1982) have shown that the increase in viscosity, by increasing the CMC (carboxy methyl cellulose) concentration, did not have an effect on gas hold-up in the "slug flow" regime, a behavior similar to that for FT-300 wax as shown in the present study.

B.4. Effect of Column Diameter

Commercial size bubble columns are expected to operate in the heterogeneous ("churn-turbulent") flow regime, while majority of the studies, with a molten wax as the liquid medium, were carried out in small diameter columns (up to 0.12 m) and thus only the ideal bubbly (homogeneous) and "slug flow" regimes were observed. Results from studies conducted in the 0.051 m ID and 0.229 m ID glass columns are reported here showing the effect of column diameter. The comparison is based on runs conducted at 265°C using the 1 mm and 1.85 mm orifice plate distributors in the 0.051 m ID column, and the 19 X 1 mm and the 19 X 1.85 mm perforated plate distributors in the 0.229 m ID column. Data from a total of 13 runs in the 0.051 m ID column and from 6 runs in the 0.229 m ID column are available for

comparison. The gas velocity range employed in these experiments was 0.01-0.12 m/s.

The major highlights of these investigations are:

- With FT-300 wax, foam consistently broke at a higher velocity in the 0.051 m ID column compared to the 0.229 m ID column. However, no significant effect of column diameter was observed in the absence of foam.

- Distributors with smaller holes (1 mm orifice plate in the 0.051 m ID column and 19 X 1.0 mm perforated plate in the 0.229 m ID column) gave higher hold-up values in the smaller column, compared to the larger column, irrespective of the presence or absence of foam.

- Experiments conducted with Sasol's Arge reactor wax did not show a significant effect of column diameter on the gas hold-up in the range of velocities investigated (0.01-0.12 m/s).

Figure V-22 compares results obtained at 265°C in the two columns using the 1.85 mm orifice plate distributor in the 0.051 m ID column and the 19 X 1.85 mm distributor in the 0.229 m ID column. The jet velocities produced by the two distributors, for a given superficial gas velocity, are very similar (the jet velocity in the smaller column was approximately 94% of the jet velocity in the larger column). The experiments, conducted using increasing order of gas velocities, show similar trends in the two columns, however, hold-up values in the "foamy" regime are consistently higher in the smaller diameter column and the transition from the "foamy" to the "slug flow" regime occurs at a higher velocity in the 0.051 m ID column. Once the foam broke, hold-up values in the two columns are similar at all subsequent velocities. Results presented in this figure are typical of the
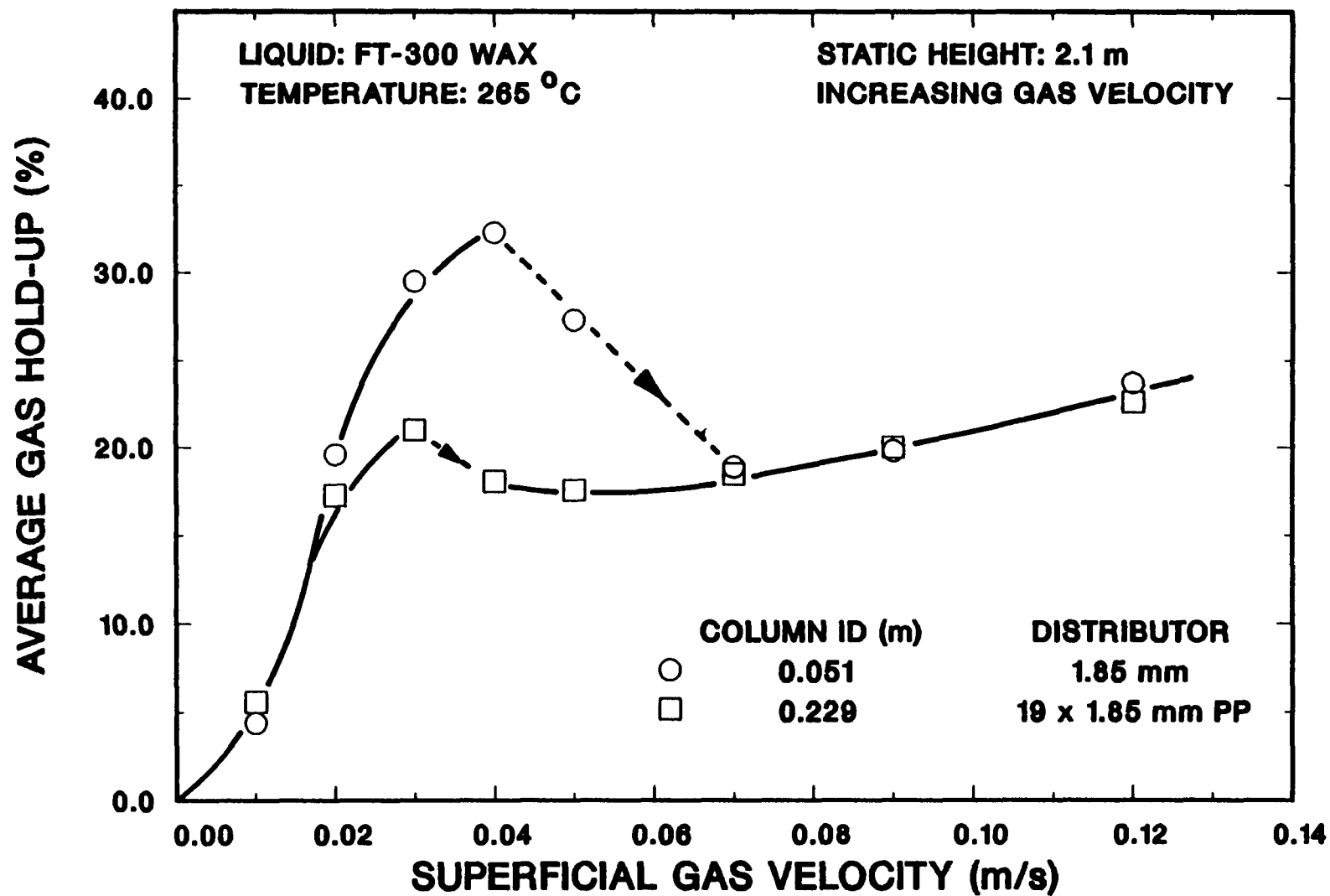
Figure V-22. Effect of column diameter on gas hold-up (Increasing order of velocities; O - Run 13-1; □ - Run 2-8)

behavior of FT-300 wax in the two columns. Figure V-23 shows a similar comparison for runs made in the two columns using decreasing order of gas velocities. These results show trends which are qualitatively similar to those observed using increasing order of gas velocities (Figure V-22). However, there were runs in which hold-up values in the 0.051 m ID column were lower than those in the 0.229 m ID column, particularly in the gas velocity range 0.03-0.07 m/s. This usually occurs when a transition from the "slug flow" regime to the "foamy" regime does not take place in the 0.051 m ID column (e.g. see Figure V-10). It appears that in such situations the dispersion in the large column, despite the obvious absence of foam, has a large concentration of tiny bubbles. These tiny bubbles increase the hold-up to levels which are similar to those obtained in the presence of foam in this column. In general, results presented in Figures V-22 and V-23 are indicative of the trends observed with hold-up values for majority of the runs conducted in the two columns.

Figure V-24 compares results from the two columns using the 1 mm orifice plate distributor in the 0.051 m ID column, and the 19 X 1 mm perforated plate distributor in the 0.229 m ID column. Once again, the jet velocities for the two distributors are similar at a given gas flow rate. These runs, conducted using increasing order of velocities, show results which are qualitatively similar to those shown earlier in Figure V-22 in the "foamy" regime. However, after an apparent foam breakup, the hold-ups in the 0.051 m ID column are consistently higher than those in the 0.229 m ID column.

Experiments were also conducted with Sasol's Arge reactor wax in the two columns at 265°C using the 1.85 mm distributor in the 0.051 m ID column
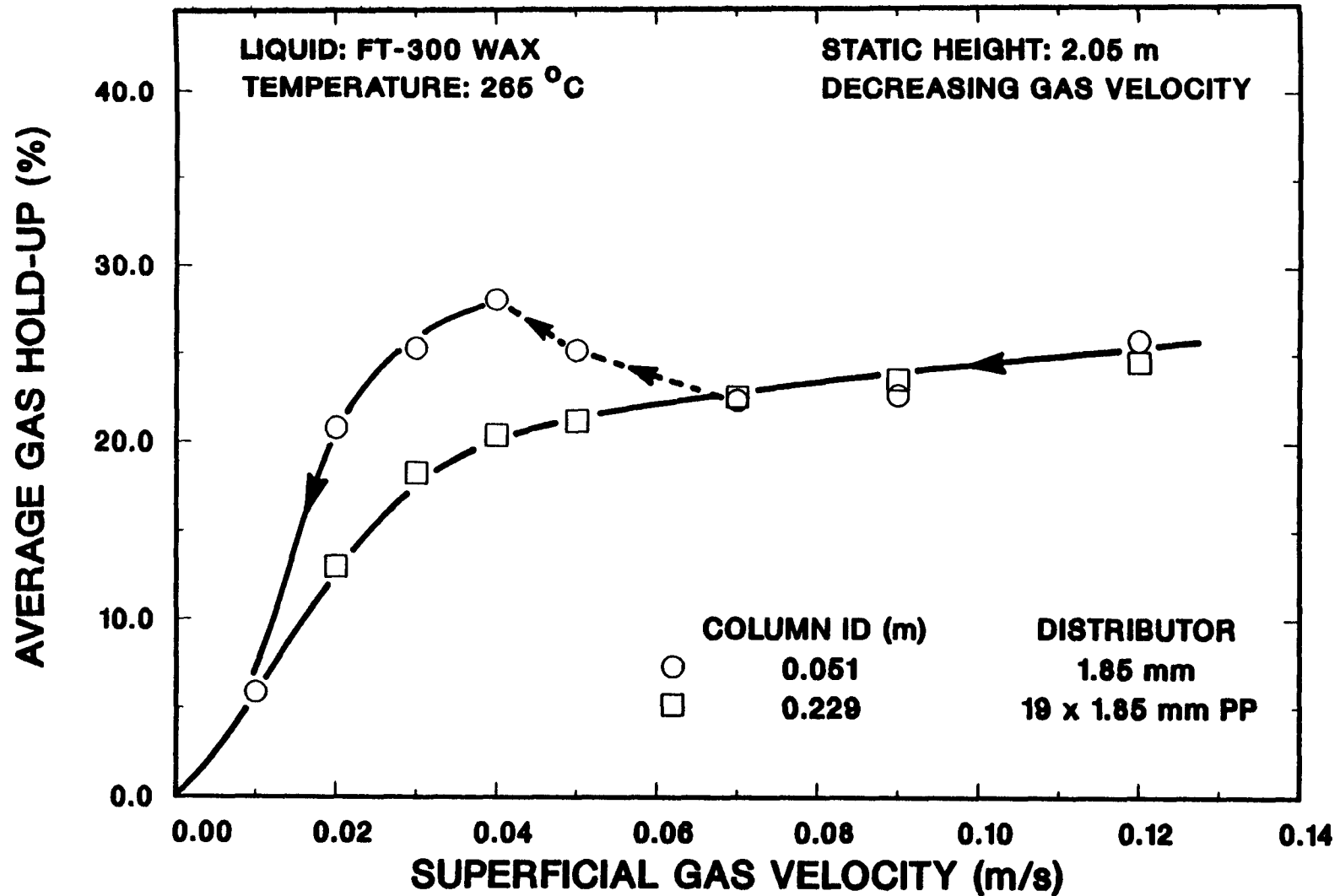
Figure V-23. Effect of column diameter on gas hold-up (Decreasing order of velocities; O - Run 13-3; □ - Run 2-9)
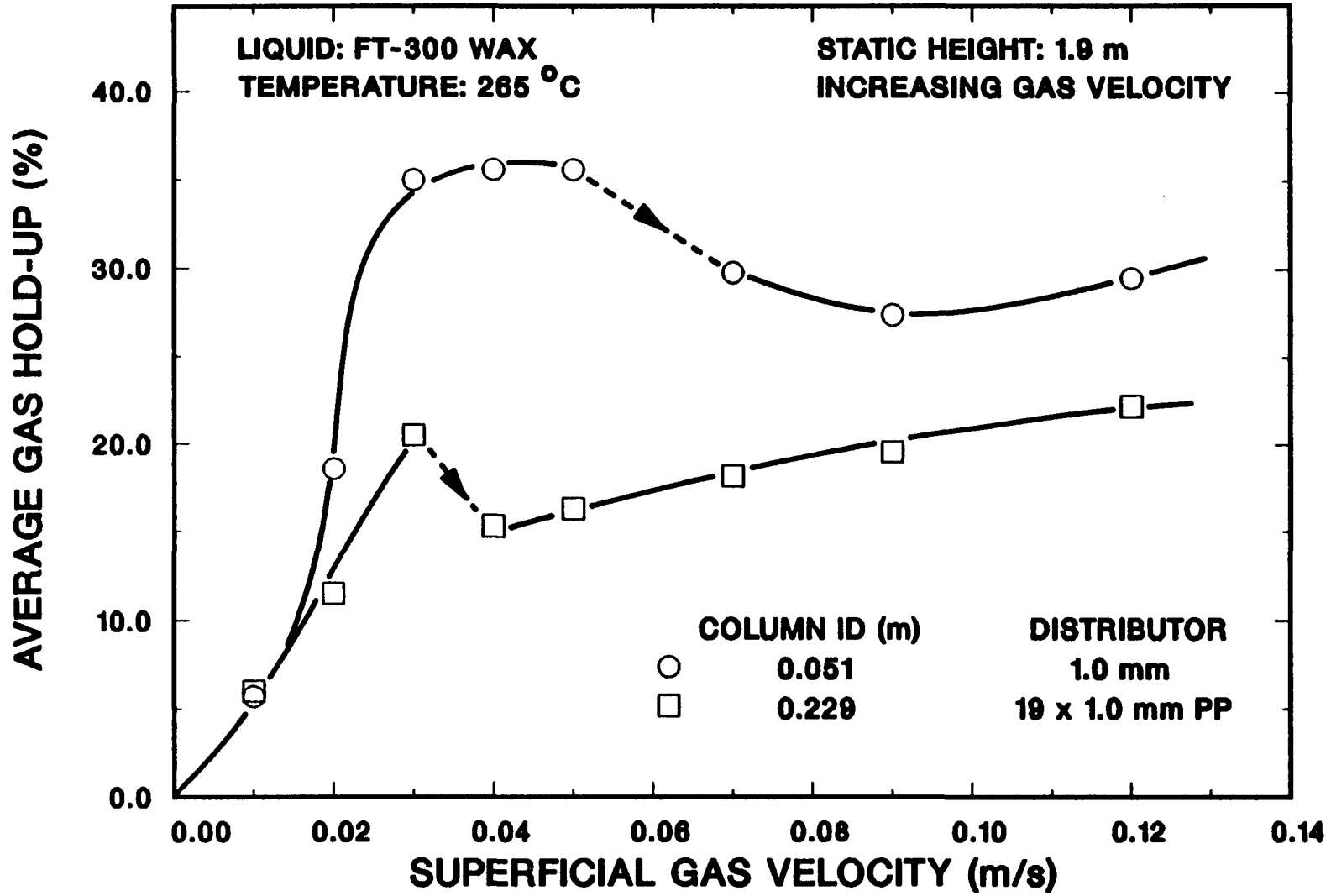
Figure V-24. Effect of column diameter on gas hold-up (O- Run 15-1; □ -Run 1-6)

and the 19 X 1.85 mm distributor in the 0.229 m ID column. No foam was produced during any of these runs and hold-up values were very similar in both columns, as shown in Figure V-25. Researchers at Mobil (Kuo et al., 1985) conducted experiments in 0.051 m ID and 0.102 m ID columns with reactor wax produced in their bench scale unit (Run CT-256-7 and CT-256-8 waxes). The hold-up values in the 0.102 m ID column were 30-40% higher than those in the 0.051 m ID column over the gas velocity range 0.015-0.065 m/s. They attributed this difference to the fewer slugs (or large bubbles) in the large column compared to the smaller column.

In general, the above results do not show a significant effect of column diameter on the gas hold-up. The major differences are in the "foamy" regime, and the earlier discussion on reproducibility showed that large deviations in hold-up are possible in this regime. These findings are consistent with results reported in literature. Researchers at Mobil (Kuo et al., 1985) conducted studies with FT-200 wax in 0.032 m ID and 0.053 m ID columns, each being 2.2 m in height, in order to assess the effect of column diameter on gas hold-up. Their results indicate that for similar jet velocities, column diameter did not have a significant effect on the gas hold-up values. Also hold-ups in the "foamy" regime were higher for runs made in the smaller diameter column, which is in agreement with the findings from the present study. Kuo et al. conducted similar studies in two tall columns (0.051 m ID and 0.102 m ID, 9.14 m tall) with FT-200 wax and reactor waxes produced in their bench scale units. These studies showed no effect of column diameter on gas hold-up for FT-200 wax, however, in experiments with reactor waxes higher hold-ups were obtained in the larger column. Deckwer et al. (1980) conducted experiments in two different
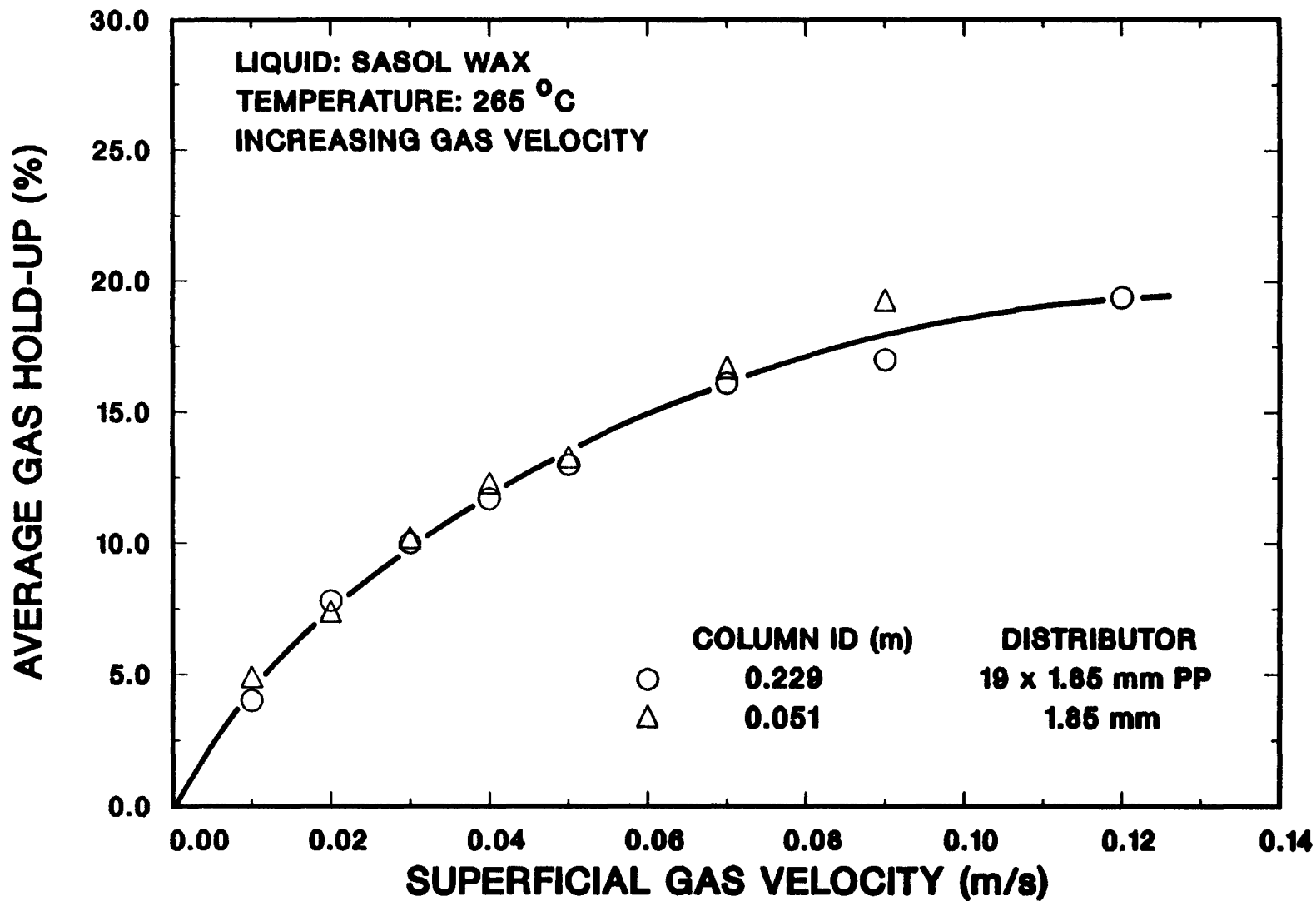
Figure V-25. Effect of column diameter on gas hold-up (O - Run 3-2; △ - Run 8-4)

diameter columns (0.041 m and 0.10 m). For temperatures below 250°C hold-up in the smaller diameter column was consistently higher than the hold-up in the 0.10 m column for the range of velocities investigated (0.005-0.03 m/s). It should be noted that foam was present under these conditions. However, for temperatures greater than 250°C, hold-up values from the two columns were similar. Shah et al. (1982) summarized the findings of various researchers, from hold-up measurements made with systems which did not produce foam (mostly air-water), which show that the effect of column diameter on the average gas hold-up is minimal. In general slightly lower hold-ups were obtained in large diameter columns compared to smaller columns.

In summary, our results show that the effect of column diameter is not very pronounced in the absence of foam. However, when foam was present, hold-up values in the smaller column (0.051 m ID) were higher than those in the larger column (0.229 m ID). This difference was more pronounced when distributors with smaller holes were used.

B.5. Effect of Distributor Type

The performance of the different distributors was investigated in the 0.051 and 0.229 m ID columns using FT-300 wax. Three orifice plate distributors (1, 1.85 and 4 mm holes) and a 40 μm sintered metal plate (SMP) distributor were evaluated in the smaller diameter column. The orifice plate distributors provided jet velocities in the range 1.6 m/s to 310 m/s for the superficial gas velocities in the range from 0.01 m/s to 0.12 m/s. Two perforated plate distributors, 19 x 1 m and 19 x 1.85 mm, used in the 0.229 m ID column gave jet velocities similar to those obtained with the 1 mm and 1.85 mm orifice plates in the 0.051 m column. A 5 x 1 mm

perforated plate was used in the large column in order to obtain jet velocities (up to 720 m/s) similar to those in the Quicker and Deckwer (1981) study. In addition to these three distributors, a 30 x 1.5 mm perforated pipe distributor (commonly encountered in fluidized beds) was also used in the larger column. Results from a few runs conducted with FT-200 wax are also presented here.

The major highlights of these investigations are:

- In the smaller diameter column, hold-up in the "foamy" regime increases with a decrease in orifice diameter, with the SMP distributor giving the highest hold-up values.

- In the large column, the distributor type does not have a significant effect on hold-up values in the "foamy" regime.

- The type of distributor does not have a significant effect on hold-up in the absence of foam in either column.

Figure V-26 shows results obtained in the 0.051 m ID column with FT-300 wax at 265°C using the four distributors. Substantial differences in hold-ups were obtained in the "foamy" regime. All measurements were conducted using increasing order of velocities, therefore, foam was produced at lower velocities, followed by a transition to the "slug flow" regime at higher velocities. These results show that in the "foamy" regime, hold-up increases with decreasing orifice size with the highest amount of foam being produced by the 40 μm SMP distributor and the lowest amount of foam being produced by the 4 mm orifice plate distributor. The velocity range, over which foaming occurs, also increases with decreasing orifice size. In general, the differences in hold-up values in the "foamy" regime with the different orifice distributors could be attributed to differences

86
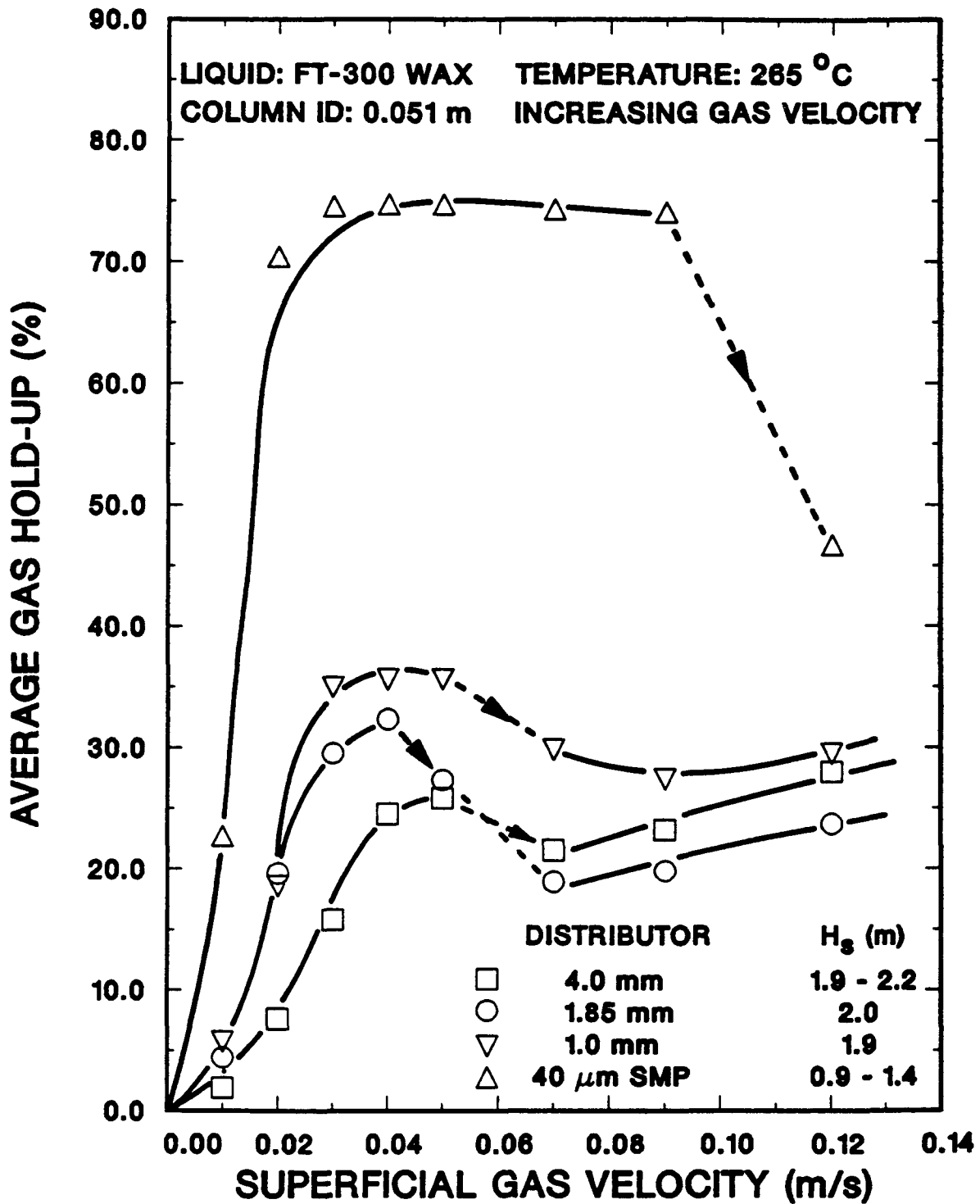
Figure V-26. Effect of distributor type on gas hold-up (☐- Run 6-2; O - Run 13-1; ▽ - Run 15-1; △ - Run 5-1)

in jet velocities. It is known that for the same superficial gas velocity, jet velocity increases with an increase in column diameter or a decrease in orifice size. A higher jet velocity would translate into a higher kinetic energy and therefore a greater number of small bubbles would be formed, resulting in higher hold-up values.

Results presented in Figure V-26 show that, once the transition from the "foamy" regime to the "slug flow" regime takes place, hold-up values for the different distributors are similar. In the run conducted using the SMP distributor, the transition from the "foamy" regime to the "slug flow" regime was not complete, and thus higher hold-up was obtained at 0.12 m/s. There is a lack of data in literature relating the effect of distributor type to hold-up in the "slug flow" or "churn-turbulent" flow " regime, with molten wax as the liquid medium. However, based on data for non-foaming systems (mostly air-water), Shah et al. (1982) found that in the "slug flow" regime, the effect of sparger type is insignificant. Heijnen and van't Riet (1984) postulate that when coalescence persists (e.g. in FT-300 wax in the absence of foam), larger bubbles are formed within a short distance of the distributor and the identity of the bubbles formed at the distributor is lost, thus hold-up values for different distributors would be similar.

Figure V-27 shows results obtained in the 0.229 m ID column with the four distributors, using FT-300 wax at 265°C. The experiments, conducted in increasing order of gas velocities, show the presence of foam at lower velocities followed by a transition from the "foamy" regime to the "churn-turbulent" regime. The trends are similar with the 19 X 1 mm and the 19 X 1.85 mm perforated plate distributors, with foam breaking in the velocity
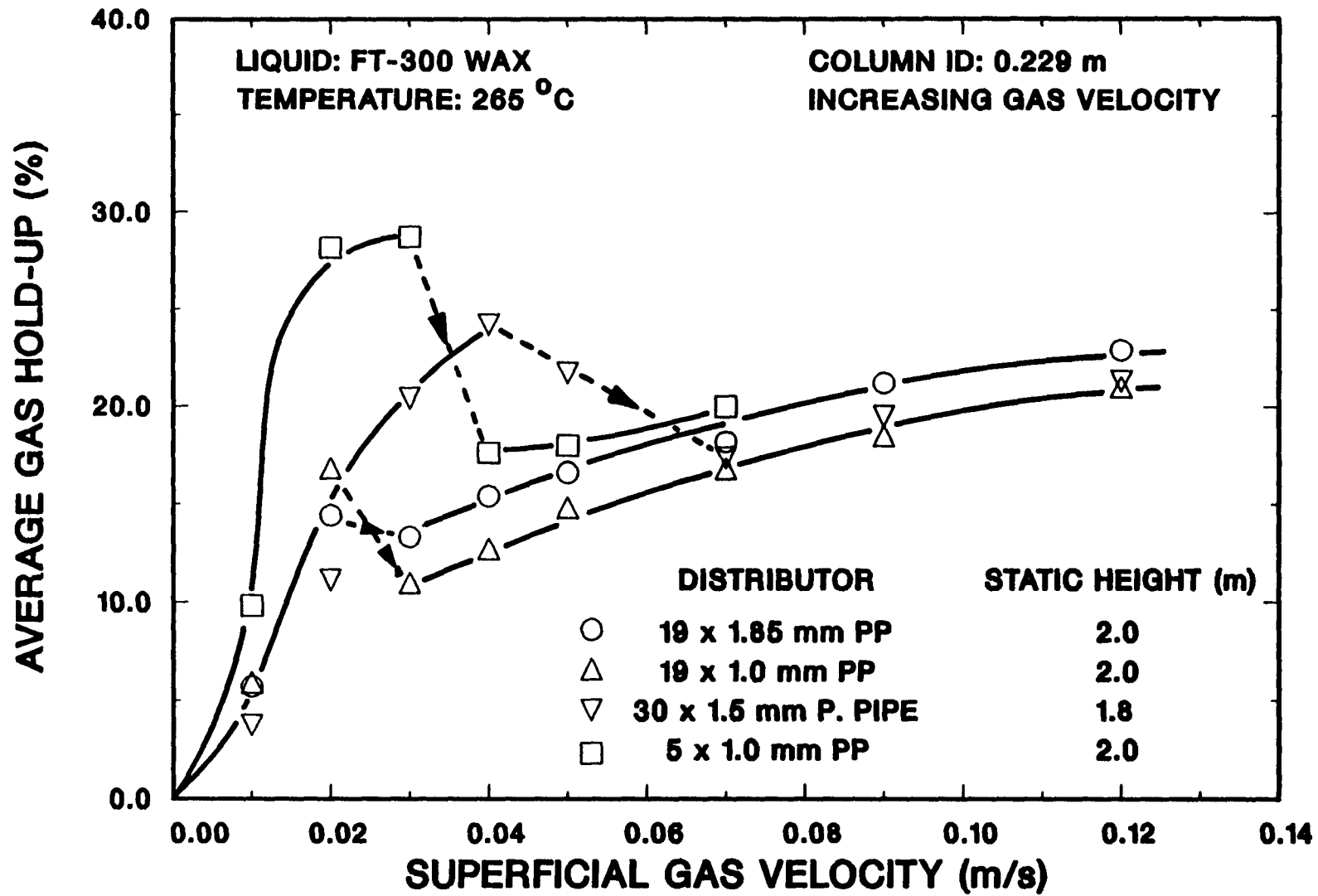
Figure V-27. Effect of distributor type on gas hold-up (O - Run 2-3; △ - Run 2-2; ▽ - Run 1-5; □ - Run 4-1)

range 0.02-0.03 m/s for both runs. The wider range of gas velocities over which foaming occurred, with the perforated pipe distributor (1.5 mm holes) is not as expected. However, only one run was conducted with this distributor and the results may not be typical of the actual behavior for this type of distributor. The 5 X 1 mm distributor gave the highest hold-up in the presence of foam. This is as expected since jet velocities associated with this distributor were significantly higher than those for the other three distributors investigated. With this distributor, foam broke in the velocity range 0.03-0.04 m/s, which is higher than the foam breakup range with the perforated plate distributors. In the "churn-turbulent" regime, hold-up values for the different distributors are very similar. The slightly higher values with the 19 X 1.85 mm distributor (around 2.5% absolute) are not as expected, however, the difference is not significant.

Figure V-28 shows hold-up values obtained with FT-200 wax in the 0.051 m ID column using the 40 μm SMP, 1 mm orifice and the 1.85 mm orifice plate distributors at 265°C. These results are qualitatively similar to those for FT-300 wax under similar conditions with higher hold-ups produced when small hole size distributors were used. Hold-ups were highest with the 40 μm SMP distributor, whereas hold-ups with the 1.85 mm orifice plate distributors were significantly lower. Most of the data presented in Figure V-28 were obtained in the presence of foam and a transition from the "foamy" regime to the "slug flow" regime was not as pronounced with FT-200 wax compared to FT-300 wax. The results for the SMP distributor do show a decrease in gas hold-up when velocity was increased from 0.09 m/s to 0.12 m/s. This could be attributed to the initiation of the foam breakage process. The trends are similar to the findings by researchers at Mobil (Kuo
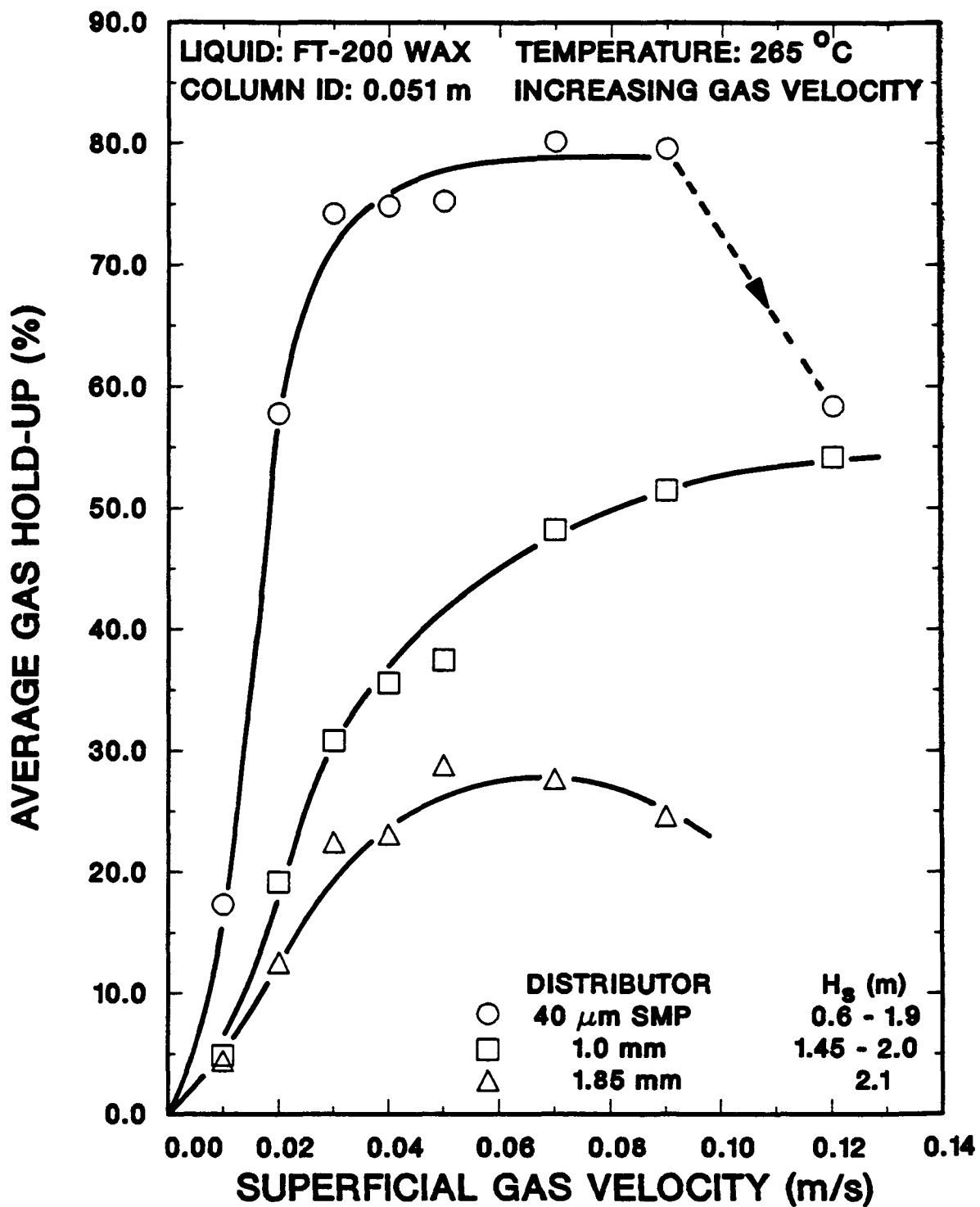
Figure V-28. Effect of distributor type on gas hold-up (O - Run 20-1; ☐ - Run 17-1; Δ - Run 11-5)

et al., 1985). Their experiments with FT-200 wax at 200°C, using three different SMP distributors (15, 60 and 100 μm) and three different orifice plate distributors (0.25, 0.39 and 0.57 mm) in a 0.032 m ID column, showed that hold-up values were highest with the 15 μm SMP distributor and lowest with the 0.57 mm orifice plate distributor. However, these investigations were carried out for superficial gas velocities less than 0.04 m/s, therefore, the transition from the "foamy" to the "slug flow" flow regime was not observed. The maximum hold-up obtained in the Mobil studies was around 70%, when foam filled the entire column (with the 15 and 60 μm SMP distributors). This value compares well with that obtained with the SMP distributor in the present study.

Experiments conducted with reactor waxes showed no significant effect of distributor type. However, hold-ups obtained using the SMP distributor were marginally higher than those obtained using the 1.85 mm orifice plate distributor in the 0.051 m ID column (see Section V-B.7.).

Experiments with FT-300 and FT-200 waxes conducted to study the effect of distributor type indicate that the effect is most significant in the presence of foam. Smaller orifice diameters and SMP distributors produce higher hold-ups compared to larger orifice distributors. However, in the absence of foam, even though there is a similar trend, its magnitude is rather small. The effect of distributor type is less pronounced in the larger (0.229 m ID) column than in the 0.051 m ID column.

B.6. Effect of Oxygenates

The hydrodynamic behavior of reactor waxes is significantly different from that of paraffin waxes (e.g. FT-200 and FT-300). The reactor waxes, in addition to long chain paraffins, also contain high molecular weight ole-

92

fins and oxygenates (primarily alcohols and acids). Smith, J. et al. (1984) postulated that oxygenates might be partly responsible for the differences in foaming characteristics between reactor waxes and paraffin waxes. Experiments were conducted in the 0.051 m ID glass column in order to investigate the effect of oxygenates (5 to 10 wt.% of 1-octadecanol and octadecanoic acid) on the hydrodynamic behavior of paraffin waxes. The 1.85 mm orifice plate and the 40 μm sintered metal plate (SMP) distributors were used in these experiments.

The major highlights of these investigations are:

• In the 0.051 m ID column, equipped with the 1.85 mm orifice plate distributor, the addition of oxygenates delayed the breakage of foam to a higher velocity, and a marginal increase in hold-up was observed.

• When the 40 μm SMP distributor was used in the 0.051 m ID column, the addition of oxygenates gave hold-up values which were essentially the same as those for pure FT-300 wax.

• In general, the addition of oxygenates did not have a significant effect on the average gas hold-up.

The experiments were conducted with mixtures of known compositions of 1-octadecanol (99% purity from Sigma Chemical Co.), octadecanoic acid (90% purity from Sigma) and FT-300 wax. All runs were conducted using increasing order of gas velocities at 265°C.

Figure V-29 shows results obtained using the 1.85 mm orifice plate distributor. The hold-up values for all three cases behave as expected, with a substantial increase in gas hold-up as foam is produced, followed by a transition from the "foamy" regime to the "slug flow" regime accompanied
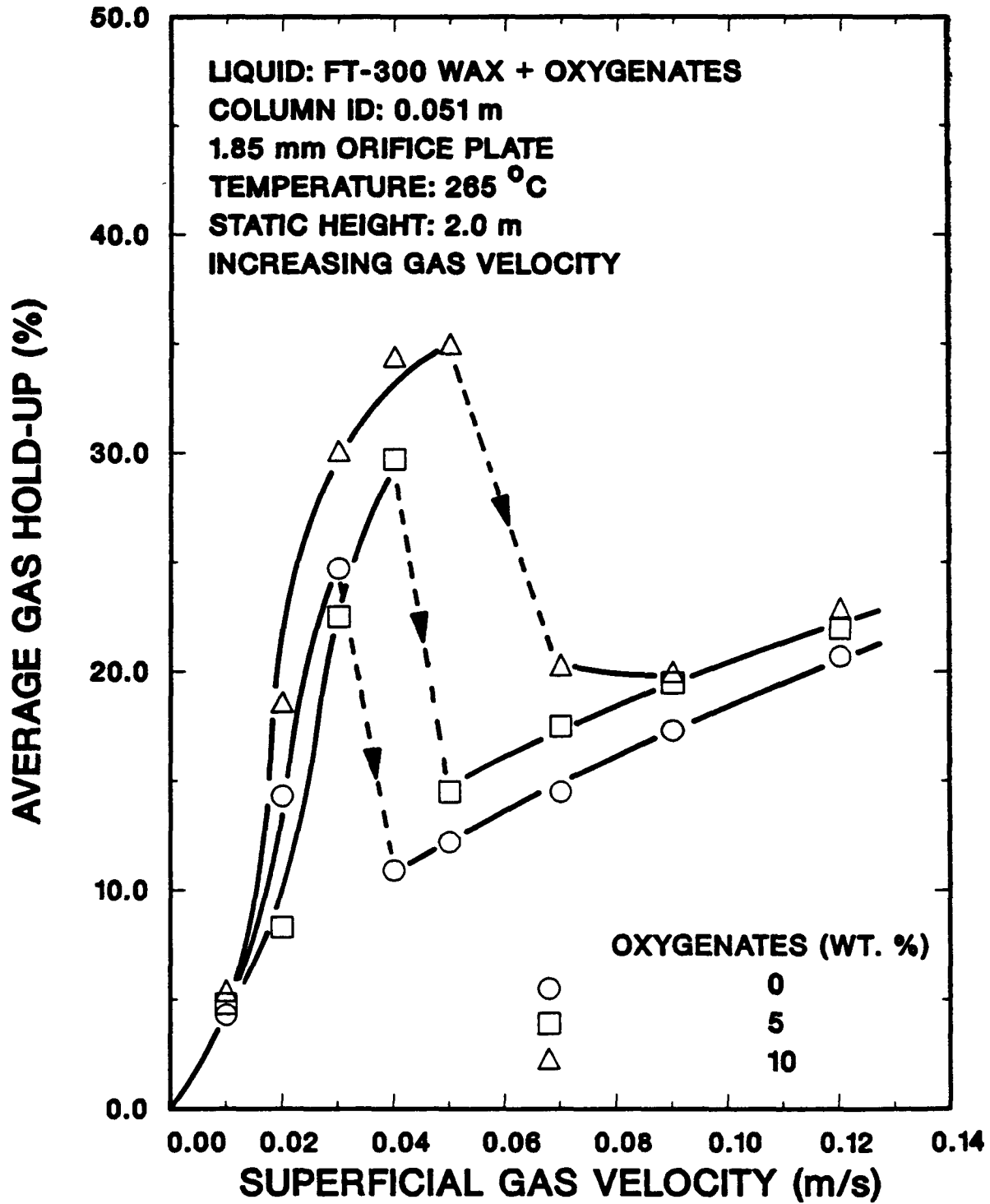
Figure V-29. Effect of oxygenates on gas hold-up (◯ - Run 4-1; ☐ - Run 4-4 - 1-octadecanol; △ - Run 4-5 - equal amounts of 1-octadecanol and octadecanoic acid)

by a sudden decrease in hold-up values. Thereafter, hold-up increases gradually as gas velocity is increased. The transition from the "foamy" regime to the "slug flow" regime shifts to higher velocities as the concentration of oxygenates increases. The maximum hold-up value in the "foamy" regime also increases in a similar manner. In the "slug flow" regime, the hold-ups for runs with oxygenates are marginally higher than those obtained in the run with pure FT-300.

Figure V-30 compares hold-up values for runs made with and without oxygenates using the 40 μm SMP distributor. Once again, these results show trends typical for this distributor, a substantial increase in hold-up to around 70% at lower velocities as foam fills the entire column, followed by a sharp drop in hold-up as the transition from the "foamy" regime to the "slug flow" regime takes place. In the "foamy" regime, hold-up values for the two cases are similar, with slightly higher hold-ups for the wax with oxygenates. These high hold-ups are typical for the SMP distributor for gas velocities in the range 0.02-0.05 m/s. Since coalescence rates for this system are already low, it is possible that the addition of coalescence inhibitors (such as oxygenates) causes no further decrease in coalescence rates. Therefore, oxygenates do not appear to have a significant influence on the hold-up values. However, foam broke earlier for the run with pure FT-300 wax (between 0.04 and 0.07 m/s) compared to run with oxygenates (between 0.07 and 0.09 m/s), but this difference is not significant. The velocity at which the transition from the "foamy" regime to the "slug flow" regime occurred was not always the same in runs with pure FT-300 wax. In some cases this transition occurred at higher velocities (0.09-0.12 m/s,
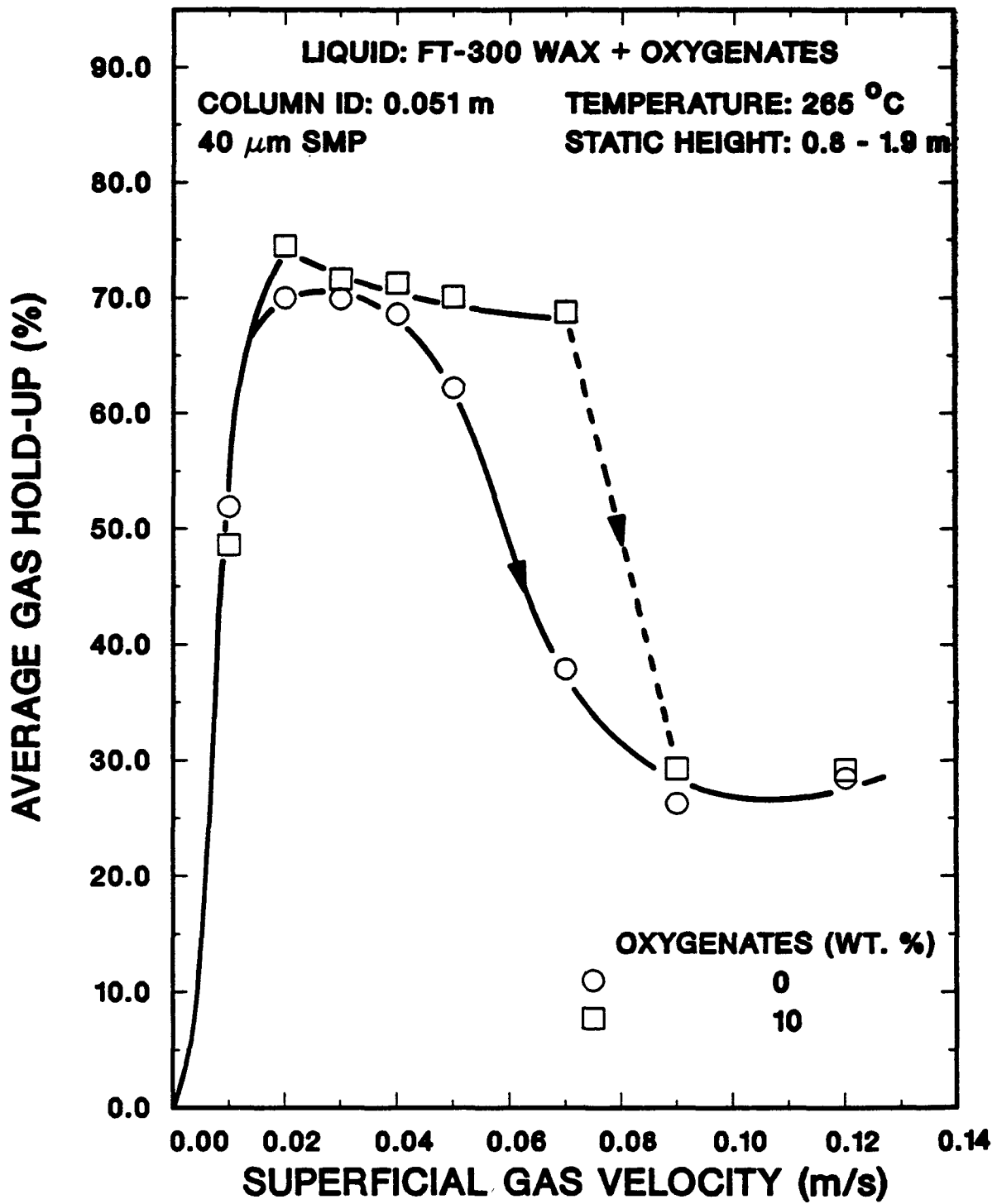
Figure V-30. Effect of oxygenates on gas hold-up (○- Run 7-2; □- Run 4-6 - equal amounts of 1-octadecanol and octadecanoic acid)

see Figure V-12). In the "slug-flow" regime, hold-up values for the two runs are similar.

The effect of the addition of oxygenates to FT-300 wax is qualitatively similar to results from studies conducted in the air-water system reported by Schugerl et al. (1977) and Kelkar et al. (1983). Their studies showed that the presence of alcohols in water resulted in higher hold-ups when compared to pure water.

The effect of oxygenates on the hydrodynamic parameters of the FT-300 wax is not significant. From our results it appears that oxygenates do not suppress foaming, and thus the reasons for low hold-ups and absence of foam in experiments with raw reactor waxes, as reported by Smith, J. et al. (1984) and Kuo et al. (1985), are not clearly understood at the present time.

B.7. Effect of Liquid Medium

It has been well established that paraffin waxes have a tendency to foam, the severity of which is dependent on a combination of factors. Bubble size measurements (see Section V-D) have revealed that FT-300 paraffin wax produces bubbles which are significantly smaller than those produced in other systems, such as the air-water system. Experiments were therefore conducted with different liquid media in order to investigate their effect on average gas hold-up. Results obtained with FT-300 wax were compared with those obtained in experiments conducted using FT-200 wax, two reactor waxes (Sasol's Arge reactor wax and Mobil's reactor wax), and distilled water. The investigations were carried out in the 0.051 m and the 0.229 m ID columns at 200 and 265°C with molten waxes, and at room temperature with distilled water. The 1 mm and 1.85 mm orifice plate, and

the 40 μm sintered metal plate (SMP) distributors were used in the 0.051 m ID column, while the 19 x 1.85 mm perforated plate distributor was used in the 0.229 m ID column.

The major highlights of these investigations are:

- Results for FT-200 wax are qualitatively similar to those for FT-300 wax in the "foamy" regime, with higher hold-ups obtained with FT-200 wax. The transition from the "foamy" regime to the "slug flow" regime is not as pronounced with FT-200 wax as was with FT-300 wax.

- Reactor waxes and water do not have a tendency to foam for the range of conditions investigated in these studies. Therefore, they do not exhibit hysteresis behavior which is characteristic of paraffin waxes.

- Hold-up values for distilled water and reactor waxes are not significantly affected by distributor type nor by temperature (for reactor waxes).

- Hold-up values for distilled water and reactor waxes in the 0.051 m ID column are very similar to those obtained with FT-300 wax in the absence of foam.

Results illustrating the effect of temperature, distributor type and gas velocity on the average gas hold-up for Sasol's Arge wax are shown in Figure V-31. All runs were conducted using increasing order of gas velocities. Hold-up values with the 1.85 mm orifice plate distributor show a gradual increase with gas velocity, whereas the ones with the SMP distributor exhibit a slight maximum at a velocity between 0.01 and 0.02 m/s. Foam was observed only in the run with the SMP distributor at 0.01 m/s during the first 30 minutes and then disappeared. However, the small bubbles produced during this brief period persisted to some extent

AVERAGE GAS HOLD-UP (%)

30.0

25.0

20.0

15.0

10.0

5.0

0.0

LIQUID: SASOL WAX
COLUMN ID: 0.051 m
INCREASING GAS VELOCITY

	T (°C)	H_s (m)	DISTRIBUTOR
O	265	2.1	1.85 mm
△	265	2.1	40 μm SMP
□	200	1.9	1.85 mm

0.00   0.02   0.04   0.06   0.08   0.10   0.12   0.14

SUPERFICIAL GAS VELOCITY (m/s)
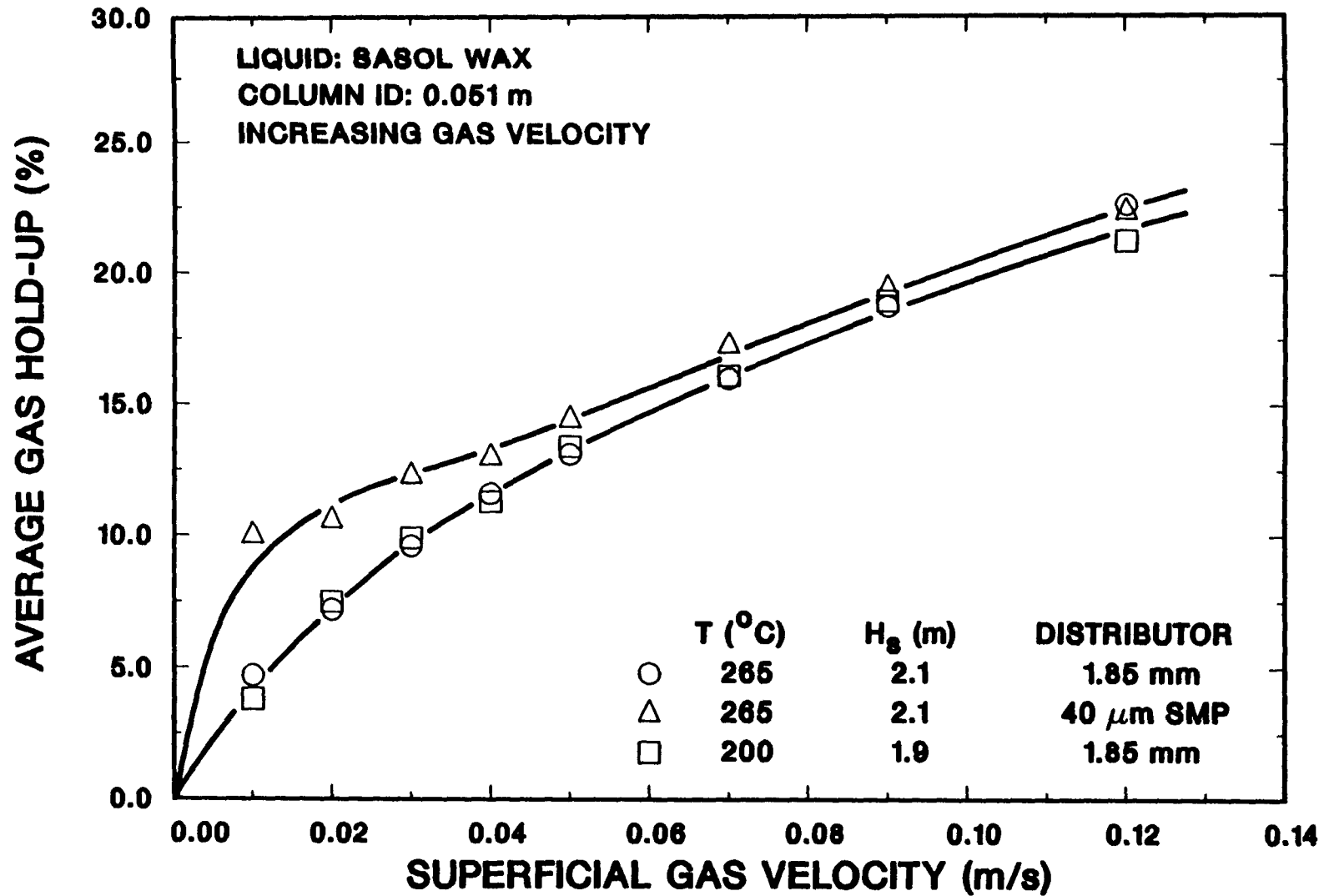
Figure V-31. Effect of superficial gas velocity, distributor type and temperature on gas hold-up (O- Run 8-1; △ - Run 8-3; □ - Run 10-1)

resulting in higher hold-up values for gas velocities up to 0.04 m/s. Hold-up values with the 1.85 mm orifice plate distributor at 200°C are marginally lower than those obtained at 265°C with the same distributor, which is as expected. At 265°C, runs were conducted using different operating procedures (i.e. start-up velocities), however, hold-up values from these runs showed no effect of the order in which gas velocities were changed (i.e. increasing or decreasing order of velocities). In both cases there was no foam produced, therefore, the hysteresis behavior (characteristic of paraffin wax) was absent for Sasol's reactor wax. Visual observations of the flow field near the wall showed that bubbles were larger than those observed previously with FT-300 wax. A notable difference was the absence of fine bubbles (less than 1 mm) that were present in large numbers in experiments with FT-300 wax. At velocities 0.03 m/s and higher, slugs occupying the entire column cross-section were observed which was also the case in experiments with the FT-300 wax. These qualitative differences in the bubble size distributions between the two waxes are reflected in the values of the Sauter mean bubble diameter (see Section V-D).

Hold-up values with Sasol wax were also measured in the 0.229 m ID column using the 19 x 1.85 mm distributor at 265°C. These results, when compared (see Figure V-25) with hold-up values obtained using Sasol wax in the 0.051 m ID column, show that column diameter did not have a significant effect on the average gas hold-up values.

Figure V-32 shows gas hold-up values obtained from experiments conducted with Mobil's reactor wax (composite wax from runs 9, 11 and 12 in their Unit CT-256). Once again foam was not observed in the runs made with

100
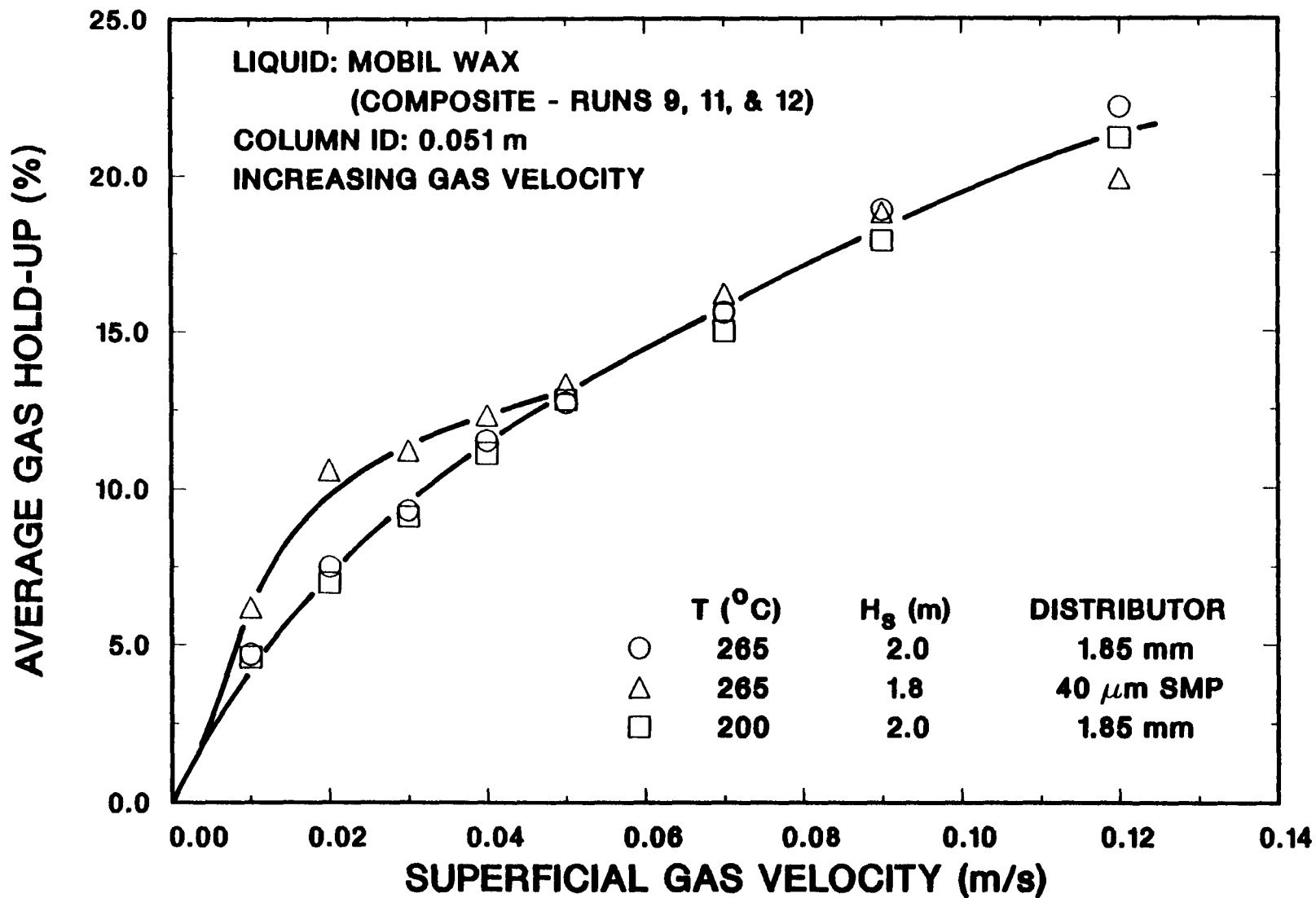
Figure V-32. Effect of superficial gas velocity, distributor type and temperature on gas hold-up (composite wax from Mobil runs CT-256-9, -11 and -12; ◯ - Run 9-3; △ - Run 9-4; ☐ -Run 9-2)

the 1.85 mm orifice plate distributor. The behavior with the SMP distributor was similar to that observed with Sasol wax, i.e. foam appeared initially at 0.01 m/s but it disappeared after approximately one hour on stream. Gas hold-up values are, in general, very similar to those obtained in the runs with Sasol wax under the same conditions. Visual observations of the flow field with this wax were limited due to its dark color which was caused by the presence of small amounts of iron catalyst particles (~ 350 ppm). However, backlighting of the column did show the presence of slugs at gas velocities of 0.03 m/s and higher.

Researchers at Mobil (Kuo et al., 1985) also conducted experiments with reactor waxes produced from runs in their pilot plant reactor (Unit CT-256). They reported hold-up values for experiments with waxes produced during runs 4,5,7 and 8. In order to compare results from the present study with those presented by Kuo et al., additional experiments were conducted with two different composites (composite of waxes produced in their runs 4 and 7; and composite of waxes produced in their runs 5 and 8). Results from these experiments and comparison with the Kuo et al. data are presented in APPENDIX E.

Figure V-33 shows results obtained from runs conducted under ambient conditions with distilled water in the 0.051 m ID column, using the 1.85 mm orifice plate and the 40 μm SMP distributor. These results show that neither the operating procedure (i.e. start-up velocity) nor distributor type had any significant effect on the average gas hold-up. As expected, foam was not observed in any of these runs. Visual observations of the flow field showed fewer and larger bubbles compared to FT-300 wax. Slugs were observed at gas velocities of 0.03 m/s and higher.
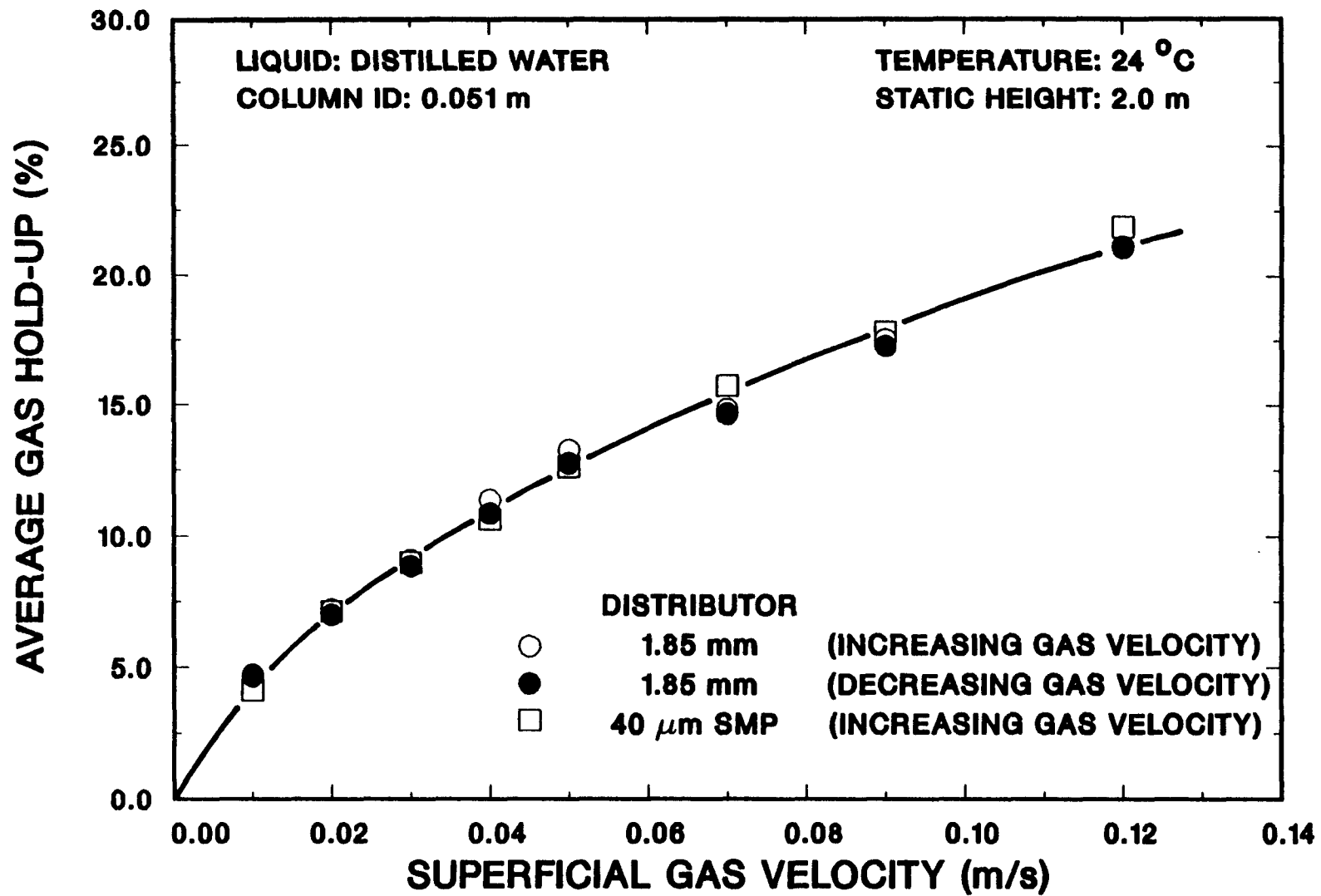
Figure V-33. Effect of superficial gas velocity, start-up procedure and distributor type on gas hold-up

Hold-up values for the five liquid media used in these studies (i.e. FT-300, FT-200, Sasol's Arge wax, Mobil's reactor wax, and distilled water) are compared in Figures V-34 to V-36 for runs conducted using increasing order of gas velocities. Results for the different systems obtained using the 1.85 mm orifice plate distributor (Figure V-34) are very similar when the "slug flow" regime persists. However, with paraffin waxes (FT-300 and FT-200) it is also possible to operate in the "foamy" regime at lower gas velocities (usually < 0.05 m/s with FT-300 wax). For this range of gas velocities, hold-ups with paraffin waxes are significantly higher than values with either reactor waxes or distilled water. For the results presented in Figure V-34, both FT-200 and FT-300 waxes showed a significant increase in hold-up as gas velocity was increased from 0.01 to 0.03 m/s. As gas velocity was further increased, a transition from the "foamy" regime to the "slug flow" regime occurred with FT-300 wax. With FT-200 wax, this transition was not as pronounced as was with FT-300. The gradual decrease in hold-up at velocities 0.05 m/s and higher could be attributed to the initiation of the foam breakage process. There were instances when foam was not produced in runs with FT-300 wax at 265°C (see Figure V-10). The hold-up values for such cases were similar to those indicated by the lower curve in Figure V-34. These results indicate that liquid medium does not have a significant effect on the average gas hold-up when foam is not produced. Figure V-35 shows results obtained using the SMP distributor. The curves for FT-200 and FT-300 waxes illustrate behavior typical for paraffin waxes, a sharp increase in gas hold-up as gas velocity increases from 0.01 m/s to 0.02 m/s accompanied by the formation of foam, followed by a sudden drop as foam breaks. There is no significant difference between

104
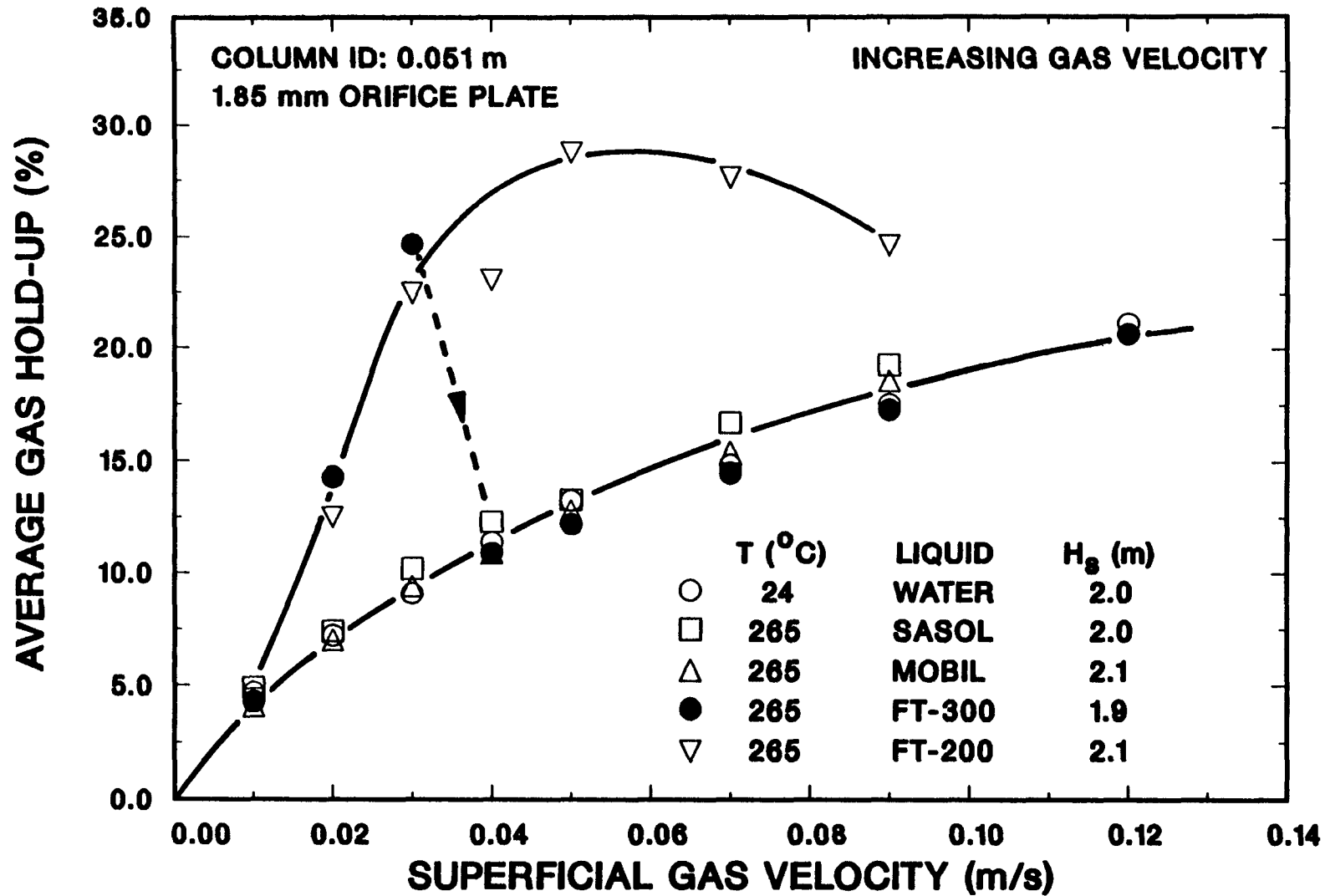
Figure V-34. Effect of liquid medium and superficial gas velocity on gas hold-up (☐ - Run 8-4; △ - Run 9-1; ● - Run 4-1; ▽ - Run 11-5)
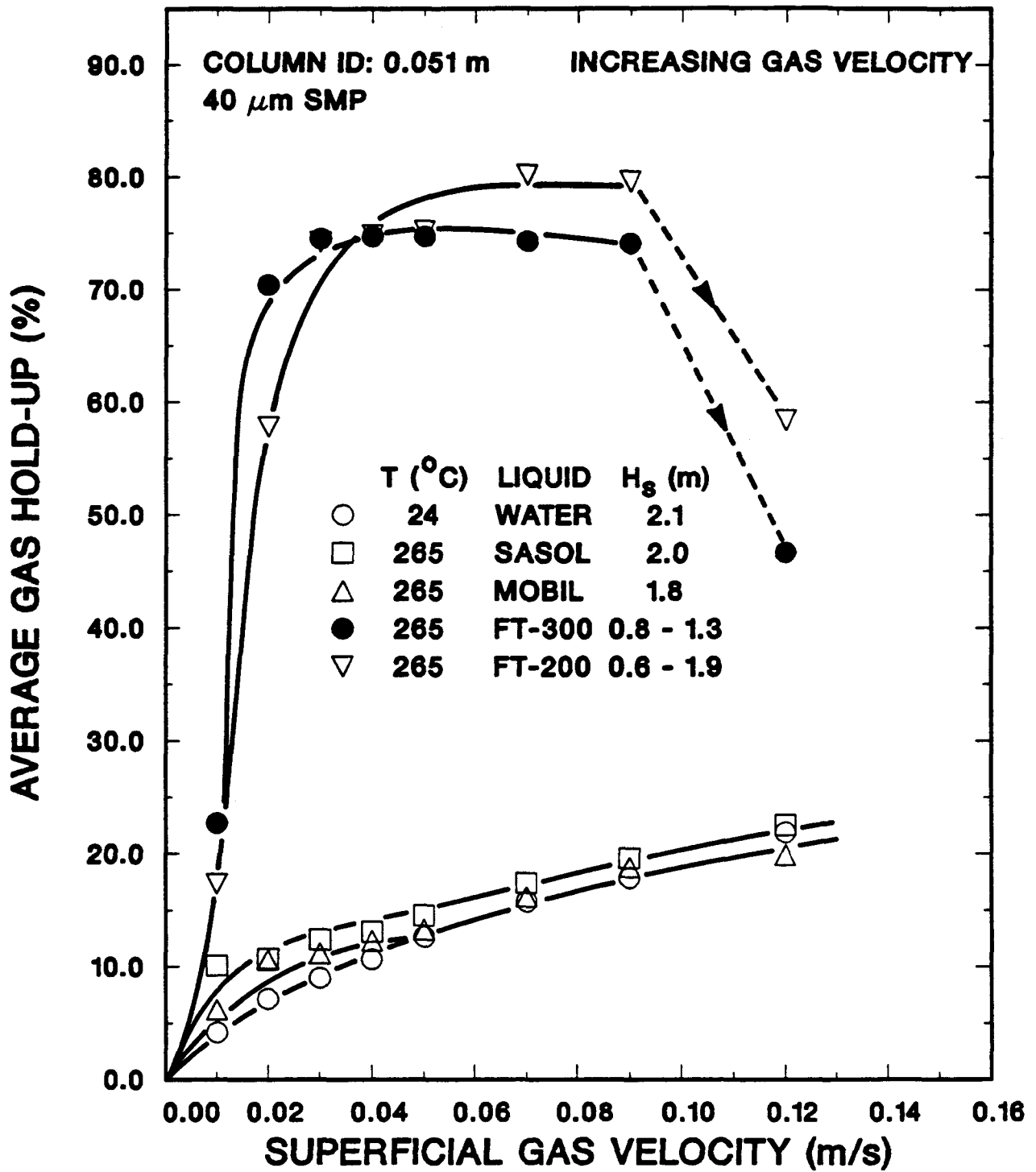
Figure V-35. Effect of liquid medium and superficial gas velocity on gas hold-up (□-
Run 10-1; △ - Run 9-4; ● - Run 5-1; ▽- Run 20-1)

hold-ups for the two waxes for the examples shown in Figure V-35. Hold-up values for the two reactor waxes and for distilled water are significantly lower than those for paraffin wax. The reactor waxes showed slightly higher hold-ups in the velocity range 0.01-0.04 m/s compared to values for distilled water. This could be attributed to the presence of fine bubbles in these waxes following the small amount of foam produced at 0.01 m/s.

Figure V-36 compares hold-up values obtained with FT-200 and FT-300 waxes using the 1 mm orifice plate distributor in the 0.051 m ID column. Results for FT-200 wax are similar to those for FT-300 wax in the velocity range 0.01-0.03 m/s. For velocities greater than 0.03 m/s, hold-ups continued to increase for FT-200 wax, while a transition from the "foamy" to the "slug flow" regime was observed with FT-300 wax. These results are as expected and illustrate the foaming capacity of paraffin waxes.

The results presented above indicate that the hydrodynamic properties of paraffin waxes (FT-200 and FT-300) are significantly different from those for the reactor waxes and distilled water. The absence of foam and lower hold-up values for the two reactor waxes and water could be attributed to high coalescence rates for these systems. Visual observations of the flow field with water showed virtually no difference in flow patterns between the run using the 1.85 mm orifice plate and the run using the SMP distributor. The presence of foam in FT-300 wax is indicative of low coalescence rates. Heijnen and van't Riet (1984) have discussed the differences between liquids that have high coalescence rates and liquids with low coalescence rates. They postulate that for the former, the flow is independent of the distributor since bubbles coalesce just above the distributor and their size continues to grow as gas
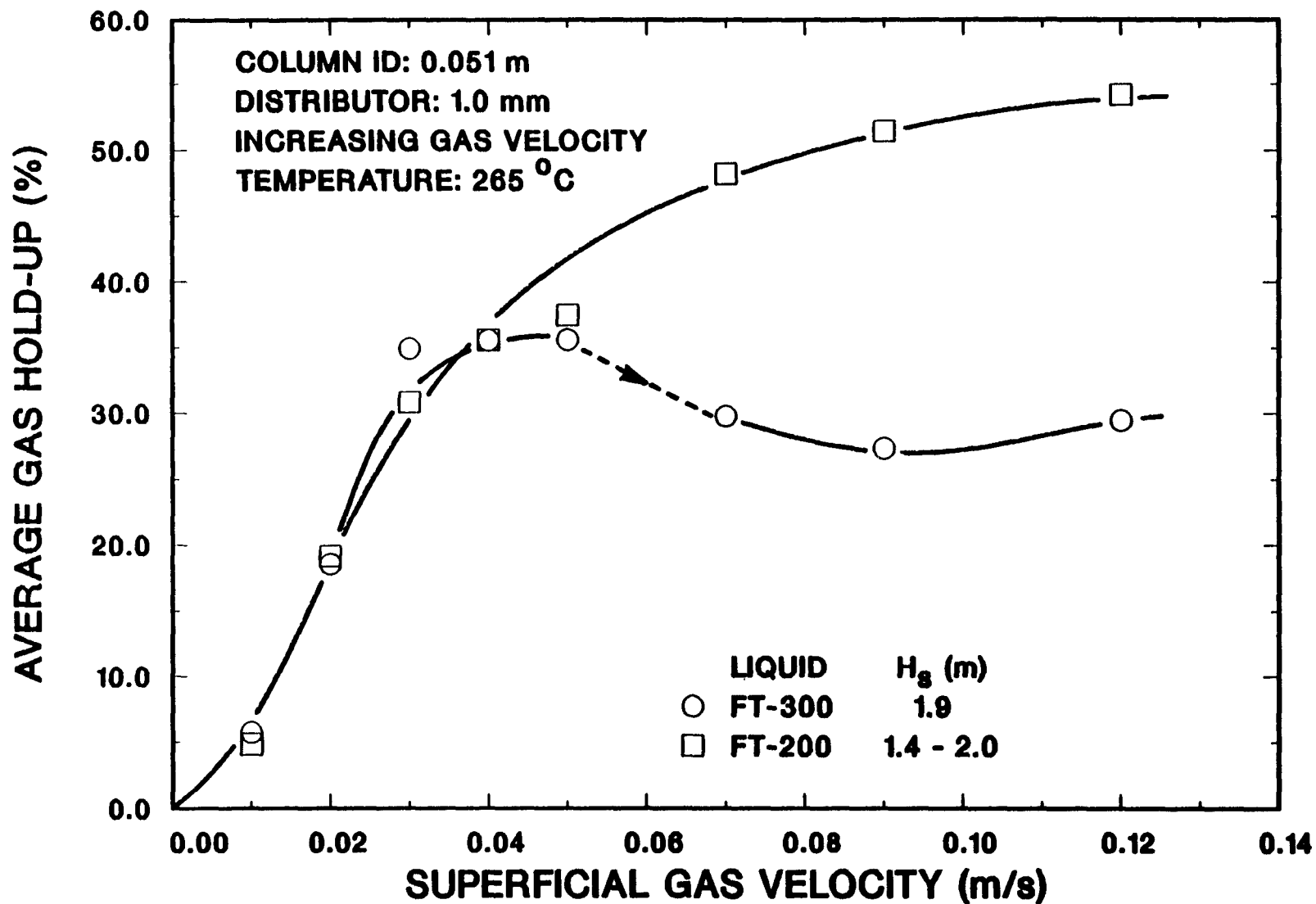
Figure V-36. Effect of liquid medium and superficial gas velocity on gas hold-up (O - Run 15-1; □ - Run 17-1)

velocity is increased. However, for liquids that have low coalescence rates, the bubbles formed at the distributor are further dispersed, forming smaller bubbles. Results from the present studies are in general agreement with these observations.

Results from dynamic gas disengagement (DGD) measurements indicate that large bubbles (slugs) are responsible for up to 85% of the gas hold-up at higher velocities (greater than 0.07 m/s) for FT-300 and the two reactor waxes when runs were conducted in the 0.051 m ID column. For FT-300 wax smaller bubbles account for most of the hold-up at velocities less than 0.07 m/s, whereas, for the other three systems, large bubbles dictate the hold-up values even at lower velocities. Vermeer and Krishna (1981) showed that hold-up in a bubble column could be classified into two components; one due to the entrained bubbles, and the other due to the large bubbles or the transport portion of the hold-up. It is expected that if the entrained portion of the hold-up is substantially greater than the transport portion, a higher hold-up value will result, e.g. with FT-300 wax in the presence of foam. However, when the transport portion of the hold-up is high, e.g. with reactor waxes and water, and with FT-300 wax at higher gas velocities, the average hold-up will be relatively lower. Since slugs with all systems are of the same relative size (i.e. almost equal to the column diameter) it is expected that in the presence of slugs, hold-up values should be independent of the liquid medium, as is the case in the present study.

The above studies with the different liquid media show that the differences between the hydrodynamic parameters for paraffin waxes and reactor waxes are significant, therefore the choice of liquid medium is

109

critical for investigations aimed at obtaining parameters for bubble column design and scale-up.

B.8. Comparison with Literature

Qualitative comparisons between average gas hold-up values obtained in the present study and those that have appeared in the literature have been made in the previous sections. Here some quantitative comparisons will be made. Only the results from runs conducted using paraffin waxes are compared here. Hold-up values obtained from runs conducted with Mobil's reactor waxes are compared with Mobil's data with similar waxes in APPENDIX E.

The major highlights of the comparisons are:

• Literature data on hold-up values obtained using the SMP distributor is limited to the "foamy" regime and shows that hold-ups increase with a decrease in pore size. Results obtained from the present studies using the 40 μm SMP distributor are in fairly good agreement with the data reported for SMP distributors having pore sizes in the range 20-60 μm.

• Results obtained using the orifice plate and the perforated plate distributors also show a dependency on the distributor hole size in the "foamy" regime. Higher hold-ups are produced with distributors having smaller holes or perforations. This is in good agreement with data reported in literature. In the absence of foam, hold-up values are not affected significantly by the distributor hole size.

B.8.a Sintered Metal Plate Distributors

Figure V-37 shows a comparison of hold-up values obtained in the present study, using the 40 μm SMP distributor in the 0.051 m ID column,
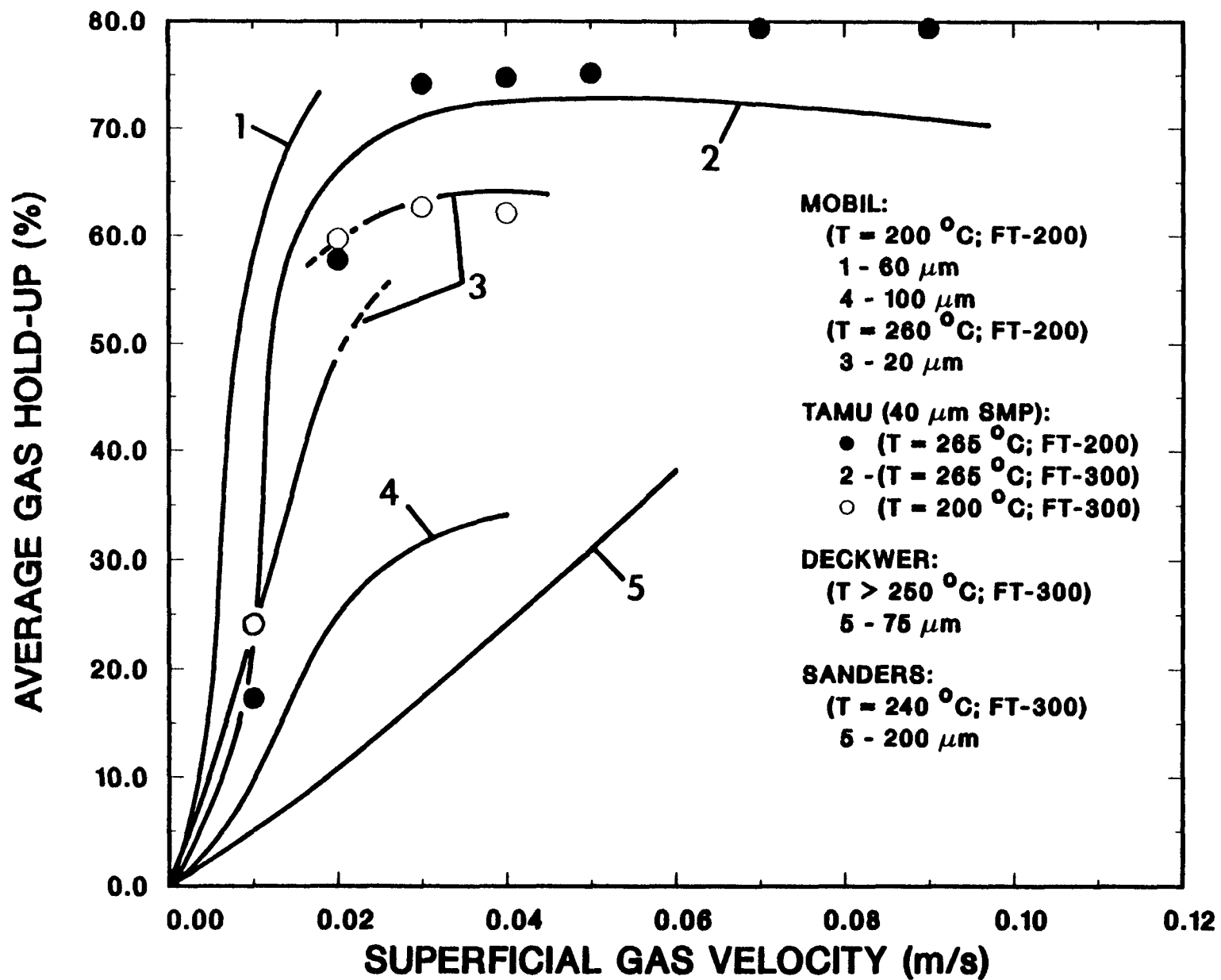
Figure V-37. Comparison of gas hold-ups obtained in studies with sintered metal plate distributors

AVERAGE GAS HOLD-UP (%) — vertical axis (0.0 to 80.0)

SUPERFICIAL GAS VELOCITY (m/s) — horizontal axis (0.00 to 0.12)

MOBIL:
(T = 200 °C; FT-200)
1 - 60 μm
4 - 100 μm
(T = 260 °C; FT-200)
3 - 20 μm

TAMU (40 μm SMP):
● (T = 265 °C; FT-200)
2 - (T = 265 °C; FT-300)
○ (T = 200 °C; FT-300)

DECKWER:
(T > 250 °C; FT-300)
5 - 75 μm

SANDERS:
(T = 240 °C; FT-300)
5 - 200 μm

with data from literature. The curve at 265°C (curve 2) represents an arithmetic average of results from 7 runs conducted using FT-300 wax, while only one run was conducted at 200°C with this wax and experimental data are shown (open circles). In the run at 200°C, foam broke when gas velocity was increased from 0.04 m/s to 0.05 m/s and a transition from the "foamy" to the "slug flow" regime took place. Results presented in Figure V-37 are only those obtained in the "foamy" regime; hold-up values obtained in the "slug flow" regime for this run were presented in Figure V-19. Also shown are hold-up values obtained for a run conducted with FT-200 wax at 265°C (solid circles). All of these runs showed hold-up values that are quite similar considering their variability in the "foamy" flow regime (see Section V-B.2). Mobil's data (Kuo et al., 1985) for FT-200 wax obtained using the 60 and 100 μm SMP distributor at 200°C, and with the 20 μm at 260°C (curves 1, 4, and 3, respectively) are also shown in Figure V-37. Results from the present studies are in fairly good agreement with these data. Mobil's data with the 20 μm distributor were obtained in a 0.051 m ID by 9.1 m tall bubble column. A discontinuity in these data is due to the fact that measurements were taken at different static liquid heights (4.83-6.40 m for the low values of u_g and 3.05 m for u_g > 0.02 m/s). Mobil's data with the 60 and 100 μm SMP distributors were obtained from experiments conducted in a short hot flow column (0.053 m ID, 1.9 m tall) at 200°C. Deckwer et al. (1980) data for a 75 μm SMP distributor (curve 5) were obtained in two bubble columns having diameters of 0.041 m and 0.10 m, using a hard paraffin wax as the liquid medium at temperatures between 250°C and 285°C. Sanders et al. (1986) data with a 200 μm SMP distributor (curve 5) were obtained in a 0. 05 m ID by 2 m tall bubble column,

112

using FT-300 wax at 240°C.

The gas hold-ups reported by Deckwer et al. (curve 5) are significantly lower than the values obtained in the present study (curve 2 and the open and solid circles), or in Mobil's study (curve 1, 3 and 4), even though the operating conditions, the reactor geometry, and the liquid medium are similar in all cases. The discrepancies are probably caused by the differences in the experimental techniques and duration of runs employed in the different studies.

In Mobil's studies with the 100 μm SMP distributor (curve 4) and Sanders et al. study with the 200 μm SMP distributor (curve 5), lower hold-ups were obtained than in the present study, which may be attributed to the use of larger pore size (100 and 200 μm vs. 40 μm).

Mobil's gas hold-ups obtained with the 60 μm SMP at 200°C (curve 1) appear to be too high in comparison to their own data as well as data from the present study. This is partly due to the poor reproducibility of results in the "foamy" regime. The discrepancy might also be caused by the use of a small static height (0.6 m) in experiments with low superficial gas velocities.

In general, there is fairly good agreement between data from the present study and that from literature for SMP distributors. The data from different sources show that the hold-up values tend to decrease with an increase in pore size for the sintered metal plate distributors, which is as expected, since smaller pore sizes would produce smaller bubbles and therefore higher hold-ups.

B.8b. <u>Orifice and Perforated Plate Distributors</u>

Gas hold-ups, obtained with orifice and perforated plate type

distributors, are presented in Figure V-38. Results from our experiments with paraffin waxes (FT-200 and FT-300) conducted in the 0.051 m ID column with the 1, 1.85 and 4 mm orifice plate distributors, and in the 0.229 m ID column with the 19 x 1.85 and 19 x 1 mm perforated plate distributors and the 30 x 1.5 mm perforated pipe distributor are presented. Data from all runs with a given distributor were divided into two groups based on the presence or absence of foam and averaged. Figure V-38 also includes data from literature for experiments conducted under similar conditions.

Gas hold-ups for the run conducted with FT-200 wax using the 1 mm orifice plate distributor in the 0.051 m ID column at 265°C, are in very good agreement with Mobil's results (Kuo et al., 1985) under similar conditions. Foam was present at all velocities with this distributor, resulting in relatively high gas hold-ups. Hold-up values with FT-300 wax in the "foamy" regime decrease as orifice size increases, which is as expected. The 1.0 mm orifice produced the highest hold-ups in this regime, and the 1.85 mm and 4 mm orifice plate distributors produced lower hold-ups. Hold-up values in the larger column (0.229 m ID) were lower than those in the 0.051 m ID in the "foamy" regime, and the effect of orifice hole diameter was rather small. Majority of the distributors employed in the present study produced foam in the velocity range 0.02-0.05 m/s. For velocities greater than 0.05 m/s a transition from the "foamy" regime to the "slug flow" regime (in the 0.051 m ID column) or the "churn-turbulent" regime (in the 0.229 m ID column) occurred.

In the absence of foam, hold-ups do not show any significant effect of distributor type for experiments conducted in the present study. Literature data for flow in this regime (i.e. "slug flow" or "churn-
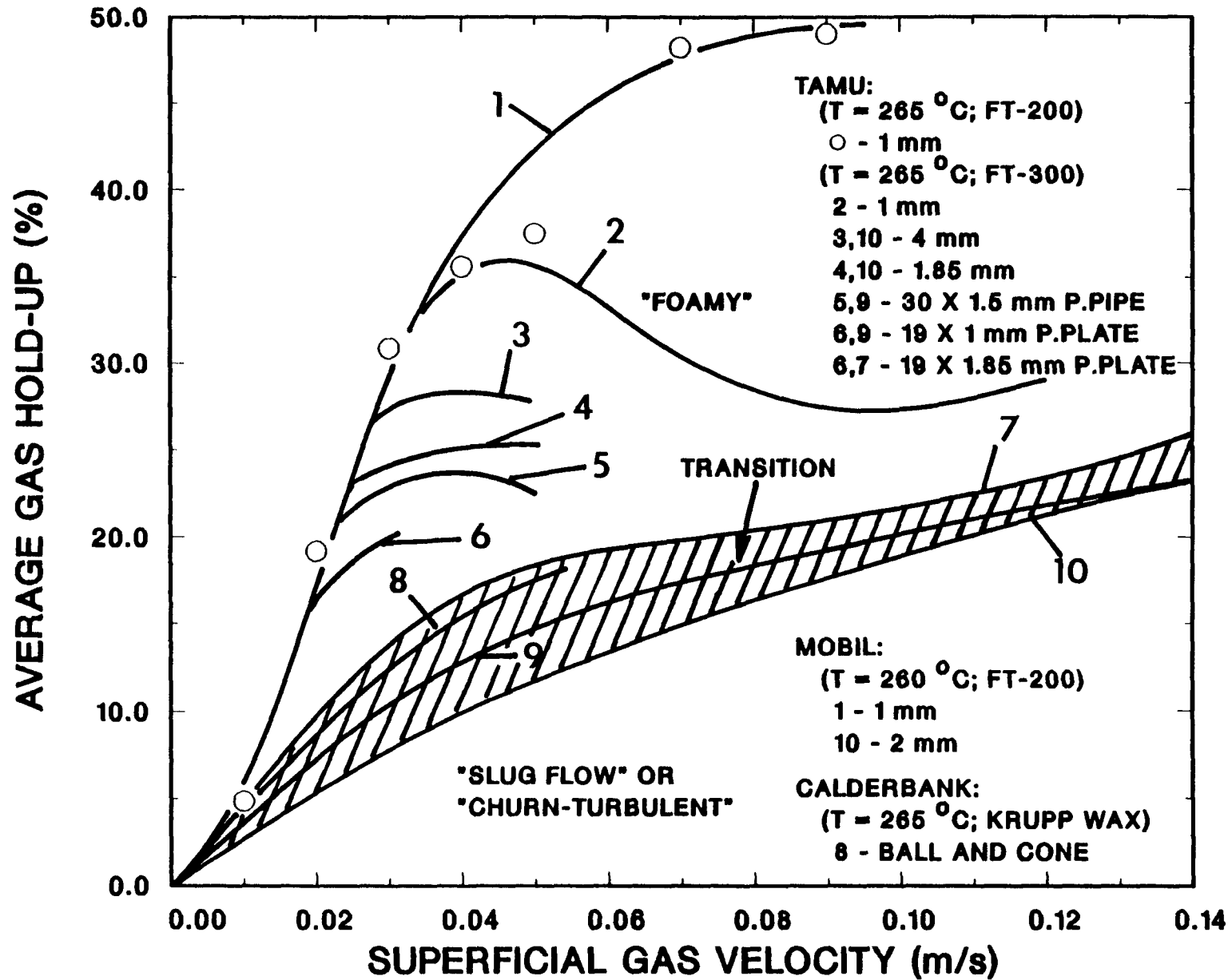
Figure V-38. Comparison of gas hold-ups obtained in studies with perforated plate distributors

turbulent") is very limited. Kuo et al. (1985) presented results from studies conducted with a 2 mm orifice plate distributor. There was no foam produced during this run for the entire range of velocities investigated (0.01-0.12 m/s). This is probably due to the use of a very tall column which provides long residence time and thus facilitates bubble coalescence. The hold-ups obtained in the Calderbank et al. (1963) study with a ball and cone distributor lie between the "foamy" data and the data obtained in the absence of foam. The slight discrepancies could be attributed to the differences in static heights and reactor geometries employed in the different studies. Hold-up values, in the absence of foam, fall in a narrow region (shaded region in Figure V-38), irrespective of the distributor type. This region represents a transition region, and lies between the "foamy" regime and "slug flow" (in small diameter columns) or "churn-turbulent" (in large diameter columns) regime. When hold-up values are in this region, a distinct layer of foam is not present, however, very fine bubbles are still present in the system. The transition region becomes narrower at higher velocities compared to velocities in the range 0.01-0.05 m/s.

Results presented in Figure V-38 show that distributors with smaller holes have a greater tendency to foam. This is consistent with observations reported in literature that in systems with foaming capacity, the "foamy" regime is obtained with SMP distributors and perforated plate distributors having smaller holes, while the "slug flow" or the "churn-turbulent" regime occurs with perforated plate distributors having larger hole diameters (e.g. Zahradnik and Kastanek, 1979; Pilhofer, 1980).

C. AXIAL GAS HOLD-UP MEASUREMENTS

Axial gas hold-up measurements were made in two stainless steel (SS) columns (0.241 m ID and 0.051 m ID by 3.0 m tall). Experiments were conducted at 265°C using FT-300 wax in the 0.051 m ID column, and FT-300 and Sasol's Arge reactor wax in the 0.241 m ID column. The 1.85 mm orifice plate and 40 μm SMP distributors were employed in the 0.051 m ID column, whereas the 19 X 1.85 mm perforated plate distributor was used in the 0.241 m ID column. Increasing order of gas velocities were used for all experiments, except for the 1.85 mm orifice plate distributor, where a run was also conducted using decreasing order of velocities.

The major highlights associated with the axial gas hold-up measurements are:

- Axial gas hold-up increases with height along the column and gas velocity in the presence of foam.

- Axial gas hold-up shows a marginal increase with height along the column in the absence of foam.

- Average gas hold-ups obtained from differential pressure measurements are in good agreement with average gas hold-ups obtained in the glass columns.

C.1. Experimental Apparatus

The two columns were constructed and operated in the same way, therefore, only a description of the differential pressure (DP) system and the operating procedure for obtaining axial gas hold-ups in the small stainless steel column will be presented.

Figure V-39 is a schematic representation of the DP system used with the small stainless steel column for axial gas hold-up measure-

FIGURE V-39

AXIAL GAS HOLD-UP APPARATUS
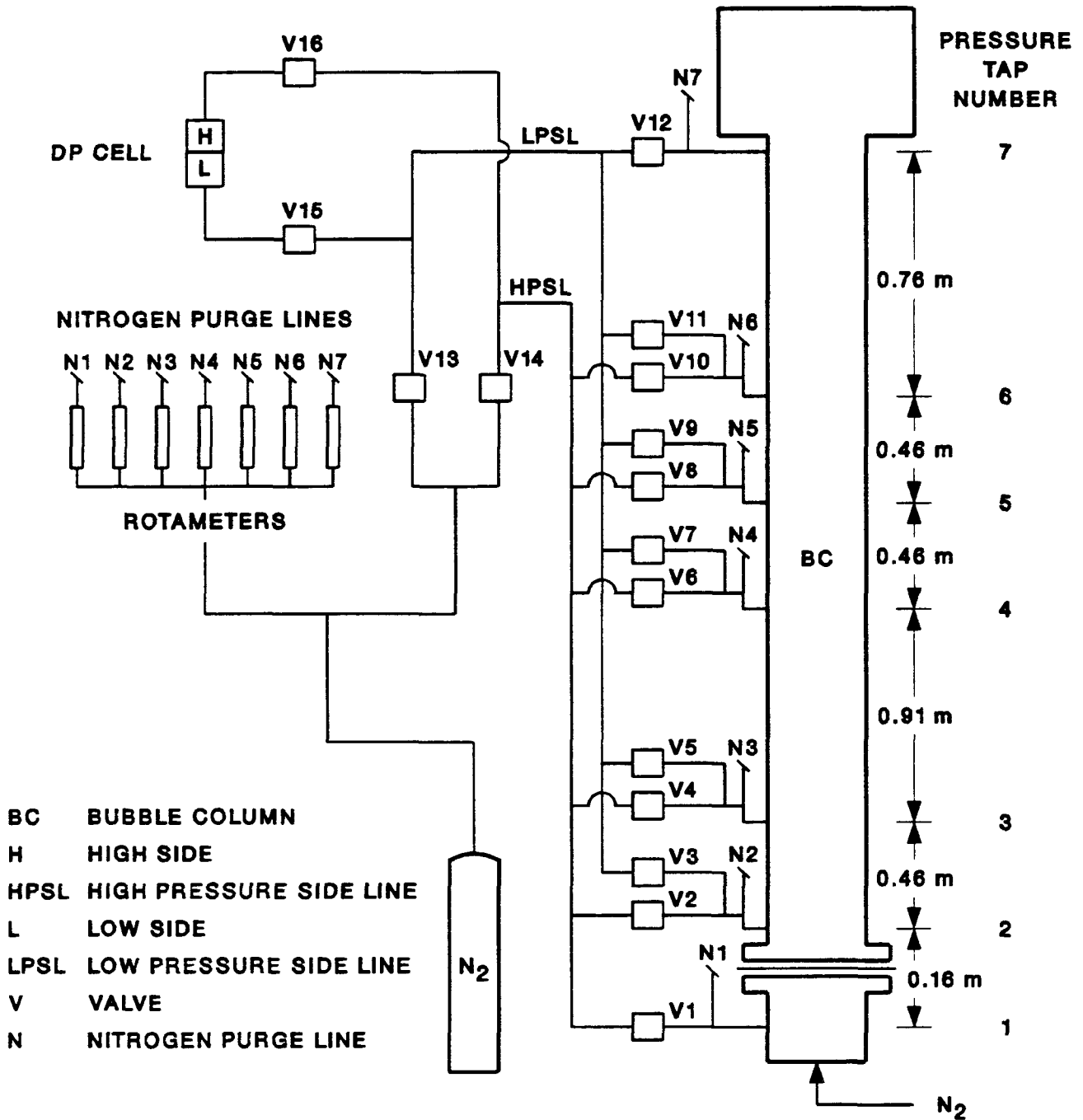
ments. The DP system consists of a series of pressure taps (1 - 7 in Figure V-39), with 0.64 mm holes at seven locations along the column height. Pressure tap 1 is located below the distributor, whereas taps 2 - 7 are located above the distributor. The pressure taps are purged with nitrogen, lines N1 - N7, in order to prevent the wax from entering the pressure tap lines. A series of rotameters (one for each pressure tap) control the nitrogen purge rates. Following the nitrogen purge lines, the pressure tap lines split and are connected to the high pressure side line (HPSL) and the low pressure side line (LPSL), with the exception of pressure taps 1 and 7. Pressure tap 1 is connected only to the HPSL and pressure tap 7 is connected only to the LPSL. Valves V1 - V12 allow axial pressure measurements across any two pressure ports. All of the pressure tap lines, the HPSL and the LPSL are electrically heated to 200°C. Valves V13 - V16 comprise the secondary nitrogen purge system which is used to clear the HPSL and the LPSL if wax enters the lines. The HPSL and the LPSL are attached to the high side (H) and the low side (L) of the DP cell (Validyne Model DP-15), respectively. A readout (Validyne Model CD-223), which is connected to the DP cell, displays the pressure. Pressure fluctuations are recorded with a chart recorder (Cole Parmer Model 8376-30).

C.2. Operating Procedure

The axial gas hold-up is calculated from the axial pressure drop measurements. While making measurements, the secondary purge line valves (V13 and V14) were kept closed and the DP cell connecting valves (V15 and V16) were opened. The DP cell was first calibrated by recording the pressure drop across the column length for different known heights of

distilled water (i.e. a liquid of known density). The rotameters, on the purge lines, were then adjusted to obtain a zero reading across all possible combinations of pressure tap pairs (one high side and low side port) when the column was empty. However, the purge flow through any given rotameter was maintained below 45 cc/min.

After adjusting the DP cell, the column was filled with wax up to the desired height and measurements commenced. The pressure drop across all possible combinations of the pressure taps was measured approximately 45 minutes to one hour after achieving the desired column temperature and gas flow rate. It was necessary to wait at least 45 minutes to ensure that steady state was achieved, particularly when foam was present. For all experiments, the liquid static height was approximately 2.0 to 2.4 m with the exception of the experiment in the small column with the SMP distributor (H_s = 1.0 m). Periodically, the HPSL and the LPSL were cleared by using the secondary nitrogen purge system (i.e. by closing valves V15 and V16 and opening valves V13 and V14).

C.3. Experimental Results

The differential pressure measurements obtained from the experiments were converted to axial and average hold-up values using the data reduction procedure outlined in APPENDIX B.

C.3a. 1.85 mm Single Hole Orifice Plate Distributor

Axial gas hold-up profiles obtained from the experiments conducted in increasing and decreasing order of gas velocities (0.051 m ID column) are shown in Figures V-40 and V-41 respectively. In the experiments conducted from low to high gas flow rates (Figure V-40), three zones of gas hold-up can be noted at the higher gas velocities: (1) low hold-ups are obtained

120
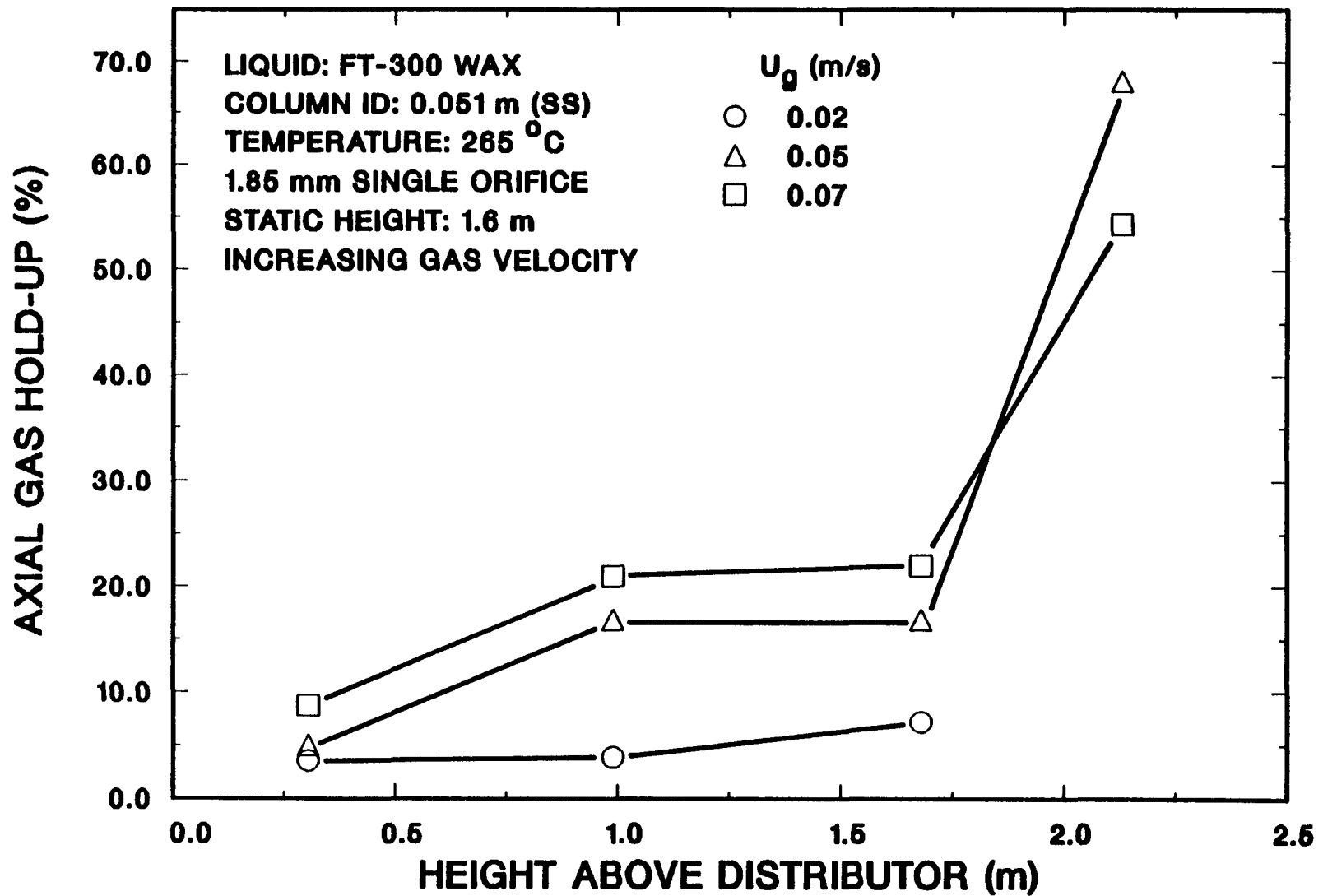
Figure V-40. Effect of superficial gas velocity and height above the distributor on axial gas hold-up (Run 3-4 - increasing order of velocities)

near the distributor; (2) higher hold-ups in the middle of the column; and (3) very high hold-ups (foam) near the top of the expanded bed. In this experiment, the transition from the "foamy" regime to the "slug flow" regime was not complete (as shown in Figure V-42). This is reflected in Figure V-40 by almost similar axial hold-up at the top of the column as velocity was increased from 0.05 to 0.07 m/s. In general, the axial gas hold-up increased with height and gas velocity. The axial gas hold-up profiles follow patterns that were expected based on visual observations. Larger bubbles produced with the 1.85 mm orifice plate distributor break into smaller bubbles as they rise within the column, and consequently the increase of gas hold-up with column height is expected. Further up in the column, the presence of foam causes the higher axial hold-up. The same type of behavior was observed in a 0.051 m ID by 9 m tall bubble column equipped with a 1 mm single hole orifice plate distributor by Mobil workers (Kuo et al., 1985) who used the FT-200 wax as the liquid medium. Towell et al. (1965) and Ueyama et al. (1980) have reported a similar increase in axial hold-up with height for experiments conducted with the air-water system. In both of these studies, froth was present at the top of the dispersion.

For the run conducted in decreasing order of gas velocities (Figure V-41), a start-up velocity of 0.07 m/s was employed. This prevented the formation of foam, and consequently much lower hold-up values were obtained than in the experiment conducted in increasing order of velocities. The axial gas hold-ups were qualitatively the same for both experiments, i.e. the gas hold-up increases with velocity and height. However, the increase of hold-up with height, at a constant superficial gas velocity,
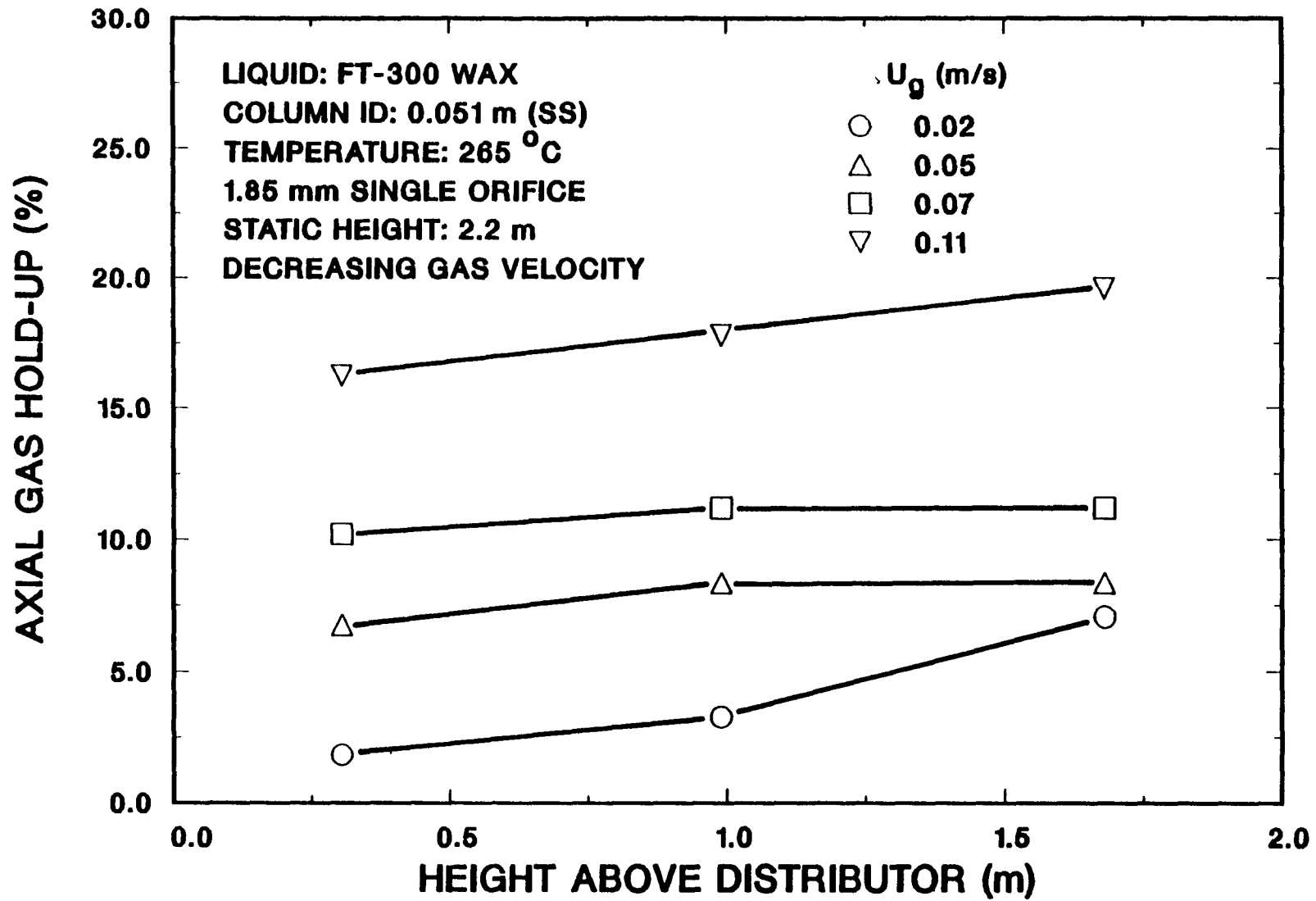
Figure V-41. Effect of superficial gas velocity and height above the distributor on axial gas hold-up (Run 3-5 - decreasing order of velocities)

is fairly small in the "slug flow" regime (Figure V-41). This is in agreement with the findings of Zahradnik and Kastanek (1979) for air-water system.

Figure V-42 shows a comparison of average gas hold-up values obtained from the 0.051 m ID SS column (using DP measurements) with those obtained from the 0.051 m ID glass column (from visual observations of the static and expanded heights). In view of the fact that the experiments were conducted in two different columns (wall surface roughness effect) under somewhat different conditions (e.g. purge flow in the SS column but not in the glass columns) and that different techniques were used to obtain the average gas hold-ups, the agreement in results is quite satisfactory. The main differences in the results are as follows. The foam breakup did not occur to a significant extent in the SS column at velocities greater than 0.05 m/s using an increasing order of gas velocities (open circles); whereas, it did occur in the glass column (open squares). A transition from the "slug flow" regime (where slugs dominate and foam is absent) to the "foamy" regime (where a stable layer of foam persists at the top of the dispersion) took place in the glass column when the velocity was decreased from 0.05 m/s to 0.03 m/s; while, for the experiment conducted in the steel column, using decreasing order of gas velocities, the transition to the "foamy" regime did not occur.

C.3b. 40 μm Sintered Metal Plate Distributor

The axial gas hold-up profiles obtained with the 40 μm SMP distributor are shown in Figure V-43. The same general trends were observed as with the 1.85 mm orifice plate distributor. At higher gas velocities, a significant amount of foam is present even in the

124
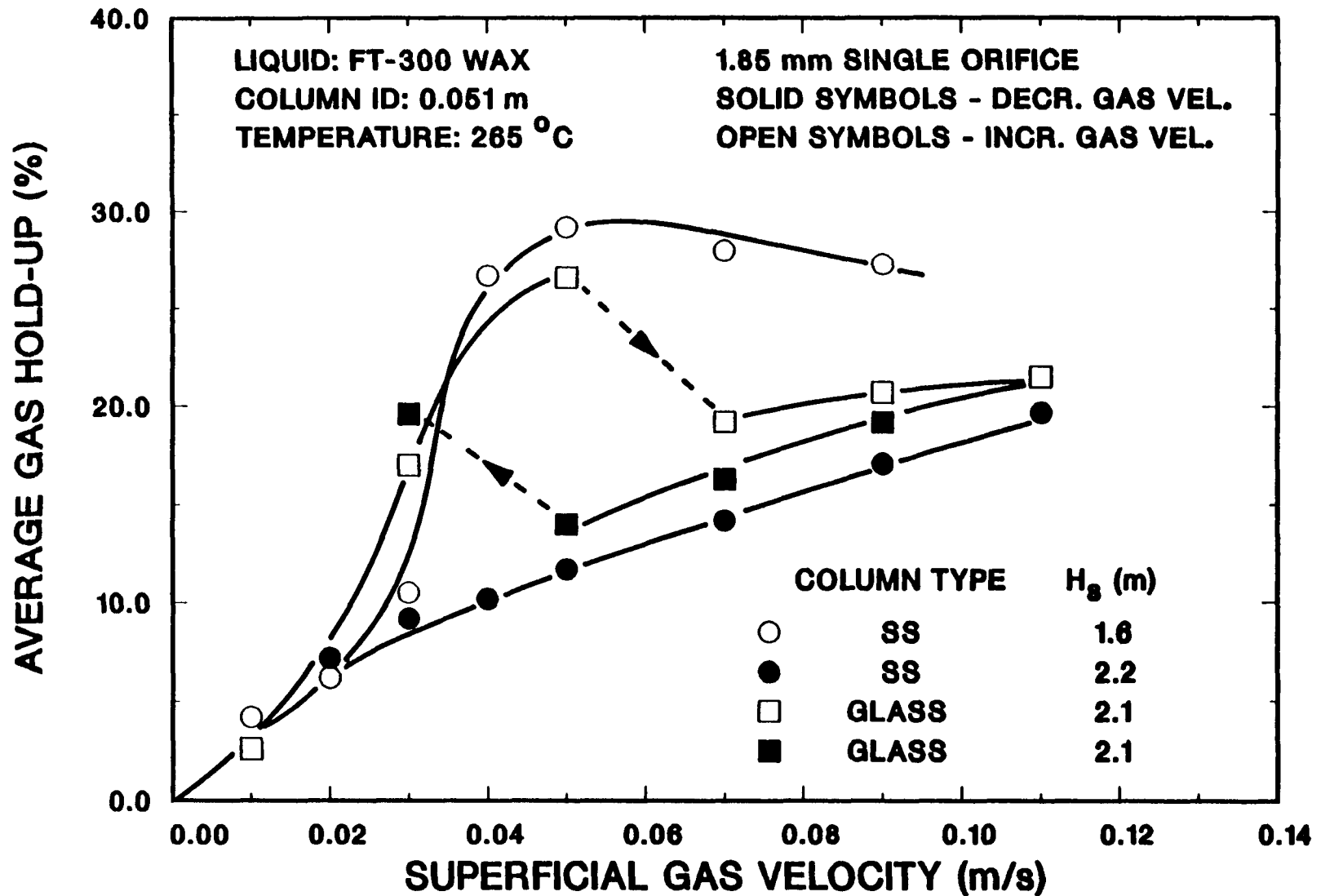
Figure V-42. Effect of superficial gas velocity on gas hold-up (O - Run 3-4; ● - Run 3-5; □,■ - Run 3-1)
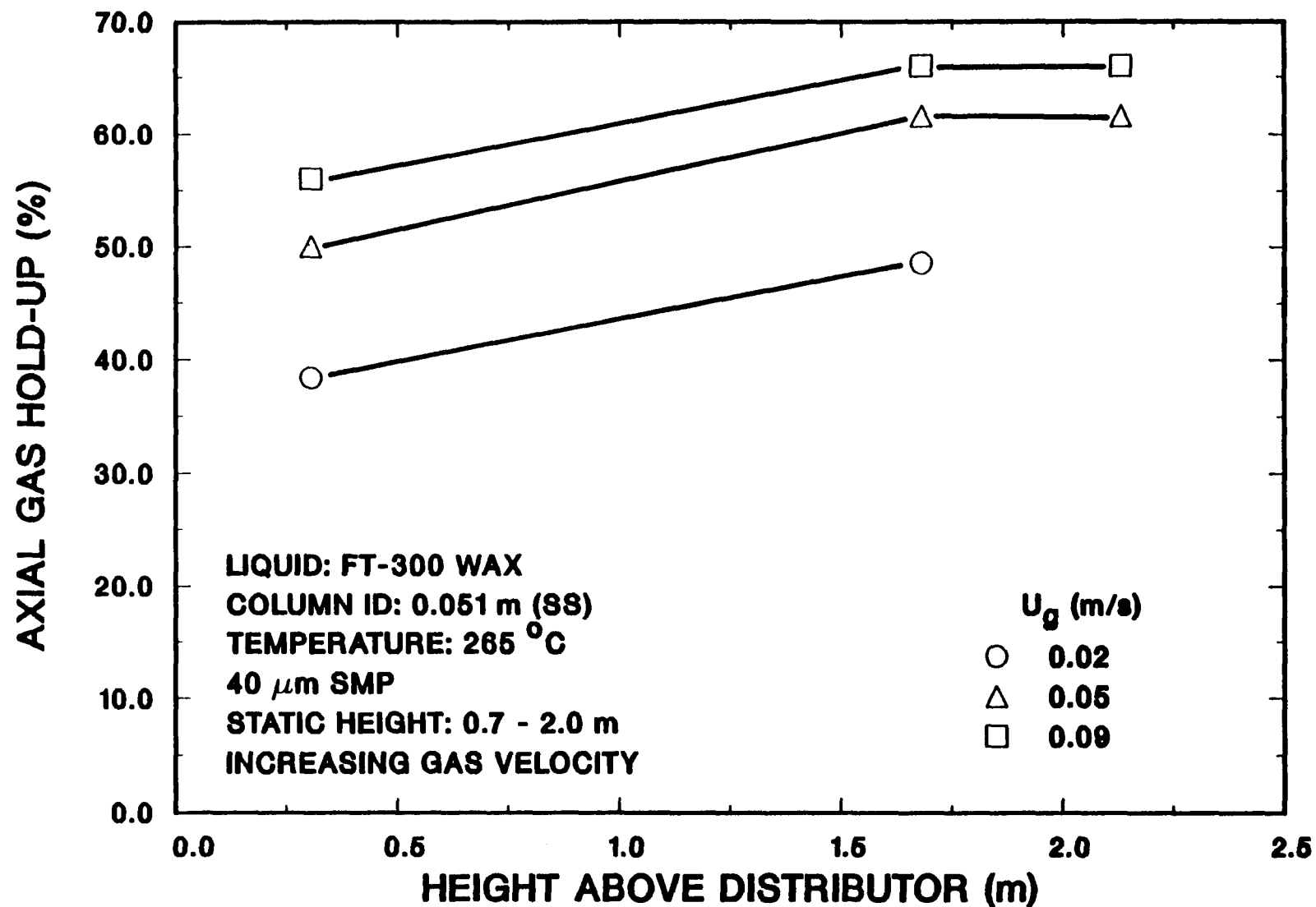
Figure V-43. Effect of superficial gas velocity and height above the distributor on axial gas hold-up (Run 3-7)

lower part of the column, which is in agreement with visual observations.

C.3c. 19 x 1.85 mm Perforated Plate Distributor

Axial gas hold-up profiles obtained in the large column with the 19 x 1.85 mm PP distributor using FT-300 as the liquid medium are shown in Figure V-44. In general, the same behavior was observed as with the axial gas hold-up measurements in the smaller diameter column (see Figure V-41). Namely, in the absence of foam, axial gas hold-up increases with gas velocity, however, it increases only slightly with an increase in column height. The average gas hold-ups at a given velocity were higher in the large SS column as opposed to the large glass column (see Figure V-45). This, along with the constant hold-up profile, indicates that smaller bubbles were present in the 0.241 m ID stainless steel column and they were uniformly dispersed (i.e. the higher average gas hold-ups were not caused by a layer of foam on top of the dispersion but rather by a higher concentration of smaller bubbles dispersed throughout the liquid medium). One possible explanation for this could be the aging of wax. Studies have shown that hold-up tends to be higher in runs conducted with wax that has been on stream for an extended period of time (see Section V-B.2.) The wax used to conduct runs in the stainless steel column was on stream longer than the wax used for the run conducted in the glass column. Therefore, it is expected that smaller bubbles would be produced in the stainless steel column, resulting in higher hold-ups.

Average gas hold-ups obtained using FT-300 as the liquid medium at 200 and 265°C in the 0.241 m ID stainless steel column are shown in Figure V-45; also shown are the average gas hold-ups obtained in the 0.229 m ID glass column. All experiments were conducted using increasing order of

127
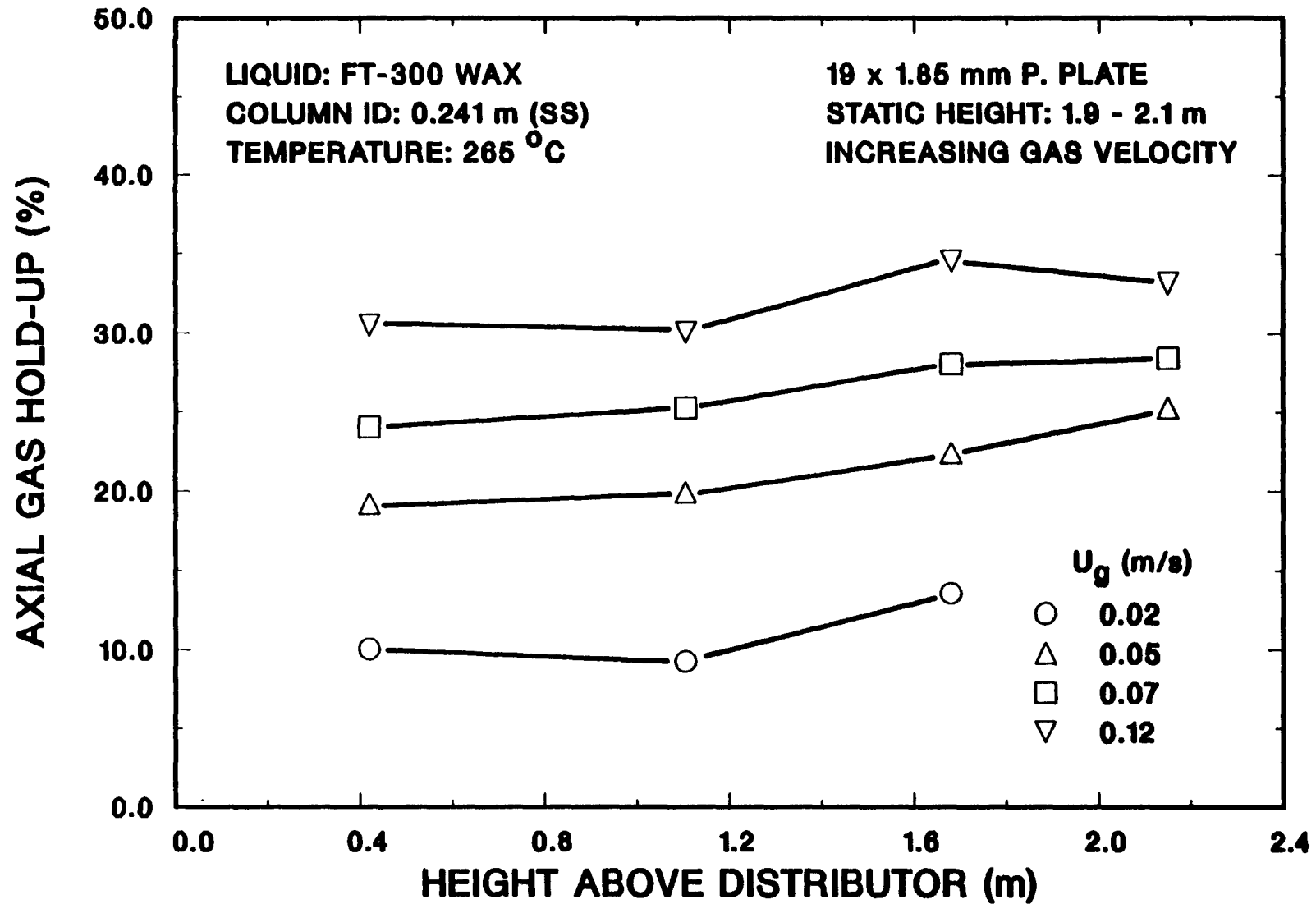
Figure V-44. Effect of superficial gas velocity and height above the distributor on axial gas hold-up (Run 2-7)
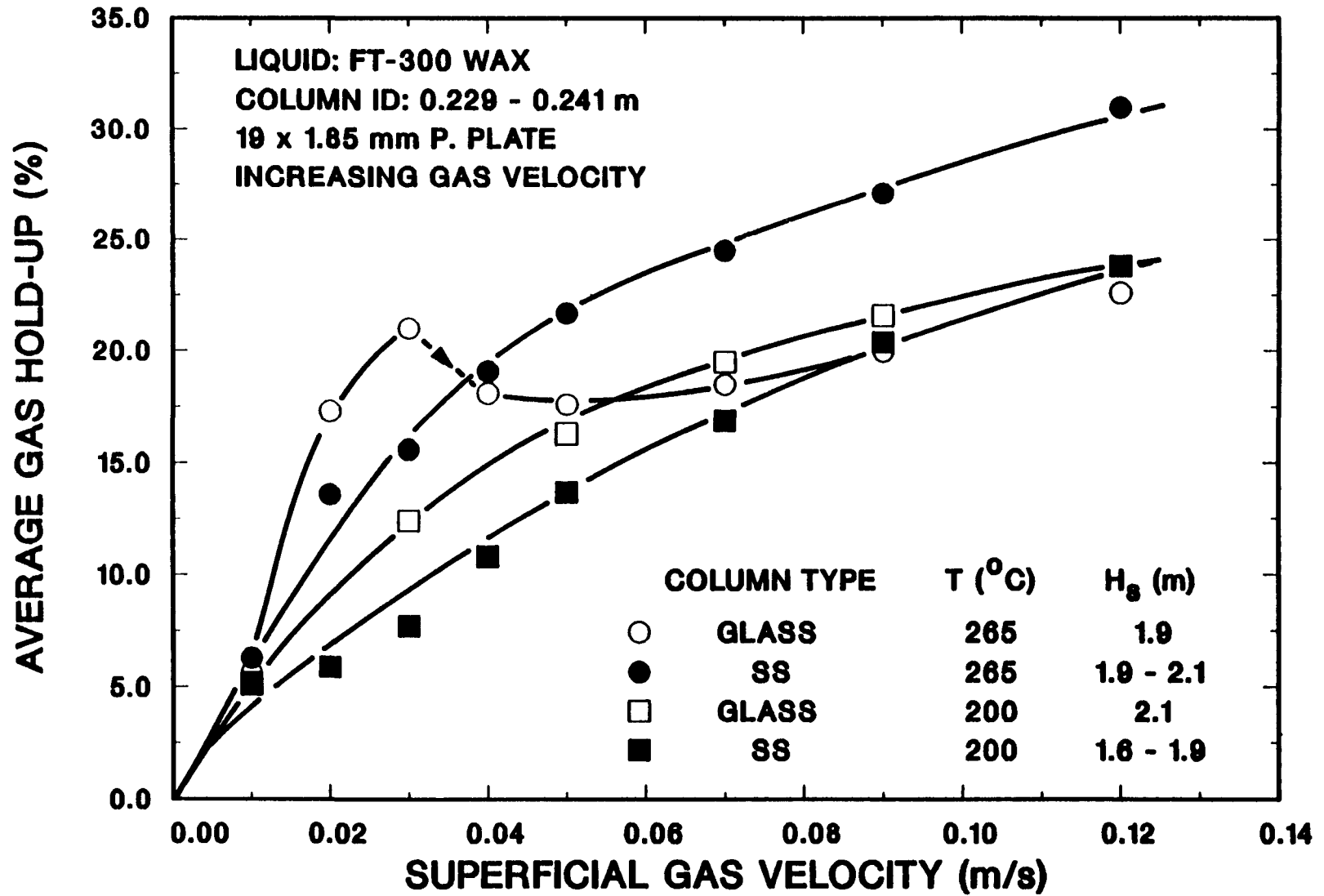
Figure V-45. Effect of superficial gas velocity on gas hold-up (◯ - Run 2-8; ● - Run 2-7; ☐ - Run 1-1; ■ - Run 2-6)

velocities. There is good agreement between the data obtained in the stainless steel column and the glass column especially at 200°C. Average gas hold-ups obtained from the experiment conducted at 265°C in the 0.241 m ID stainless steel column were larger than the values obtained in the "churn-turbulent" regime in the glass column; yet, lower than the values obtained in the "foamy" regime at 0.02 and 0.03 m/s. On the other hand, the gas hold-ups obtained at 200°C in the stainless steel column were slightly lower than those obtained in the glass column at 200°C. A similar trend was observed with Sasol wax in the large column (see Figure V-47) and in the small column with FT-300 wax (see Figure V-42, decreasing order of velocities). This is probably due to overestimating the slurry density in the uppermost section of the column.

Figure V-46 shows the axial gas hold-ups for Sasol wax in the 0.241 m ID stainless steel column. The profiles are different from those obtained with FT-300 wax. Our results with Sasol wax indicate a minimum axial gas hold-up midway along the column height. Sasol wax has a greater tendency to coalesce than does FT-300. For this type of medium, it is possible to reach a maximum stable bubble size along the column height. Above this point, the bubbles may remain unchanged or disperse. This is a possible explanation for the type of behavior we saw with Sasol wax. Kuo et al. (1985) conducted axial hold-up measurements with reactor wax produced in their bench scale unit (Run CT-256-7 wax). Their results indicate a gradual decrease in the axial gas hold-up as column height is increased (for $u_g >$ 0.025 m/s). Since their runs were conducted in a 0.051 m ID column, the presence of slugs would have a significant effect on axial hold-up. It has been shown that in a column of this size, slugs are present for this
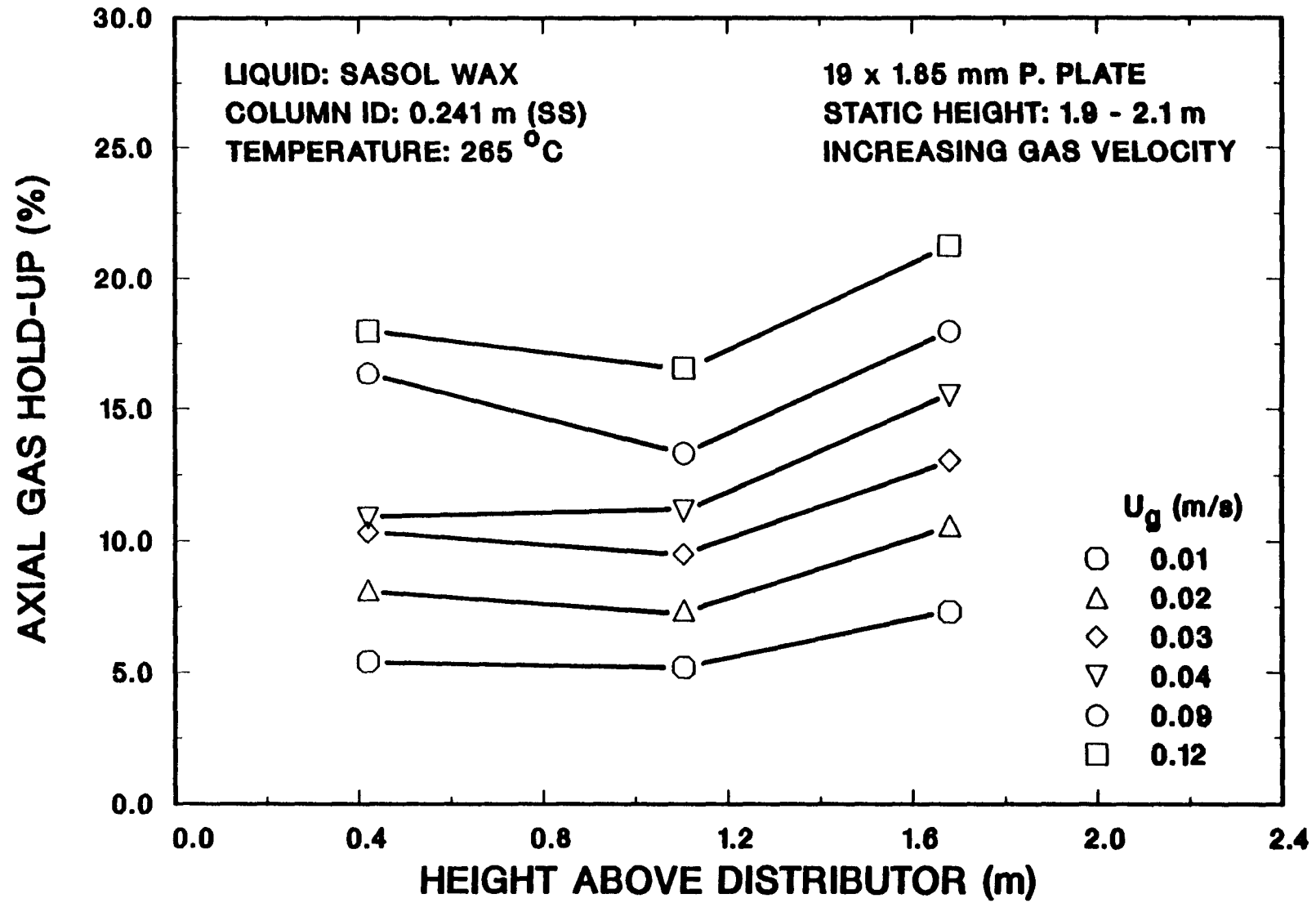
Figure V-46. Effect of superficial gas velocity and height above the distributor on axial gas hold-up (Run 3-1)
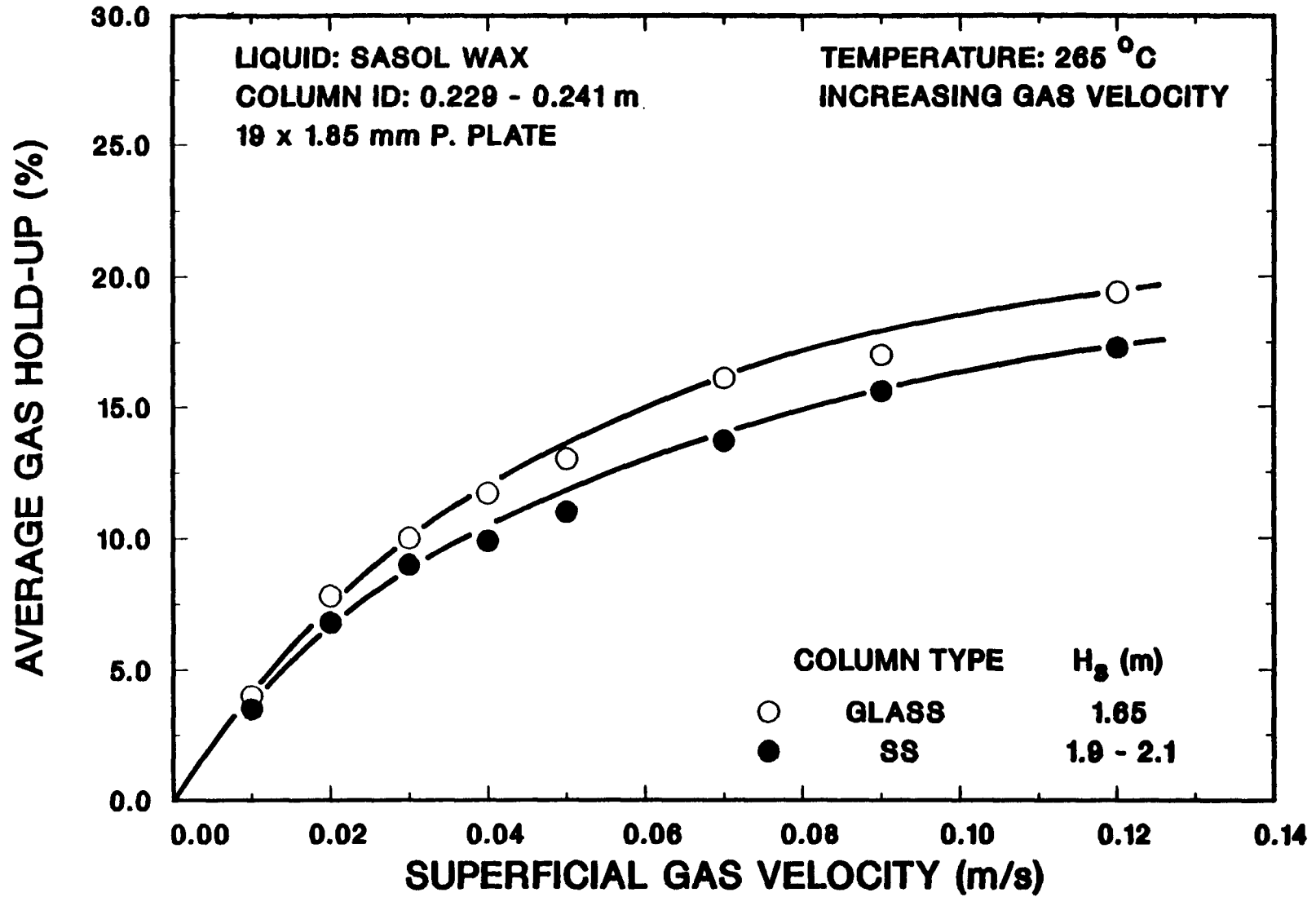
Figure V-47. Effect of superficial gas velocity on gas hold-up (O- Run 3-2; ●- Run 3-1)

velocity range, and therefore, the axial hold-up is expected to decrease with an increase in column height. Whereas, in the present study, where a larger column was used (0.241 m ID), flow is mostly in the "churn-turbulent" regime, where large bubbles are more uniformly mixed with a lot of fine bubbles, therefore, axial hold-up tends to remain constant or increase slightly with column height.

Axial hold-up measurements show that hold-up profiles along the length of the column are dependent on the flow regime. In the presence of foam the gas hold-ups near the top of the dispersion are significantly higher than those in the lower portion of the column. However, in the absence of foam and for systems with a high coalescence rate, the increase in hold-up with column height is only marginal. An increase in gas velocity shifts the axial gas hold-up profile upwards (towards higher values) irrespective of whether the foam is present or not.

D. BUBBLE SIZE DISTRIBUTION MEASUREMENTS

The bubble size distribution, together with the average gas hold-up determines the gas-liquid interfacial area available for mass transfer. Bubble properties such as bubble size and rise velocity, and the axial and radial profiles of bubble size distributions are very important in analyzing the hydrodynamics and gas-liquid mass transfer in the slurry bubble column reactor. Studies were undertaken to determine the bubble size distributions for FT-300 wax and reactor waxes (Sasol's Arge reactor wax and Mobil reactor wax). The effect of operating and design parameters were also investigated during the course of these studies.

The Sauter mean bubble diameter (d_s) is commonly used to represent the bubble size distributions for mass transfer studies in two-phase systems. It is a volume to surface ratio and together with the average hold-up value (ϵ_g) determines the specific gas-liquid interfacial area (a).

The specific gas-liquid interfacial area is the total surface area of all bubbles in the dispersion divided by the volume (V_T) of the dispersion. However, V_T can be obtained by dividing the total volume of the bubbles by the void fraction (or gas hold-up). Assuming spherical bubbles, the following equations can then be used to obtain a definition for the Sauter mean bubble diameter:

$$a = \frac{\Sigma \pi d_i^2}{V_T} = \frac{6 \epsilon_g \Sigma d_i^2}{\Sigma d_i^3} = \frac{6 \epsilon_g}{d_s} \qquad (V-2)$$

where

$$d_s = \frac{\Sigma d_i^3}{\Sigma d_i^2} \qquad (V-3)$$

The diameters of bubbles in a representative sample of the bubble population can now be used to determine the Sauter mean bubble diameter and therefore the specific interfacial area.

D.1. Selection of Techniques

Several techniques are available for the measurement of bubble size distributions. Detailed reviews of these techniques along with their limitations are available in literature (e.g. Buchholz and Schugerl, 1979). Two such techniques were selected for our work; the photographic technique and the dynamic gas disengagement (DGD) technique. These techniques were the most suitable for the hostile environment in the hot flow columns. The photographic technique provides point estimates of the bubble size distributions at various locations in the bubble column, whereas the DGD technique gives an average bubble size distribution for the entire dispersion.

D.2. Bubble Size Distribution Using The Photographic Technique

The photographic method is a direct procedure for measuring bubble size distributions. Despite the tedious process of identifying individual bubbles, this technique is by far the most widely used method for obtaining bubble sizes. The photographic technique was used to obtain estimates of bubble size distributions in FT-300 wax. Selected photographs of the bubbles were enlarged and bubble sizes measured using image analysis. Experiments were conducted in the 0.051 m ID and 0.229 m ID glass columns, and the 0.241 m ID stainless steel column in order to study the effect of various parameters on the bubble size distribution. Majority of the experiments were conducted at 265°C, with a few at 200°C in order to study the effect of temperature. The 1.85 mm orifice plate and the 40 μm sintered metal plate (SMP) distributors were employed in the 0.051 m ID column,

while the 19 X 1.95 mm perforated plate distributor was used in the 0.229 and 0.241 m ID columns.

The major highlights of these investigations are:

- The Sauter mean bubble diameter (d_s) decreases with an increase in height above the distributor. The extent of this decrease depends on the flow regime, with more significant decreases in cases where foam is present.

- The presence of foam results in lower Sauter mean bubble diameters compared to values when foam is absent. Sauter mean diameter for pure foam was found to be around 0.5 mm.

- The value of d_s appears to be fairly constant with changes in superficial gas velocity in the 0.051 m ID column, however in the large columns (0.229 m ID glass and 0.241 m ID SS), it decreases marginally with an increase in superficial gas velocity. In general, d_s approaches a fairly constant value for higher values of u_g (> 0.07 m/s).

- The 40μm SMP distributor produced significantly smaller bubbles (d_s = 0.5-0.7 mm at 265°C) compared to the 1.85 mm orifice plate distributor (d_s = 1.2-2.2 mm under similar conditions). However, d_s in the 0.229 m and 0.241 m columns, with improvements in the technique (significantly larger bubble count), were around 0.5 mm at the wall and around 0.8 mm at the center (for velocities greater than 0.05 m/s). The latter values are comparable with results reported in literature for studies conducted using molten wax as the liquid medium.

- Sauter mean diameter is greatly affected by radial position with larger values in the center of the column than at the column wall.

136

This is compatible with observations reported in literature for the air-water system.

- In the presence of oxygenates lower Sauter mean bubble diameters were obtained.

- Temperature did not have a significant effect on d_s for the 0.051 m ID column, whereas d_s decreased (between 25-50% relative) in the 0.241 m ID column as temperature was decreased from 265°C to 200°C.

D.2a. Image Analysis

Photographs selected for analysis were enlarged to 8" by 10" and analyzed on a Zeiss image analyzer located in the Biology Department at the University of Texas at Austin. An illustration of the image analysis system is shown in Figure V-48. A description of the hardware and software associated with image analysis is given below.

D.2a.1. Hardware

The TV camera (1) converts an image of the photograph falling on its light sensitive pickup tube into an analog electrical signal. This signal is sent to an array processor, IBAS II (3), where it is converted to numerical form by an analog to digital converter so that it can be manipulated by the computer. Processed images are sent through a digital to analog converter and then to a display monitor (2). The image analyzer is only able to distinguish between shades of gray, therefore, when bubbles overlap, the image analyzer treats such bubbles as a single bubble. However, IBAS II allows the user to edit the original image in order to circumvent this problem. This is done using the digitizer tablet with mouse or light pen (7). With the light pen the user can trace over the bubbles that are to be analyzed. Once this is complete, a variety of object speci-

137

FIGURE V-48
IMAGE PROCESSING SYSTEM
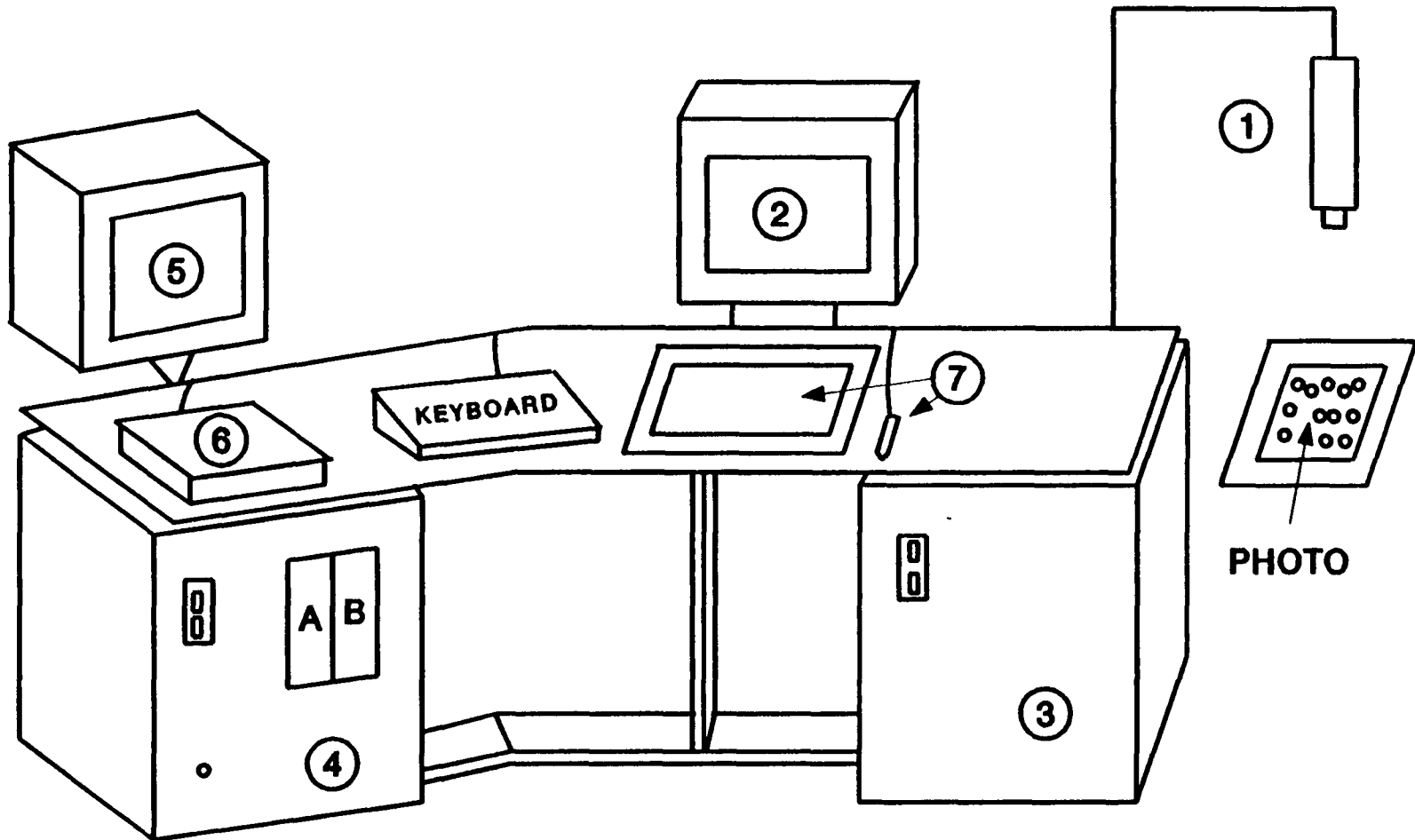
1 - TV CAMERA   2 - DISPLAY MONITOR   3 - IBAS II   4 - IBAS I
5 - DATA MONITOR   6 - PRINTER   7 - DIGITIZER TABLET & LIGHT PEN

fic parameters can be calculated and displayed on the data monitor (5) and/or printer (6). A host computer, IBAS I (4), performs the tasks of a manager. It communicates with the user, manages the image processing programs (or software) for IBAS II, and is also capable of some statistical analysis. IBAS I is equipped with floppy disk drives and hard disk drives that allow the storage of parameters for further analysis.

D.2a.2. Software

The image analysis software consists of two separate programs, the first program controls the operations of the array processor (IBAS II) and the second program is used to perform statistical analysis on data generated by IBAS II. Both programs are stored on a floppy disk and are loaded into the computer's memory using the disk drives in IBAS I.

IBAS II Controller Program: This program consists of predefined function groups and functions that allow the image analyzer to perform the various tasks necessary for bubble size measurements. Following is a list of tasks handled by this program:

a.   Input of image into the computer.

b.   Scaling of the image or calibration: A wire piece of known length (usually 12 mm long) is glued to the wall of the bubble column in the field of the camera used to take photographs. Thus, every photograph of the bubbles also contains an image of this reference piece. During the calibration process the user locates the two ends of the reference piece on the TV image and marks them using the light pen and digitizer tablet. A corresponding value of the actual length is also entered into the computer. The computer then evaluates the scaling factor.

c. Enhancement of the image in order to correct for uneven lighting or poor contrast in the photographs.

d. Interactive editing, which allows the user to trace the individual bubbles using the light pen and digitizer. Bubbles that overlap or touch one another are separated by redrawing them in open spaces on the image. At the end of this step only those bubbles have been identified which are clear and distinct. This step involves some subjective judgement on the part of the user, thus introducing human error. There is a definite bias toward the inclusion of a greater proportion of larger bubbles at the expense of tiny bubbles. The implication of this prejudice towards larger bubbles is discussed later in the Section V-D.2e.

e. The actual sizing and classification of bubbles based on the parameters selected (see Section V-D.2b.).

Statistical Analysis Program: This program requires very little user interaction. It reads the data output by the previous program and performs the necessary statistical calculations. After the initial classification of bubble sizes into 40 classes, it was found that in majority of the cases 95% of the bubbles were classified in the first 15 to 20 classes with the other 5% distributed in the remaining 20 to 25 classes. In order to improve upon this distribution, bubbles in the first 15 to 20 classes were reclassified into 40 classes instead. As a result, for each photograph, bubbles were distributed in 60 to 65 classes or groups based on the diameter of the area equivalent circle (d_B). Three user-defined parameters were estimated for each bubble; $(d_{MAX}+d_{MIN})/2$, d_B^2, and d_B^3. The following statistical

quantities were also calculated for each of these parameters for all bubbles in a given photograph: arithmetic and geometric means, variance, and the second and third moments. The program also produced a plot of the number frequency of bubbles as a function of bubble diameter (histogram) and a cumulative frequency plot (or a plot of the total number of bubbles smaller than a given diameter versus bubble diameter) of bubbles in a given photograph, based on the d_B values for the groups.

D.2a.3. Data Reduction - Sauter Mean Diameters

Data obtained from image analysis were used to estimate the Sauter mean diameter d_s for bubbles in individual photographs. Two values of Sauter mean diameter were calculated. The first was estimated from diameters of individual bubbles using Equation (V-4).

$$d_s = \frac{\Sigma d_{Bi}^3}{\Sigma d_{Bi}^2} \qquad (V-4)$$

where d_{Bi} is the diameter of the area equivalent circle. The second value of d_s was estimated for the bubble groups (classified during the image analysis step). The groups were formed according to the size of bubbles, and typically between 60 to 65 bubble groups were formed for a given photograph. The upper and lower size limits for each group were averaged and it was assumed that this averaged value represented the diameter of all bubbles in that group. Equation (V-5) was then used to estimate a d_s value for these groups.

$$d_s = \frac{\Sigma n_i d_{Bi}^3}{\Sigma n_i d_{Bi}^2} \qquad (V-5)$$

where d_{Bi} is the representative diameter for the i'th group and n_i is the number of bubbles in that group. The difference between the two values of

d_s was less than 0.1% for most cases. Therefore, parameters based on groups were used in subsequent analysis. A cumulative density function was generated for each photograph analyzed.

D.2b. <u>Parameter Selection for Bubble Size Measurements</u>

The photographic technique to measure bubble size distributions approximates the true particle size distribution (particles having three dimensions) by a profile size distribution (measurements in two dimensions). Errors involved in this approximation depend partly on the parameter chosen to represent the diameter of the bubble. The size of a particle or bubble in profile can be characterized by four different measures (Weibel, 1980).

a.   Maximum and minimum diameters: These are also defined as the largest and smallest caliper diameters. A caliper diameter is defined as the distance between two parallel lines that are tangent to the particle profile. These dimensions in effect describe the shape of the particle. An average of these two dimensions could be used as a representative diameter of the particle.

b.   Feret diameter: This is a random caliper diameter. It is measured by the distance between two parallel lines that are tangent to a particle which is in any random orientation. However, when a profile is used to measure the diameter of a solid particle, the mean Feret diameter would be a better representation of the particle's dimension.

c.   Chord or intercept length: This is the intercept of a random test line by the particle's boundaries. A mean value for this length could be used as the particle diameter.

d. Area equivalent diameter: This is the diameter of the circle which has
    the same area as the particle.

The image analysis system can measure all four diameters, however the
area equivalent diameter requires the least amount of computation. It has
been shown (Weibel, 1980) that for a circle, the mean Feret diameter and
the area equivalent diameter are the same, however the mean chord length is
slightly lower (mean chord length = 0.79 times area equivalent diameter).
However, for ellipses of axial ratio greater than one, the following rela-
tion holds true:

mean Feret diameter > area equivalent diameter > mean chord length

The four parameters discussed above were estimated from image analysis
results for photographs of the FT-300 wax - nitrogen system. The results
are summarized in Table V-1. These values are in agreement with the rela-
tionship given above for ellipses.

Akita and Yoshida (1974) used the average of the minimum and maximum
diameters to represent the size of bubbles obtained from photographic
measurements in their study. In the present study it was decided that the
area equivalent diameter would be used as an estimate of the bubble
diameter. The choice of the area equivalent diameter is justified by two
factors; (1) it requires the least amount of computation, and (2) the
primary purpose of measuring diameter is to use it to estimate the Sauter
mean diameter, which assumes a spherical particle. As shown in Table V-1,
the area equivalent diameter is between 4 to 10% lower than the average of
the maximum and minimum diameters. This difference is not too significant
considering other sources of error.

Table V-1. Comparison between parameters used for bubble diameter measurements (FT-300 wax, 265°C, 0.051 m ID column, 1.85 mm orifice plate distributor).

u_g (m/s)	Height (m)	Parameter value (mm)			
		d_{ave}	d_{Feret}	d_{chord}	d_{circ}
0.01	0.3	0.69	0.74	0.45	0.65
0.01	1.2	0.81	0.87	0.54	0.77
0.01	1.8	0.52	0.56	0.35	0.50
0.02	1.2	0.61	0.66	0.39	0.58
0.03	0.3	0.59	0.63	0.38	0.56
0.03	1.2	0.59	0.63	0.38	0.55
0.03	1.8	0.45	0.52	0.26	0.40
0.04	0.3	0.63	0.72	0.35	0.56
0.04	1.2	0.67	0.76	0.37	0.60
0.04	1.8	0.46	0.52	0.26	0.41
0.07	1.2	0.51	0.58	0.29	0.46
0.09	0.3	0.53	0.62	0.30	0.49
0.09	1.2	0.58	0.62	0.30	0.52

D.2c. <u>Experimental Procedure</u>

Various lighting arrangements, cameras, and lenses were tried in the 0.051 m ID column in order to improve the quality of photographs for bubble size measurements. The best arrangement for this column consisted of two 1000 watt lights (Colortran) placed at angles of 90° with respect to the front of the column in a staggered position (i.e. one 0.15 m above the field of view and the other 0.15 m below the field of view). A shield (flat black metal plate) was placed between the lower light and the field of view. Milar paper was placed between the field of view and the light at the top in order to reduce the glare. A Canon, AE1/P (35 mm SLR) camera was used with Canon auto bellows and a 135 mm Canon lens with a polarized filter. Photographs were taken for all velocities (0.01 to 0.12 m/s) at heights of 0.45, 1.20 and 1.95 m, except when foam filled the entire column (photographs were taken only at 1.20 m for such cases).

Two different lighting arrangements were used while photographing bubbles in the 0.229 m ID column, one for low gas velocities (< 0.05 m/s) and one for gas velocities greater than 0.05 m/s. A Vivitar Model 283 flash was attached to the Canon camera for all photographs. The flash was mounted approximately 0.25 m from the column at an angle of 45° with respect to the front face of the column. At low gas velocities, the Canon 135 mm lens mounted on the Canon auto bellows with an extension of 110 mm was employed. At higher velocities, a 50 mm Canon lens was mounted on the Canon auto bellows with an extension of 70 mm. An f/stop of 16 was found to produce the best results. Photographs were taken for all velocities at heights of 0.41, 1.12 and 1.96 m. The arrangement used in the 0.241 m ID stainless steel column (viewing port) was the same as that used with the 0.229 m ID

145

column at higher gas velocities.

The photographs were taken after a run time of one hour at a given velocity, for velocities of 0.01 to 0.05 m/s, and after 45 minutes for gas velocities greater than 0.05 m/s. A minimum of four photographs were taken at each velocity using Kodak 400 ASA Tri-X Pan film. In the 0.229 m ID column, photographs were also taken just after the gas input to the column was shut off, after each velocity. This was done in order to obtain bubble size distributions after the large bubbles had disengaged from the dispersion.

A major problem with the use of the photographic technique with cylindrical columns is the 'curvature effect' The curvature of the column wall distorts the image of the bubbles in the column since the wall behaves like a convex lens. In order to alleviate this problem, the area of the column that was photographed was kept at a minimum (approximately 15 X 20 mm). The distance between the lens and the column wall was typically between 30 to 50 mm. This also helped in the image analysis procedure since the individual bubbles were more distinct when photographed at a close range.

D.2d. <u>Experimental Results</u>

The photographic technique could be used only with FT-300 wax because of its clarity and water-like appearance. Measurements were made mostly in the 0.051 m ID and 0.229 m ID glass columns, with some photographs of the flow field near the center of the column taken through the specially con-structed port (see Figure V-49) in the 0.241 m ID stainless steel column. It was not possible to use this technique with the Mobil and Sasol reactor waxes due to their dark color.
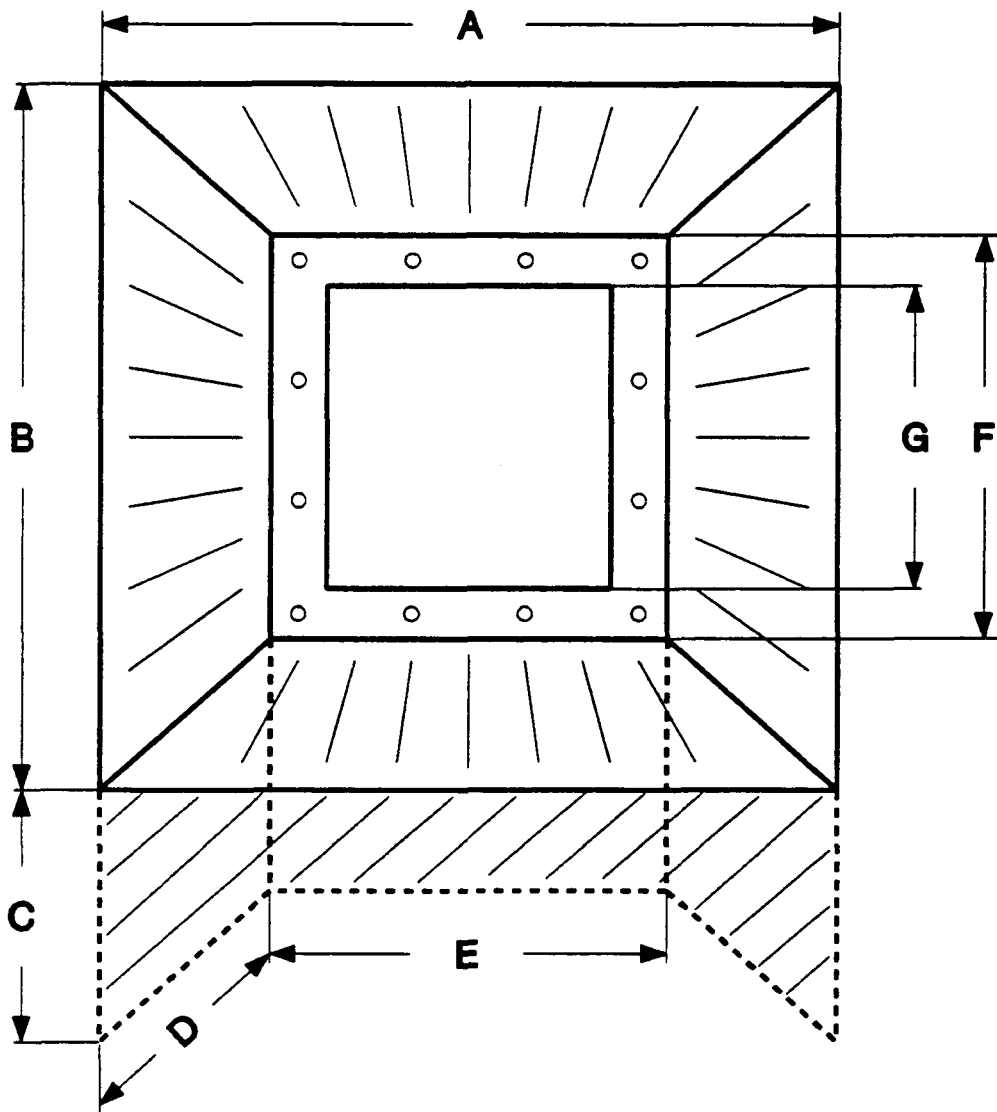
A = 0.20 m   B = 0.20 m   C = 0.05 m   D = 0.11 m

E = 0.10 m   F = 0.10 m   G = 0.08 m

ure V-49. Viewing port in the 0.241 m I.D. SS column

Results from photographs taken in the 0.051 m ID column are discussed qualitatively because of the relatively small number of bubbles sized per condition (400 - 500). The effect of large bubbles is significant for this case (see Section V-D.2e.). However, the technique was improved when used in the 0.229 m ID glass column and quantitative analysis was possible for this case. Data from two photographs were used at each condition for this column and the number of bubbles sized was considerably larger (1500 - 1700). As a result it would not be prudent to assess the effect of column diameter based on the photographic data.

D.2d.1. Effect of Height Above Distributor

Figure V-50 shows the Sauter mean diameter for FT-300 wax from measurements made in the 0.051 m ID column. The measurements were made at 265°C using the 1.85 mm orifice plate distributor. Results are shown for three different superficial gas velocities, 0.01, 0.03 and 0.09 m/s. Approximately 400-500 bubbles were catalogued and sized at each condition. These results show that d_s does not vary significantly in the lower half of the column (up to about 1.25 m above the distributor), however, d_s decreases above this point. The maximum drop in the value of d_s appears to be at a gas velocity of 0.03 m/s, from 1.7 mm to 0.8 mm at a height of 1.75 m. The cumulative frequency distributions presented in Figure V-51 support the trends observed in Figure V-50. At a superficial gas velocity of 0.03 m/s, Figure V-51 shows similar bubble size distributions at heights of 0.45 and 1.2 m above the distributor, however, the distribution shifts to the left at a height of 1.95 m, indicating the presence of smaller bubbles. These curves also indicate that the bubble size distribution at a height of 1.95 m above the distributor is narrower than those at lower heights (i.e.
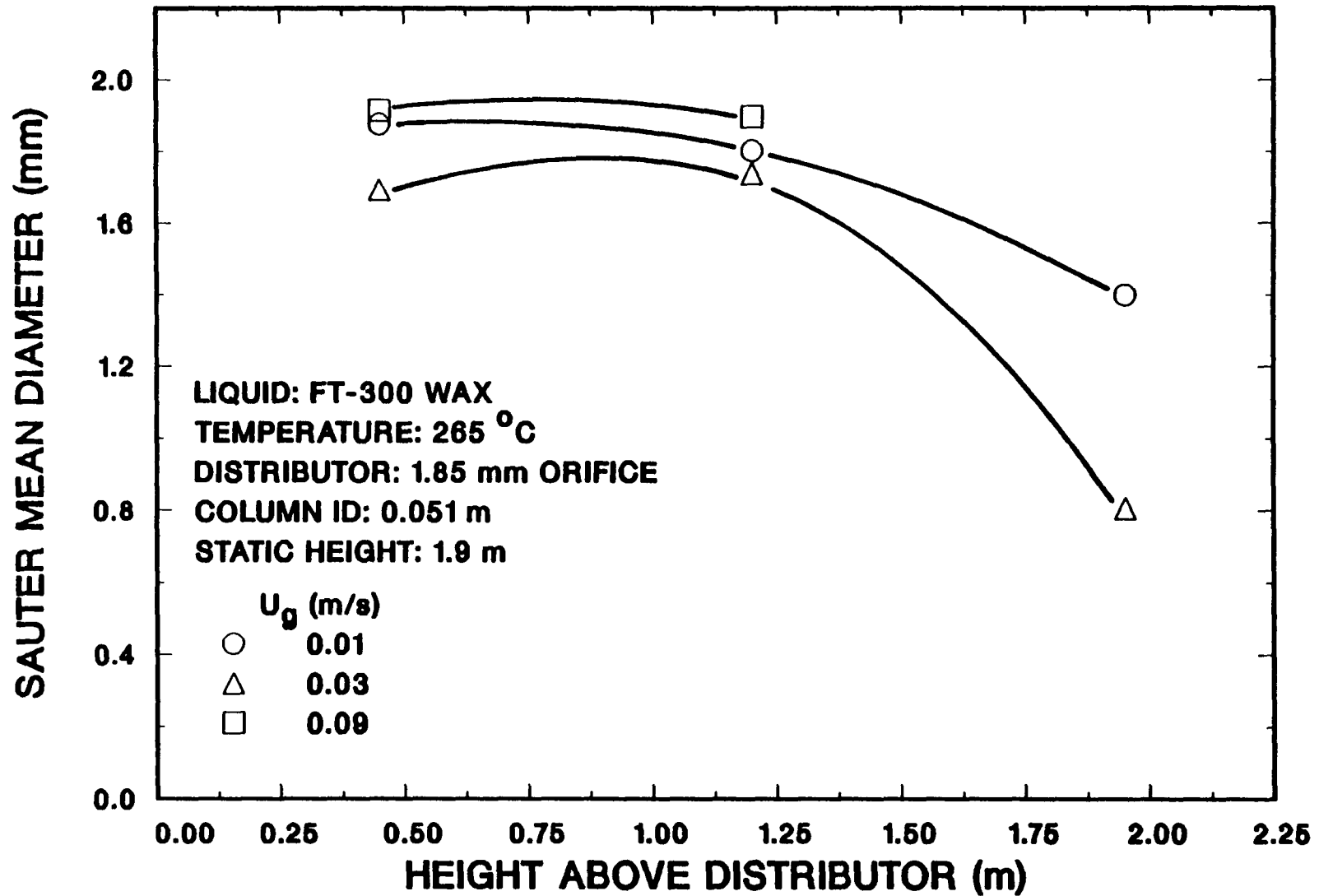
Figure V-50. Effect of superficial gas velocity and height above the distributor on the Sauter mean bubble diameter (Run 4-1)
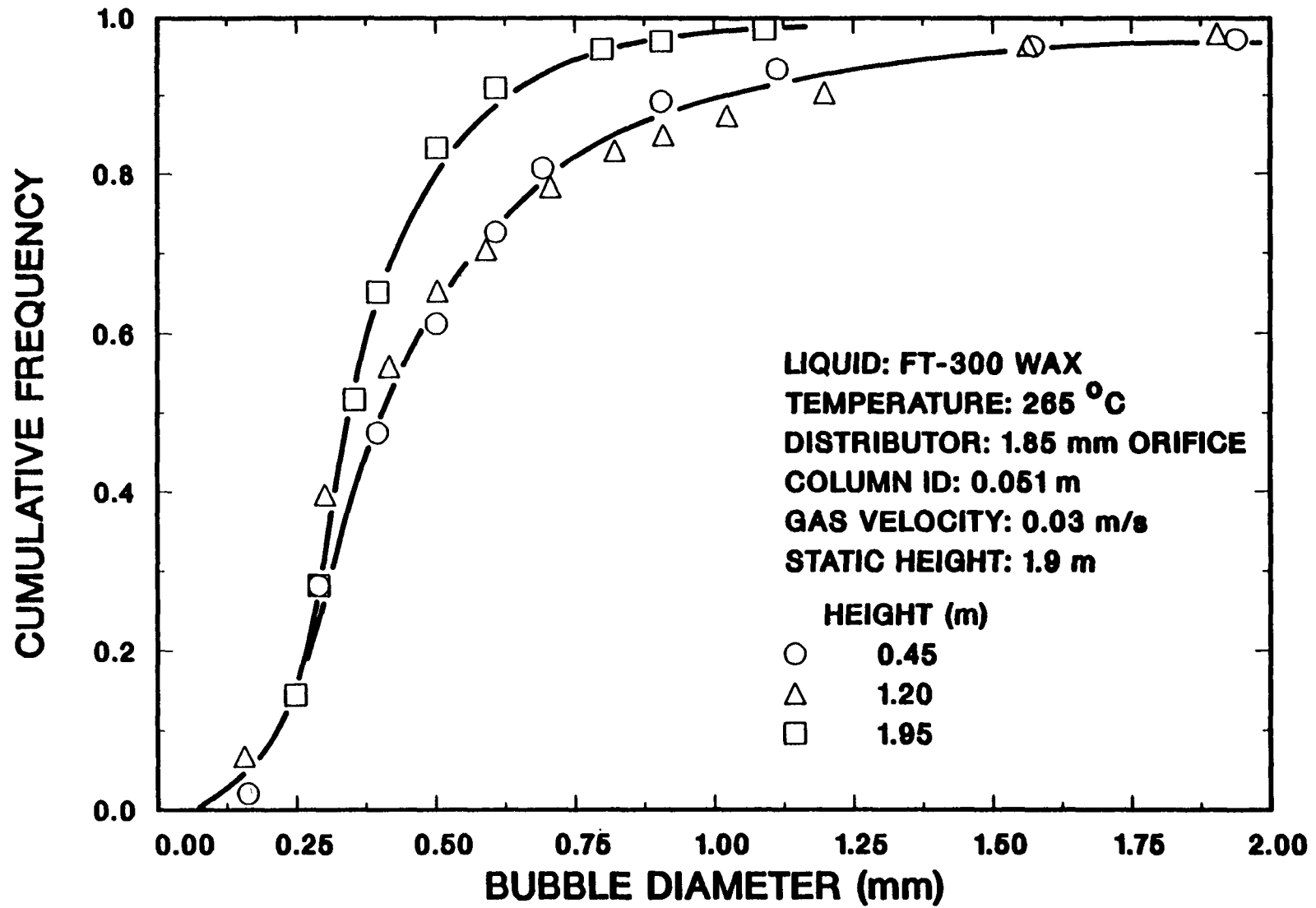
Figure V-51. Effect of height above the distributor on the bubble size distribution (Run 4-1)

0.45 and 1.2 m). Similar trends were observed at other velocities as well.

Figure V-52 shows the variation of d_s with height above distributor for a run conducted in the 0.229 m ID column with FT-300 wax at 265°C using a 19 X 1.85 mm perforated plate distributor. Results obtained at superficial gas velocities of 0.01, 0.05 and 0.09 m/s are presented in this figure. In this case two photographs were selected and analyzed for each condition, and d_s for the individual photographs was calculated. Results from the two photographs were then combined and d_s for the combined data was calculated. Thus, approximately 1500-1700 bubbles were catalogued and sized at each condition. The various symbols in Figure V-52 represent d_s from combined data, while the vertical bars connect d_s values from individual photographs. Only one photograph could be analyzed at 0.09 m/s for a height of 1.12 m above the distributor. The results once again indicate trends which are similar to those observed in the 0.051 m ID column, however, they are not as significant as in the previous case. At 0.01 m/s, d_s for the combined data (from the two photographs at each condition) decreases from 1.2 mm at 0.41 m above the distributor to 1.0 mm at a height of 1.96 m above the distributor, a relative difference of less than 20%. The significance of this difference is further diminished because of the variability in d_s values from the individual photographs for a given condition. For example, at 0.01 m/s and at a height of 0.41 m above the distributor, d_s from individual photographs is 0.9 mm and 1.5 mm compared to a d_s value of 1.2 mm for the combined data. This translates into a relative difference of ±25% between the individual and combined values. However, similar comparisons at the other conditions reveal significantly lower variations, as can be seen in Figure V-52. The limited results
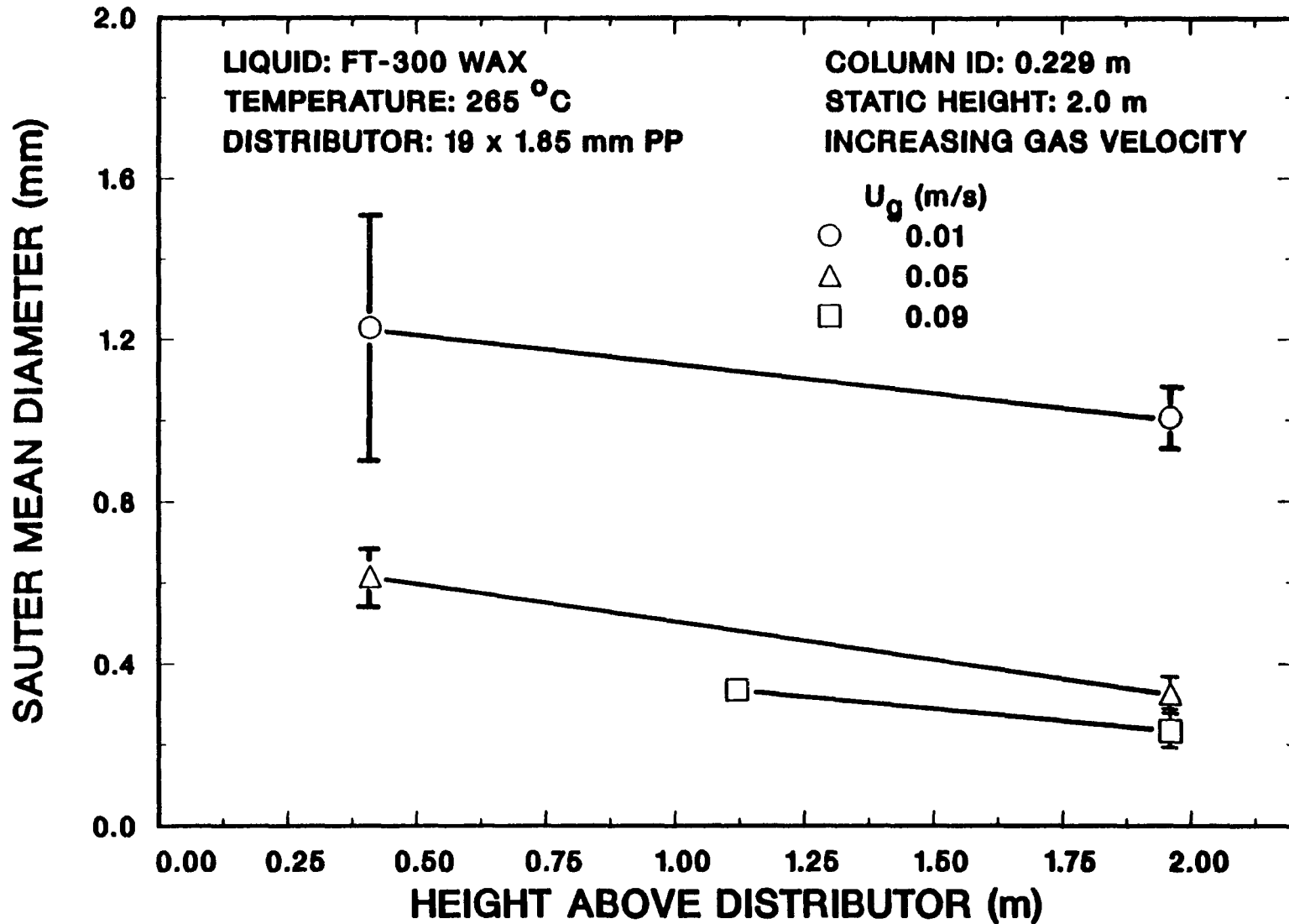
Figure V-52. Effect of superficial gas velocity and height above the distributor on the Sauter mean bubble diameter (Run 2-3; vertical bars join Sauters from individual photographs, symbols represent Sauters when results from two photos were combined)

presented in Figure V-52 also show that the variability between individual photographs is considerably lower at greater heights above the distributor (e.g. at 1.96 m) compared to values near the distributor (at a height of 0.41 m). This might be a consequence of narrower bubble size distributions at 1.96 m compared to those at 0.41 m.

The results presented above imply that, in general the Sauter mean bubble diameter has a tendency to decrease with an increase in height above the distributor. This behavior is supported by visual observations and by results obtained from axial hold-up measurements (see Section V-C.3.). Figure V-40 shows that local hold-up values at different axial locations along the column increases with height. The extent of increase was more pronounced when foam was present in the system (e.g. at 0.05 and 0.07 m/s in Figure V-40). Since higher hold-ups are caused by smaller bubbles, axial hold-up measurements imply that bubble size decreased with an increase in column height. This is in agreement with the relatively large decreases in d_s at 0.03 m/s in Figure V-50, where foam was present. However, in the absence of foam, axial hold-up values show only a marginal increase with an increase in column height (e.g. Figure V-41). This is once again in agreement with the weak trends shown by d_s under similar conditions (Figure V-52). Visual observations of the flow-field near the bottom of the column reveal relatively large bubbles with high rise velocities - resulting in the lower hold-ups and larger d_s values at this location. However, these bubbles begin to disperse resulting in smaller bubbles and higher hold-ups higher up in the column. At velocities where foam is produced, a large number of very fine bubbles are present in the system, producing higher hold-ups and lower Sauters towards the top of the column.

153

Towell et al. (1965) present some results from experiments conducted in a 0.406 m diameter and 3.05 m tall column with the air-water system. They report a variation in axial hold-up which is similar to that observed in the present study, however, bubble size distribution measurements, using the photographic technique, did not reveal any trends. A possible explanation for this could be that Towell et al. measured bubble sizes up to a height of 2.59 m above the distributor, while the expanded height was around 3 m. Therefore, it is likely that the layer of froth (that they refer to in their investigations), which is expected to be accompanied by smaller bubbles was not accounted for in their photographic measurements. Furthermore, the air-water system studied by Towell et al., is less conducive to producing the fine bubbles present in the molten wax-nitrogen system, thus, the effect of height above distributor might be different in the two systems despite similar variations in axial hold-up values. Similar results have been reported more recently by Ueyama et al. (1980) in studies that were also conducted with the air-water system. They used a medium size (0.6 m diameter and 3.03 m tall) bubble column in their investigations and made bubble size distribution measurements using both, the photographic technique and electric resistivity probes. Their studies also reveal that bubble size does not vary significantly with height above the distributor even though they report the presence of a layer of froth on top of the dispersion. Results obtained in the present study in the absence of foam (higher gas velocities) and in the larger column (0.229 m ID) show a weak dependence of d_s on column height, which is in agreement with the findings of Towell et al. and Ueyama et al.

D.2d.2. <u>Effect of Flow Regime and Operating Procedure</u>

Results presented earlier (see Section V-B.2.) indicate that the flow regime at a given velocity is affected by the operating procedure. The tendency to foam was greater when increasing order of gas velocities were employed compared to runs conducted using decreasing order of gas velocities. Therefore, the effects of flow regime and operating procedure are grouped together in the following discussion.

Figure V-53 shows the cumulative frequency curves obtained from photographs taken in the 0.051 m ID column equipped with the 1.85 mm orifice plate distributor using FT-300 wax at a temperature of 265°C and a gas velocity of 0.03 m/s. The open circles indicate results obtained when foam was present (increasing order of velocities), while the solid circles denote results in the absence of foam (decreasing order of velocities). The differences between the two curves are obvious. In the presence of foam, a greater number of smaller bubbles are produced in the dispersion compared to the case where foam is absent. Results at other heights indicate similar trends, i.e. d_s was lower in the presence of foam. This was illustrated in Figure V-50, where d_s at a gas velocity of 0.03 m/s (when foam was present) was consistently lower than d_s at other velocities.

Figure V-54 gives cumulative frequency curves obtained using the 40 μm sintered metal plate (SMP) distributor under conditions similar to those for the 1.85 mm distributor. However, the superficial gas velocity in this instance is 0.07 m/s. These results indicate that bubble sizes are significantly greater in the presence of foam when compared to the case when no foam was present. However, it should be noted that foam, when present, filled the entire column ($\epsilon_g \simeq 70\%$) in experiments with SMP.

155
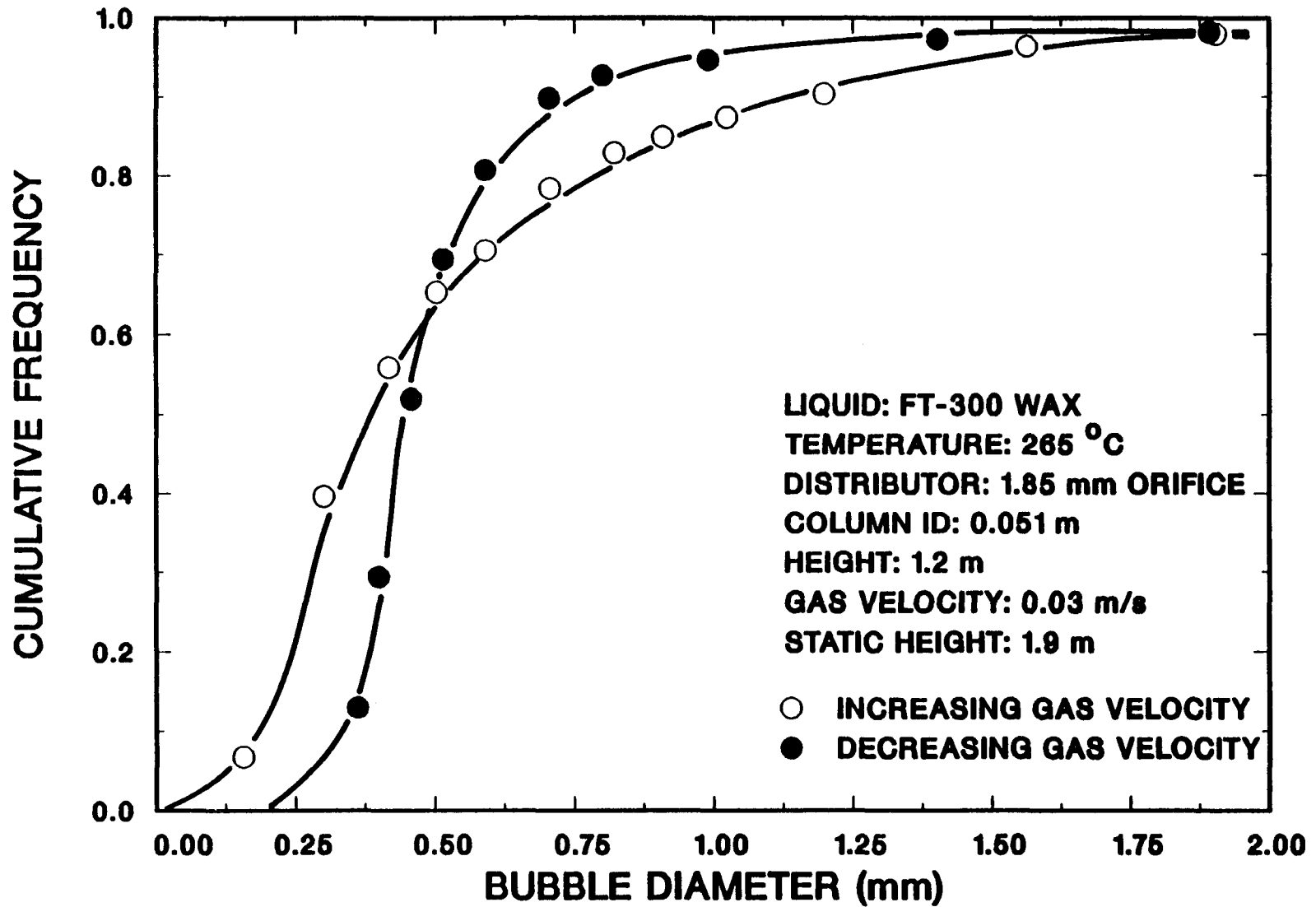
Figure V-53. Effect of flow regime on the bubble size distribution (◯- Run 4-1; ●-Run 4-2)
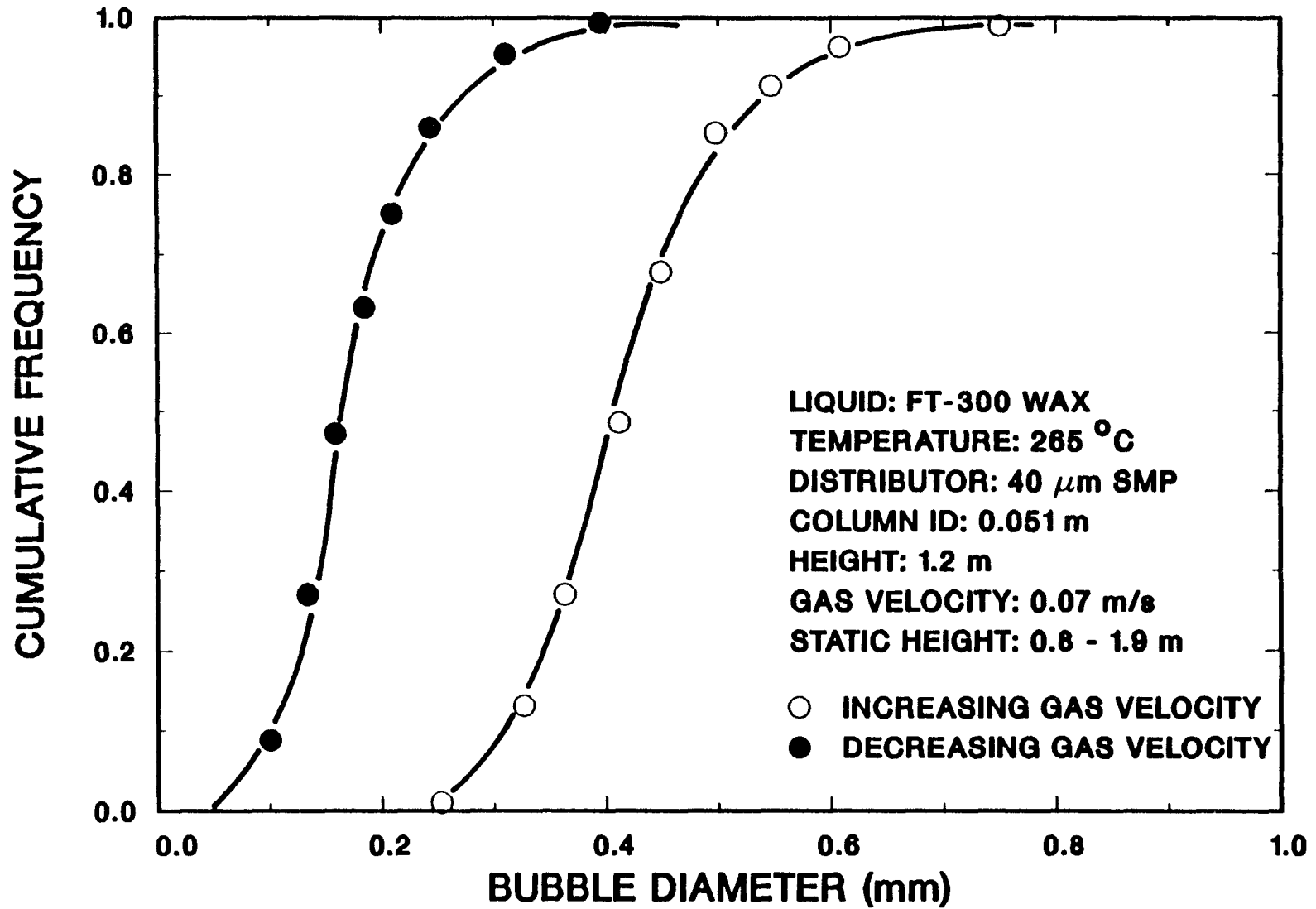
Figure V-54. Effect of flow regime on the bubble size distribution (○- Run 5-1; ●-Run 5-2)

Therefore, the photographs taken under these conditions were of foam. Whereas, in experiments conducted with the 1.85 mm orifice plate distributor, foam does not fill the entire column; hence, photographs taken are those of the bubbles in the gas-liquid dispersion near the wall of the column. Photographs of the foam reveal that the d_s for foam is around 0.5 mm and the bubble frequency distribution is relatively narrow, as can be seen from Figure V-54. The difference in trends observed with the SMP distributor, compared to the 1.85 mm orifice plate distributor, can be explained by the fact that foam tends to be comprised of larger bubbles than those in the liquid (except for slugs). Results for this distributor at other velocities (0.01 and 0.03 m/s) showed similar behavior. Foam was present in the whole column and d_s was consistently around 0.5 mm at these velocities.

Results illustrating the effect of operating procedure on the bubble size distribution, for the 0.229 m ID column, are presented in Figure V-55. These runs were conducted at 265°C using a 19 X 1.85 mm perforated plate distributor. The photographs were taken at a height of 1.12 m above the distributor using a superficial gas velocity of 0.02 m/s. Bubbles produced using increasing order of velocities appear to be smaller than those produced using decreasing order of velocities, however, the difference does not appear to be significant and can be accounted for by the differences in hold-up values for the two cases (14.4% with increasing order of velocities and 12.0% with decreasing order of velocities).

D.2d.3. <u>Effect of Superficial Gas Velocity</u>

The effect of velocity on Sauter mean diameter for experiments conducted in the 0.051 m ID column using the 1.85 mm orifice plate

158
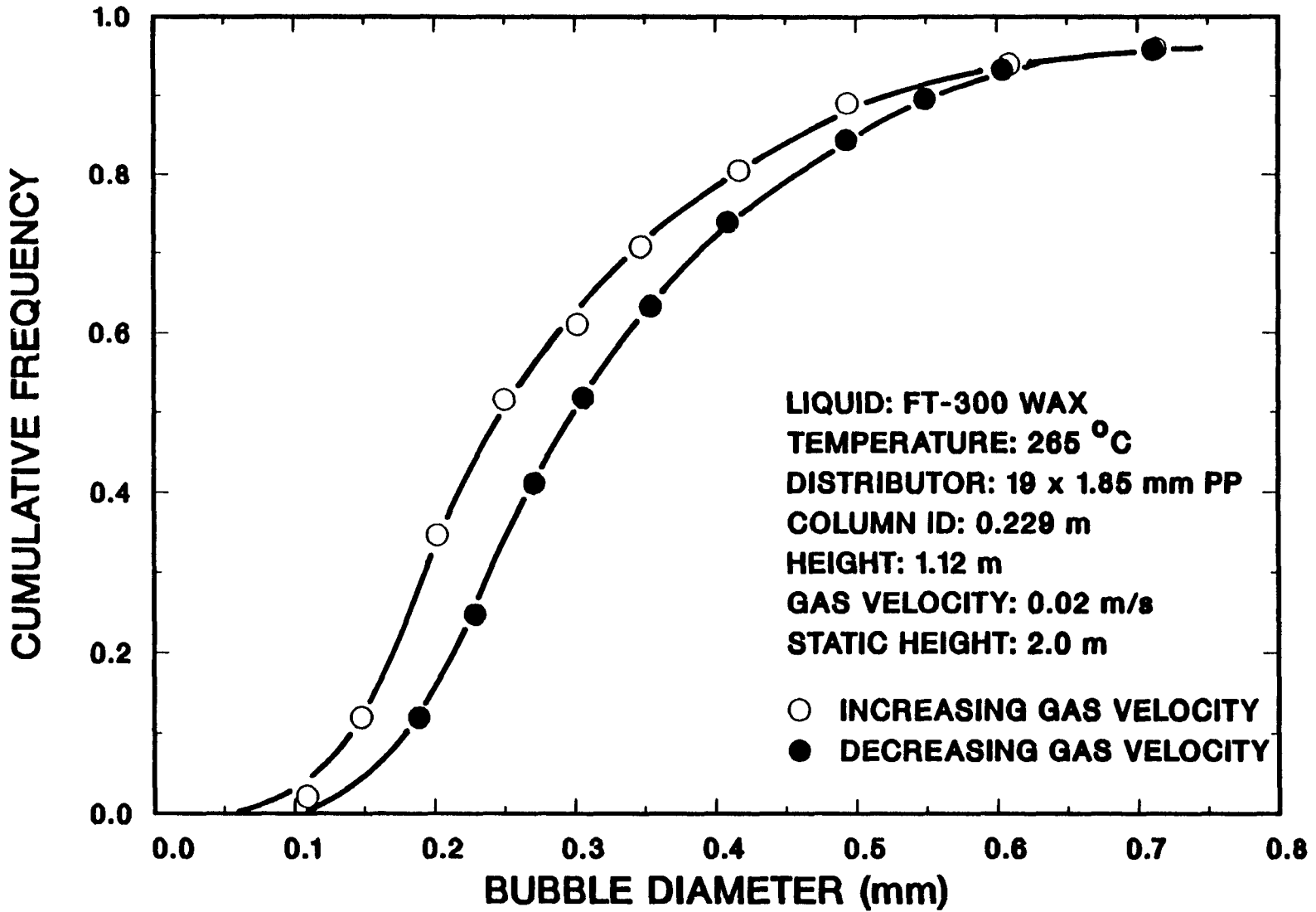
Figure V-55. Effect of flow regime on the bubble size distribution (O- Run 2-3; ●-Run 2-4)

distributor at 265°C is shown in Figure V-56 for a height of 1.2 m above the distributor. In general, d_s appears to remain fairly constant (around 1.8 mm) regardless of operating procedure and gas velocity. The effect of large bubbles is more pronounced for these results because of the limited number of bubbles sized (around 400 to 500 per condition). This might help explain the scatter in results shown in Figure V-56. Results obtained using the 40 μm SMP distributor are shown in Figure V-57. The Sauter mean diameter for this distributor also appears to remain fairly constant around 0.6 mm over the range of gas velocities employed. Zaidi et al. (1979) and Deckwer et al. (1980) report Sauter mean diameters of about 0.7 mm for molten paraffin wax in bubble columns equipped with porous plate spargers which is in good agreement with results obtained in our study.

Figure V-58 illustrates the effect of gas velocity on the Sauter mean diameter for experiments conducted in the 0.229 m ID glass column. These results indicate that the Sauter mean diameter tends to decrease initially as gas velocity is increased and approaches a constant value at higher gas velocities. At 0.41 m above the distributor d_s decreases from approximately 1.2 mm at 0.01 m/s to approximately 0.7 mm at higher velocities. Visual observations of the flow field support these results. However, at 1.12 m and 1.96 m above the distributor, bubbles are significantly smaller at high velocities, approaching 0.4 mm at a gas velocity of 0.09 m/s. Again, this is in agreement with visual observations. At high velocities, bubbles near the wall form a very fine dispersion.

Quicker and Deckwer (1981) estimated d_s for FT-300 wax in a bubble column using porous plate and perforated plate spargers. They took photographs of bubbles along the column wall for experiments performed in the
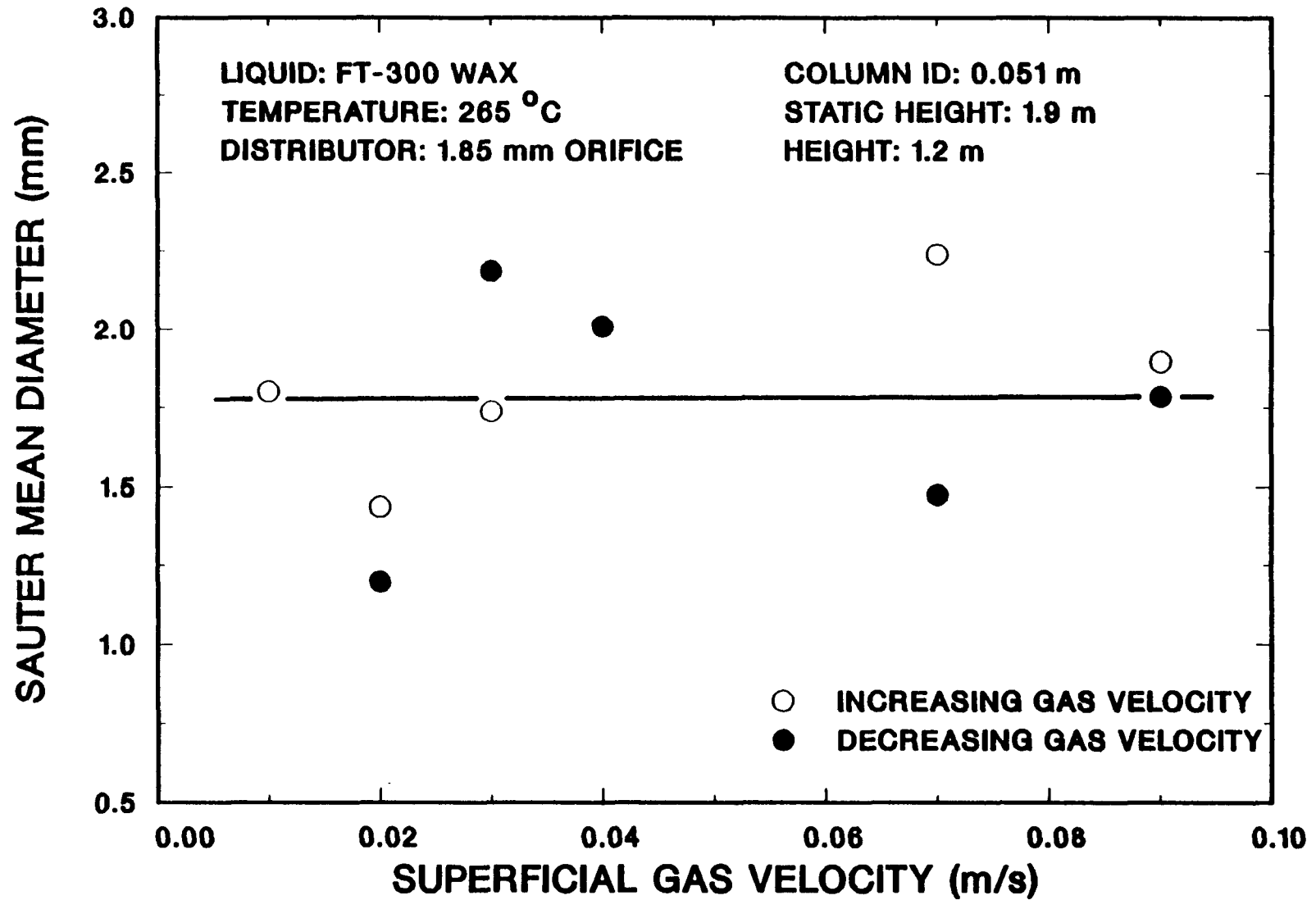
Figure V-56. Effect of superficial gas velocity on the Sauter mean bubble diameter (O- Run 4-1; ● - Run 4-2)
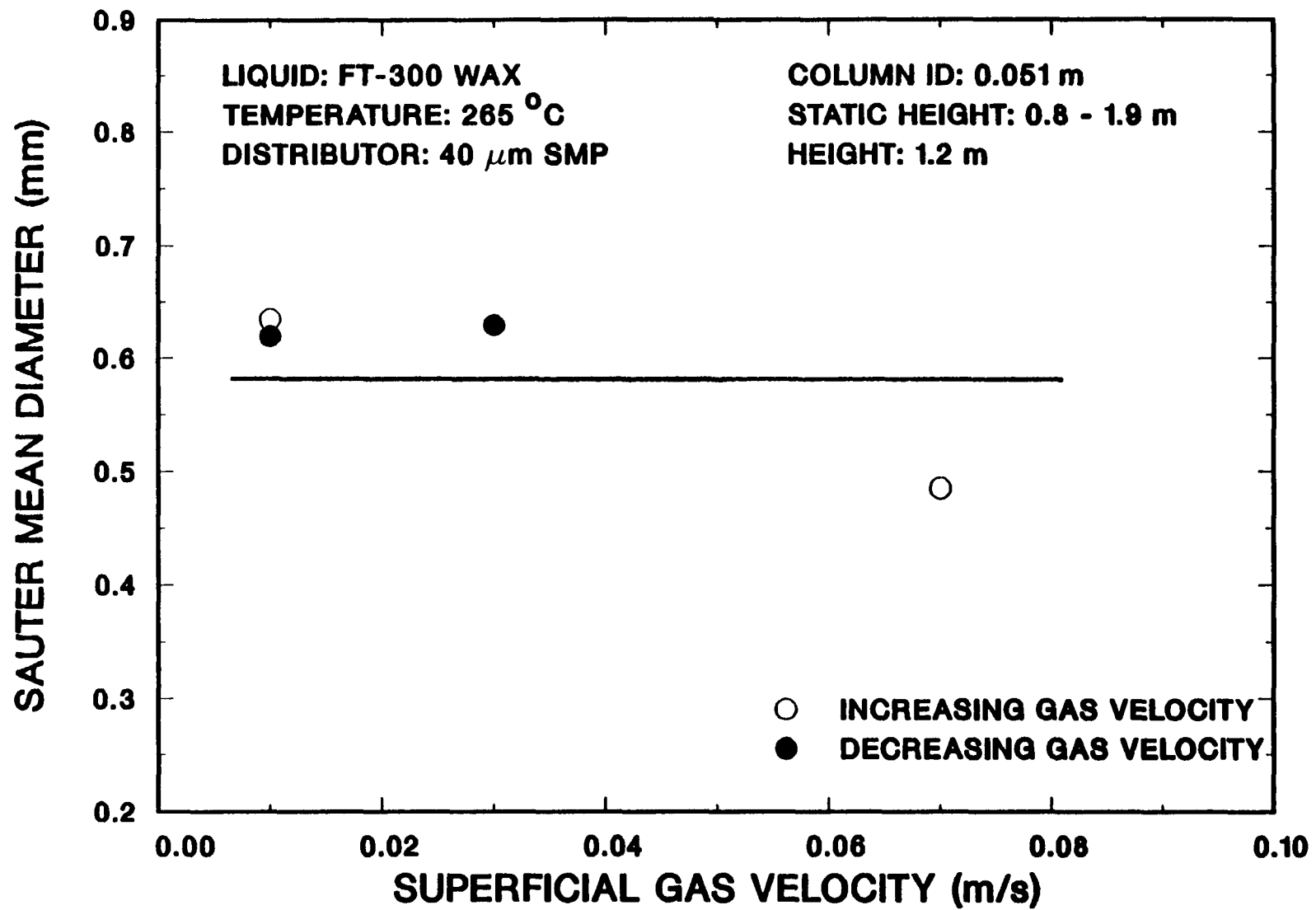
Figure V-57. Effect of superficial gas velocity on the Sauter mean bubble diameter (O- Run 5-1; ● - Run 5-2)
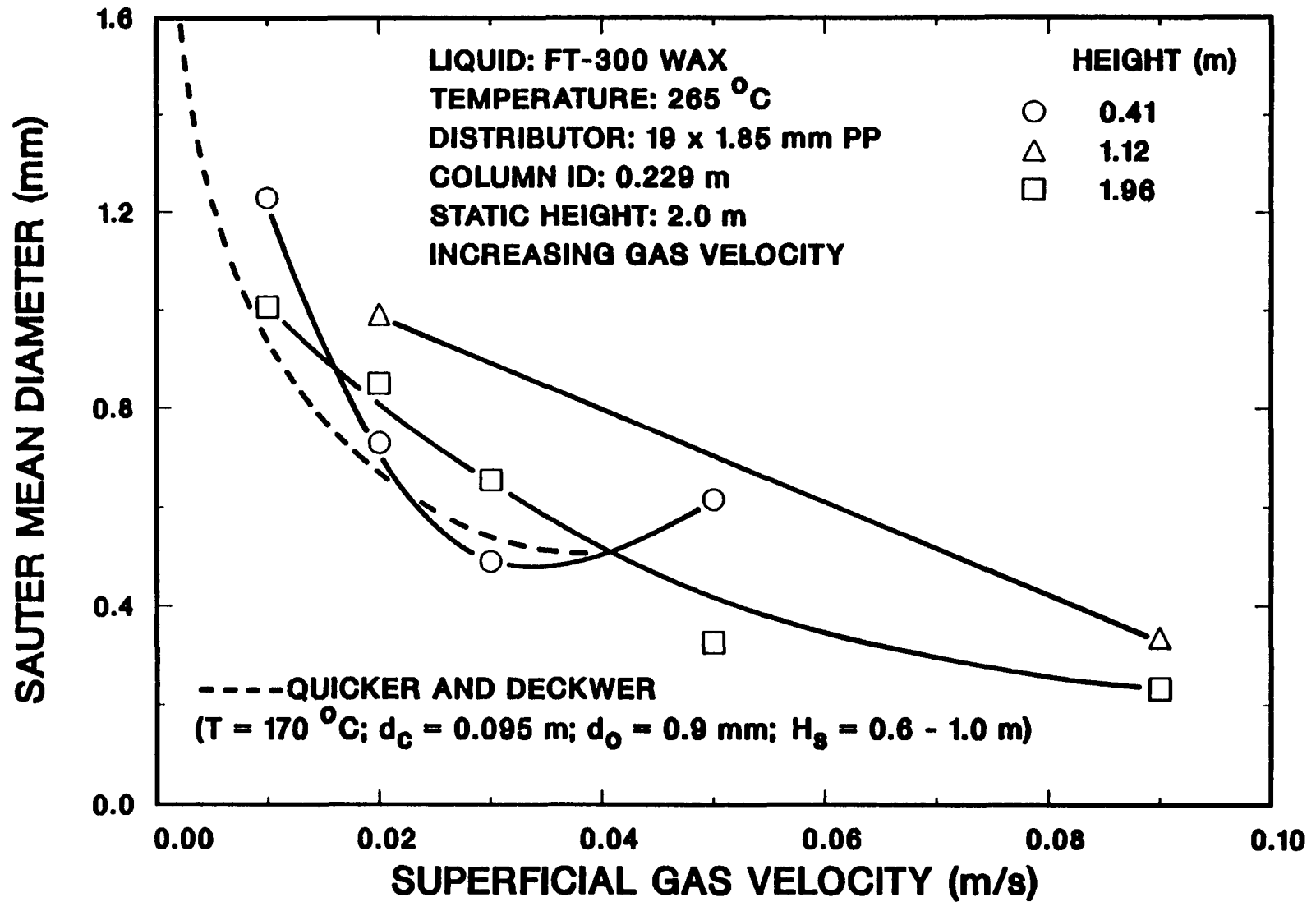
Figure V-58. Effect of superficial gas velocity on the Sauter mean bubble diameter and comparison with literature (Run 2-3)

homogeneous flow regime. Their results show that d_s is around 1.5 mm at low velocities (u_g = 0.005 m/s) and it decreases to about 0.5 mm at a velocity of 0.035 m/s (Figure V-58). Sauter mean diameters for FT-300 wax from the current study at a height of 0.41 m above the distributor are in good agreement with the findings of these workers considering the differences in distributors and operating conditions.

Figure V-59 shows results from photographs taken at a temperature of 265°C in the 0.241 m ID stainless steel column through the special viewing port located at a height of 1.37 m above the distributor. Two photos at each velocity were selected and analyzed, and d_s from the individual photos was calculated. The data from the two photographs were then combined and d_s for the combined data was also calculated. Approximately 1500-1700 bubbles were catalogued and sized at each velocity (combined total from the two photographs). The open circles in Figure V-59 represent d_s for the combined data, whereas the d_s values for individual photographs are connected by the vertical bar at each velocity. Sauter mean diameters reach a maximum of 1.5 mm at 0.03 m/s and then stabilize at approximately 0.9 mm for higher velocities. Sauter mean diameters from the individual photographs compare satisfactorily considering the limitations of this procedure. These results indicate that for gas velocities in the range 0.02-0.04 m/s larger bubbles were present near the center of the column. However, bubbles were much smaller at velocities greater than 0.04 m/s. This indicates that at lower gas velocities, there might be significant circulation patterns in the column when larger bubbles are moving upwards in the center of the column. However, at higher gas velocities when flow is in the "churn-turbulent" regime, these circulations give way to intense mixing, resulting in
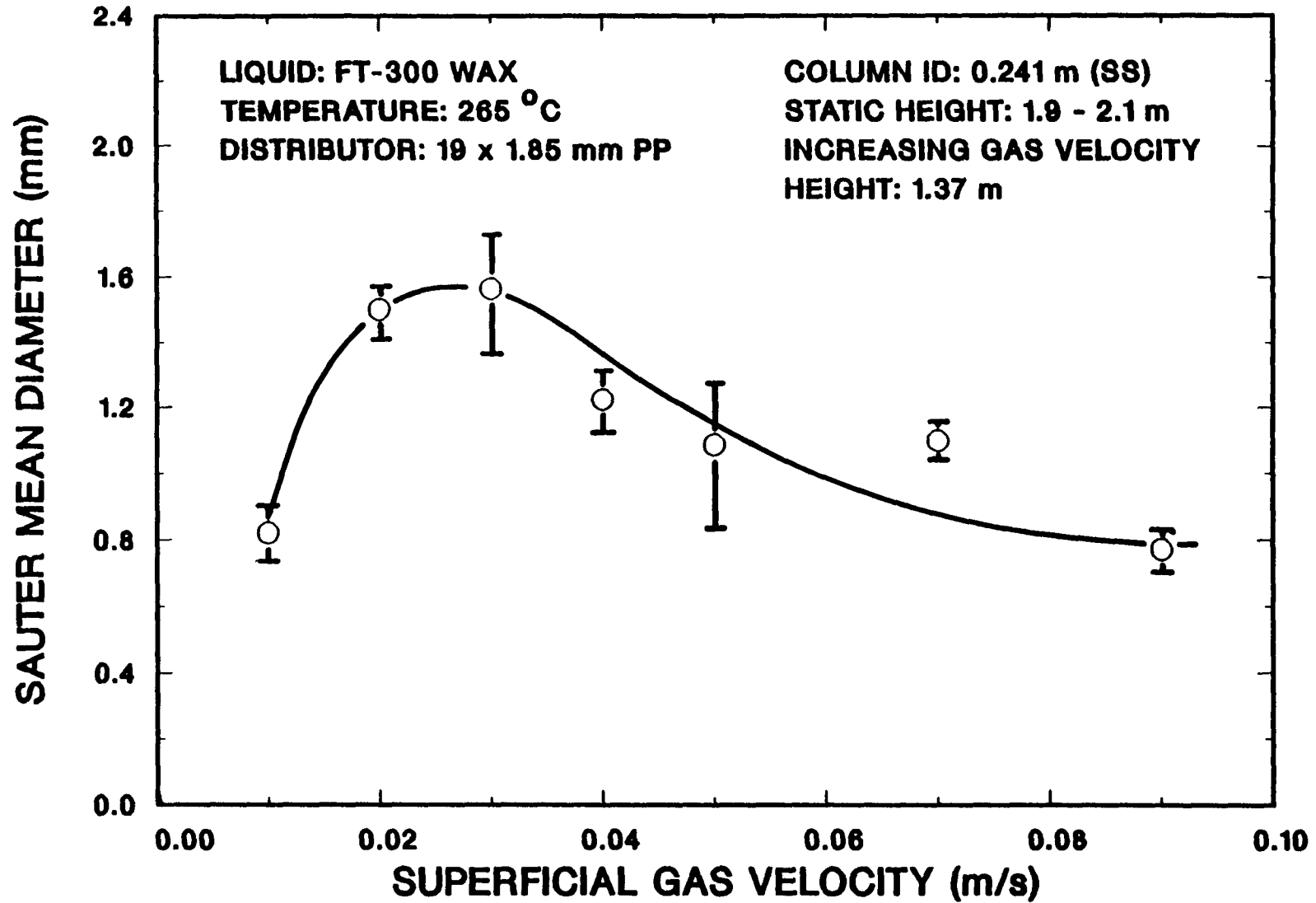
Figure V-59. Effect of superficial gas velocity on the Sauter mean bubble diameter (Run 2-7 - vertical bars join Sauter mean diameters from individual photographs, open circles represent Sauter mean diameters when results from the two photos were combined)

relatively small bubble sizes. Visual observations of the dispersion support these findings.

Selected cumulative frequency curves for measurements made in the 0.24 m ID column are shown in Figure V-60. As expected, these curves show that the size of small bubbles remains almost constant at all velocities. However, the large bubbles change in size with gas velocity and this is reflected by the variation in the upper half of these curves. The change in distributions with gas velocity is in agreement with the trend shown in Figure V-59. At 0.01 m/s the bubbles are small and the distribution is relatively narrower (implying homogeneous flow). However, as velocity is increased to 0.03 m/s, larger bubbles start forming as a result of coalescence and higher gas flow rates. As velocity is further increased to 0.05 m/s these large bubbles begin to breakup due to increased turbulence and the distribution once again shifts to the left (towards smaller bubble sizes). Further increases in velocity result in only a marginal shift in the cumulative frequency curve (e.g. the curve at 0.09 m/s).

D.2d.4. Effect of Distributor

This effect was investigated only in the 0.051 m ID column. Cumulative frequency curves for measurements made at 265°C and at a gas velocity of 0.07 m/s are presented in Figure V-61. The photographs were taken at a height of 1.2 m above the distributor. It was not possible to compare results for the 1.85 mm distributor and the SMP distributor at velocities where foam was present because of reasons mentioned earlier (see Section V-B.2.). The results presented in Figure V-61 show that the SMP distributor produced smaller bubbles compared to the 1.85 mm orifice plate distributor. This is expected for a medium with low coalescence rates, such as paraffin
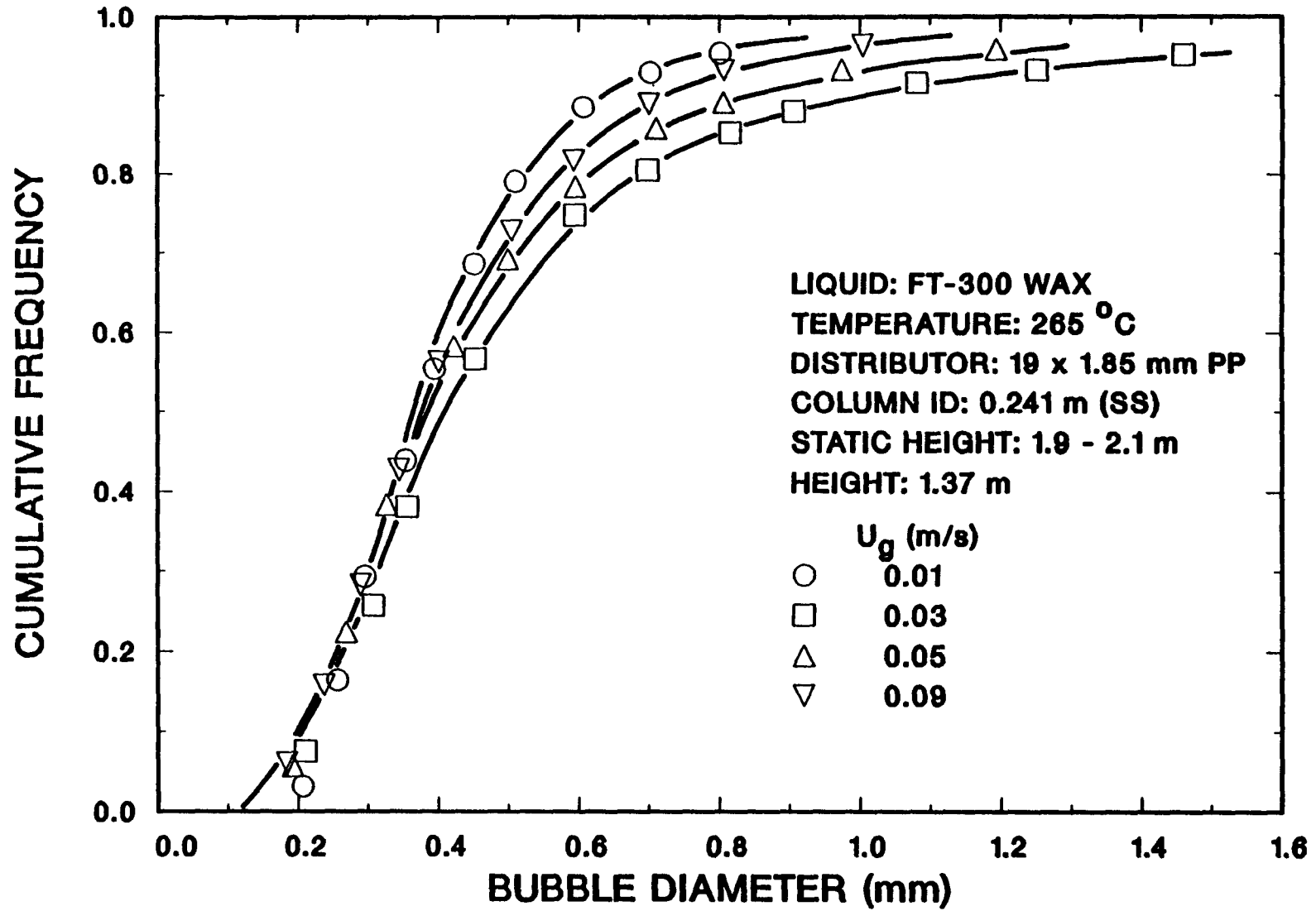
Figure V-60. Effect of superficial gas velocity on the bubble size distribution (Run 2-7)
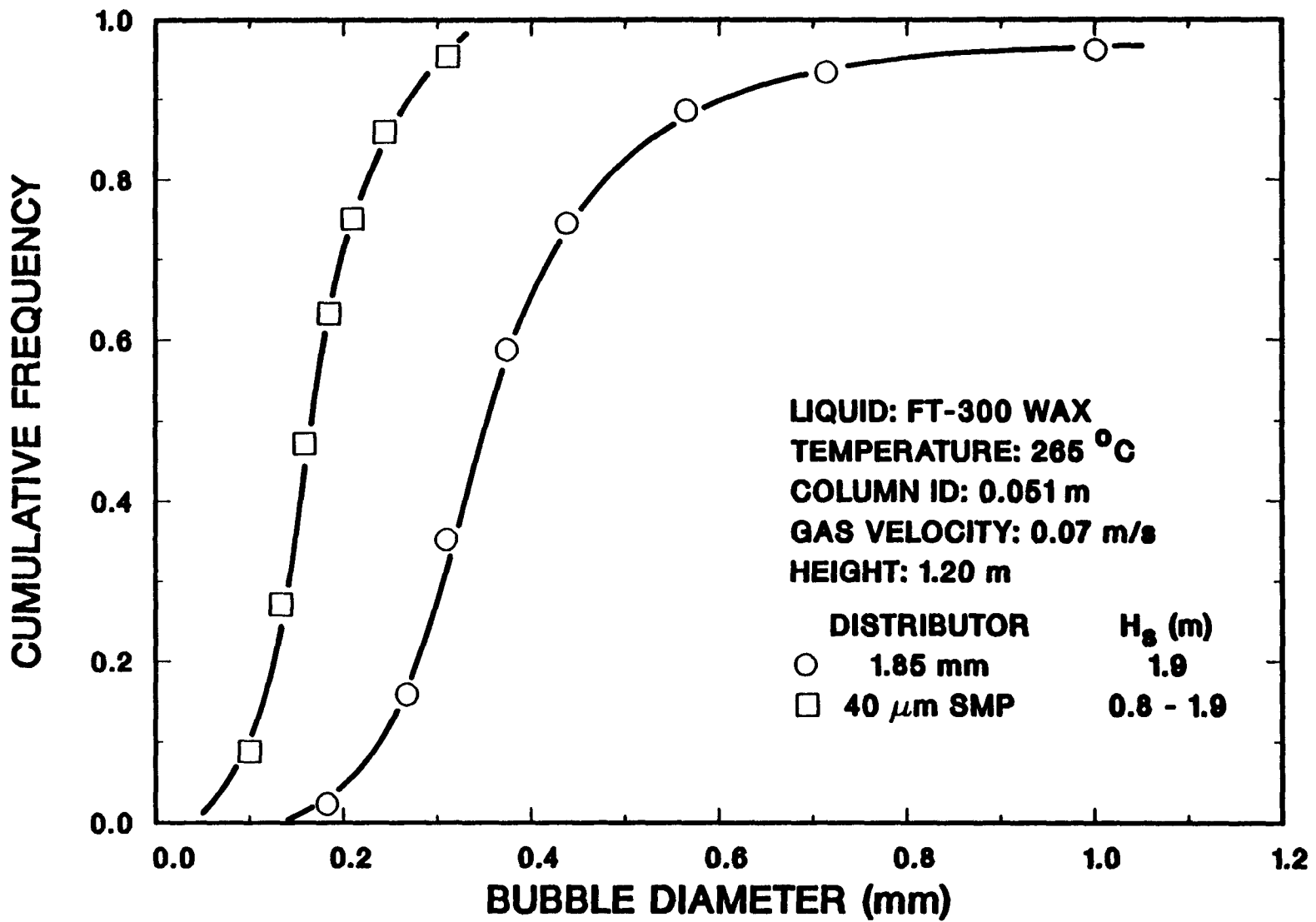
Figure V-61. Effect of distributor type on the bubble size distribution (○- Run 4-1; □- Run 5-1)

waxes. These results are qualitatively in agreement with the arguments put forward by Heijnen and van't Riet (1984) relating the bubble sizes in a non-coalescing medium with the type of distributor used.

D.2d.5. Effect of Radial Position

The special viewing port constructed in the 0.241 m ID stainless steel column made it possible to compare the results obtained at the wall with those obtained from photographs taken near the center of the column (approximately 0.028 m from the center of the column). One of the major limitations of the photographic technique is its inability to predict the bubble size distribution across the entire cross-section for a non-homogeneous flow field. The following results illustrate this limitation clearly.

Sauter mean diameters near the center of the column were obtained in the 0.241 m ID column from photographs taken at a height of 1.37 m above the distributor and the results were shown in Figure V-59. Photographs of bubbles near the wall were taken in the 0.229 m ID glass column at three different heights (0.41 m, 1.12 m and 1.96 m above the distributor). These results, presented in Figure V-52, showed that the Sauter mean diameter did not change significantly with height above the distributor. Therefore, it can be assumed that d_s values at a height of 1.37 m, near the wall, should be approximately the same as those at 1.12 m or 1.96 m. Based on this assumption, it is possible to study the effect of radial position on the Sauter mean bubble diameter. Figure V-62 shows the variation of d_s with the normalized radial position at a temperature of 265°C for different superficial gas velocities. Values at the wall are based on photographs taken at a height of 1.96 m above the distributor.

169
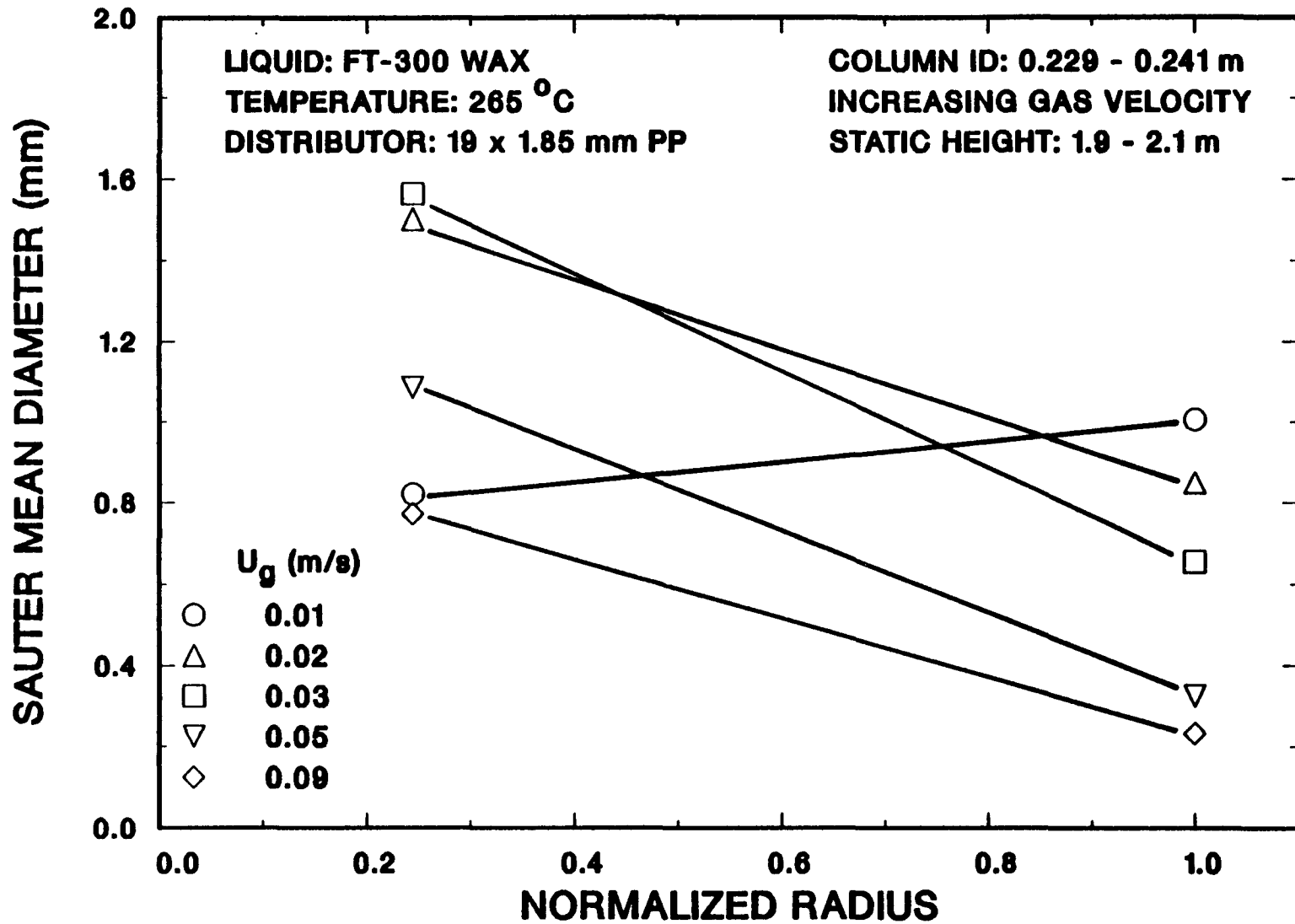
Figure V-62. Effect of radial position and superficial gas velocity on the Sauter mean bubble diameter (photos near the center - Run 2-7; photos near the wall - Run 2-3)

Results presented in Figure V-62 show that d_s is significantly affected by radial position at all velocities, except at 0.01 m/s. At 0.01 m/s the Sauter mean diameter is approximately the same at the two locations. These results imply that the dispersion is not homogeneous at this height (1.37 m above the distributor) once the gas velocity exceeds 0.01 m/s and significant gradients begin to develop. Figure V-63 shows cumulative frequency distribution curves for the two locations at a superficial gas velocity of 0.03 m/s. These results show that the bubble size distribution at the wall is significantly different from that near the center of the column.

Shah et al. (1985) have presented radial gas hold-up profiles for studies conducted in the air-water system. These profiles indicate that the hold-up is the highest at the column center and gradually decreases to a minimum at the column wall. Ueyama et al. (1980) also report similar findings with their studies with the air-water system. Ueyama et al. also present radial profiles for the bubble sizes based on measurements made using photography and electrical resistivity probes. Their results show trends which are similar to those found in the present study with FT-300 wax. Smith, D.N. et al. (1984a) conducted studies with the aqueous ethanol and nitrogen system and found that bubble size increased slightly from the column wall to the center of the column, however, d_s was found to be fairly constant within a distance of half a radius from the column center. Radial gas hold-up profiles from their studies are similar to those reported by Ueyama et al. Gas hold-up profiles presented in literature are as expected since it is well known that the greater part of the gas moves through the central core of the bubble column. For the column used in the present
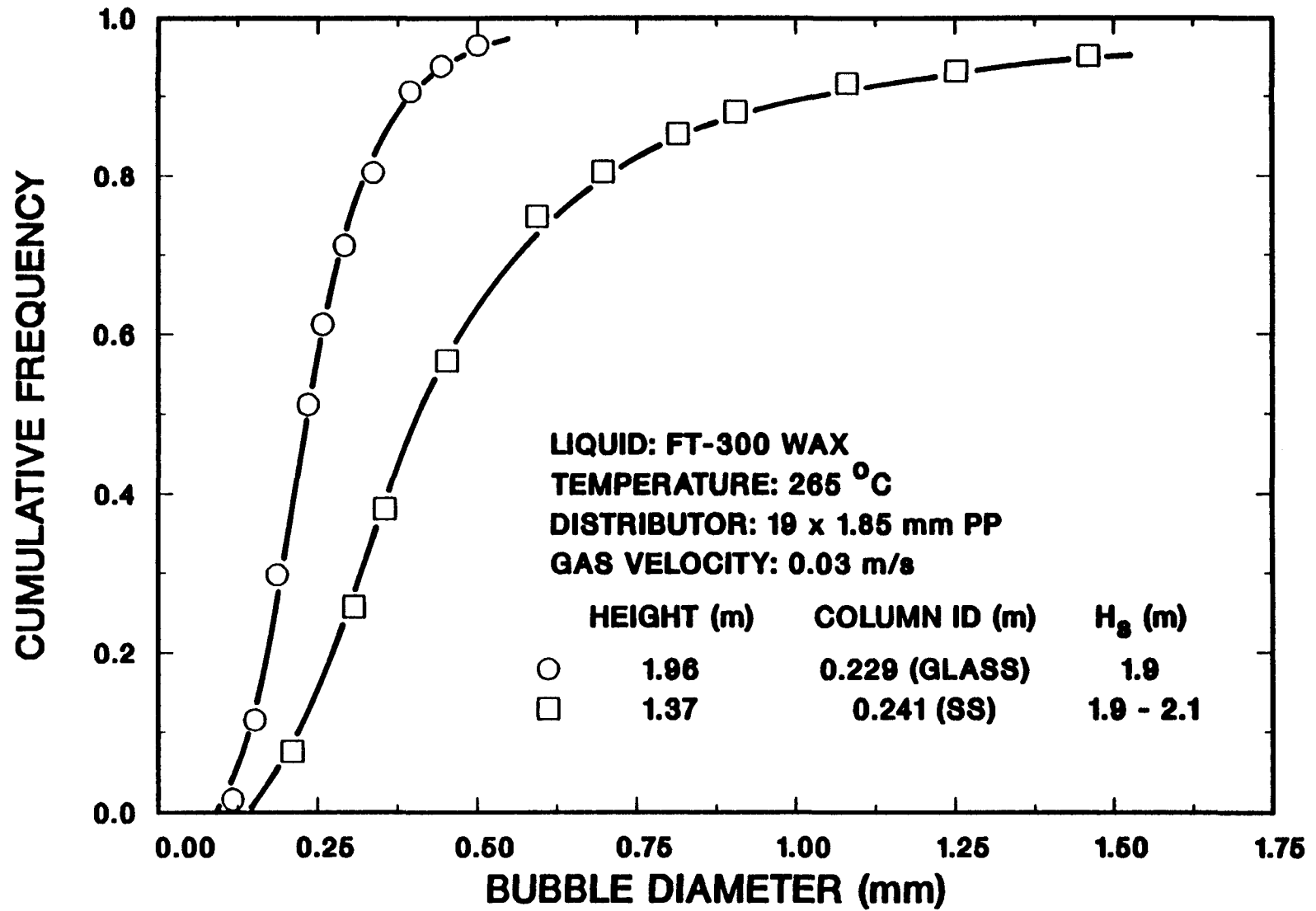
Figure V-63. Effect of radial position on the bubble size distribution (○- Run 2-3; □- Run 2-7)

study, circulation patterns begin to develop in the column so that large bubbles move upwards in the center of the column and small bubbles entrained in the liquid move down along the wall of the column. This phenomenon explains the difference in results between photographs taken at the wall of the column and those taken near the center of the column.

D.2d.6. Effect of Oxygenates

The effect of oxygenates was investigated using mixtures of known composition of 1-octadecanol, octadecanoic acid (stearic acid) and FT-300 wax. These runs were made in the 0.051 m ID column using increasing order of velocities at 265°C. Both, the SMP and 1.85 mm orifice plate distributors were used in these studies. Up to 10 wt.% of oxygenates were added to FT-300 wax during these experiments.

For runs made using the 1.85 mm distributor, the addition of oxygenates resulted in a decrease in the value of the Sauter mean bubble diameter (around 1 mm for velocities greater than 0.03 m/s compared to around 1.8 mm with pure FT-300 wax). This can be partially explained by the fact that in the runs with oxygenated compounds, slightly higher hold-ups were obtained than in runs without oxygenates. Results from measurements made using the SMP distributor are qualitatively similar to those obtained using the 1.85 mm distributor. Zieminski et al. (1967) and Keitel and Onken (1982) conducted studies to investigate the effect of the addition of electrolytes to the air-water system. Their studies using alcohols show that the Sauter mean bubble diameter for the air-water system decreases with an increase in the length of the carbon chain of the alcohol.

D.2d.7. Effect of Operating Temperature

The effect of operating temperature (200 and 265°C) was investigated

173

in the 0.051 m ID column using both, the SMP and the 1.85 mm orifice plate distributors; and in the 0.241 m ID stainless steel column using the 19 X 1.85 mm perforated plate distributor. Results from measurements made in the 0.051 m ID column revealed little or no effect of temperature on the bubble size distributions. Sauter mean diameters at 200°C were similar to those at 265°C. Photographs taken near the center of the column in the 0.24 m ID column showed that the value of d_s dropped as temperature was decreased from 265°C to 200°C. At 0.02 m/s d_s at 265°C was 1.5 mm compared to around 1.3 mm at 200°C, a relative decrease of around 13%. Similarly, at 0.07 m/s the relative difference was about 50% (1.1 mm compared to 0.5 mm). These results are contrary to the belief that lower temperatures result in higher viscosities and therefore should produce larger bubbles (as shown by DGD measurements). However, Quicker and Deckwer (1981) reported similar re-sults with FT-300 wax. Their results show a decrease in d_s of as much as 50% at 0.01 m/s, when temperature was decreased from 170°C to 130°C, and about 10% at a velocity of 0.03 m/s. Results for other systems show that an increase in viscosity (equivalent to a decrease in temperature) results in an increase in d_s (e.g. Schugerl, 1981). There appears to be no obvious explanation for the results with FT-300 wax.

D.2e. <u>Limitations of the Photographic Method</u>

There are several limitations and drawbacks to the photographic technique for determining the Sauter mean diameter. The photographic technique only allows for the analysis of bubbles near the wall of the column which may not be representative of the bubbles in the entire column. However, in the present work the severity of this limitation was alleviated to a great extent by constructing a special viewing port in the 0.241 m ID

stainless steel column. This port, shown in Figure V-49, is indented into the column for the purpose of obtaining photographs of bubbles near the center of the column. The construction of such a port is likely to influence the flow field because it creates an obstruction. However, the possibility of such an occurrence was greatly reduced by constructing a skirt (or a curtain) below the window as shown in Figure V-49. This metal piece extended around 0.05 m below the window. The purpose was to trap the bubbles close to the wall and allow the bubbles near the center of the column to proceed upwards unhindered. Visual observations of the flow field, through the viewing port confirm this. However, occasionally a sudden surge of small bubbles could be seen at the viewing port. This happens when the cavity under the window is saturated with tiny bubbles and as a result the bubbles are suddenly released in a large swarm. The photographs of the flow field were taken between such surges.

Once photographs of bubbles have been taken, the bubble sizes associated with the bubbles in the picture need to be determined by either a mechanical method or by image analysis equipment. Regardless of the method employed, the bubble sizes will be biased toward larger bubbles. The prejudice toward larger bubbles arises from the fact that in general, most of the large bubbles will be sized in a photograph (since they are clearly defined and in focus); whereas, not all of the small bubbles will be sized (too many and a lot are out of focus). In addition to this the measuring process involves some subjectivity and therefore introduces a certain amount of human error as well. Due to the finite number of bubbles which are counted the Sauter mean diameter will be significantly affected by the presence of large bubbles. This is evident in the following example.

Given a bimodal distribution with 500 bubbles of 0.5 mm diameter and 1 bubble 10 mm in diameter, the Sauter mean diameter is 4.7 mm (using Equation (V-5)). However, given 500 bubbles of 1 mm in diameter and 1 bubble 10 mm in diameter, the Sauter mean diameter is 2.5 mm. These results show that for a distribution containing smaller bubbles (0.5 mm), the Sauter mean bubble diameter is significantly greater than the distribution containing larger bubbles (1 mm), i.e. 4.7 mm for the former versus 2.5 mm for the latter. The obvious problem is the presence of the one large (10 mm) bubble in each of the distributions. If 100,000 small bubbles were sized instead of 500, only then does the value of d_s approaches 0.5 mm for the first case and 1.0 mm for the second. For the molten wax - nitrogen system the problem is further aggravated because of the large number of fine bubbles present in the dispersion, whereas only a few large bubbles are visible. Therefore, by counting only a relatively small number of these fine bubbles the calculated values for the Sauter mean diameter will be larger than the actual values. The margin of this type of error can be reduced by increasing the bubble count (by analyzing more than one photograph per condition). However, this is an arduous task.

D.3. Bubble Size Distribution Using the Dynamic Gas Disengagement Method

Bubble size measurements were made using the dynamic gas disengagement technique (DGD) developed by Sriram and Mann (1977). Experiments were conducted in the 0.051 m ID and the 0.229 m ID glass columns in order to study the effect of operating temperature (200 and 265°C), distributor type, column diameter, and wax type. Majority of the experiments were conducted in the 0.051 m ID column using FT-300 wax, and reactor waxes

(Sasol's Arge reactor wax and Mobil's reactor wax). A few measurements were made in the 0.229 m ID column with FT-300 wax. The 1.85 mm and 4 mm orifice plate, and the 40 μm SMP distributors were used in the small column, while the 19 X 1.85 mm perforated plate distributor was used in the 0.229 m ID column.

The major highlights of these investigations are:

- 1.85 and 4 mm orifice plate distributors gave similar values for d_s with FT-300 wax, while measurements could not be made with the 40μm SMP distributor due to excessive foaming.

- Column diameter did not have a significant effect on the d_s value for FT-300 wax.

- The presence of foam had a strong effect on d_s values. At 265°C the Sauter mean diameter for FT-300 wax was approximately 0.5 mm, irrespective of the amount of foam (or hold-up). However, results from the DGD method obtained in the presence of foam should be interpreted with caution.

- Temperature had a significant effect on the Sauter mean bubble diameter (d_s), with values at 200°C being significantly larger than values at 265°C for all wax types, despite relatively small differences between hold-up values at the two temperatures.

- Distributor type (SMP and 1.85 mm orifice plate) did not have a significant effect on d_s for reactor waxes, however, values with the SMP distributor were consistently lower than those with the 1.85 mm orifice plate distributor.

- Wax type had a significant effect on d_s values, with the smallest bubbles being produced by FT-300 wax and the largest by Mobil reactor

177

wax. The trends were similar at both 200°C and at 265°C. At 265°C
Sauter mean diameters for FT-300 wax were around 0.8 mm for
superficial gas velocities greater than 0.05 m/s; while those for
Sasol reactor wax approached 2 mm and Mobil reactor wax gave values
around 4 to 5 mm.

D.3a. <u>Theory</u>

Sriram and Mann (1977) developed the dynamic gas disengagement (DGD)
technique for obtaining the bubble rise velocity and the bubble size
distribution in bubble columns. This technique requires the knowledge of
the change in liquid level as a function of time, once the gas flow to the
bubble column is shut off.

Sriram and Mann showed that the gas hold-up, $\epsilon_g(t)$, after a time, t,
is given by

$$\epsilon_g(t) = \epsilon_{go} \int_o^\infty \left\{ f(d_B) \left[1 - \frac{t u(d_B)}{H(t)} \right] \right\} d(d_B) \qquad (V-6)$$

where $(1-tu(d_B)/H(t))$ is the fraction of the volume fraction of bubbles
remaining in the dispersion after an elapsed time, t, ϵ_{go} is the average
gas hold-up at time zero, $f(d_B)d(d_B)$ is the volume fraction of the bubbles
having size between d_B and d_B + $d(d_B)$, and $u(d_B)$ is the rise velocity
associated with a bubble of size d_B. Equation (V-6), based on a theoretical
approach, implies that the bubble size distribution is initially axially
homogeneous and that significant bubble interactions do not occur during
the disengagement process.

D.3a.1. <u>Discretization for N Classes of Bubbles</u>

A generalized theory for obtaining the bubble size distribution from
DGD is developed here. Equations for the specific cases involving bimodal

178

and trimodal distributions (most commonly encountered in the present work) are presented in APPENDIX C, together with examples and sample calculations. Equation (V-6) is valid for a continuous bubble size distribution, and its discretized version for N classes of bubbles is given by

$$\epsilon_g(t) = \epsilon_{go} \sum_{i=1}^{N} f_i \left[1 - \frac{tu_{Bi}}{H} \right] \qquad (V-7)$$

where i represents the individual bubble classes, f_i is the volume fraction of bubbles in class i, and u_{Bi} is the rise velocity associated with this class of bubbles. It is assumed that class N comprises of the largest bubbles and class 1 contains the smallest bubbles.

After a time, t_1^*, all of the bubbles in class N will have disengaged along with some bubbles in the other N-1 classes. Similarly, after a time t_2^* ($t_2^* > t_1^*$) all of the bubbles in class N-1 will have disengaged, and so on (see Figure V-64). By this assumption, the term $(1-tu_{BN}/H)$ becomes zero at time t_1^*, the term $(1-tu_{BN-1}/H)$ becomes zero at time t_2^*, leading to the following general equation for the dynamic hold-up, $\epsilon_g(t)$:

$$\epsilon_g(t) = \epsilon_{go} \sum_{i=1}^{k} f_i \left[1 - \frac{tu_{Bi}}{H} \right] \qquad t_{N-k+1}^* \geq t > t_{N-k}^* \qquad (V-8)$$

Equation (V-8) can be rearranged so as to relate the normalized liquid level (H/H_o) to time elapsed (t) to obtain the following equation (see APPENDIX C for details of its derivation):

$$\frac{H}{H_o} = \frac{H_s/H_o}{1 - \sum_{i=1}^{k} \epsilon_{goi}} - t \frac{\sum_{i=1}^{k} \epsilon_{goi} u_{Bi}}{H_o \left[1 - \sum_{i=1}^{k} \epsilon_{goi} \right]} \qquad t_{N-k+1}^* \geq t > t_{N-k}^*$$

$$(V-9)$$

where $\epsilon_{goi} = \epsilon_{go} f_i$, and H_s is the height of the ungassed liquid (or static height).

According to Equation (V-9) a plot of the normalized liquid level (H/H_o) versus time elapsed (t) would result in a series of straight lines, one for each of the time intervals, with intersections (or break points) occurring at times t_1^*, t_2^*, and so on. This is graphically illustrated in Figure V-64.

D.3a.2. <u>Procedure for Obtaining ϵ_{goi}, u_{Bi} and f_i</u>

Assuming that the experimental normalized liquid level versus time elapsed data can be represented by N straight lines, as shown in Figure V-64, the following procedure can be used to obtain estimates for ϵ_{goi} and u_{Bi}. In Figure V-64, t_N^* represents the time when all bubbles have disengaged from the liquid, therefore, the straight line beyond t_N^* represents the static liquid level. The slope of this line is zero ($s_o = 0$) and the intercept is H_s/H_o (i.e. $b_o = H_s/H_o$).

The first step is to obtain the slopes and intercepts of the N straight line segments (see Figure V-64). Let s_1 to s_N represent the slopes of these lines, and let b_1 to b_N represent the intercepts of these lines. Equation (V-9) can be used to obtain the expressions for the slope and intercept of the straight lines. General equations for estimating ϵ_{goi} and u_{Bi} from s_i and b_i are developed here.

For the k'th straight line the following expressions represent the slope and the intercept:

180
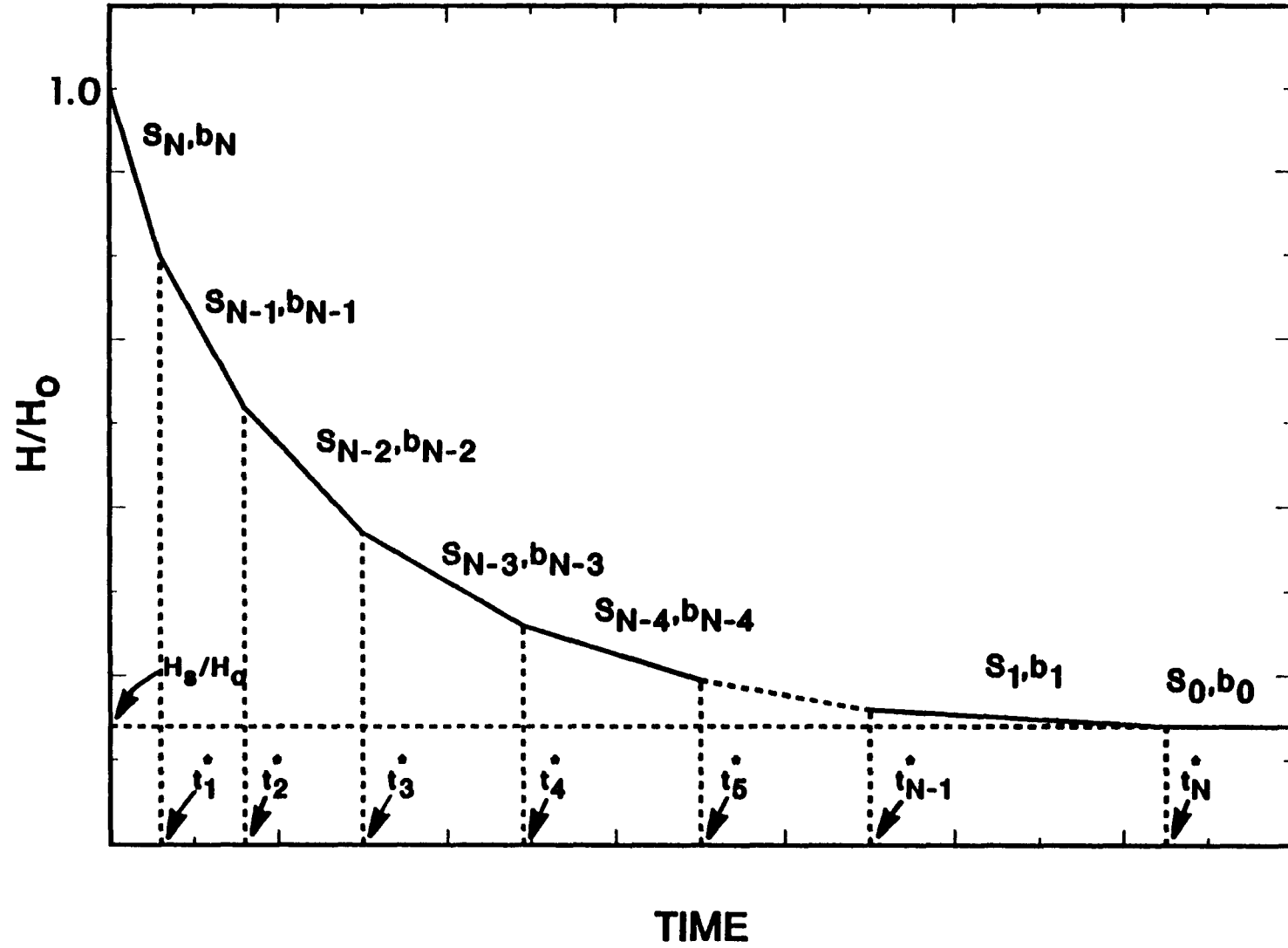
Figure V-64. Change in normalized liquid level with time during DGD for a dispersion with N bubble size classes

$$\text{slope:} \qquad s_k = - \frac{\sum\limits_{i=1}^{k} \epsilon_{goi} u_{Bi}}{H_o \left[1 - \sum\limits_{i=1}^{k} \epsilon_{goi} \right]} \qquad\qquad \text{(V-10)}$$

$$\text{intercept:} \qquad b_k = \frac{H_s/H_o}{1 - \sum\limits_{i=1}^{k} \epsilon_{goi}} \qquad\qquad \text{(V-11)}$$

These equations can be manipulated to obtain the following expressions for ϵ_{goi} and u_{Bi} (see APPENDIX C for details).

$$\epsilon_{goi} = \frac{H_s}{H_o} \left[\frac{1}{b_{i-1}} - \frac{1}{b_i} \right] \qquad\qquad i = 1 \to N \qquad \text{(V-12)}$$

$$u_{Bi} = \frac{H_o \left[b_i s_{i-1} - b_{i-1} s_i \right]}{b_i - b_{i-1}} \qquad\qquad i = 1 \to N \qquad \text{(V-13)}$$

Equations (V-12) and (V-13) can now be used to estimate ϵ_{goi} and u_{Bi} for the N classes of bubble sizes. The fraction of bubbles in class i, f_i, is given as:

$$f_i = \frac{\epsilon_{goi}}{\epsilon_{go}} \qquad\qquad i = 1 \to N \qquad\qquad \text{(V-14)}$$

182

D.3a.3. <u>Procedure for Obtaining Bubble Size (d_{Bi}) and Number of Bubbles (n_i)</u>

There are several correlations available in literature for obtaining bubble sizes based on the bubble rise velocity. Two of these correlations were selected for use in this study.

Abou-el-Hassan (1983) has presented a generalized bubble rise velocity correlation based on dimensionless groups that account for the parameters affecting bubble rise velocity as well as bubble interaction. It is independent of flow regimes and is applicable for Reynolds numbers between 0.1 and 10^4. The correlation is in good agreement with literature data for air-bubble motion in Newtonian fluids and covers the following range of conditions:

liquid-phase density = 710 to 1180 kg/m^3

liquid-phase viscosity = 0.233 to 59 mPa.s

interfacial tension = 0.015 to 0.072 N/m

The correlation is given by:

$$V = 0.75 \ [\log(F)]^2 \qquad \text{(V-15)}$$

where V (velocity number) and F (flow number) are defined as:

$$V = \frac{u_B d_B^{2/3} \rho_\ell^{2/3}}{\mu^{1/3} \sigma^{1/3}} \qquad \text{(V-16)}$$

$$F = \frac{g d_B^{8/3} (\rho_\ell - \rho_g) \rho_\ell^{2/3}}{\mu^{4/3} \sigma^{1/3}} \qquad \text{(V-17)}$$

The correlation is valid for velocity numbers in the range of 0.1 to 40 and flow numbers in the range of 1 to 10^6.

For bubble rise velocities greater than 0.15 m/s it was found that the correlation failed. Another correlation was used to determine the bubble

183

size for bubble rise velocities greater than 0.2 m/s (Clift et al., 1978),

$$u_B = \left[\frac{2.14\sigma}{\rho_\ell d_B} + 0.505gd_B \right]^{1/2} \qquad (V-18)$$

The equation was developed from experimental data for air bubbles rising in distilled water, and is valid for bubble sizes greater than 1.3 mm.

For the range of bubble rise velocities not covered by the above two correlations, bubble diameters were obtained by interpolation. Figure V-65 shows the relation between rise velocity and bubble diameter for FT-300 wax at 265°C, with the interpolated values indicated by the broken line. These correlations can now be used to estimate d_{Bi} values using bubble rise velocities (u_{Bi}) obtained from the procedure outlined in the previous section.

The number of bubbles (n_i) of size d_{Bi} can be calculated as follows. The overall or average gas hold-up is given by:

$$\epsilon_{go} = \frac{V_g}{V_T} \qquad (V-19)$$

where V_g is the volume of gas in the gas-liquid dispersion and V_T is the expanded volume. Equation (V-19) can be rewritten as:

$$\epsilon_{go} = \sum_{i=1}^{N} n_i V_i / V_T \qquad (V-20)$$

where n_i is the number of bubbles of size d_{Bi} and V_i is the volume associated with this group of bubbles. Therefore, the hold-up associated with bubbles of size d_{Bi} can be expressed as:
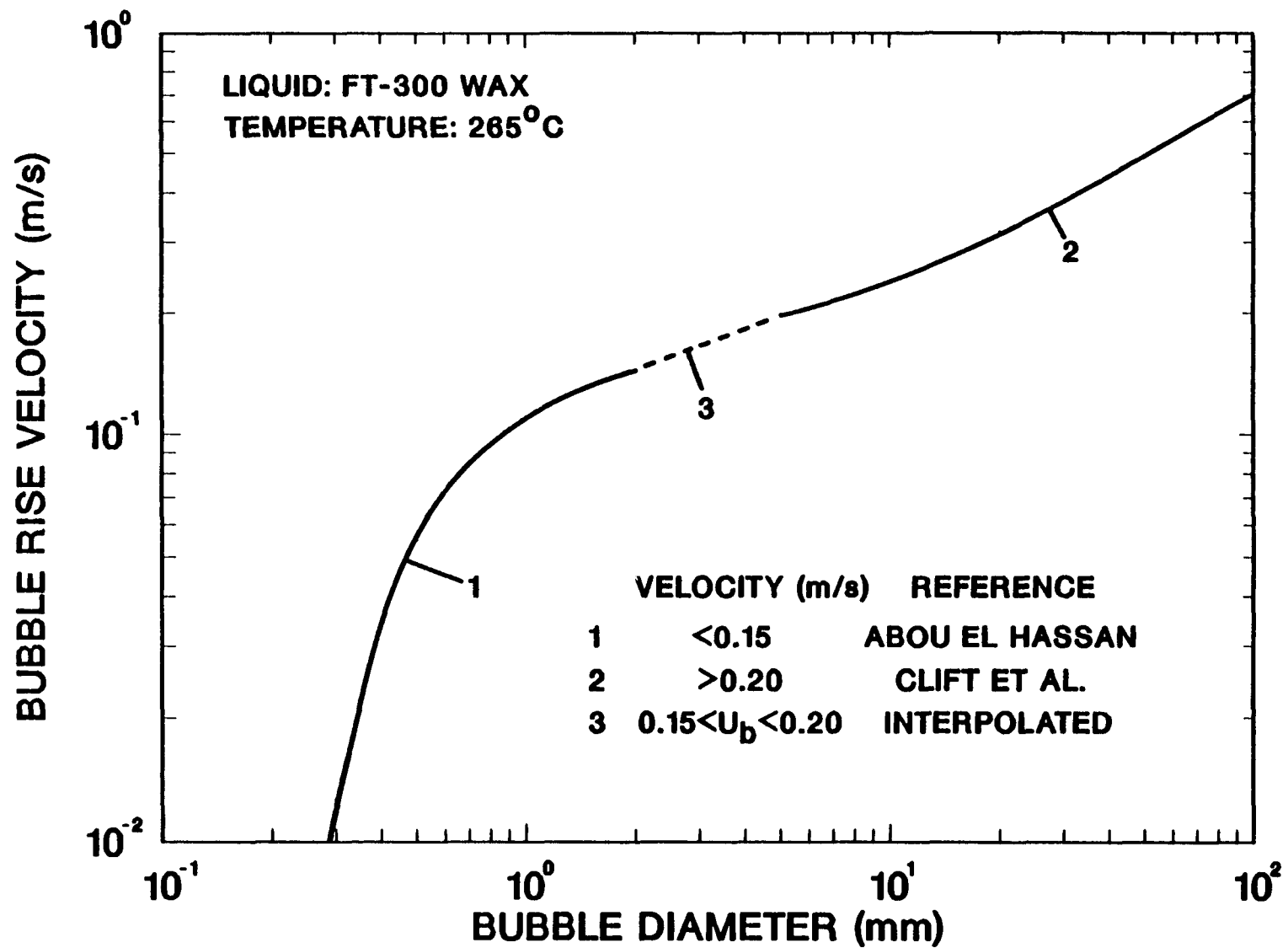
Figure V-65. Correlation of bubble rise velocity as a function of bubble diameter

$$\epsilon_{goi} = \frac{n_i V_i}{V_T} \qquad \text{(V-21)}$$

or

$$n_i = \frac{\epsilon_{goi} V_T}{V_i} \qquad \text{(V-22)}$$

The volume associated with bubbles of size d_{Bi} is given by:

$$V_i = \frac{\pi d_{Bi}^3}{6} \qquad \text{(V-23)}$$

and the total volume is:

$$V_T = \frac{\pi d_c^2 H_o}{4} \qquad \text{(V-24)}$$

where d_c is the column diameter. Substituting Equations (V-23) and (V-24) into Equation (V-22) yields:

$$n_i = \frac{3 \epsilon_{goi} d_c^2 H_o}{2 d_{Bi}^3} \qquad \text{(V-25)}$$

which may be used to calculate the number of bubbles of size d_{Bi}.

D.3a.4. <u>Sauter Mean Diameter</u>

By definition, the Sauter mean bubble diameter, d_s, is:

$$d_s = \frac{\sum\limits_{i=1}^{N} n_i d_{Bi}^3}{\sum\limits_{i=1}^{N} n_i d_{Bi}^2} \qquad \text{(V-26)}$$

Substituting Equation (V-25) into Equation (V-26), yields upon rearrangement:

186

$$d_s = \frac{\sum_{i=1}^{N} \epsilon_{goi}}{\sum_{i=1}^{N} \epsilon_{goi}/d_{Bi}} \qquad (V-27)$$

D.3b. Experimental Procedure

A videocamera and a VCR unit were used to record the drop in liquid level during the disengagement process. A vertical ruler mounted next to the column (in the camera's field of view) was used to obtain the actual heights. After the completion of a run with a given gas velocity, the gas flow was shut off using a solenoid valve and the drop in liquid level recorded. The level dropped rapidly during the first 5 to 10 s after the gas flow was shut off, due to the disengagement of the large bubbles. Thereafter, the level dropped slowly as the medium size and small bubbles disengaged from the dispersion. The recording was completed when the level reached a stationary value (corresponding to the static height). Towards the end of the recording period, a large number of very tiny bubbles could be seen rising through the dispersion.

The data analysis procedure involved the analysis of the video tape followed by the data reduction procedure. The video tape was scanned and the time elapsed (t) recorded for different values of height (H) as the level dropped during the disengagement process. The data were recorded directly into a personal computer. The frequency at which time was recorded ranged from every 0.05 m drop in level (during the initial period when the level dropped rapidly) to every 0.005 m drop in level (towards the end when tiny bubbles were disengaging). This procedure was repeated three to four times for each velocity to reduce errors. Following this step, the normalized liquid level (H/H_o) plot was directly displayed on the screen.

Appropriate break points were then selected by the user and plots similar to those shown in Figure C-1 (APPENDIX C) obtained. The slopes and intercepts of the straight line segments were then computed and the corresponding rise velocities and hold-up fractions obtained. The computer then calculated bubble sizes for each class of bubbles, the number of bubbles in each class and finally the Sauter mean diameter. A summary data sheet for every run, similar to those shown in APPENDIX D, was then printed out.

D.3c. Experimental Results

DGD measurements were made after a minimum of one and a half hour per velocity for velocities between 0.01 and 0.05 m/s, and a minimum of 1 hour for velocities greater than 0.05 m/s except for a few runs as discussed below. It was necessary to wait for this duration to ensure that steady state was achieved, particularly when foam was present. Summary of results for selected runs are included in APPENDIX D.

D.3c.1. Effect of Operating Temperature

Figure V-66a is a plot of the Sauter mean bubble diameter (d_s) as a function of superficial gas velocity for experiments conducted with FT-300 wax in the 0.051 m ID column using a 1.85 mm orifice plate distributor. Average gas hold-up values for these runs are shown in Figure V-66b. Figures V-68a and V-68b show similar results for runs conducted with Sasol's Arge wax.

Sauter mean diameter values for FT-300 wax at 265°C (Figure V-66a) are consistently lower than values at 200°C for all velocities, except at 0.01 m/s. In the presence of foam (u_g = 0.02 to 0.05 m/s), d_s at 200°C is 50% higher than d_s at 265°C (0.75 mm compared to around 0.5 mm). This
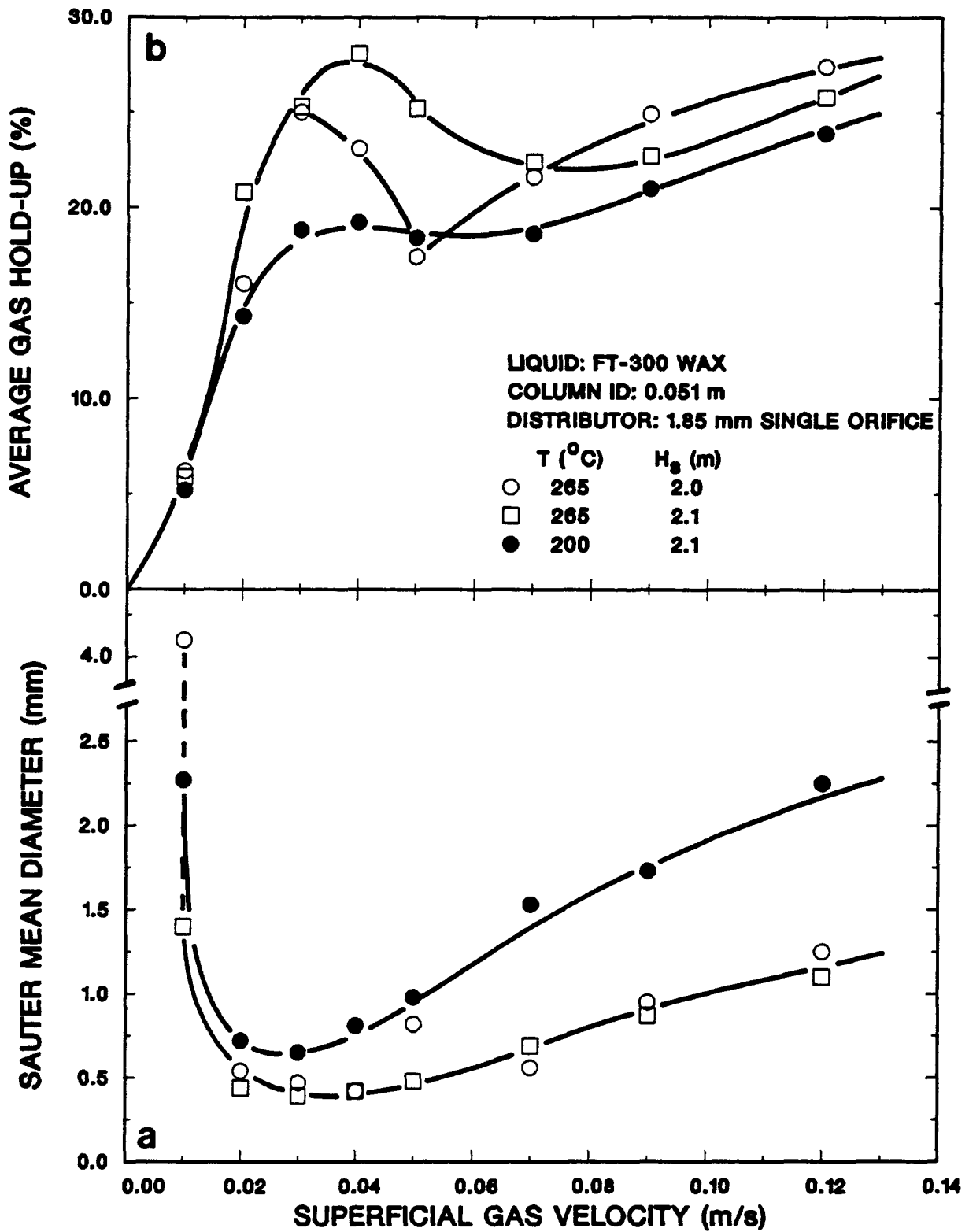
Figure V-66. Effect of temperature and superficial gas velocity on the Sauter mean bubble diameter (a) and gas hold-up (b) (◯- Run 6-1; ☐ - Run 13-3; ●- Run 13-2)

difference increases as u_g increases and at 0.12 m/s d_s at 200°C is approximately twice as large as d_s at 265°C (2 mm compared to 1 mm). Results for Sasol reactor wax (Figure V-68a) show a similar effect of temperature on the Sauter mean diameters. Studies were also conducted with Mobil reactor wax to investigate the effect of temperature. Results from these studies showed trends that were the same as those for FT-300 and Sasol waxes, therefore, they are not shown here.

The significant differences between d_s values at the 200°C and 265°C can be attributed mainly to the different viscosities of the waxes at these temperatures. Viscosity for the three waxes investigated were between 50 to 65% higher at 200°C than at 265°C. Therefore, the effect of temperature on Sauter mean diameters can be viewed as the effect of liquid viscosity.

Figure V-67a shows the effect of gas velocity on the small and large bubble sizes for the runs conducted at 200°C and 265°C with FT-300 wax. The variation in the volume fraction of large bubbles with gas velocity at the two temperatures is shown in Figure V-67b. The results for the two runs are given in Tables D-1 and D-2 (APPENDIX D). These results show that small bubbles determine the value of d_s at most velocities. However, at higher gas velocities, the volume fraction of large bubbles reaches as high as 80% and large bubbles have some effect on the value of d_s. This causes the Sauter mean bubble diameter to increase slightly for velocities 0.05 m/s and higher. Figure V-67a shows that the diameter of small bubbles was not affected by gas velocity, however, large bubbles increased in diameter at higher velocities (u_g = 0.07 - 0.12 m/s) mainly due to the growing number of slugs. The diameter of small bubbles at 265°C was around 0.33 mm, while the diameter for small bubbles at 200°C was around 0.45 mm. The diameters

190
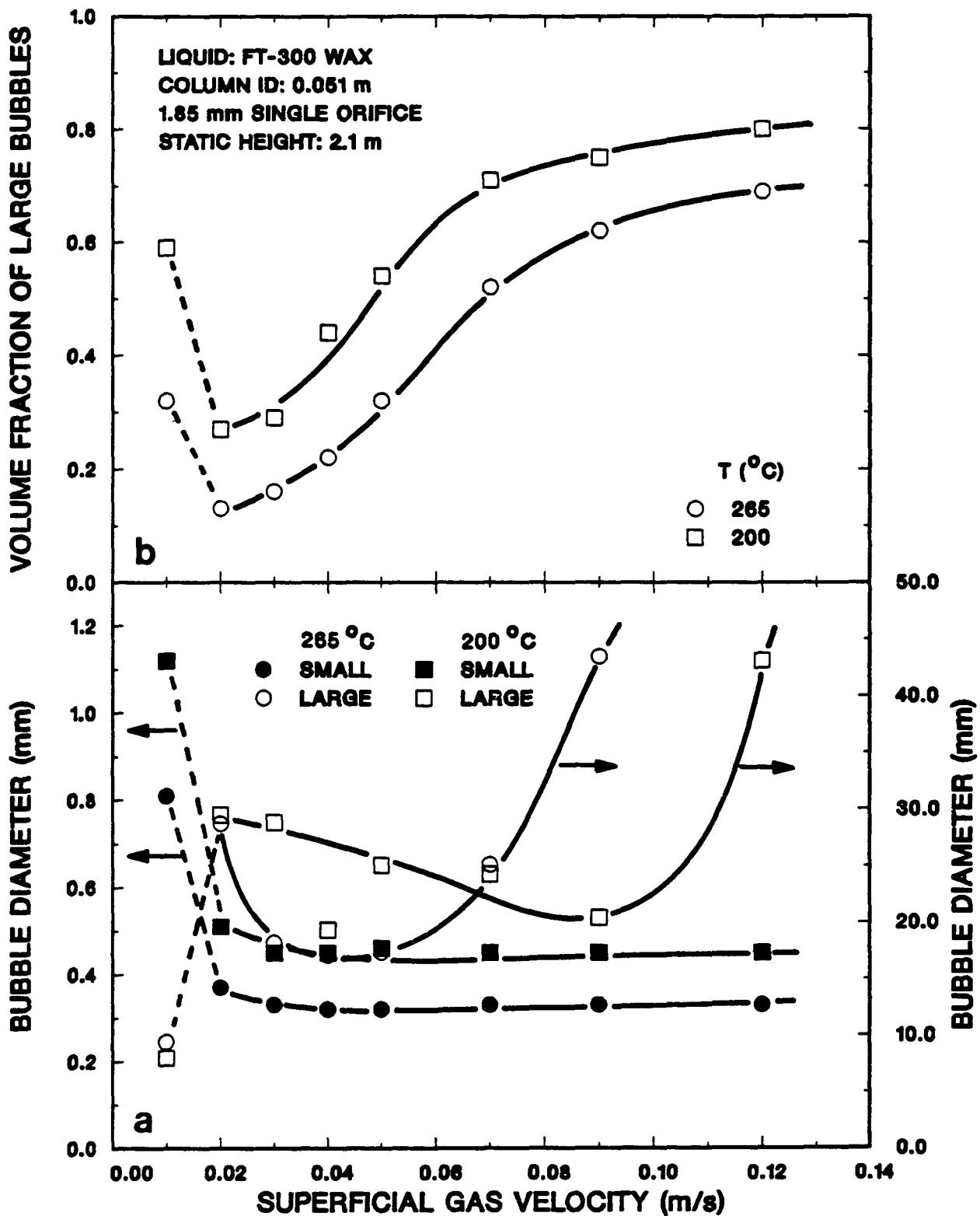
Figure V-67. Effect of temperature and superficial gas velocity on bubble size (a) and volume fraction of large bubbles (b) (O - Run 13-3; □ - Run 13-2)
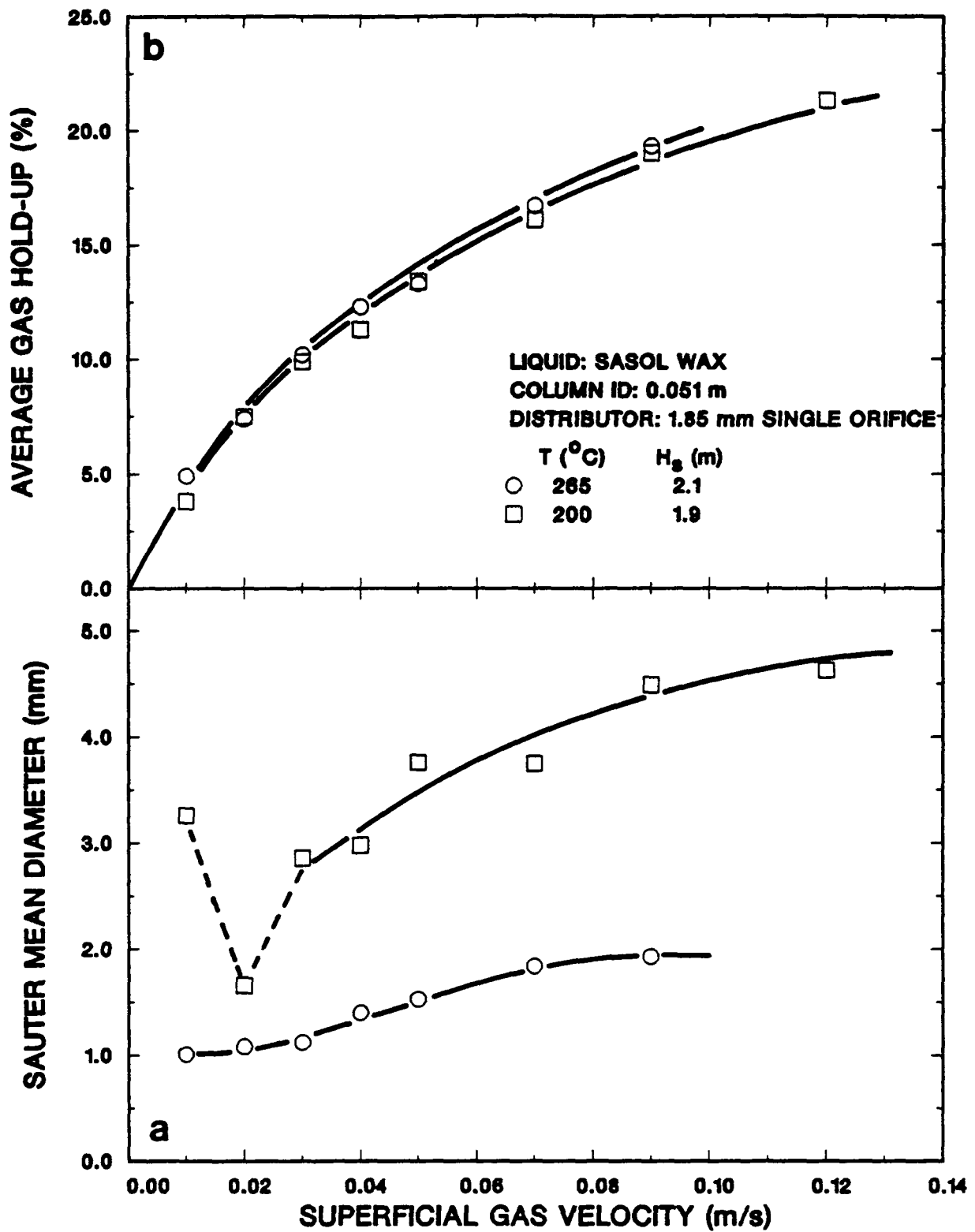
Figure V-68. Effect of temperature and superficial gas velocity on the Sauter mean bubble diameter (a) and gas hold-up (b) (○- Run 8-4; □- Run 8-3)

of large bubbles are similar at the two temperatures. These results show that small bubbles are mainly responsible for the differences in d_s values at the two temperatures. This is in agreement with results reported by Schugerl (1981), who conducted studies with glycerine solutions and showed that bubbles in that system could be classified into three size ranges. The small bubbles had the strongest influence on d_s. Schugerl's studies also indicate that d_s increases with viscosity and superficial gas velocity.

Hold-ups at 200°C were consistently lower than at 265°C with all waxes for the range of superficial gas velocities employed in these studies. Figure V-66b shows a significant difference between hold-up values at the two temperatures for velocities between 0.02 and 0.05 m/s, however this is not reflected in the d_s values. The difference in hold-ups is mainly due to the extent of foaming, which was different for the different runs. In the presence of foam the number of small bubbles is exceedingly high and exerts a strong influence on d_s. However, the diameter of these bubbles is not influenced by the amount of foam and remains fairly constant (as shown in Figure V-67a), therefore, d_s, in the presence of foam, is independent of the hold-up value. Figure V-66a also illustrates reproducibility of results (d_s values) for the two runs conducted at 265°C. Results from the two runs at 265°C are in good agreement, except for discrepancies between d_s values at 0.01 and 0.05 m/s, which could be attributed to the foaming character-istics (at 0.05 m/s) or to errors in the measurement process (at 0.01 m/s). At 0.05 m/s, foam was still present in Run 13-3 but it was absent in Run 6-1.

D.3c.2. Effect of Distributor Type

Figures V-69 and V-71a illustrate the effect of distributor type on

193
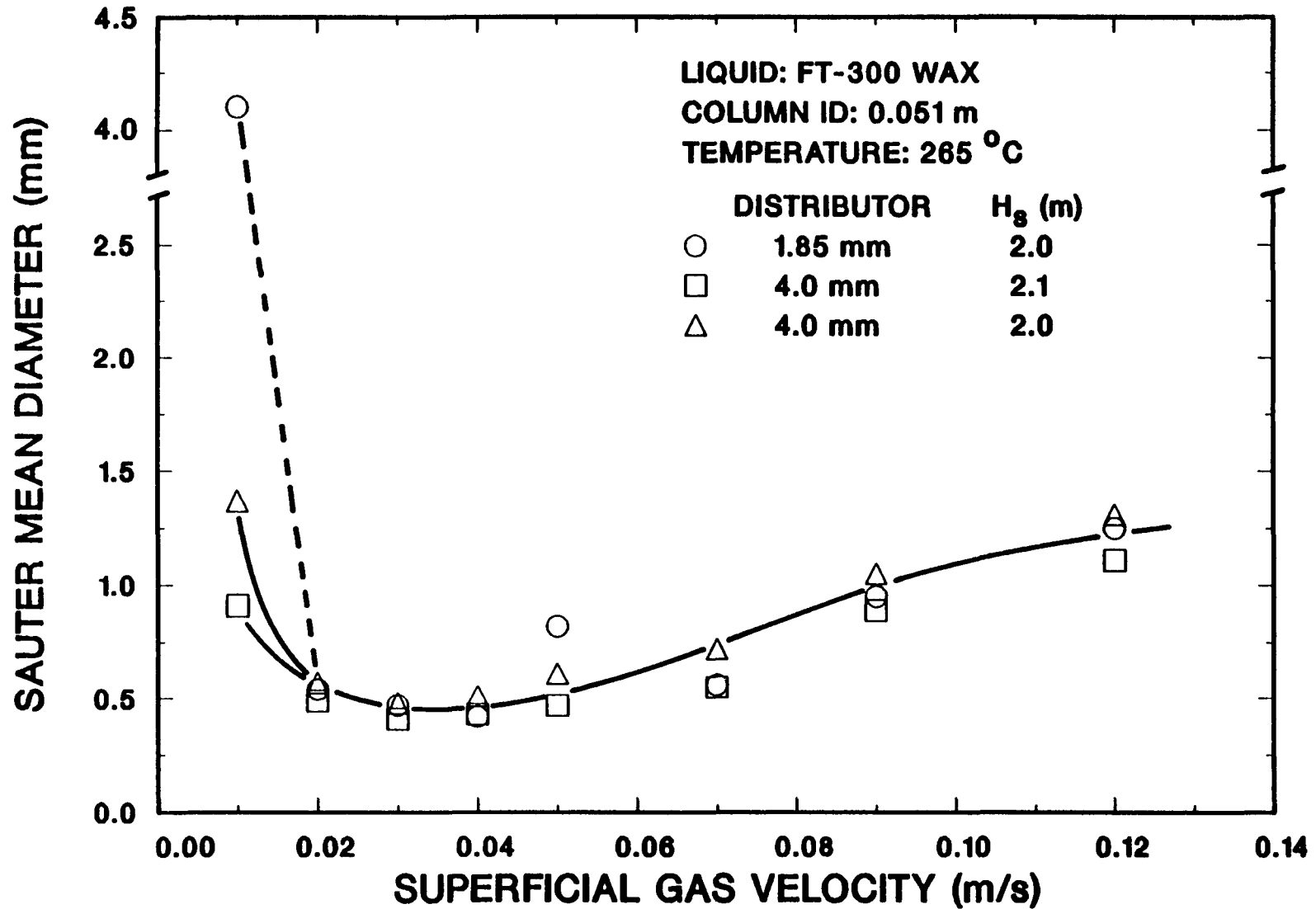
Figure V-69. Effect of distributor type and superficial gas velocity on the Sauter mean bubble diameter (O- Run 6-1; □- Run 6-2; △- Run 6-3)

the Sauter mean diameter for FT-300 and Mobil reactor wax. Results for Sasol reactor wax are qualitatively similar to those for Mobil wax and are not shown. Only orifice plate distributors (1.85 mm and 4 mm) were used in experiments with FT-300 wax. Runs with a $40\mu m$ SMP distributor caused excessive foaming preventing the use of the DGD technique for bubble size distribution measurements. The 1.85 mm orifice plate distributor and the $40\mu m$ SMP were used for experiments with the reactor waxes. With these waxes foaming was not a problem and DGD measurements could be made with both distributors. All runs were conducted at a temperature of 265°C. Figure V-71b shows hold-up values for the two runs conducted using Mobil reactor wax.

Results for runs made using FT-300 wax (Figure V-69) show no significant effect of distributor type, with similar d_s values resulting for both 1.85 and 4 mm distributors. There is, however, significant variation in d_s values at a superficial gas velocity of 0.01 m/s. This variation might be indicative of the inability of the DGD technique to predict Sauter mean diameters at very low gas velocities (or low gas hold-up values). However, trends are similar for all runs made with FT-300 wax, i.e. d_s is significantly greater at 0.01 m/s compared to values in the velocity range 0.02 - 0.05 m/s. Results for FT- 300 wax once again show that when foam is present the Sauter mean diameter is approximately constant (i.e. independent of the gas velocity and the amount of foam present).

Figure V-70a shows the effect of gas velocity on the small and large bubble diameters for experiments conducted with the 1.85 mm and 4 mm orifice plate distributors using FT-300 wax. The size of small bubbles, with the 4 mm orifice, is around 0.35 mm which is similar to values with the
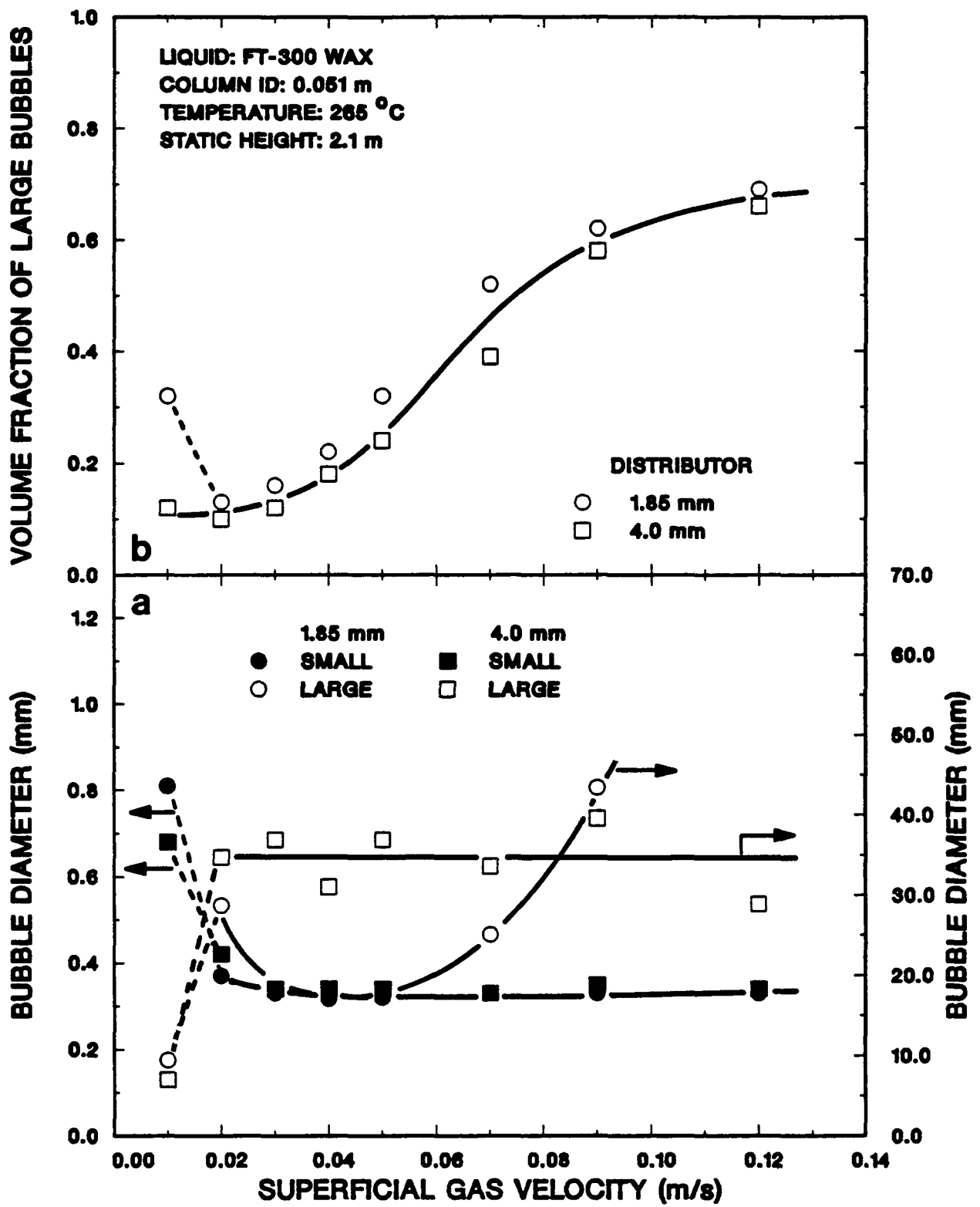
Figure V-70. Effect of distributor type and superficial gas velocity on bubble size (a) and volume fraction of large bubbles (b) (O - Run 13-3; □ - Run 6-2)

1.85 mm orifice (0.33 mm). Table D-3 (APPENDIX D) gives results for experiments with the 4 mm distributor. These results indicate little variation in the size of small bubbles with gas velocity, similar to observations with the 1.85 mm distributor. The variation in the volume fraction of large bubbles with gas velocity is similar for the two runs (Figure V-70b). Therefore, the influence of large bubbles on the Sauter mean diameters for the two distributors (for u_g > 0.05 m/s) is expected to be the same, as is shown in Figure V-69. Figure V-69 once again shows that results from two different runs with FT-300 wax, using the 4 mm orifice plate distributor, are in fairly good agreement with one another.

Results from experiments conducted with Mobil reactor wax (Figure V-71a) showed a minimal effect of distributor type, with the SMP distributor resulting in d_s values that are somewhat lower than those with the 1.85 mm orifice plate distributor. Sauter mean diameter increased with gas velocity from around 1 mm at 0.01 m/s to approximately 5 mm at 0.12 m/s using the 1.85 mm distributor. These values are about 20% higher than those with the SMP distributor at most velocities.

Most of the literature dealing with the influence of distributor type on bubble size indicates that bubble sizes in fully established gas-liquid dispersion is independent of distributor type (e.g. Akita and Yoshida, 1974; Mersmann, 1978). Findings from the present study with waxes appear to be in good agreement with trends reported in literature.

D.3c.3. Effect of Column Diameter

The effect of column diameter was investigated using FT-300 wax in the 0.051 m ID and 0.229 m ID glass columns. Figure V-72 shows results from these studies. Sauter mean diameters from three runs in the 0.229 m ID

197
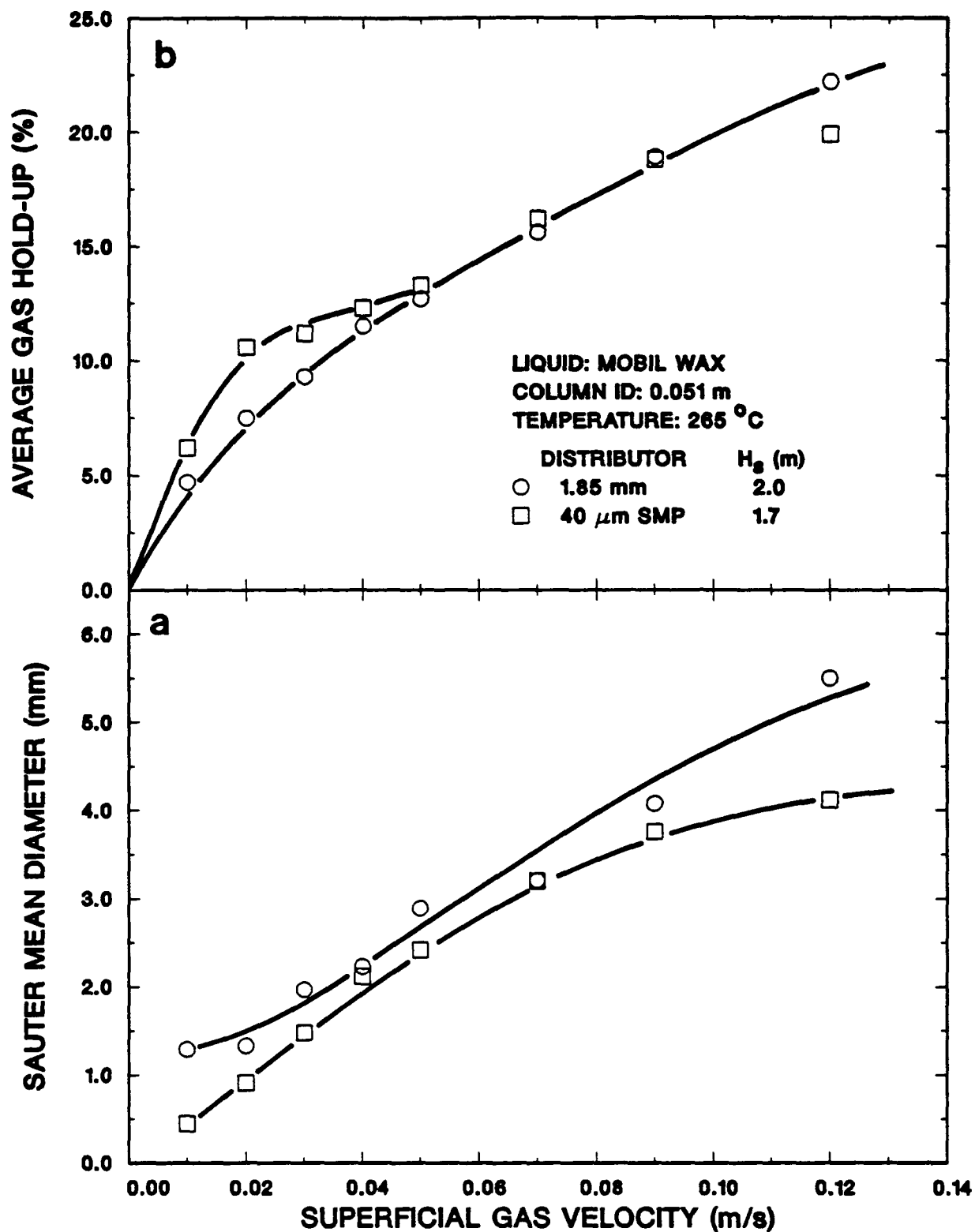
Figure V-71. Effect of distributor type and superficial gas velocity on the Sauter mean bubble diameter (a) and gas hold-up (b) (O - Run 9-3; □ - Run 9-4)

column and one run in the 0.051 m ID column are presented in Figure V-72a. Figure V-72b shows hold-up values for these runs. All runs were conducted at a temperature of 265°C. A 19 X 1.85 mm distributor was used for runs made in the large column, while the 1.85 mm orifice plate distributor was used in the 0.051 m ID column.

Sauter mean diameters from runs made in the two columns appear to be qualitatively similar with d_s approaching a constant value of around 0.8 mm at higher velocities (u_g greater than 0.05 m/s). The flow field in the two columns is different, with runs in the smaller column having a greater tendency to produce more foam and slugs were present at higher velocities. This difference manifests itself in the shape of the curves shown in Figure V-72. All runs in the 0.051 m ID column produced slugs that were distributed along the entire column length at u_g values greater than 0.05 m/s, however, this was not seen in the larger column. Churn-turbulent flow prevailed in this column for these high gas flow rates. The effect of gas velocity on the small and large bubbles for the run in the 0.051 m ID column and one run in the 0.229 m ID column is shown in Figure V-73a. The variation in the volume fraction of large bubbles with gas velocity for the two runs is shown in Figure V-73b. A significant difference between the two columns is the contribution of large bubbles to the Sauter mean diameter. The volume fraction of large bubbles (f_L) in the 0.051 m ID column increased steadily with gas velocity and reached 70% at 0.12 m/s, whereas f_L in the large column appears to reach a constant value of around 50% for gas velocities above 0.05 m/s. Slugs in the smaller column are stabilized by the wall and continue to grow in size with an increase in gas velocity, however, large bubbles in the 0.229 m ID column are relatively

199
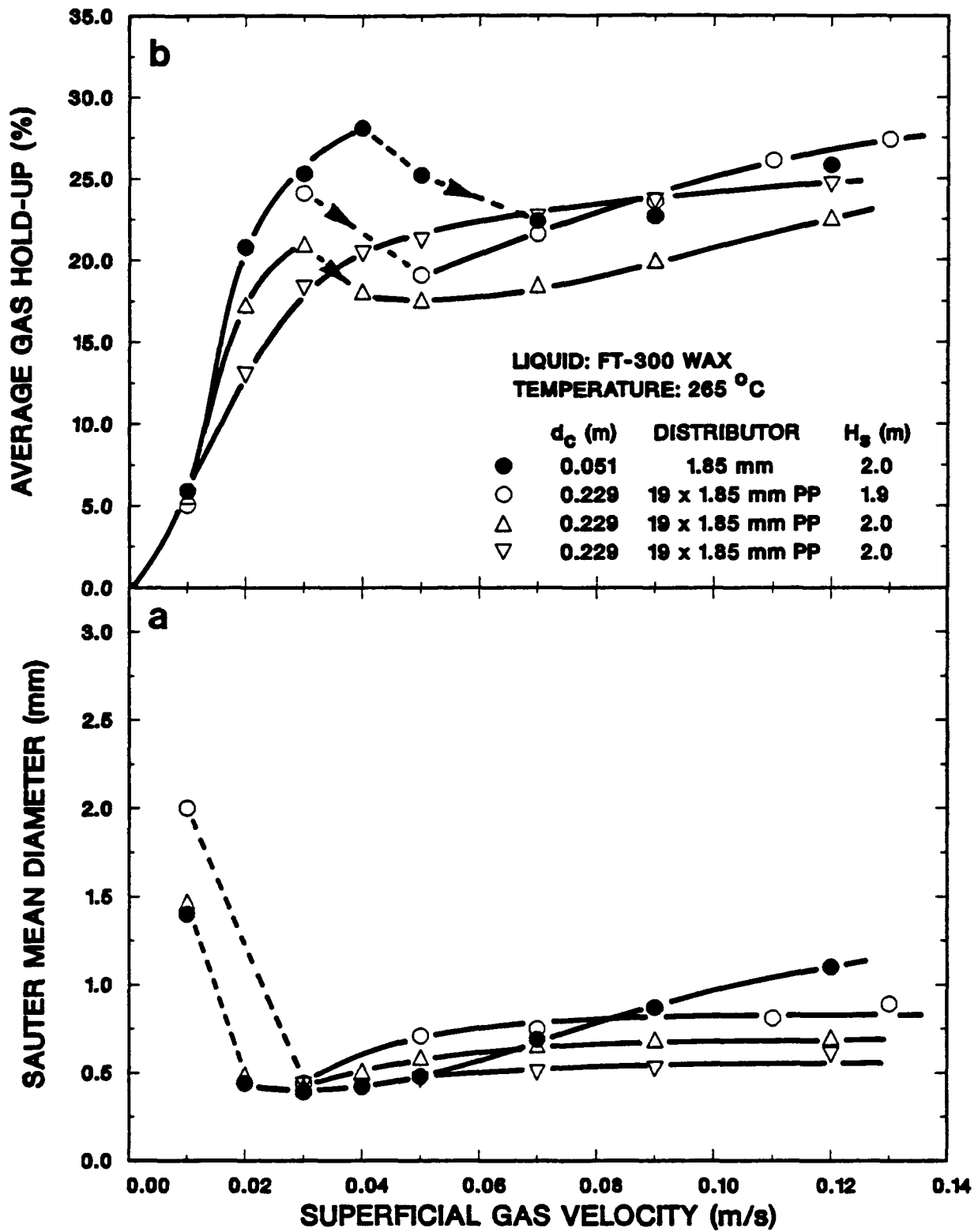
Figure V-72. Effect of column diameter and superficial gas velocity on the Sauter mean bubble diameter (a) and gas hold-up (b) (● - Run 13-3; ○ - Run 1-3; △ - Run 2-8; ▽- Run 2-9)
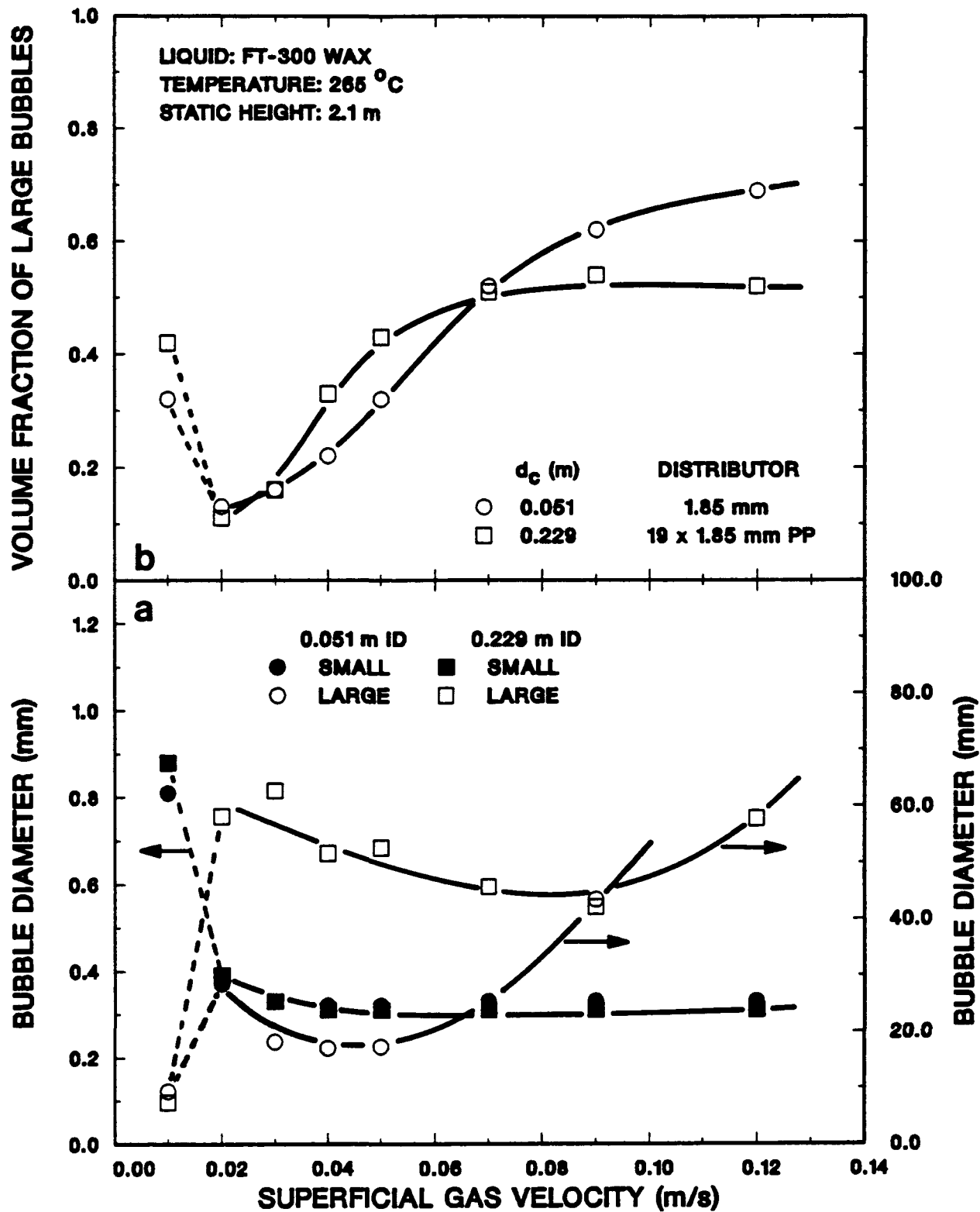
Figure V-73. Effect of column diameter and superficial gas velocity on bubble size (a) and volume fraction of large bubble (b) (○- Run 13-3; □- Run 2-8)

unstable and do not grow with an increase in gas velocity. Figure V-73a shows that in the 0.229 m ID column, large bubbles remained between 50 and 60 mm in diameter for gas velocities greater than 0.02 m/s, however, results for the 0.051 m ID column indicate that large bubbles (or slugs) continue to grow for velocities greater than 0.05 m/s. This explains the different trends observed for the variation of d_s with u_g in the two columns. The diameter of small bubbles for the large column is 0.31 mm and remains fairly constant over the entire range of superficial gas velocities (Table D-4). This value compares well with the value of 0.33 mm for the 0.051 m ID column (Table D-1). This is also illustrated in Figure V-73a.

The correlation presented by Akita and Yoshida (1974), based on studies conducted with other systems, indicates that d_s should be higher for 0.051 m ID column compared to d_s for the 0.229 m ID column. This is not clear from results illustrated in Figure V-72 due to the discrepancy in values from the different runs made in the 0.229 m ID column.

Results from the three runs in the 0.229 m ID column show similar trends, i.e. d_s reaches a fairly constant value at around 0.05 to 0.07 m/s, however, there is some discrepancy between values from the different runs. This can be partly attributed to different run times employed and to different foaming characteristics. Run 1-3 was conducted using shorter run times compared to Runs 2-8 and 2-9 (20-30 minutes per velocity for the former compared to 60-90 minutes for the latter runs). Hold-up values for the runs conducted in the 0.229 m ID column (Figure V-72b) reflect these differences.

D.3c.4. <u>Effect of Wax Type</u>

Figure V-74a illustrates the effect of wax type on the Sauter mean bubble diameter. Results are presented for runs made in the 0.051 m ID column using a 1.85 mm orifice plate distributor at a temperature of 265°C. Figure V-74b shows the effect of wax type on the volume fraction of large bubbles (f_L). Hold-up values for the three runs are shown in Figure V-75. Results for these three runs are summarized in Tables D-1, D-5 and D-6 in APPENDIX D.

Sauter mean diameters for the three waxes are significantly different as shown in Figure V-74a. FT-300 wax shows a decrease in d_s as gas velocity increases from 0.01 m/s to 0.02 m/s, and stays at around 0.5 mm for velocities in the range 0.02 to 0.05 m/s. It increases to around 1 mm as u_g approaches 0.12 m/s. These values for the Sauter mean diameter are in good agreement with those reported in literature. Quicker and Deckwer (1981) have reported a value of around 0.7 mm for FT-300 wax. Workers at Mobil (Kuo et al., 1985) conducted DGD studies with FT-200 wax and reported average bubble diameters of 2.2 mm at 0.012 m/s and 1.2 mm at 0.022 m/s. The decrease in d_s values when the flow regime changes from bubbly flow (u_g around 0.01 m/s) to foamy flow regime was also observed by Quicker and Deckwer.

Sauter mean diameters for Sasol wax are around 1 mm at a gas velocity of 0.01 m/s and increase steadily to around 2 mm at 0.09 m/s. Similarly, Mobil wax gives d_s values that range from around 1 mm at 0.01 m/s to 5.5 mm at 0.12 m/s. The volume fraction of large bubbles shows similar behavior for these two reactor waxes (Figure V-74b). In the absence of foam, the concentration of larger bubbles increases due to coalescence. FT-300 wax,
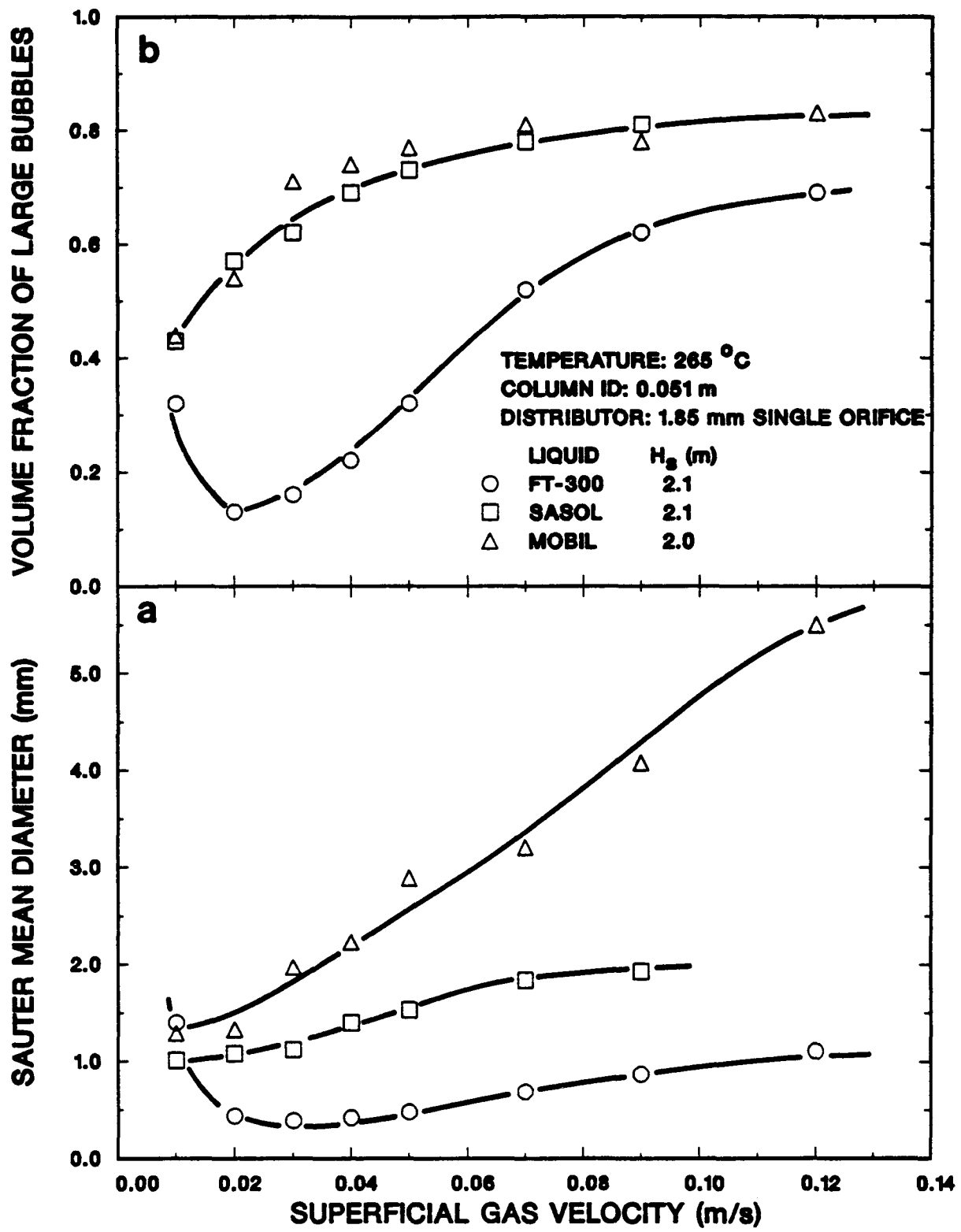
Figure V-74. Effect of liquid medium and superficial gas velocity on the Sauter mean bubble diameter (a) and volume fraction of large bubbles (b) (O- Run 13-3; □- Run 8-4; △- Run 9-3)

on the other hand, has a large fraction of small bubbles which remains entrained in the dispersion. However, once gas velocities reach around 0.05 to 0.07 m/s, slugs begin to dominate and the hold-up begins to be dominated by large bubbles. Therefore, f_L appears to increase beyond this point, showing a trend similar to that for the reactor waxes.

Figure V-75 shows that hold-up values for the two reactor waxes (Sasol and Mobil) are very similar, despite significant differences in the Sauter mean bubble diameters (as shown in Figure V-74a). Hold-up values for FT-300 wax are significantly higher than those for the reactor waxes in the velocity range 0.02-0.07 m/s, therefore, the lower Sauters for this wax are as expected. For velocities above 0.07 m/s, the difference in hold-ups is less than 5% (absolute), however, d_s values for FT-300 wax are still significantly lower. These results indicate that even though different waxes give similar hold-ups, the Sauter mean bubble diameters can be significantly different.

Experiments were also conducted at 200°C with the three waxes using the 1.85 mm orifice plate distributor. The trends observed in these experiments are qualitatively similar to those at 265°C and are not shown here.

Schumpe and Grund (1986) have recently applied the DGD technique to study the gas hold-up structure for the air-water system in a bubble column. In their studies, two distinct bubble classes were observed for all experiments. They show that the rise velocity for small bubbles (and therefore the diameter of small bubbles) remained almost constant for the velocity range 0.01-0.20 m/s. This is similar to the behavior of small bubbles found in the present work.
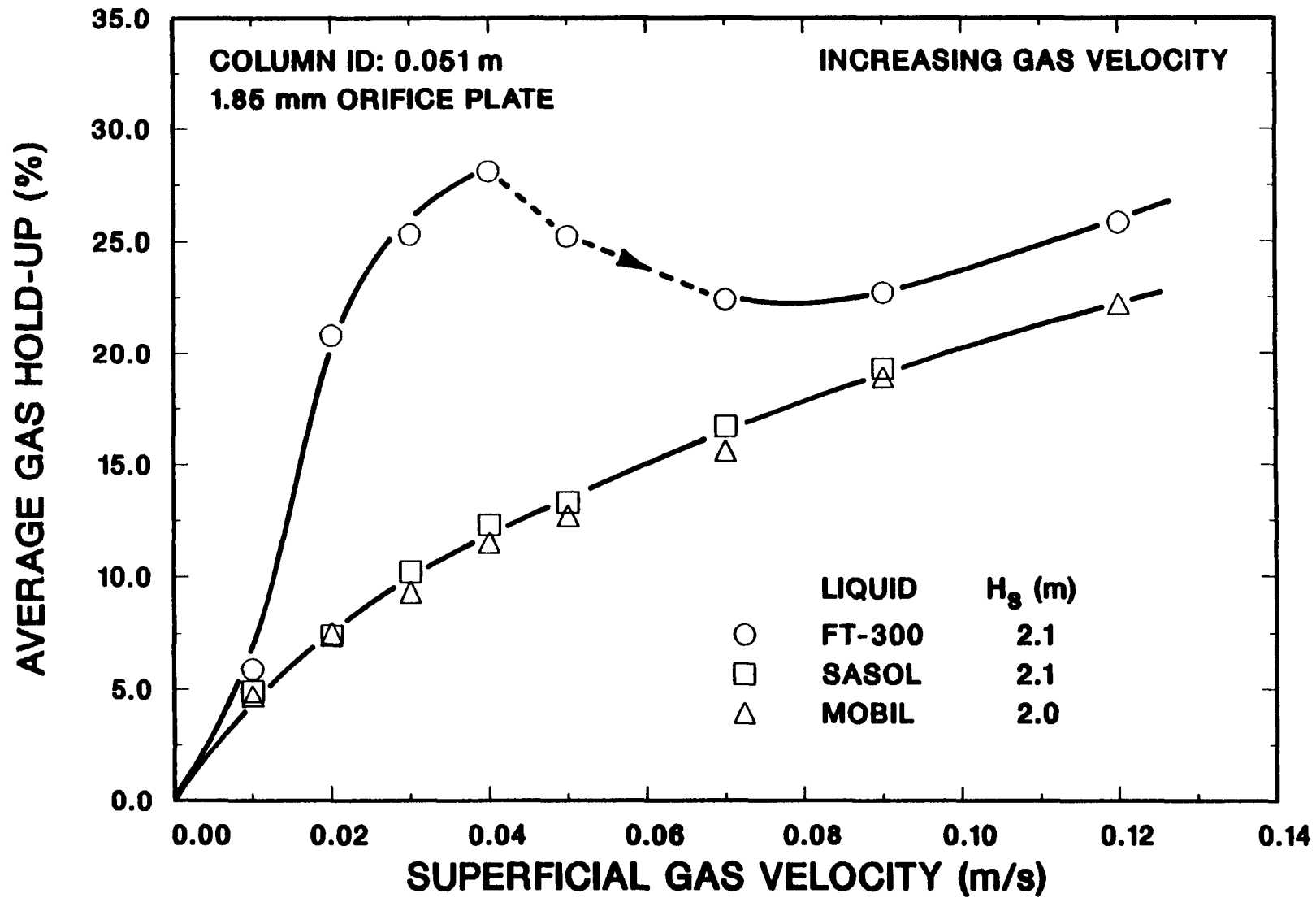
Figure V-75. Effect of liquid medium and superficial gas velocity on gas hold-up (O - Run 13-3; □ - Run 8-4; △ - Run 9-3)

D.3d. <u>Limitations of the DGD Technique</u>

The dynamic gas disengagement technique provides a convenient method for the characterization of the bubble size distributions in the bubble column. However, there are problems and limitations associated with this technique which need to be understood in order to appreciate their effect on the results.

The assumption of initial axial homogeneity of the bubble size distribution (see Section V-D.3a.) is in fairly good agreement with the phenomena observed in the bubble column for majority of gas flow rates employed. However, at superficial gas velocities between 0.02 and 0.04 m/s, where slugs are present only in the top half of the column, the above assumption is likely to introduce errors. Axial homogeneity implies that the time t_1^* (see Figure V-64) corresponds to the time taken for a large bubble (bubble in class N) to travel from just above the distributor to the top of the dispersion. Therefore, the technique overestimates the rise velocity for this class of bubbles when they are distributed over only a portion of the column, as is the case with slugs. Since bubble size is obtained using the rise velocity (Figure V-65), a larger bubble size would be obtained for this class of bubbles. However, the effect of this error on the Sauter mean diameter (d_s) is insignificant. As an example, let us consider the data for FT-300 wax (Run 13-3, 265°C, u_g = 0.03 m/s). The value for d_s is 0.394 mm (see Table D-1) using a value of 18.2 mm as the diameter (d_{BL}) for the large class of bubbles. If d_{BL} was reduced to 10 mm instead (55% of the original value), the value for d_s becomes 0.393 mm, a difference of less than 0.5%. The value for d_s in this range of superficial gas velocities (0.03-0.04 m/s) is governed by the diameter of the large number of small

207

bubbles (for the example in consideration, there were 5.15 x 10^7 small bubbles and only 73 large bubbles), therefore, errors in the estimated value of large bubble diameters in this velocity range do not have a significant effect on d_s.

The theory for DGD also assumes that significant bubble interactions do not occur during the disengagement process. Such interactions do occur since liquid flowing downwards, to displace the large bubbles that are disengaging, will affect the disengagement of the fine bubbles. Even though the magnitude of these interactions can not be quantified, it is believed that this does not have a significant effect on the results.

The experimental procedure employed, to measure the rate at which the expanded height drops, has a certain amount of subjectivity associated with it. The disengagement process lasts typically between 60 to 80 s (in some instances, where foam is present, it takes up to 120 to 140 s for bubbles to disengage). During this period, "weeping" of wax into the plenum chamber is inevitable despite the back pressure of the gas trapped below the distributor. The amount of "weeping" obviously depends on the distributor used; with negligible drainage for SMP and relatively higher amounts draining with the 4 mm distributor. Therefore, towards the end of the disengagement process, when only the very small bubbles are disengaging, special care has to be taken to interpret the rate at which the level drops. It is possible that some of the drop in the liquid level is caused by "weeping". Table V-2 compares the observed change in static height between two velocities to the change in level attributed to the small class of bubbles for a run with FT-300 wax. The observed change in static height is the difference between visual measurements of the static height at two

Table V-2. Effect of "weeping" on small bubble diameter obtained by DGD (FT-300 wax, Run 13-3, 265°C, 0.051 m ID column, 1.85 mm orifice plate distributor).

u_g (m/s)	Drop in height (m) weeping	Drop in height (m) Small bubble disengagement	Error[a] (%)
0.01	0.0	0.057	0.0
0.02	0.010	0.321	3.0
0.03	0.010	0.456	2.1
0.04	0.006	0.450	1.4
0.05	0.010	0.340	2.8
0.07	0.023	0.192	12.2
0.09	0.011	0.164	7.0
0.12	_[b]	0.186	_[b]
	Average error due to weeping		3.5

[a] Error is calculated as follows:

$$\frac{\left\{ \begin{array}{c} \text{Height due to} \\ \text{small bubble} \\ \text{disengagement} \end{array} \right\} - \left\{ \begin{array}{c} \text{Height due} \\ \text{to weeping} \end{array} \right\}}{\left\{ \begin{array}{c} \text{Height due to} \\ \text{small bubble} \\ \text{disengagement} \end{array} \right\}} \times 100$$

[b] drop in height not measured

209

consecutive velocities. The drop in height attributed to the disengagement of the small bubbles was obtained from the H/H_o versus t plot by subtracting the static height (H_s) from the height corresponding to the intercept (b_s) of the line for the small class of bubbles (i.e. b_s X (H_o - H_s)). Assuming that the change in static height is purely due to "weeping" of wax into the plenum chamber, and further assuming that this phenomenon occurs only during the disengagement of the small bubbles, values in Table V-2 show that for Run 13-3 this causes, on an average, a 3.5% error in the level drop attributed to disengagement of small bubbles. This translates into a 3 to 4% error in the rise velocity associated with this class of bubbles. For a superficial gas velocity of 0.07 m/s, when the error due to "weeping" appears to be significant (12.2%), the Sauter mean diameter changes from 0.69 mm to 0.68 mm after correcting for "weeping", a difference of less than 2%. This example illustrates that even though "weeping" is a problem during DGD, its affect on the value of d_s is not significant.

The application of the DGD technique has a severe limitation under conditions where foam is produced at the top of the gas-liquid dispersion. For FT-300 wax foam was present for superficial gas velocities in the range 0.02 to 0.05 m/s in most cases. Under these conditions, the bubbles of interest are those which are in the dispersion between the distributor and the foam- liquid interface. In order to circumvent this problem, researchers at Mobil (Kuo et al., 1985) followed the drop in the foam-liquid interface during the disengagement process instead of the top of the foam. However the use of this alternative was not found useful in our experiments. First, the foam-liquid interface is not distinct at most

velocities; it usually consists of a zone 0.05 to 0.10 m in height where foam appears to be thoroughly mixed with the liquid. Secondly, the foam-liquid interface, when distinct, appears to drop initially when large bubbles disengage, however, it begins to rise beyond this point. Even though small bubbles are still disengaging, the breakage of foam (which is approximately 30% liquid) results in a net increase in the liquid level. Consequently, all measurements made in this study are based on the rate of drop of the top of the dispersion (including foam, when present). There-fore, d_s values for instances where foam was present, should be interpreted with caution. A possible solution for this problem is to recalculate d_s after subtracting the hold-up attributed to foam (which is measured during the experiments) from the hold-up corresponding to small bubbles.

The data reduction step also involves a certain amount of subjectivity. The selection of the number of break points for a given set of data, which in turn determines the number of bubble classes (see Figure V-64, for example), is subject to some variability. For majority of cases this was not a problem and break points were obvious. For instances where this was not the case, several different break points were tried and the lines that gave the lowest value for sum of squared errors were selected. Since the value for d_s is dictated by the size of the small bubbles, its sensitivity to errors in the selection of break points is of importance. Earlier calculations for problems due to "weeping" showed that an error of 12.2% in the height corresponding to the disengagement of small bubbles (which is approximately equal to a 12.2% error in the slope for the line corresponding to this class of bubbles, or the rise velocity for these bubbles) translated to an error of less than 2% in the d_s value. This is

because bubble diameter is not very sensitive to variations in rise velo-
city in this range (refer to Figure V-65 for rise velocities between 0.03
and 0.10 m/s). Therefore, the error caused by the subjectivity in the
selection of break points is not expected to be significant.

The process of converting rise velocities to bubble diameters involves
the use of available correlations as discussed previously. Even though
these correlations are dependent on the physical properties of the liquid
medium, the assumption that they can be used for waxes cannot be verified
due to lack of data. The following discussion is therefore limited to the
sensitivity of DGD results to errors in the measurement of physical
properties. Experimentally determined values for density and viscosity
appear to be in agreement with values reported in the literature (see
Section VI-A.). The relative error in density measurements is expected to
be less than 3%, while the error in viscosity measurements is less than 5%
(based on variation in measurements with fluids of known viscosities). The
effect of these errors on the value of d_s was determined for FT-300 wax
(Run 13-3, 265°C, 0.051 m ID column). At a superficial gas velocity of 0.07
m/s, d_s is 0.69 mm. An error of 5% in the value for viscosity translates to
a change of less than 3% in the d_s value. Similarly, an error of 3% in
density measurements translates to a change of approximately 1% in the
value of d_s. Therefore, d_s values are expected to have a maximum relative
error of less than 5%, based on possible errors in physical property
measurements.

The contribution from the various problems and limitations to the
overall error in results obtained from DGD measurements is expected to be
within an acceptable range, as shown above. Even though the applicability

212

of the technique to instances where foam is present is questionable, results for FT-300 wax are in good agreement with values obtained using the photographic method, in the present study and those reported for paraffin waxes by Deckwer and coworkers.

D.4. Comparison of Techniques Used to Measure Bubble Size Distributions

Three different approaches were used to estimate the Sauter mean diameters of bubbles in the large columns (0.229 m ID and 0.24 m ID) and two techniques were used in the smaller column (0.051 m ID). Results from the various techniques are compared here. The discussion is limited to results from the larger columns since results are qualitatively similar for the two cases.

The dynamic gas disengagement (DGD) technique gives an average value of the Sauter mean bubble diameter for the entire column; whereas photographs near the column wall and center give only point estimates of the Sauter mean bubble diameter. Results from the DGD technique could be considered as the base case since this technique accounts for all bubbles unlike the photographic technique. Figure V-76 shows the variation of Sauter mean bubble diameter for FT-300 wax at 265°C in the large columns equipped with the 19 X 1.85 mm perforated plate distributor. Results obtained using DGD, photos at the wall (at a height of 1.96 m above the distributor), and photos obtained near the center of the column (at a height of 1.37 m above the distributor) are included in this figure. These results show that d_s values obtained from DGD measurements lie between those obtained from photographs near the center and near the wall of the column (for gas velocities greater than 0.04 m/s). This is as expected, since the DGD gives

213
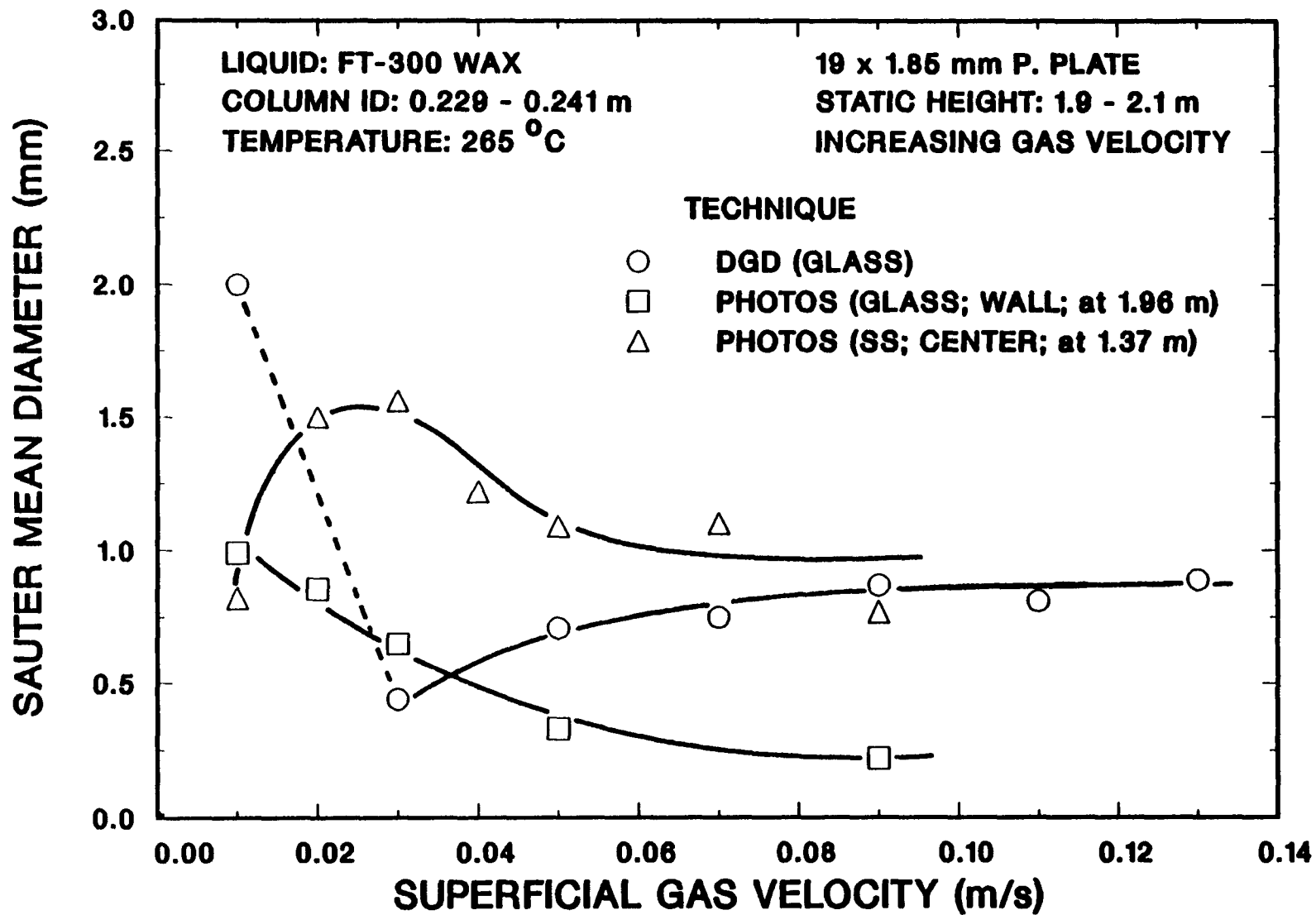
Figure V-76. Comparison of techniques used to determine the Sauter mean bubble diameter (O - Run 1-3; □ - Run 2-3; △ - Run 2-7)

an average Sauter mean diameter for the entire dispersion (i.e. it includes bubbles near the center and near the wall of the column). However, photographs taken near the wall of the column produced significantly lower Sauter mean bubble diameters. The d_s value from DGD at 0.03 m/s is significantly lower than that from photographs taken near the center of the column because foam was present at this range velocity. The DGD technique has serious limitations in the presence of foam and d_s for such conditions is dictated by the large number of bubbles in the foam, thus, lowering the Sauter mean bubble diameter. However, d_s in the presence of foam was found to be consistently around 0.5 mm using the DGD technique. A similar value for d_s was found when photographs of pure foam (with SMP distributor in the 0.051 m ID column) were analyzed.

Results from DGD and photography suggest that the Sauter mean diameter for FT-300 wax at 265°C is around 0.8 mm. The DGD technique showed that d_s increases significantly with a decrease in temperature. The photographic technique was not able to discern the effect of temperature on d_s in the 0.051 m ID column, while trends in the larger column were opposite than those obtained by DGD.

Figure V-77 compares the size of small bubbles obtained using DGD with bubble sizes obtained from photographic measurements near the wall for the 0.229 m ID column. The photographs were taken just after the gas flow to the column was shut off after a given velocity. Arithmetic average bubble diameters are used for values from photographic measurements. Figure V-77 shows that the two sets of diameters compare well except at 0.01 m/s.

The above discussion illustrates that the photographic technique can be used to estimate the interfacial area in bubble columns, if proper

215

modifications are made and precautions taken in order to counter its limi-

tations.
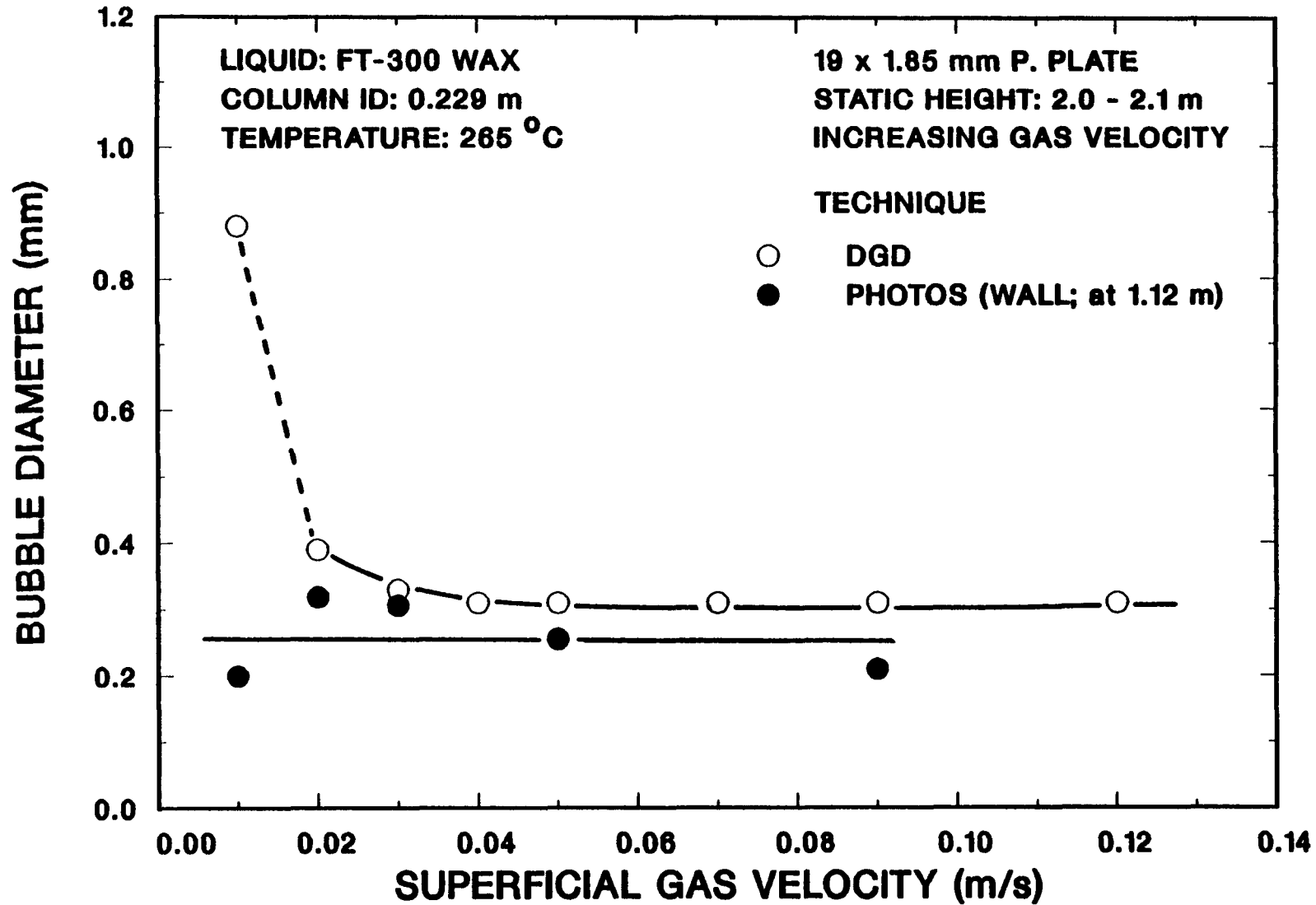
Figure V-77. Comparison of small bubble diameters estimated from DGD and photographic techniques (O- Run 2-8; ●- Run 2-3)

VI. TASK 4 - CORRELATION DEVELOPMENT AND DATA REDUCTION

A. PHYSICAL PROPERTY MEASUREMENTS

The density and viscosity of the various waxes used in the present study were measured at different temperatures to better understand the role of physical properties in determining the hydrodynamic properties of these waxes. The physical properties of the different liquid media are also needed for correlation of data. It was not possible to measure the surface tension of the waxes and literature values for this property were used. Physical properties obtained from measurements made in the present study are compared with existing literature data in Table VI-1.

A.1. Density Measurements

Densities of the various liquid media were estimated by measuring the pressure drop across known heights of liquid in the 0.051 m ID glass column. The differential pressure (DP) cell (Validyne Model DP-15) was connected to the 0.051 m ID glass column so as to measure the pressure drop across the column. The column was filled with the test liquid up to a height of about 2.5 m (height was measured on a vertical scale placed along the column). The pressure drop was recorded for this height and some of the liquid was drained out and the pressure drop recorded again. This process was repeated for every 0.25 m drop in the liquid level. Measurements were first made using distilled water in order to calibrate the DP cell. The column was then preheated to the desired temperature and hot wax introduced into the column. The density for the wax at that temperature was obtained from the slope of the pressure drop versus height plot, after appropriate corrections for the calibration factor.

Results from the density measurements are included in Table VI-1.

218

Table VI-1. Physical properties of waxes.

Wax Type	Temp. (°C)	Density (kg/m^3)	Viscosity (mPa.s)	Surface Tension (N/m)	Reference
Krupp wax	200	723	3.0		Calderbank et al.
	230	705	2.2		(1963)
	260	694	1.6		
Paraffin wax	143	730	13.0	0.029	Deckwer et al.
	220	690	4.0	0.024	(1980)
	260	670	2.0	0.021	
FT-200 wax	149		4.4		Kuo et al. (1985)
	204		2.2		
	260	720	1.7	0.024	
FT-200 wax	150		4.4		This work
	200	712	2.8		
	230		2.4		
	265	675	1.9 *		
FT-300 wax	150		6.4		This work
	200	722	4.2		
	230	706	3.6		
	265	681	2.7 *		
SASOL's Arge wax	150		4.2		This work
	200	701	2.9		
	230		2.5		
	265	655	2.0 *		

* estimated from data at lower temperatures.

Table VI-1. Physical properties of waxes (contd.).

Wax Type	Temp. (°C)	Density (kg/m³)	Viscosity (mPa.s)	Surface Tension (N/m)	Reference
MOBIL REACTOR WAXES					
Run CT-256-4	149		6.1		Kuo et al. (1985)
	204		4.3		
	260		3.4	0.026 - 0.027	
Run CT-256-5	149		17.6		Kuo et al. (1985)
	204		8.5		
	260		5.5	0.028	
Run CT-256-7	149		8.2		Kuo et al. (1985)
	204		4.1		
	260		2.3	0.026 - 0.027	
Run CT-256-8	149		13.1		Kuo et al. (1985)
	204		6.8		
	260		-	0.026 - 0.027	
Run CT-256-9	149		5.7 - 7.5		Kuo et al. (1985)
	204		3.1 - 4.0		
Run CT-256-11	149		6.1 - 6.7		Kuo et al. (1985)
	204		3.2 - 3.7		
Run CT-256-4 CT-256-7 composite	150 200 230 265		9.1 5.5 4.5 3.9 *		This work
Run CT-256-5 CT-256-8 composite	150 200 230 265		13.9 7.3 5.7 3.9 *		This work
Run CT-256-9, CT-256-11, CT-256-12 composite	150 200 230 265	716 674	6.5 3.8 3.1 2.3 *		This work

* estimated from data at lower temperatures.

These values are in good agreement with densities for different waxes reported in literature (Calderbank et al., 1963; Deckwer et al., 1980; Kuo et al., 1985). Calderbank et al. used a pyknometer to measure densities, while the procedure used by other workers is not known. The effect of temperature on density is as expected, i.e. density increases as temperature is decreased. These results also show that the different types of waxes have similar densities (between 655 and 694 kg/m^3 in the temperature range 260-265°C).

A.2. <u>Viscosity Measurements</u>

Viscosity measurements were made in a Brookfield viscometer (LV series, 2.5X) using a cylindrical spindle (SC4-18) operating at 60 RPM. A Brookfield Thermosel system allowed measurements up to temperatures of 250°C. The measurements were made in the temperature range 150-230°C and the wax viscosity at higher temperatures was estimated from data at lower temperatures assuming Arrhenius type of dependence of viscosity with temperature. The system was first calibrated using fluids of known viscosities. Three fluids were used; water (0.89 mPa.s), and two viscosity standards (5.1 and 8.9 mPa.s - supplied by Brookfield). The standards were used before and after viscosity measurements with waxes to prevent errors due to device drift. Each measurement required a 8 ml sample of the test fluid.

Results obtained from these measurements are presented in Table VI-1 along with data from literature. Calderbank et al. (1963) measured viscosity of Krupp wax with an Ostwald viscometer (capillary type). Other workers (Deckwer et al., 1980; Kuo et al., 1985) did not provide information on experimental methods used to determine physical properties.

Comparison of data obtained with the same type of wax is possible only for FT-200 and some of Mobil's reactor waxes. Values of viscosity of the FT-200 paraffin wax obtained in this study and Mobil's study (Kuo et al., 1985) are in good agreement at low (~150°C) and high (~260°C) temperatures, whereas the agreement is less than satisfactory at intermediate temperatures (~200°C). Viscosities of the composite Mobil reactor wax from runs 4 and 7 are consistently higher than values reported by Kuo et al. for either run 4 or run 7 waxes, whereas viscosities of the composite, from runs 5 and 8, are between values reported by Kuo et al. for waxes from the two runs. Viscosities of the composite from runs 9, 11 and 12 are in good agreement with values reported by Kuo et al. for waxes produced in runs 9 and 11. Kuo et al. reported values of viscosity of wax samples produced at different times during a given run. In Table VI-1 only the lowest and the highest values obtained during the entire run are listed.

A.3. Surface Tension

The surface tension of different waxes was not measured in the present study. However, from the data reported in literature it may be concluded that different waxes have similar values of surface tension (e.g. compare results of Deckwer et al., 1980; and Kuo et al., 1985; shown in Table VI-1).

The data summarized in Table VI-1 show that physical properties of different waxes at a given temperature are similar. In particular there are no significant differences in physical properties between the paraffin and the reactor waxes at higher temperatures (260-265°C).

B. CORRELATIONS FOR AVERAGE GAS HOLD-UP

The average gas hold-up values measured for the different waxes under the various conditions were divided into the following four groups:

Group 1: Data from experiments conducted in the "foamy" regime using orifice type distributors (in the 0.051 m ID column), and perforated plate or perforated pipe type of distributors (in the 0.229 m ID column).

Group 2: Data from experiments conducted in the "slug flow" regime using orifice type distributors (in the 0.051 m ID column), and in the "churn-turbulent" regime using perforated plate or perforated pipe type of distributors (in the 0.229 m ID column).

Group 3: Data from experiments conducted in the "foamy" regime using the 40 μm SMP distributor (in the 0.051 m ID column).

Group 4: Data from experiments conducted in the "slug flow" regime using the 40 μm distributor (in the 0.051 m ID column).

Various correlations were used with each of these groups and the goodness of fit was determined. The average gas hold-up values in all correlations presented here are expressed on a percentage basis (i.e. percent of the dispersion occupied by the gas phase).

The major findings from this section are:

• Hold-up values in the "foamy" regime with orifice and perforated plate distributors show a dependency on column diameter and distributor type, and can be predicted by:

$$\epsilon_g \ (\%) = 12(Bo)^{-0.19}(We)^{0.13}(Ga)^{0.11}(Fr)^{0.19} \qquad 0.01 \leq u_g \leq 0.07 \ m/s$$

$$(VI-14)$$

• Hold-up values in the "slug flow" regime (in the 0.051 m ID column) and in the "churn-turbulent" regime (in the 0.229 m ID column) are

223

independent of column diameter and distributor type and can be predicted by:

$$\epsilon_g \ (\%) = 25(Bo)^{0.15}(Fr)^{0.60} \qquad 0.01 \le u_g \le 0.15 \ \text{m/s} \qquad (VI\text{-}16)$$

- Hold-up values in the "foamy" regime with the SMP distributor show a weak dependence on superficial gas velocities greater than 0.02 m/s and can be predicted by:

$$\epsilon_g \ (\%) = \frac{10560u_g}{1+130u_g} \qquad 0.01 \le u_g \le 0.12 \ \text{m/s} \qquad (VI\text{-}17)$$

- Hold-up values in the "slug flow" regime with the SMP distributor show an increase with an increase in the superficial gas velocity and can be predicted by:

$$\epsilon_g \ (\%) = 98u_g^{0.61} \qquad 0.01 \le u_g \le 0.12 \ \text{m/s} \qquad (VI\text{-}18)$$

B.1. Correlations Based on Dimensional Analysis

The factors affecting the gas hold-up are the physical properties of the liquid medium, ρ_ℓ (density), μ_ℓ (viscosity) and σ (surface tension); gas density, ρ_g; column diameter, d_c, superficial gas velocity, u_g; jet velocity, u_j; orifice diameter, d_o; and gravity, g. By dimensional analysis, the following functional form for the average gas hold-up is obtained:

$$\epsilon_g = fn \ [Bo, \ We, \ Ga, \ Fr] \qquad (VI\text{-}1)$$

where

$$Bo = \frac{d_c^2 \rho_\ell g}{\sigma} \qquad \text{Bond number} \qquad (VI\text{-}2)$$

$$We = \frac{d_o \rho_g u_j^2}{\sigma} \qquad \text{Weber number} \qquad (VI\text{-}3)$$

$$Ga = \frac{d_c^3 g \rho_\ell^2}{\mu_\ell^2} \qquad \text{Galileo number} \qquad (VI\text{-}4)$$

224

$$Fr = \frac{u_g}{\sqrt{d_c g}} \qquad \text{Froude number} \qquad (VI-5)$$

In Equation (VI-1), the Weber number (We) is based on the orifice diameter and the jet velocity through the orifice. Therefore, for correlations involving hold-up for SMP distributors, this quantity is not applicable and Equation (VI-1) reduces to:

$$\epsilon_g = fn \ [Bo, \ Ga, \ Fr] \qquad (VI-6)$$

Hold-up correlations were also developed using a modified form of Equation (VI-1). Equation (VI-7) was used for orifice and perforated plate type of distributors, and Equation (VI-8) was used for the SMP distributor.

$$\frac{\epsilon_g}{100 - \epsilon_g} = fn \ [Bo, \ We, \ Ga, \ Fr] \qquad (VI-7)$$

$$\frac{\epsilon_g}{100 - \epsilon_g} = fn \ [Bo, \ Ga, \ Fr] \qquad (VI-8)$$

The range of values for the various parameters and dimensionless groups used in these correlations are summarized in Table VI-2.

B.2. Empirical Hold-up Correlations

Two empirical correlations were selected to fit hold-up values obtained during the present study. These correlations relate the average gas hold-up to the superficial gas velocity.

$$\epsilon_g = k_1 u_g^{k_2} \qquad (VI-9)$$

$$\epsilon_g = \frac{k_1 u_g}{1 + k_2 u_g} \qquad (VI-10)$$

The first of these correlations (Equation (VI-9)) was used to describe hold-up data by various researchers (e.g. Deckwer et al., 1980).

Table VI-2. Range of values for various parameters used in the correlations

PARAMETER	RANGE
liquid density (ρ_ℓ)	655 - 730 kg/m^3
liquid viscosity (μ_ℓ)	1.9 - 6.4 mPa.s
surface tension (σ)	0.020 - 0.028 N/m
gas density (ρ_g)	0.660 - 0.843 kg/m^3
column diameter (d_c)	0.051, 0.229 m
superficial gas velocity (u_g)	0.01 - 0.17 m/s
jet velocity (u_j)	1.63 - 331 m/s
orifice or perforated plate pore size (d_o)	1 - 4 mm
Bond number (Bo)	703 - 16738
Weber number (We)	0.058 - 3282
Galileo number (Ga)	3.82X10^7 - 1.28X10^{10}
Froude number (Fr)	0.0067 - 0.2403

B.3. Correlations from Literature

A large number of correlations for gas hold-up have been proposed in the literature based on measurements made with various gas-liquid systems. The correlations presented by Akita and Yoshida (1973), Bach and Pilhofer (1978), Mersmann (1978) and Hikita et al. (1980) are based on a large number of experimental data and are often used to predict the average gas hold-up. These correlations were used to predict hold-ups for the waxes used in the present study and it was found that Bach and Pilhofer's correlation provides a very good fit for data obtained in the "slug flow" regime (in the 0.051 m ID column) and the "churn-turbulent" regime (in the 0.229 m ID column). This correlation is based on measurements made using pure organic liquids as the liquid media. Figure VI-1 compares the values predicted by Bach and Pilhofer's correlation to those obtained in the present study at 265°C. The physical properties of FT-300 wax at 265°C were used in the correlation. Also included in this figure are results from experiments conducted by Calderbank et al. (1963) with Krupp wax using a ball and cone type of distributor, and from experiments conducted by Kuo et al. (1985) with FT-200 wax using a 2 mm orifice plate distributor. The agreement between the experimental and predicted values is very good. Therefore, this correlation was selected and the constants reevaluated for our data:

$$\frac{\epsilon_g}{100 - \epsilon_g} = k_1 \left[\frac{u_g^3 \rho_\ell^2}{\mu_\ell g (\rho_\ell - \rho_g)} \right]^{k_2} \tag{VI-11}$$

Akita and Yoshida's (1973) correlation is based on measurements made using water, methanol, and glycol solution as the liquid media. The hold-up values predicted by their correlation were significantly lower than those
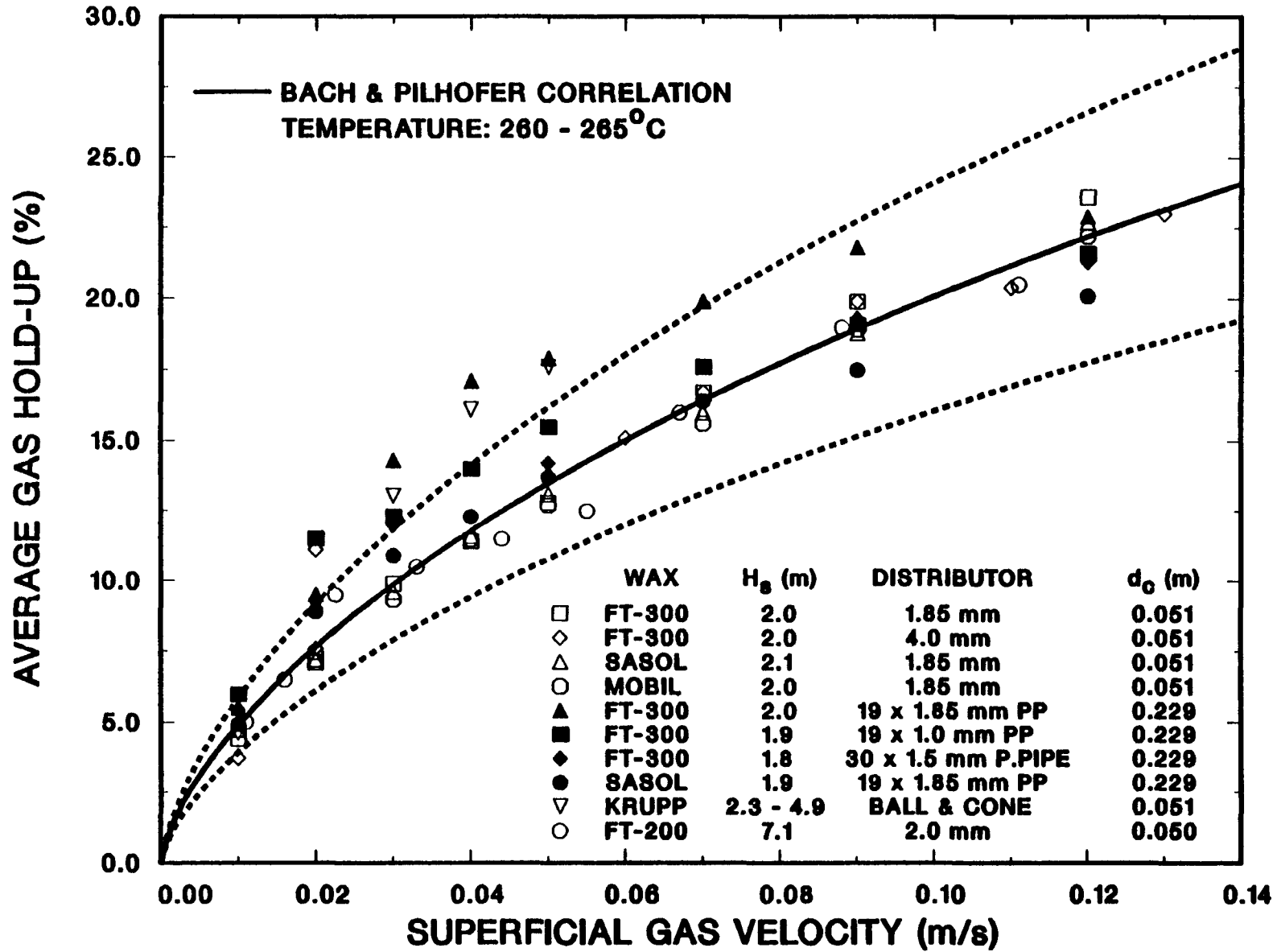
Figure VI-1. Comparison between experimental gas hold-ups and predictions from the Bach and Pilhofer correlation (solid line - Bach and Pilhofer correlation; dashed lines - ±20% relative deviation from the correlation; △ - Calderbank et al., 1963; ○- Kuo et al., 1985; remaining data are from present study)

obtained in the present study, however, the dimensionless groups involved with this correlation are similar to those presented earlier (Equation (VI-1)). Therefore, the constants for their correlations were reevaluated using data from the present study. The functional form of this correlation is:

$$\frac{\epsilon_g}{(100-\epsilon_g)^4} = fn\,[Bo,\ Ga,\ Fr] \qquad (VI-12)$$

B.4. Tests for Goodness of Fit

The constants for the different correlations were evaluated using non-linear regression (i.e. the NLIN procedure in the SAS package) of the hold-up data. In order to compare the various correlations two different criteria were used. The first of these is the Mean Square Error (MSE) and is given as:

$$MSE = \frac{\sum_{i=1}^{N} (\epsilon_g - \epsilon_{gp})^2}{N} \qquad (VI-13)$$

where ϵ_g is the actual or measured hold-up, ϵ_{gp} is the hold-up value predicted by the correlation, and N is the number of data points used to obtain the correlation. The second criterion is the percent of data points that are within ±30% of the values predicted by the correlation. The correlation with the lowest MSE and the greatest percentage of data points within ±30% provides the best representation of the experimental data.

B.5. Results from Statistical Analysis

The six correlations presented earlier were used with each of the four data groups. Tables VI-3 to VI-5 summarize results from the goodness of fit tests and values of the parameters (constants) associated with the various correlations. Table VI-3 shows MSE values and percentage of data points

Table VI-3. Goodness of fit and parameters for hold-up correlations based on dimensionless groups (using data for all waxes; ϵ_g - %).

Correlation 1:

$$\epsilon_g = k_1(Bo)^{k_2}(Ga)^{k_3}(Fr)^{k_4}(We)^{k_5}$$

Correlation 2:

$$\frac{\epsilon_g}{100 - \epsilon_g} = k_1(Bo)^{k_2}(Ga)^{k_3}(Fr)^{k_4}(We)^{k_5}$$

	ORIFICE	TYPE	SMP[a]	
Foam	Yes	No	Yes	No
No. of points	175	349	61	36

MEAN SQUARE ERROR:

Correlation 1	26.9	7.85	158	_[b]
Correlation 2	28.8	7.89	182	_[b]

PERCENTAGE OF POINTS WITHIN ±30%:

Correlation 1	86.9	90.8	86.9	_[b]
Correlation 2	82.9	91.7	88.5	_[b]

PARAMETERS FOR CORRELATION 1:

k_1	11.9	23.7	0.06	_[b]
k_2	-0.19	0.15	1.20	_[b]
k_3	0.11	0.01	-0.03	_[b]
k_4	0.19	0.62	0.14	_[b]
k_5	0.13	-0.01		

PARAMETERS FOR CORRELATION 2:

k_1	0.06	0.35	3.04×10^{-8}	_[b]
k_2	-0.41	0.17	2.53	_[b]
k_3	0.23	0.01	0.10	_[b]
k_4	0.18	0.74	0.23	_[b]
k_5	0.22	-0.01		

[a] Weber number (We) was not included in correlations for this distributor.

[b] Parameters could not be estimated from these data due to convergence problems.

within the ±30% error band for correlations based on dimensional analysis. Problems with convergence prevented the correlation of hold-up data obtained using SMP distributors in the "slug flow" regime. Hold-up values obtained using orifice type distributors in the "slug flow" and "churn-turbulent" regimes have excellent reproducibility (see Section V-B.2.), therefore, the MSE for these data is significantly lower than for the other data groups. Greater than 90% of these data are within ±30% of the predicted values. These results also show that both correlations give similar fits for the different data groups, although the first correlation gives marginally lower MSE values than the second correlation. Table VI-4 summarizes goodness of fit tests for the two empirical correlations. In general the MSE values with these correlations are higher than those from correlations based on dimensional analysis. This would be expected since the empirical correlations have fewer parameters (constants) and therefore lower degrees of freedom. Table VI-5 shows goodness of fit test results for literature correlations. Convergence could not be obtained when Akita and Yoshida's correlation was used with three of the four data groups. For hold-up data in the "slug flow" and "churn-turbulent" regimes, obtained using orifice type distributors, this correlation gave a significantly higher MSE compared to other correlations and the fit was relatively poor. As expected, Bach and Pilhofer's correlation provides an excellent fit for data in the "slug flow" and "churn-turbulent" regimes.

.Based on the lowest MSE values, the correlations that best describe hold-up data from the present study are presented here.

231

Table VI-4. Goodness of fit and parameters for empirical hold-up correlations (using data for all waxes; ϵ_g - %).

Correlation 1:

$$\epsilon_g = k_1 u_g{}^{k_2}$$

Correlation 2:

$$\epsilon_g = \frac{k_1 u_g}{1 + k_2 u_g}$$

	ORIFICE	TYPE	SMP	
Foam	Yes	No	Yes	No
No. of points	175	349	61	36

MEAN SQUARE ERROR:

Correlation 1	50.4	8.17	162	16.4
Correlation 2	46.7	8.45	162	17.4

PERCENTAGE OF POINTS WITHIN ±30%:

Correlation 1	70.3	90.8	86.9	94.4
Correlation 2	72.0	91.4	90.2	86.1

PARAMETERS FOR CORRELATION 1:

k_1	93.7	84.3	105.9	98
k_2	0.41	0.59	0.15	0.61

PARAMETERS FOR CORRELATION 2:

k_1	1425	466	10560	409
k_2	29.44	11.59	130	6.82

Table VI-5. Goodness of fit and parameters for hold-up correlations from literature (using data for all waxes; ϵ_g - %).

Correlation 1 (Akita and Yoshida):

$$\frac{\epsilon_g}{(100 - \epsilon_g)^4} = k_1(Bo)^{k_2}(Ga)^{k_3}(Fr)^{k_4}$$

Correlation 2 (Bach and Pilhofer):

$$\frac{\epsilon_g}{(1 - \epsilon_g)} = k_1 \left[\frac{u_g^3 \rho_\ell^2}{\mu_\ell g(\rho_\ell - \rho_g)} \right]^{k_2}$$

	ORIFICE	TYPE	SMP	
Foam	Yes	No	Yes	No
No. of points	175	349	61	36

MEAN SQUARE ERROR:

Correlation 1	$-^a$	32.00	$-^a$	$-^a$
Correlation 2	46.5	8.14	185	17.1

PERCENTAGE OF POINTS WITHIN ±30%:

Correlation 1	$-^a$	75.2	$-^a$	$-^a$
Correlation 2	71.4	91.7	88.5	94.4

PARAMETERS FOR CORRELATION 1:

k_1	$-^a$	3.85×10^5	$-^a$	$-^a$
k_2	$-^a$	0.14	$-^a$	$-^a$
k_3	$-^a$	0.08	$-^a$	$-^a$
k_4	$-^a$	1.02	$-^a$	$-^a$

PARAMETERS FOR CORRELATION 2:

k_1	0.321	0.128	2.174	0.133
k_2	0.19	0.24	0.08	0.27

[a] Parameters could not be estimated from these data due to convergence problems.

Group 1 - Orifice type distributors in the "foamy" regime:

$$\epsilon_g \ (\%) = 12(Bo)^{-0.19}(We)^{0.13}(Ga)^{0.11}(Fr)^{0.19} \qquad 0.01 \leq u_g \leq 0.07 \ m/s$$

(VI-14)

The above correlation for hold-up in the "foamy" regime shows that hold-up tends to increase with an increase in the Weber number (i.e. the jet velocity). This is as expected since our results show that hold-up in the "foamy" regime increases as hole size of the distributor is decreased (see Section V-B.5.). It was also shown earlier (see Section V-B.4.) that hold-up in the larger column (0.229 m ID) was lower than hold-up in the smaller column (0.051 m ID) in the "foamy" regime. In the above correlation, column diameter (d_c) is associated with the Bond number (Equation (VI-2)), Galileo number (Equation (VI-4)) and the Froude number (Equation (VI-5)). This implies that the gas hold-up is proportional to $d_c^{-0.15}$, i.e. hold-up decreases as column diameter increases. Figure VI-2 shows the parity plot for this correlation. In general, predicted hold-up values are in fairly good agreement with experimental data.

Group 2 - Orifice type distributors in the "slug flow" and "churn turbulent" regimes:

$$\epsilon_g \ (\%) = 24(Bo)^{0.15}(We)^{-0.01}(Ga)^{0.01}(Fr)^{0.62} \qquad 0.01 \leq u_g \leq 0.15 \ m/s$$

(VI-15)

A comparison of Equation (VI-15) with Equation (VI-14) shows that in the "slug flow" and "churn-turbulent" regimes, the Weber number does not have a significant effect on the gas hold-up. This implies that the type of distributor used has no effect on the gas hold-up. This is in agreement with results presented earlier (see Section V-2.5.). The terms involving the Bond number, Galileo number and the Froude number can be simplified to

234
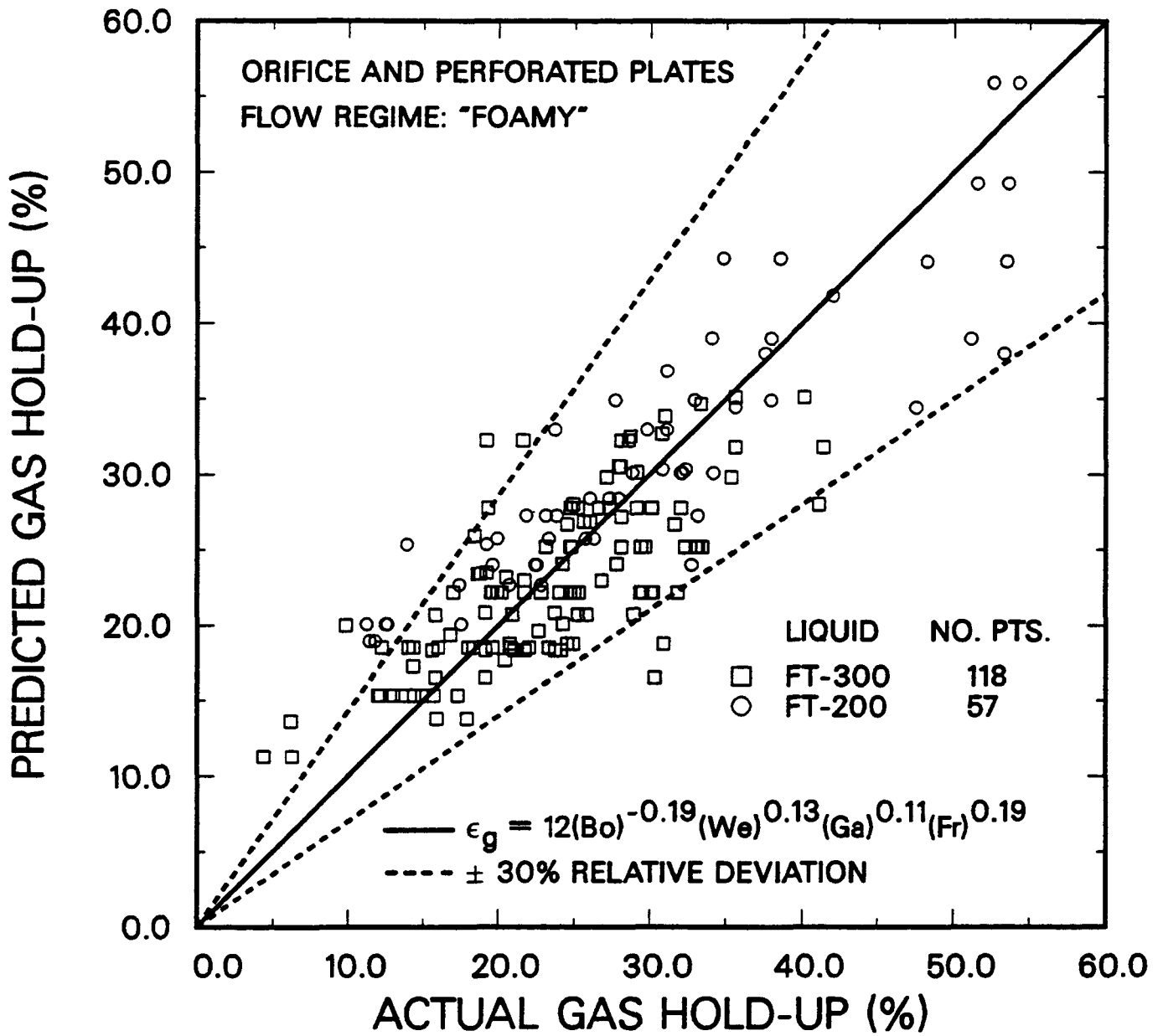
Figure VI-2. Comparison between experimental and predicted gas hold- ups

show that column diameter has no effect on the average gas hold-up. This is once again as expected and is in agreement with results presented earlier (see Section V-B.4.). Equation (VI-15) shows a weak dependence of hold-up on the Weber number and the Galileo number, therefore, the parameters (constants) for the correlation were reevaluated after dropping off these two groups. The resulting equation is:

$$\epsilon_g \ (\%) = 25(Bo)^{0.15}(Fr)^{0.60} \qquad 0.01 \leq u_g \leq 0.15 \ m/s \qquad (VI-16)$$

This equation also shows that column diameter has no effect on the average gas hold-up. The simplified equation increased the MSE from 7.85 (for Equation (VI-15)) to 7.90, however, the percentage of points within ±30% of the predicted values remained the same for the two equations. A parity plot for this correlation is shown in Figure VI-3. The agreement between the predicted and measured values of gas hold-up is very good, with 91% of the data within ±30% of the predicted values.

Group 3 - SMP distributor in the "foamy" regime:

$$\epsilon_g \ (\%) = \frac{10560u_g}{1+130u_g} \qquad 0.01 \leq u_g \leq 0.12 \ m/s \qquad (VI-17)$$

Hold-up values with the SMP distributor, in the presence of foam, remained fairly constant around 70% for velocities greater than 0.02 m/s. For gas velocities of 0.01 and 0.02 m/s hold-up varied between 20 and 60 %. Therefore, it is expected that an equation of the type shown above (Equation (VI-17)) would best describe this type of behavior. A parity plot for this correlation is shown in Figure VI-4.

Group 4 - SMP distributor in the "slug flow" regime:

$$\epsilon_g \ (\%) = 98u_g^{0.61} \qquad 0.01 \leq u_g \leq 0.12 \ m/s \qquad (VI-18)$$

A parity plot for this correlation is shown in Figure VI-5. Majority of
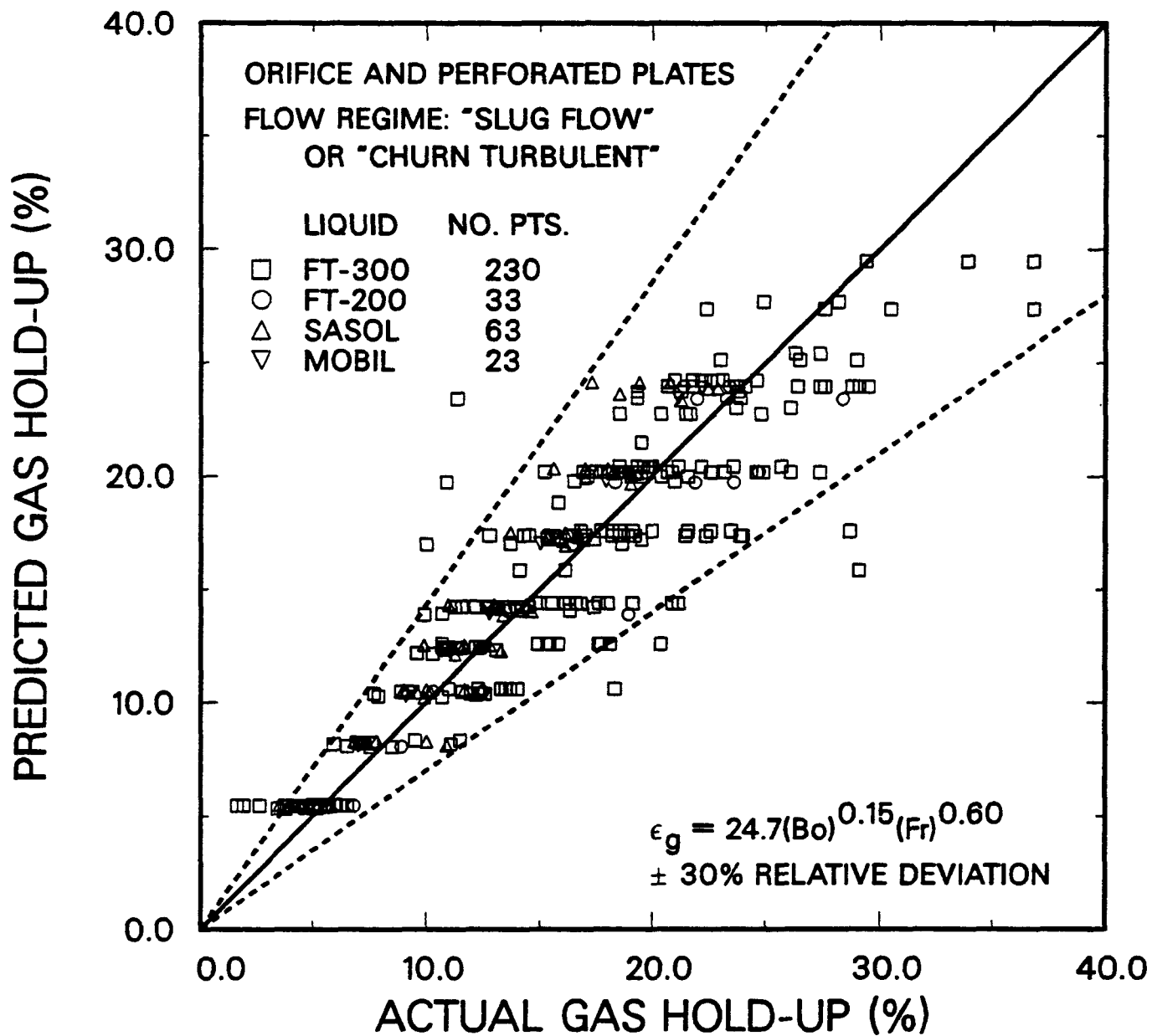
Figure VI-3. Comparison between experimental and predicted gas hold- ups
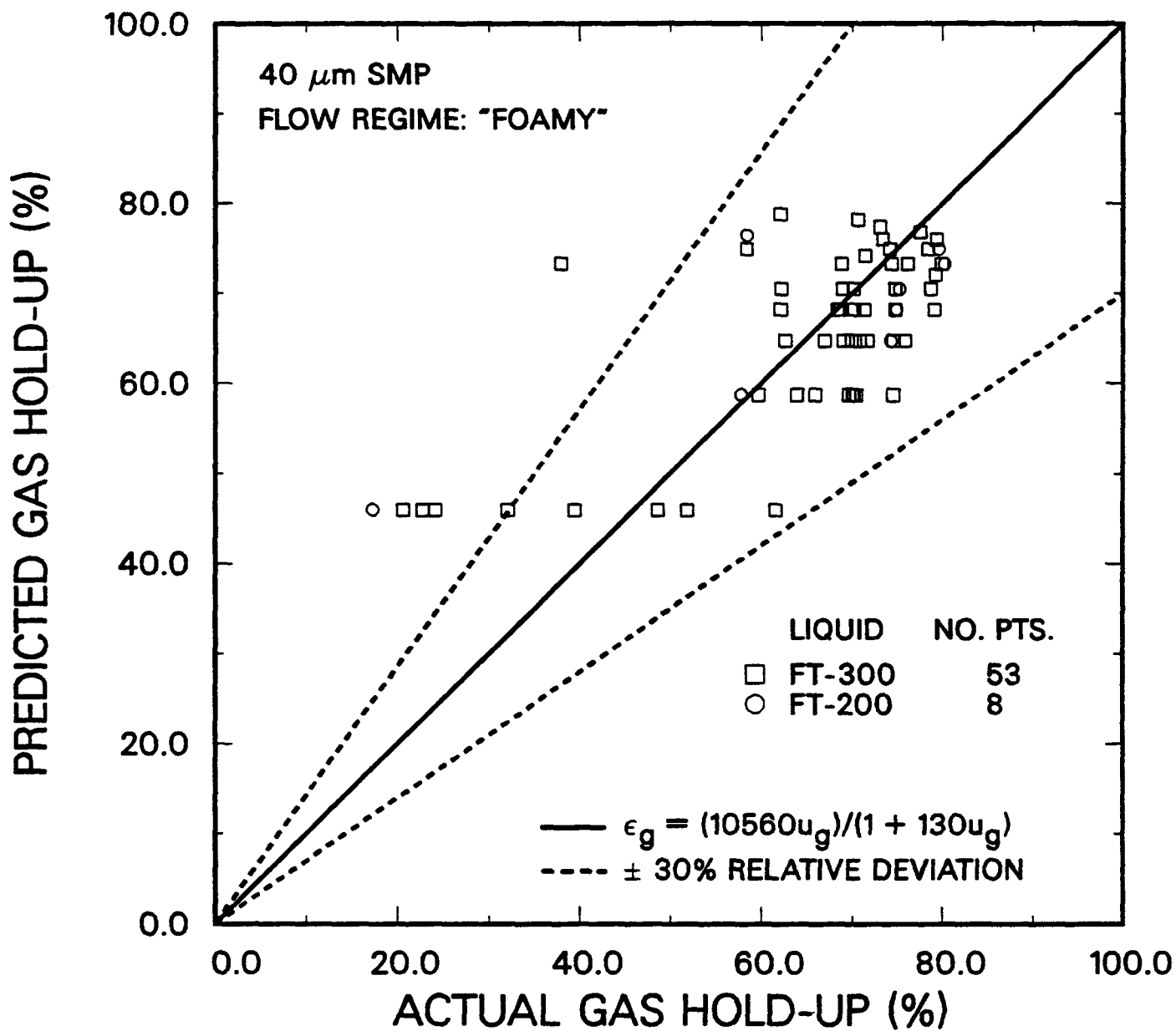
Figure VI-4 Comparison between experimental and predicted gas hold- ups
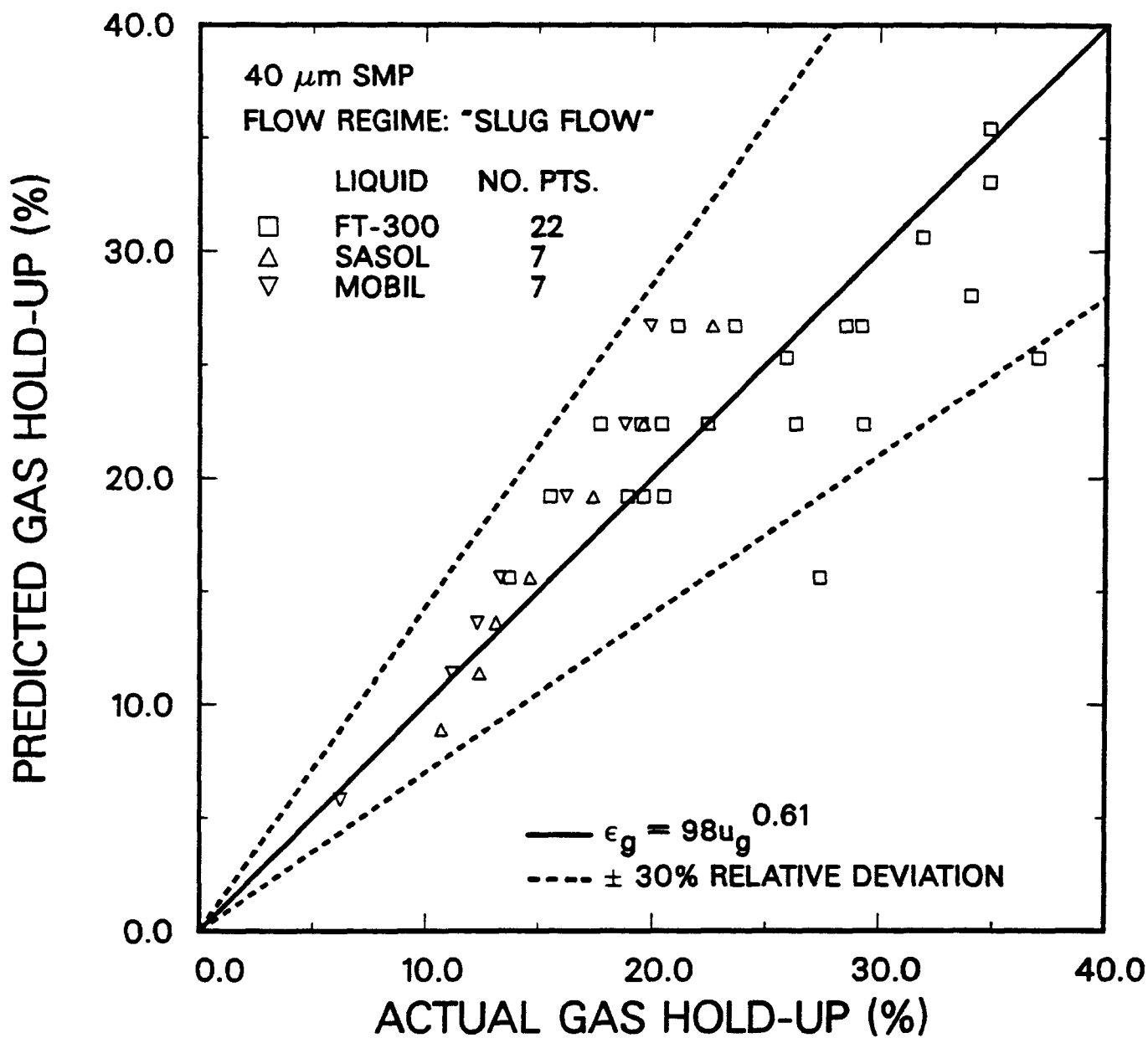
Figure VI-5. Comparison between experimental and predicted gas hold- ups

these data were obtained from runs conducted with reactor waxes at 265°C and hold-up appeared to be affected by gas velocity alone. The correlation presented in Equation (VI-18) provides the best description of these data.

B.6. Comparison with Literature

Bach and Pilhofer's correlation provides an excellent fit for average gas hold-up data in the "slug flow" and "churn turbulent" regimes (Figure VI-1). The constants in this equation were reevaluated and the new equation is:

$$\frac{\epsilon_g}{100 - \epsilon_g} = 0.128 \left[\frac{u_g^3 \rho_\ell^2}{\mu_\ell (\rho_\ell - \rho_g)} \right]^{0.24} \qquad 0.01 \le u_g \le 0.15 \text{ m/s} \qquad \text{(VI-19)}$$

The new coefficient is 0.128 compared to 0.115 for the original equation and the new exponent is 0.24 compared to 0.23 for the original equation. The new values compare very well with those for the equation proposed by Bach and Pilhofer. Hold-up data for FT-300 wax obtained at 265°C in the "slug flow" and "churn turbulent" flow regimes were also correlated separately and the constants for Bach and Pilhofer's equation reevaluated. These values are 0.140 and 0.23 respectively, and are essentially the same as the ones in the Bach and Pilhofer correlation.

Deckwer et al. (1980) used an empirical equation to correlate hold-up values obtained using molten paraffin wax, which is given by

$$\epsilon_g \text{ (\%)} = 840 u_g^{1.1} \qquad u_g \le 0.04 \text{ m/s} \qquad \text{(VI-20)}$$

The above equation is based on measurements made using gas velocities less than 0.04 m/s. Recently Sanders et al. (1986) obtained hold-up values with FT-300 wax for gas velocities up to 0.06 m/s and found that their data could be described with Equation (VI-20). When data obtained in the present study in the "foamy" regime were correlated with a similar equation, the

following equation was obtained

$$\epsilon_g \ (\%) = 94u_g^{0.41} \qquad 0.01 \le u_g \le 0.07 \ m/s \qquad (VI-21)$$

for orifice type distributors and

$$\epsilon_g \ (\%) = 106u_g^{0.15} \qquad 0.01 \le u_g \le 0.12 \ m/s \qquad (VI-22)$$

for the 40 μm SMP distributor. When data in the "slug flow" and "churn turbulent" flow regime were correlated the following equation was obtained

$$\epsilon_g \ (\%) = 84u_g^{0.59} \qquad\qquad (VI-23)$$

for orifice type distributors and

$$\epsilon_g \ (\%) = 98u_g^{0.61} \qquad\qquad (VI-24)$$

for the 40 μm SMP distributor. The equation proposed by Deckwer et al. (Equation (VI-20)) shows that hold-up increases almost proportionally with superficial gas velocity, while results from the present study showed that hold-up values tend to level off at higher gas velocities. A possible explanation for the discrepancy is the range of velocities employed in the two studies. Equation (VI-20) is based on measurements made for gas velocities less than 0.04 m/s. For this range of gas velocities, hold-up values (in the presence of foam) tend to increase proportionally with gas velocity as was observed in the present study. Similar observations were also made by Kuo et al. (1985) in their studies with FT-200 wax. The correlation used to fit some of their data for gas velocities less than 0.06 m/s is

$$\epsilon_g \ (\%) = 1030u_g^{1.1} \qquad u_g \le 0.06 \ m/s \qquad (VI-25)$$

The correlations developed in the present work are applicable to a greater range of gas velocities than the existing correlations for molten waxes. It is obvious from the present study that a single correlation cannot be used to predict hold-up data, since hold-up is significantly

affected by the presence or absence of foam. The correlations presented above are based on a large number of data points, therefore, it is expected that they describe the hold-up behavior of molten waxes fairly well. For the mode of operation in the "foamy" regime, with orifice and perforated plate distributors, Weber number and column diameter have a significant effect on the gas hold-up, therefore a correlation that accounts for these effects is necessary for predicting the average gas hold-up values. Equation (VI-14) provides a good fit of data in this regime. In the "slug flow" and "churn-turbulent" regimes, hold-up is independent of column diameter and distributor type. Equation (VI-16) should be used to predict hold-up values in this flow regime. Hold-ups with the SMP distributor are essentially functions of the gas velocity alone. In the "foamy" regime, the dependence on u_g is very weak at velocities greater than 0.02 m/s and Equation (VI-17) can be used to predict hold-ups under these conditions. In the "slug flow" regime, with the SMP distributor, a limited amount of data were available and they could be correlated with Equation (VI-18).

C. CORRELATIONS FOR SPECIFIC INTERFACIAL AREA

The dynamic gas disengagement technique allowed the estimation of the Sauter mean diameter at different superficial gas velocities during a given run. The Sauters along with the corresponding average gas hold-up values were then used to estimate specific interfacial area from

$$a = \frac{6\epsilon_g}{d_s} \qquad \text{(VI-26)}$$

The specific interfacial area values were divided into the following six groups:

Group 1: Data from experiments conducted with FT-300 wax at 200°C.

Group 2: Data from experiments conducted with FT-300 wax at 265°C.

Group 3: Data from experiments conducted with Sasol's Arge wax at 200°C.

Group 4: Data from experiments conducted with Sasol's Arge wax at 265°C.

Group 5: Data from experiments conducted with Mobil reactor wax at 200°C.

Group 6: Data from experiments conducted with Mobil reactor wax at 265°C.

Two empirical correlations were tested with each of these groups and the goodness of fit determined. In these correlations the superficial gas velocity was used as the only independent variable and the units of area are m^{-1}.

$$a = k_1 u_g^{k_2} \tag{VI-27}$$

$$a = k_1 u_g^{k_2} e^{-k_3 u_g} \tag{VI-28}$$

The first of these correlations has the same functional form as that used by Deckwer et al. (1980) to obtain the specific interfacial area. The second correlation has the same functional form as the Gamma function (a skewed Gaussian distribution). FT-300 wax has a tendency to foam at lower gas velocities ($u_g < 0.06$ m/s), therefore, it is expected that the specific interfacial area would go through a maximum in the "foamy" regime and then decrease as the foam breaks. Equation (VI-28) can therefore be used to correlate this type of behavior.

The major highlights of these studies are:

• The specific interfacial area (m^{-1}) for FT-300 wax at 265°C can be predicted using two separate correlations depending on the superficial gas velocity employed:

$$a = 3.3 \times 10^8 u_g^{2.72} e^{-71 u_g} \qquad u_g < 0.08 \text{ m/s} \tag{VI-29}$$

$$a = 971 u_g^{-0.216} \qquad 0.08 \leq u_g \leq 0.15 \text{ m/s} \tag{VI-30}$$

- The specific interfacial area (m^{-1}) for Sasol's Arge reactor wax at 265°C can be predicted using

$$a = 1000u_g^{0.25} \qquad 0.01 \leq u_g \leq 0.12 \text{ m/s} \qquad (VI-31)$$

- The specific interfacial area (m^{-1}) for Mobil's reactor wax at 265°C can be predicted using

$$a = 300u_g^{0.01} \qquad 0.01 \leq u_g \leq 0.12 \text{ m/s} \qquad (VI-33)$$

C.1. <u>Results from Statistical Analysis</u>

The goodness of fit for the correlations was tested using criteria similar to those used for the average gas hold-up correlations. The mean square errors (MSE) were estimated for each case, and the percentage of points within a ±30% band determined. Tables VI-6 and VI-7 summarize results from the goodness of fit tests and the parameters (constants) for the different correlations.

Results for FT-300 wax at 200 and 265°C are shown in Table VI-6. A limited amount of data was available at 200°C (data from only 1 run) and the correlations appear to fit the data fairly well, with 75% of data within ±30% of the values predicted by the second correlation. The fit for data at 265°C is relatively poor and at best only 53.1% of the data were within a ±30% error band. The primary reason for the poor fit is the relatively high scatter in the original data. Results presented in Table VI-6 show that by using a Gamma function type of correlation, the MSE value for FT-300 wax at 265°C was reduced from $1.11X10^6$ (for the first correlation) to $6.85X10^5$. Therefore, data for FT-300 wax at 265°C were subdivided into two groups, the first contained data for $u_g < 0.08$ m/s and the other contained data for $u_g > 0.08$ m/s. The break point was determined at 0.08 m/s since specific interfacial areas for gas velocities below 0.08

Table VI-6 Goodness of fit and parameters for area correlations - FT-300 wax.

Correlation 1:

$$a = k_1 u_g{}^{k_2}$$

Correlation 2:

$$a = k_1 u_g{}^{k_2} e^{-k_3 u_g}$$

Temperature (°C)	200	265
No. of points	8	64

MEAN SQUARE ERROR:

Correlation 1	2.01×10^5	1.11×10^6
Correlation 2	7.50×10^4	6.85×10^5

PERCENTAGE OF POINTS WITHIN ±30%:

Correlation 1	62.5	43.8
Correlation 2	75.0	53.1

PARAMETERS FOR CORRELATION 1:

k_1	997	2411
k_2	0.021	0.071

PARAMETERS FOR CORRELATION 2:

k_1	1.31×10^6	9.51×10^5
k_2	1.61	1.43
k_3	42	31

m/s showed a Gaussian behavior and could be fitted using Equation (VI-28), while values for gas velocities above 0.08 m/s showed a behavior that could be fitted using Equation (VI-27). This procedure reduced the mean square error to 5.21×10^5 for the entire data set with 61.0 percent of data within the ±30% error band. Figure VI-6 compares the predicted values with the experimental specific interfacial area values for FT-300 wax at 265°C. The specific gas-liquid interfacial area correlations for FT-300 wax at 265°C are:

$$a = 3.3 \times 10^8 u_g^{2.72} e^{-71u_g} \qquad u_g < 0.08 \text{ m/s} \qquad (VI-29)$$

$$a = 971 u_g^{-0.216} \qquad 0.08 \leq u_g \leq 0.15 \text{ m/s} \qquad (VI-30)$$

Results for Sasol's Arge reactor wax are summarized in Table VI-7. The correlations fit the data fairly well for this case, with 80 to 85% of the data within the ±30% band. The marginally better fit with the second correlation could be as a result of the extra parameter involved in that equation. Since there was no foam present for this wax, the Gamma function type of correlation does not lead to a significant improvement in the goodness of fit. The correlations for specific gas-liquid interfacial area at the two temperatures are:

$$a = 1000 u_g^{0.25} \qquad 0.01 \leq u_g \leq 0.12 \text{ m/s} \qquad (VI-31)$$

at 265°C and

$$a = 492 u_g^{0.256} \qquad 0.01 \leq u_g \leq 0.12 \text{ m/s} \qquad (VI-32)$$

at 200°C. The different temperatures do not appear to have a significant affect on the exponent, only the coefficient appears to change. As expected, lower temperatures give smaller specific interfacial area, a direct consequence of larger bubbles present at 200°C compared to 265°C. The experimental values of the specific interfacial area are compared with

Table VI-7. Goodness of fit and parameters for area correlations - Sasol's Arge wax and Mobil reactor wax.

Correlation 1:

$$a = k_1 u_g{}^{k_2}$$

Correlation 2:

$$a = k_1 u_g{}^{k_2} e^{-k_3 u_g}$$

	SASOL WAX		MOBIL WAX	
Temperature (°C)	200	265	200	265
No. of points	8	20	8	13

MEAN SQUARE ERROR:

Correlation 1	1940	11610	240	1240
Correlation 2	1700	9090	170	740

PERCENTAGE OF POINTS WITHIN ±30%:

Correlation 1	87.5	80.0	100.0	100.0
Correlation 2	87.5	85.0	100.0	100.0

PARAMETERS FOR CORRELATION 1:

k_1	492	1000	165	300
k_2	0.26	0.25	0.01	0.01

PARAMETERS FOR CORRELATION 2:

k_1	1569	8368	378	1110
k_2	0.53	0.75	0.20	0.31
k_3	5.7	10.2	4.4	6.6
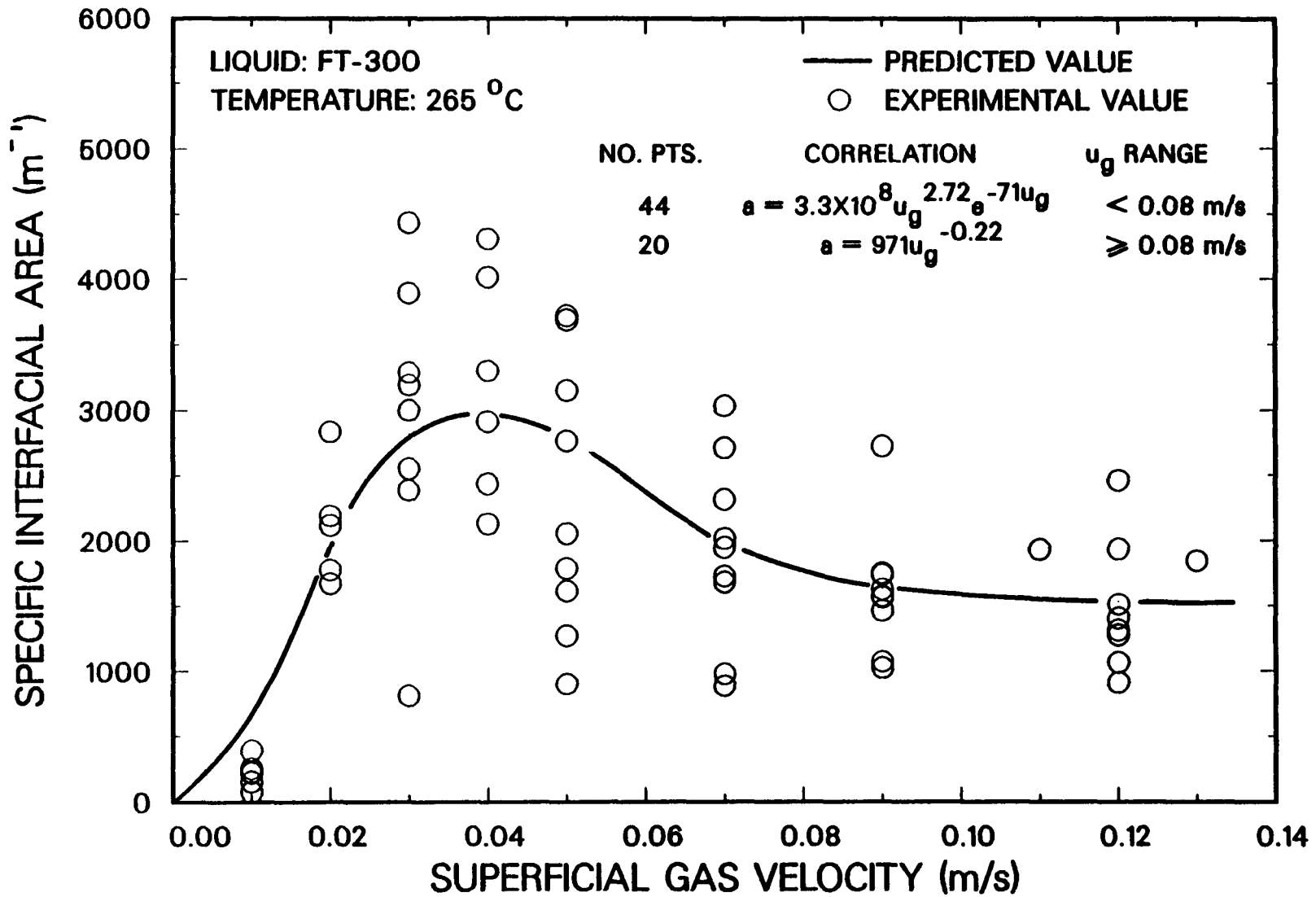
Figure VI-6. Comparison between experimental specific gas-liquid interfacial areas and predictions

the predicted values in Figure VI-7. Despite some scatter, the correlation appears to fit the data fairly well.

Table VI-7 also summarizes results for Mobil reactor wax. Both correlations provide an excellent fit for the data. All data are within ±20% of the predicted values. The correlations for specific gas-liquid interfacial area at the two different temperatures are:

$$a = 300u_g^{0.01} \qquad 0.01 \leq u_g \leq 0.12 \text{ m/s} \qquad \text{(VI-33)}$$

at 265°C and

$$a = 165u_g^{0.01} \qquad 0.01 \leq u_g \leq 0.12 \text{ m/s} \qquad \text{(VI-34)}$$

at 200°C. Once again the different temperatures only affect the coefficient for reasons similar to those mentioned above. These correlations also show that for Mobil wax, specific interfacial area has a weak dependence on the superficial gas velocity. This is further illustrated in Figure VI-8 where the experimental values are compared with the values predicted by the correlation. The specific interfacial area remains fairly constant over the range of gas velocities employed.

The results presented above show that wax type has a significant effect on the specific interfacial area. FT-300 wax produces the greatest interfacial area due to the large number of tiny bubbles, whereas, Mobil reactor wax gives the smallest specific interfacial area. The specific interfacial area for FT-300 wax is an order of magnitude larger than that for Mobil reactor wax. Sasol's Arge reactor wax produces interfacial areas that are approximately twice as large as those for Mobil reactor wax. Results from DGD studies showed that, for superficial gas velocities greater than 0.05 m/s, the typical value of the Sauter mean diameter for FT-300 wax at 265°C is around 0.8 mm with orifice and perforated plate
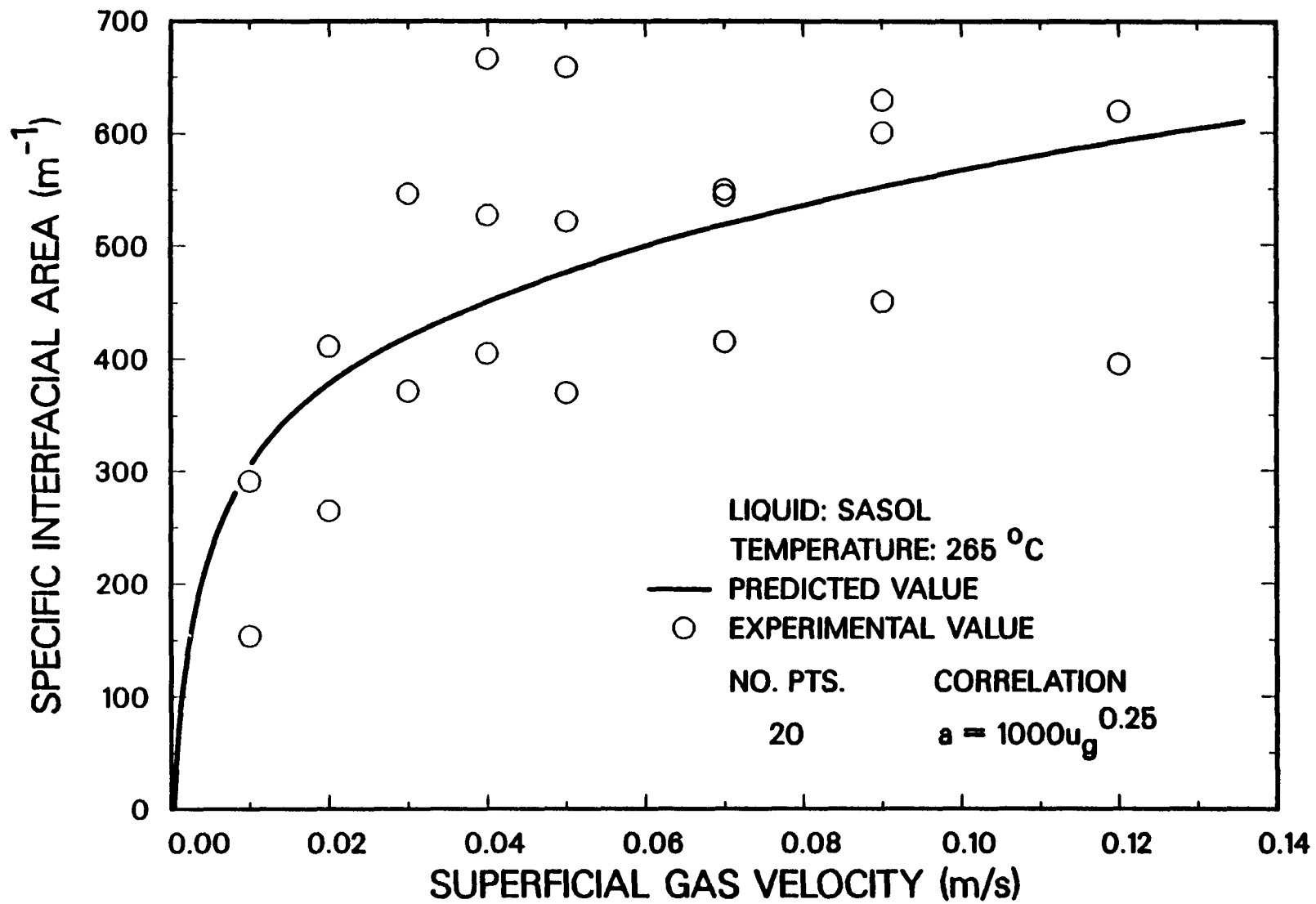
Figure VI-7. Comparison between experimental specific gas-liquid interfacial areas and predictions
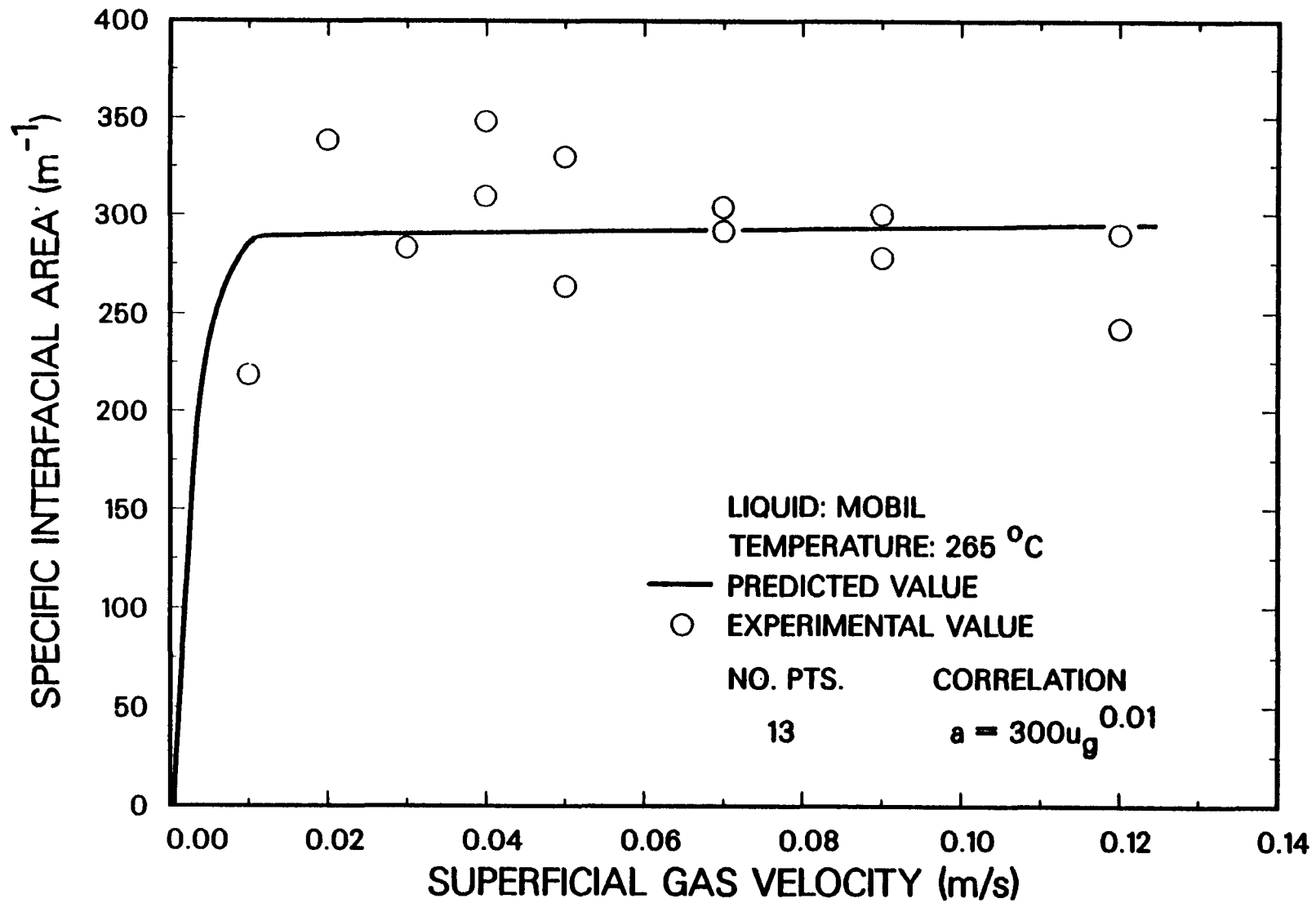
Figure VI-8. Comparison between experimental specific gas-liquid interfacial areas and predictions

distributors and around 0.6 mm with the 40 μm SMP distributor (from photography). These values can be used together with the hold-up correlations (Equations (VI-23) and (VI-24)) to obtain the following correlations for the specific interfacial area (according to Equation (VI-26)):

$$a = 6323u_g^{0.59} \qquad 0.05 \leq u_g \leq 0.15 \text{ m/s} \qquad \text{(VI-35)}$$

for orifice type distributors and

$$a = 9820u_g^{0.61} \qquad 0.01 \leq u_g \leq 0.12 \text{ m/s} \qquad \text{(VI-36)}$$

for the 40μm SMP distributor. Similarly for Sasol wax d_s is around 2 mm at 265°C and the resulting correlation for the specific gas-liquid interfacial area (using Equation (VI-23) for ϵ_g) is

$$a = 2529u_g^{0.59} \qquad 0.07 \leq u_g \leq 0.12 \text{ m/s} \qquad \text{(VI-37)}$$

For Mobil wax d_s is around 4 mm, giving the following correlation for area

$$a = 1265u_g^{0.59} \qquad 0.07 \leq u_g \leq 0.12 \text{ m/s} \qquad \text{(VI-38)}$$

Deckwer et al. (1980) obtained a correlation for the specific interfacial area (Equation (VI-39)) by using their correlation for average gas hold-up and a Sauter mean bubble diameter of 0.7 mm. The correlation is based on experiments conducted with the SMP distributor for $u_g < 0.04$ m/s (the "foamy" regime).

$$a = 71320u_g^{1.1} \qquad \text{(VI-39)}$$

The correlation for ϵ_g, based on data obtained from the present study with the SMP distributor in the "foamy" regime, can be used with a d_s value of 0.6 mm to obtain

$$a = 10600u_g^{0.15} \qquad \text{(VI-40)}$$

At 0.04 m/s this correlation gives a value of 6541 m^{-1} while Deckwer's correlation (Equation (VI-39)) gives 2068 m^{-1}. The correlation with the SMP

252

distributor, based on data obtained in the "slug flow" regime (Equation (VI-36)), gives a specific interfacial area of 1378 m^{-1}. The difference between specific interfacial area from Deckwer's correlation and that from Equation (VI-40) could be due to the differences in the amount of foam present in the two studies.

The correlations presented above show that for FT-300 waxes, the specific interfacial area can be predicted using two different equations, depending on the superficial gas velocity employed. For u_g < 0.08 m/s, Equation (VI-29) may be used, while for u_g > 0.08 m/s Equation (VI-30) is recommended. Specific gas-liquid interfacial area for Sasol's Arge reactor wax can be predicted using Equation (VI-31) at 265 °C and for Mobil's reactor wax using Equation (VI-33).

VII. NOMENCLATURE

a	specific gas-liquid interfacial area, $6\epsilon_g/d_s$ (m^{-1})
b_i	intercept associated with the i-th line
d_B	bubble diameter (mm)
d_{B_i}	diameter of bubbles in class i (mm)
d_{MAX}	largest dimension or caliper diameter of a bubble (mm)
d_{MIN}	smallest dimension or caliper diameter of a bubble (mm)
d_{ave}	average of d_{MIN} and d_{MAX} (mm)
d_{cat}	catalyst particle size (μm)
d_{chord}	chord diameter of a bubble (mm)
d_{circ}	area equivalent diameter of a bubble (mm)
d_c	bubble column diameter (m)
d_{Feret}	Feret diameter of a bubble (mm)
d_o	orifice diameter (mm)
d_{ocr}	critical orifice diameter (mm)
d_s	Sauter mean bubble diameter (mm)
f_i	volume fraction of bubbles of size d_{B_i}
g	gravitational constant = 9.81 m/s^2
H	expanded bed height at time t (m)
H_o	expanded bed height at time 0 (m)
H_s	static bed height (m)
k_L	liquid side mass transfer coefficient (m/s)
n_i	number of bubbles of size d_{B_i}
n_o	number of holes in a perforated plate
N	number of bubble size classes from DGD technique

P	pressure (Pa)
s_i	slope associated with the i-th line
s_d	specific gravity of the gas-liquid dispersion (-)
s_ℓ	specific gravity of the liquid (-)
t	time (s)
T	operating temperature (°C)
u_{B_i}	rise velocity associated with bubbles of size d_{B_i} (m/s)
u_g	superficial gas velocity (m/s)
u_j	jet velocity or gas velocity through the orifice (m/s)
V_g	volume of gas in the gas-liquid dispersion (m^3)
V_i	volume of a gas bubble of size d_{B_i} (mm^3)
V_T	total volume of the gas-liquid dispersion (m^3)
w_{cat}	weight percent catalyst in the slurry (%)

Greek Letters

ϵ_g	average gas hold-up (%)
ϵ_{go}	average gas hold-up (-)
ϵ_{goi}	gas hold-up due to the presence of bubbles of size d_{B_i} (-)
ϵ_{gp}	predicted value of average gas hold-up (%)
μ, μ_ℓ	liquid viscosity (mPa.s)
ρ_d	density of the gas-liquid dispersion (kg/m^3)
ρ_g	density of gas (kg/m^3)
ρ_{H_2O}	density of water (kg/m^3)
ρ_ℓ	density of liquid (kg/m^3)
σ	surface tension (N/m)

Dimensionless Numbers

Bo	Bond number, $d_c^2 \rho_\ell g / \sigma$
F	flow number, $g d_B^{8/3} (\rho_\ell - \rho_g) \rho_\ell^{2/3} / \mu^{4/3} \sigma^{1/3}$
Fr	Froude number, $u_g / \sqrt{d_c g}$
Ga	Galileo number, $d_c^3 g \rho_\ell^2 / \mu_\ell^2$
V	velocity number, $u_B d_B^{2/3} \rho_\ell^{2/3} / \mu^{4/3} \sigma^{1/3}$
We	Weber number (orifice), $d_o \rho_g u_j^2 / \sigma$

Acronyms

DGD	dynamic gas disengagement
DOE	Department of Energy
DP	differential pressure
FT, F-T	Fischer Tropsch
HPSL	high pressure side line - DP system
ID	inside diameter
KW	Krupp wax
LPSL	low pressure side line - DP system
MP	molten paraffin wax
MSE	mean square error
PP	perforated plate
PW	product wax
SMP, SP	sintered metal plate
SN	single nozzle
SS	stainless steel

Subscripts

B	bubble
g	gas
ℓ	liquid
L	large bubbles
M	medium size bubbles
o	at time t=0
S	small bubbles

VIII. REFERENCES

Abou-el-Hassan, M.E., A generalized bubble rise velocity correlation, Chem. Eng. Commun., 22, 243 (1983).

Akita, K. and Yoshida, F., Gas holdup and volumetric mass transfer coefficients in bubble columns, Ind. Eng. Chem. Proc. Des. Dev., 12, 77 (1973).

Akita, K. and Yoshida, F., Bubble size, interfacial area, and liquid-phase mass transfer coefficient in bubble columns, Ind. Eng. Chem. Proc. Des. Dev., 13, 84 (1974).

Anderson, J.L. and Quinn, J.A., Bubble columns: flow transitions in the presence of trace contaminants, Chem. Eng. Sci., 25, 373 (1970).

Bach, H.F. and Pilhofer, T., Variation of gas hold-up in bubble columns with physical properties of liquids and operating parameters of columns, Ger. Chem. Eng., 1, 270 (1978).

Buchholz, R. and Schügerl, K., Methods for measuring the bubble size in bubble column bioreactors - II, Europ. J. Appl. Microbiol. Biotechnol., 6, 315, (1979).

Calderbank, P.H., Evans, F., Farley, R., Jepson, G. and Poll, A., Rate processes in the catalyst-slurry Fischer-Tropsch reaction, Catalysis in Practice - Instn. Chem. Engnrs., 66 (1963).

Clift, R., Grace, J.R. and Weber, M.E., Bubble Drops and Particles, Academic Press, New York, 171 (1978).

Deckwer, W.D., Louisi, Y., Zaidi, A. and Ralek, M., Hydrodynamic properties of the Fischer-Tropsch slurry process, Ind. Eng. Chem. Proc. Des. Dev., 19, 699 (1980).

Deckwer, W.D., Serpemen, Y., Ralek, M. and Schmidt, B., Modeling the Fischer-Tropsch synthesis in the slurry phase, Ind. Eng. Chem. Proc. Des. Dev., 21, 231 (1982).

Farley, R. and Ray, D.J., Gamma radiation absorption measurement of density and gas hold-up in a three-phase catalytic reactor, Brit. Chem. Eng., 9, 830 (1964a).

Farley, R. and Ray, D.J., The design and operation of a pilot-scale plant for hydrocarbon synthesis in the slurry phase, J. Inst. Petrol., 50, 27 (1964b).

Heijnen, J.J. and van't Riet, R.K., Mass transfer, mixing and heat transfer phenomena in low viscosity bubble column reactors, Chem. Eng. J., 28, B21 (1984).

Hikita, H., Asai, S., Tanigawa, K., Segawa, K. and Kitao, M., Gas hold-up in bubble columns, Chem. Eng. J., 20, 59 (1980).

Keitel, G. and Onken, U., Inhibition of bubble coalescence by solutes in air/water dispersions, Chem. Eng. Sci., 37, 1635 (1982).

Kelkar, B.G., Godbole, S.P., Honath, M.F., Shah, Y.T., Carr, N.L. and Deckwer, W.D., Effect of addition of alcohols on gas holdup and backmixing in bubble columns, AIChE J., 29, 361 (1983).

Kölbel, H., Ackermann, P. and Engelhardt, F., New developments in hydrocarbon synthesis, Proc. Fourth World Petrol. Cong., Section IV/C, 227, Carlo Colombo Publishers, Rome (1955).

Kölbel, H. and Ralek, M., The Fischer-Tropsch synthesis in the liquid phase, Cat. Rev. Sci. Eng., 21, 225 (1980).

Kuo, J.C.W., et al., Two-stage process for conversion of synthesis gas to high quality transportation fuels, Final Report to the Department of Energy for Contract No. DE-AC22-83PC60019 (1985).

Maruyama, T., Yoshida, S. and Mizushina, T., The flow transition in a bubble column, J. Chem. Eng. Japan, 14, 352 (1981).

Mersmann, A., Design and scale-up of bubble and spray columns, Ger. Chem. Eng., 1, 1 (1978).

O'Dowd, W., Smith, D.N. and Ruether, J.A., Slurry F-T hydrodynamics and scale-up, Proceedings of the Fifth DOE Indirect Liquefaction Contractor's Meeting, Houston, Texas, Dec. 2-5 (1985).

O'Dowd, W., Smith, D.N. and Ruether, J.A., Slurry F-T reactor hydrodynamics and scale-up, Proceedings of the Sixth DOE Indirect Liquefaction Contractor's Meeting, p 147, Pittsburgh, Pennsylvania, Dec 2-4 (1986).

Ohki, Y. and Inoue, H., Longitudinal mixing of the liquid phase in bubble columns, Chem. Eng. Sci., 25, 1 (1970).

Ostergaard, K., Gas-liquid-particle operation in chemical reaction engineering, Advances in Chemical Engineering, 7, Academic Press, New York, NY (1980).

Pilhofer, T., Effect of plate geometry on gas-holdup in bubble columns, Chem. Eng. Commun., 5, 69 (1980).

259

Quicker, G. and Deckwer, W.D., A further note on mass transfer limitations in the Fischer-Tropsch slurry process, Chem. Eng. Sci., 36, 1577 (1981).

Richardson, D.R., How to design fluid-flow distributors, Chem. Eng., 83 (1961).

Riquarts, H., Model representation of homogeneous and heterogeneous two-phase flow in fluidized beds and bubble columns, Ger. Chem. Eng., 2, 268 (1979).

Sanders, E., Ledakowicz, S. and Deckwer, W.D., Fischer-Tropsch synthesis in bubble column slurry reactors on Fe/K-catalyst, Can. J. Chem. Eng., 64, 133 (1986).

Satterfield, C.N., Huff, G.A. and Stenger, H.G., Effect of carbon formation on liquid viscosity and performance of Fischer-Tropsch bubble column reactors, Ind. Eng. Chem. Proc. Des. Dev., 20, 666, (1981).

Schügerl, K., Oels, U. and Lücke, J., Bubble column bioreactors, Adv. Biochem. Eng., 7, 1 (1977).

Schügerl, K., Oxygen transfer into highly viscous media, Adv. Biochem. Eng., 19, 71 (1981).

Schumpe, A. and Grund, A., The gas disengagement technique for studying gas holdup structure in bubble columns, Can. J. Chem. Eng., 64, 891 (1986).

Shah, Y.T., Kelkar, B.G., Godbole, S.P. and Deckwer, W.D., Design parameters estimations for bubble column reactors, AIChE J., 28, 353 (1982).

Shah, Y.T., Joseph, S., Smith, D.N. and Ruether, J.A., On the behavior of the gas phase in a bubble column with ethanol-water mixtures, Ind. Eng. Chem. Proc. Des. Dev., 24, 1140 (1985).

Smith, D.N., Fuchs, W., Lynn, R.J., Smith, D.H. and Hess, M., Bubble behavior in a slurry bubble column reactor model, ACS Symposium Series, 237, Chemical and Catalytic Reactor Modeling, Ed.: Dudukovic, M.P. and Mills, P.L., 125 (1984a).

Smith, D.N., O'Dowd, W., Ruether, J.A., Stiegel, G.J. and Shah, Y.T., Slurry F-T reactor hydrodynamics and scale-up, Proceedings of the Fourth DOE Indirect Liquefaction Contractor's Meeting, Washington, Oct. 30-31 (1984b).

Smith, J., Gupte, K.M., Leib, T.M. and Kuo, J.C.W., Hydrodynamic studies of Fischer-Tropsch bubble column systems, Paper presented at the AIChE 1984 Summer National Meeting, Philadelphia, August 19 (1984).

Sriram, K. and Mann, R., Dynamic gas disengagement: a new technique for assessing

the behavior of bubble columns, Chem. Eng. Sci., 32, 571 (1977).

Towell, G.D., Strand, C.P. and Ackerman, G.H., Mixing and mass transfer in large diameter bubble columns, AIChE - Inst. Chem. Eng. Symp. Ser., No. 10, 97 (1965).

Ueyama, K., Morooka, S., Koide, K., Kaji, H. and Miyauchi, T., Behavior of gas bubbles in bubble columns, Ind. Eng. Chem. Proc. Des. Dev., 19, 592 (1980).

van Landegham, H., Multiphase reactors: mass transfer and modeling, Chem. Eng. Sci., 35, 1912 (1980).

Vermeer, D.J. and Krishna, R., Hydrodynamics and mass transfer in bubble columns operating in the churn-turbulent regime, Ind. Eng. Chem. Proc. Des. Dev., 20, 475 (1981).

Wallis, G.B., One-dimensional two-phase flow, McGraw-Hill: New York (1969).

Weibel, E.W., Stereological methods - theoretical foundations, vol. 2, Academic Press (1980).

Zahradnik, J. and Kastanek, F., Gas holdup in uniformly aerated bubble column reactors, Chem. Eng. Commun., 3, 413 (1979).

Zaidi, A., Louisi, Y., Ralek, M. and Deckwer, W.D., Mass transfer in the liquid phase Fischer-Tropsch synthesis, Ger. Chem. Eng., 2, 94 (1979).

Zieminski, S.A., Caron, M.M. and Blackmore, R.B., Behavior of air bubbles in dilute aqueous solutions, Ind. Eng. Chem. Fund., 6, 233 (1967).

IX. ACKNOWLEDGEMENT

APPENDIX A

SUMMARY OF EXPERIMENTS AND EXPERIMENTAL CONDITIONS

The various experiments conducted during the present study were distinguished by run numbers. A run number consists of two parts; the first part is the batch-number for the wax used in that run, and the second part is the experiment number with the given batch of wax. For example, Run 3-2 corresponds to the second experiment with wax batch-number 3. The set of run numbers used for experiments conducted in the 0.051 m ID glass and stainless steel columns are different from the set used for experiments conducted in the 0.229 m ID glass and 0.241 m ID stainless steel columns. This is because two different wax storage tanks were used for the two different sets of columns (see Section IV-B.), each with its own set of wax batch-numbers.

A new batch of wax was used once the old wax began to turn dark yellow (i.e. FT-200 and FT-300 waxes, which originally are clear) or when experiments with a new type of wax were to be conducted. During the first two wax changes (i.e. between wax batch numbers 1a and 1b, and between 1b and 1c), the entire batch of old wax was not replaced with fresh wax. Instead, the new batch consisted of a large amount of fresh wax added to a small amount of the old wax (from the previous batch). Since the three batches of wax originated from the same batch of fresh wax, they were numbered 1a, 1b and 1c. On an average, six runs were conducted with a batch of FT-300 wax before a change was necessary. A relatively large number of runs were conducted with batch-numbers 1a to 3 in the 0.051 m ID columns because the wax during these runs was stored in the large storage tank (0.085 m^3 capacity) while the small storage tank (0.009 m^3 capacity) was used for batch-numbers 4 and higher.

Three different types of solvents were used to clean the bubble column

apparatus during the present studies. Kerosene, which is relatively inexpensive, was used for series 1a runs, however, due to its dark color, kerosene was replaced by a mineral spirit (varsol) after Run 1c-5. Toluene was used in addition to varsol from Run 2-5 onwards. The use of varsol was limited to instances when the column was fairly dirty.

The column and the distributor section were cleaned with toluene between runs. Approximately 1 liter of the solvent was introduced into the column and the temperature maintained between 100 and 150°C. The toluene vapors rose through the column and condensed along the walls, stripping any wax remaining on the walls. After approximately 20 minutes the toluene was drained through the distributor, removing any wax present in that section. A small nitrogen flow was maintained during the cleaning process. For instances when the column was fairly dirty (i.e. when walls were significantly stained with wax), the toluene wash was preceded by a varsol wash. The varsol was introduced into the column up to a height of approximately 1.5 m and a relatively high flow rate of nitrogen maintained for 20 to 30 minutes, after which the solvent was drained through the distributor. When a different type of wax was to be used, the cleaning process also included the wax storage tank and the wax inlet line. The varsol was drained from the column into the storage tank, through the wax inlet line and then drained through the opening under the storage tank. This process was then repeated using toluene.

Periodically the columns were removed and cleaned manually using steel wool and a detergent. The columns were then rinsed with distilled water and dried. A similar procedure was used to clean the distributor section and the plenum chamber.

265

All experiments conducted during the course of this study are summarized in Tables A-1 and A-2. Table A-1 summarizes runs conducted in the 0.051 m ID glass and stainless steel columns, and Table A-2 summarizes runs conducted in the 0.229 m ID glass and the 0.241 m ID stainless steel columns.

Table A-1. Summary of experiments performed in the small bubble columns (0.051 m ID).

Run No.	Wax Type	Column ID (m)	Temperature (°C)	Distributor	Start-up velocity (m/s)	Static height (m)
1a-1	FT-300	0.051 (glass)	230-280	1.85 mm	0.01	2.2
1a-2	"	"	230-265	"	0.03	2.1
1a-3	"	"	230,250	"	0.065	1.9
1a-4	"	"	265	"	0.055	"
1a-5	"	"	280	"	0.066	1.9-2.1
1a-6	"	"	265	"	0.024	1.7-2.2
1a-7	"	"	250,265	"	0.09	1.7-1.9
1a-8	"	"	230,250	"	"	1.8-2.2
1a-9	"	"	230	"	0.10	2.2
1a-10	"	"	265	"	0.067	1.8-2.2
1a-11	"	"	160	"	0.07	2.0
1a-12	"	"	280	"	0.045	1.4-1.7
1a-13	"	"	230	4.0 mm	0.093	1.9
1a-14	"	"	265	"	"	1.7
1a-15	"	"	280	"	"	1.5-2.1
1b-1	"	"	230	40 μm SMP	0.09	1.3-2.0
1b-2	"	"	265	"	"	0.9-2.1
1b-3	"	"	280	"	"	0.8-1.7
1b-4	"	"	265,280	"	0.02	1.6
1c-1	"	"	230	1.85 mm	0.10	2.0
1c-2	"	0.051 (SS)	265	"	0.01	2.3
1c-3	"	"	"	4.0 mm	"	2.2
1c-4	"	"	"	40 μm SMP	"	0.6-1.9
1c-5	"	0.051 (glass)	"	1.85 mm	0.10	2.0
1c-6	"	"	"	4.0 mm"	"	1.9-2.0
1c-7	"	"	"	40 μm SMP	"	1.2-2.0
1c-8	"	"	"	1.85 mm	0.09	1.6-1.9
1c-9	"	"	"	"	"	1.8
2-1	"	"	"	"	"	"
2-2	"	"	"	"	0.01	2.2
2-3	"	"	"	"	0.02	2.1
2-4	"	"	"	"	0.01	"

Table A-1. (contd.)

Run No.	Wax Type	Column ID (m)	Temperature (°C)	Distributor	Start-up velocity (m/s)	Static height (m)
2-5	FT-300	0.051 (glass)	265	4.0 mm	0.01	2.1
2-6	"	"	"	"	0.09	"
2-7	"	"	"	1.85 mm	0.01	1.8-2.2
2-8	"	"	"	"	0.09	1.8
2-9	"	"	"	40 μm SMP	0.01	0.6-1.7
2-10	"	"	"	"	0.17	0.7-1.8
3-1	"	"	"	1.85 mm	0.01	2.1
3-2	"	"	"	"	"	"
3-3	"	"	"	40 μm SMP	"	0.8-1.2
3-4	"	0.051 (SS)	"	1.85 mm	"	1.8
3-5	"	"	"	"	0.09	"
3-6	"	"	"	4.0 mm	0.01	1.7
3-7	"	"	"	40 μm SMP	"	"
3-8	"	0.051 (glass)	"	1.85 mm	"	"
4-1	"	"	"	"	"	1.9
4-2	"	"	"	"	0.12	"
4-3	"	"	200	"	0.01	"
4-4	FT-300[a]	"	265	"	"	2.0
4-5	FT-300[b]	"	"	"	"	"
4-6	FT-300[b]	"	"	40 μm SMP	"	0.8-1.5
5-1	FT-300	"	"	"	"	0.8-1.9
5-2	"	"	"	"	0.12	0.8-2.1
5-3	"	"	200	"	0.01	1.0-1.8
6-1[c]	"	"	265	1.85 mm	"	1.8-2.2
6-2	"	"	"	4.0 mm	"	2.1
6-3	"	"	"	"	0.12	"
7-1	"	"	"	1.85 mm	0.01	"
7-2	"	"	"	40 μm SMP	"	0.9-1.4
7-3[c]	"	"	"	1.85 mm	0.12	2.1

[a] FT-300 + 5% stearyl alcohol by weight.
[b] FT-300 + 5% stearyl alcohol + 5% stearic acid by weight.
[c] Long term stability run - Duration - 4 hours per velocity.

Table A-1. (contd.)

Run No.	Wax Type	Column ID (m)	Temperature (°C)	Distributor	Start-up velocity (m/s)	Static height (m)
8-1	SASOL	0.051 (glass)	265	1.85 mm	0.01	1.9
8-2	"	"	"	"	0.12	"
8-3	"	"	200	"	0.01	"
8-4	"	"	265	"	"	"
9-1	MOBIL[d]	"	"	"	"	2.1
9-2	"	"	200	"	"	"
9-3	"	"	265	"	0.12	2.0
9-4	"	"	"	40 μm SMP	0.01	1.8
10-1	SASOL	"	"	"	"	2.1
11-1	FT-200	"	"	1.85 mm	"	"
11-2	"	"	200	"	"	"
11-3	"	"	265	"	0.12	"
11-4	"	"	200	"	0.01	"
11-5	"	"	265	"	"	"
12-1	"	"	200	"	"	1.8-2.1
12-2	"	"	265	"	"	2.2
13-1	FT-300	"	"	"	"	2.1
13-2	"	"	200	"	"	"
13-3	"	"	265	"	0.12	"
14-1	"	"	"	"	0.01	2.0
14-2	"	"	"	"	0.12	2.1
15-1	"	"	"	1.0 mm	0.01	1.9
15-2	"	"	"	"	0.12	1.8
16-1	"	"	"	4.0 mm	0.01	2.1
16-2	"	"	"	"	0.12	1.7
17-1	FT-200	"	"	1.0 mm	0.01	1.5-2.0
17-2	"	"	"	"	0.12	1.4
18-1	"	"	"	1.85 mm	0.01	1.6
18-2	"	"	"	"	0.12	"
19-1	"	"	200	"	0.01	1.9
20-1	"	"	265	40 μm SMP	"	.6-1.9

[d] Composite from Mobil's runs CT-256-9, -11 and -12.

269

Table A-1. (contd.)

Run No.	Wax Type	Column ID (m)	Temperature (°C)	Distributor	Start-up velocity (m/s)	Static height (m)
21-1	MOBIL[e]	0.051 (glass)	265	1.85 mm	0.01	1.9
21-2	"	"	"	40 μm SMP	"	"
21-3	"	"	"	1 mm	"	"
21-4	"	"	200	1.85 mm	"	2.0
22-1	MOBIL[f]	"	265	40 μm SMP	"	1.9
22-2	"	"	"	1 mm	"	2.0
22-3	"	"	"	1.85 mm	"	1.9
22-4	"	"	200	"	"	"
23-1	MOBIL[e] +1% FT-200	"	265	40 μm SMP	"	2.0
23-2	MOBIL[e] +3% FT-200	"	"	"	"	"
23-3	"	"	"	1 mm	"	"
24-1	MOBIL[f] +1% FT-200	"	"	"	"	2.1
24-2	MOBIL[f] +3% FT-200	"	"	"	"	"
24-3	MOBIL[f] +5% FT-200	"	"	"	"	2.2

[e] Composite from Mobil's runs CT-256-4 and -7.
[f] Composite from Mobil's runs CT-256-5 and -8.

Table A-2. Summary of experiments performed in the large bubble columns (0.229 - 0.241 m ID).

Run No.	Wax Type	Column ID (m)	Temperature (°C)	Distributor	Start-up velocity (m/s)	Static height (m)
1-1	FT-300	0.229 (glass)	200	19 x 1.85 mm	0.01	1.9
1-2	"	"	265	"	"	"
1-3	"	"	"	"	"	"
1-4	"	"	"	"	0.09	2.0
1-5	"	"	"	30 x 1.5 mm [a]	0.01	1.8
1-6	"	"	"	19 x 1.0 mm	"	"
2-1	"	"	200	"	"	2.1
2-2	"	"	265	"	"	2.0
2-3	"	"	"	19 x 1.85 mm	"	"
2-4	"	"	"	"	0.12	"
2-5	"	0.241 (SS)	"	"	0.01	1.3-2.0
2-6	"	"	200	"	"	1.8
2-7	"	"	265	"	"	2.1
2-8	"	0.229 (glass)	"	"	"	"
2-9	"	"	265	"	0.12	2.0
3-1	SASOL	0.241 (SS)	"	"	0.01	"
3-2	"	0.229 (glass)	"	"	"	1.7
3-3	"	"	"	"	"	2.0
3-4	"	"	200	"	"	"
4-1	FT-300	"	265	5 x 1.0 mm	"	2.1
4-2	"	"	170	"	"	1.9

[a] perforated pipe distributor.

271

APPENDIX B

ESTIMATION OF AXIAL HOLD-UP FROM DIFFERENTIAL PRESSURES

The equations used to estimate axial and average hold-ups values from differential pressure measurements (see Section V.C) are developed here.

The gas hold-up in a gas-liquid system can be expressed in terms of the liquid density, ρ_ℓ, and the density of gas-liquid dispersion, ρ_d (i.e. density of the expanded liquid) as,

$$\epsilon_g = \frac{\rho_\ell - \rho_d}{\rho_\ell - \rho_g} \simeq 1 - \frac{\rho_d}{\rho_\ell} \tag{B-1}$$

since the density of the gas, ρ_g, is small in comparison to the density of the liquid at low pressures.

The density of the expanded liquid between any two pressure taps, i and j, (see Figure V-39) can be calculated from the measured pressure drop $(\Delta P)_{i-j}$ and the known distance between the pressure taps, h_{i-j},

$$(s_d)_{i-j} = \frac{(\Delta P)_{i-j}}{h_{i-j}} \quad \text{and} \quad (\rho_d)_{i-j} = (s_d)_{i-j}\rho_{H_2O} \tag{B-2}$$

where $(s_d)_{i-j}$ is the specific gravity of the dispersion between pressure taps i and j, and $j > i$, $i = 2,3,4,5$ or 6. By substituting this expression into Equation (B-1), one obtains

$$(\epsilon_g)_{i-j} = 1 - \frac{(\Delta P)_{i-j}}{s_\ell h_{i-j}} \tag{B-3}$$

The major sources of error in calculating the average gas hold-up within a segment, h_{i-j}, are in the measurements of $(\Delta P)_{i-j}$ and s_ℓ. The pressure drop is a rapidly fluctuating quantity, particularly at higher gas flow rates due to the passage of slugs. In calculations, the arithmetic average of the maximum and the minimum observed values was employed. The specific gravity (i.e. the density) of the molten paraffin wax represents the slope of a straight line formed by plotting the measured pressure drop versus the actual liquid height. The densities for the various liquids at

273

265°C are given in Table VI-1 (see Section VI-A.).

The expanded bed height and the average gas hold-up can also be determined from the differential pressure measurements. Let the expanded height be in the i-th segment (see Figure B-1), i.e. the top of the dispersion is between pressure taps i and (i+1). Then, the height of the gas-liquid dispersion in this segment is given by:

$$H' = \frac{(\Delta P)_{i-(i+1)}}{(s_d)_{i-(i+1)}} \qquad (B-4)$$

where $(\Delta P)_{i-(i+1)}$ is the pressure drop across this segment. However, the specific gravity of the gas-liquid dispersion in this segment can not be calculated using Equation (B-2), because the expanded height does not occupy the entire length of the segment, i.e. in general $H' < h_{i-(i+1)}$. In order to calculate H' an estimate for the density of gas-liquid dispersion in this segment is required. This can be obtained using either

$$(s_d)_{i-(i+1)} = (s_d)_{(i-1)-i} \qquad (B-5)$$

i.e. by assuming that the density of dispersion (or the gas hold-up) in the segment i is the same as in the previous segment, (i-1), or

$$(s_d)_{i-(i+1)} = (s_d)_{2-i} \qquad (B-6)$$

i.e. the specific gravity in the segment i is the same as the average specific gravity in the column up to this segment. The latter is calculated from

$$(s_d)_{2-1} = \frac{(\Delta P)_{2-i}}{h_{2-i}} \qquad (B-7)$$

When the axial hold-up does not vary appreciably along the column the estimated values obtained from Equations (B-5) and (B-6) are about the
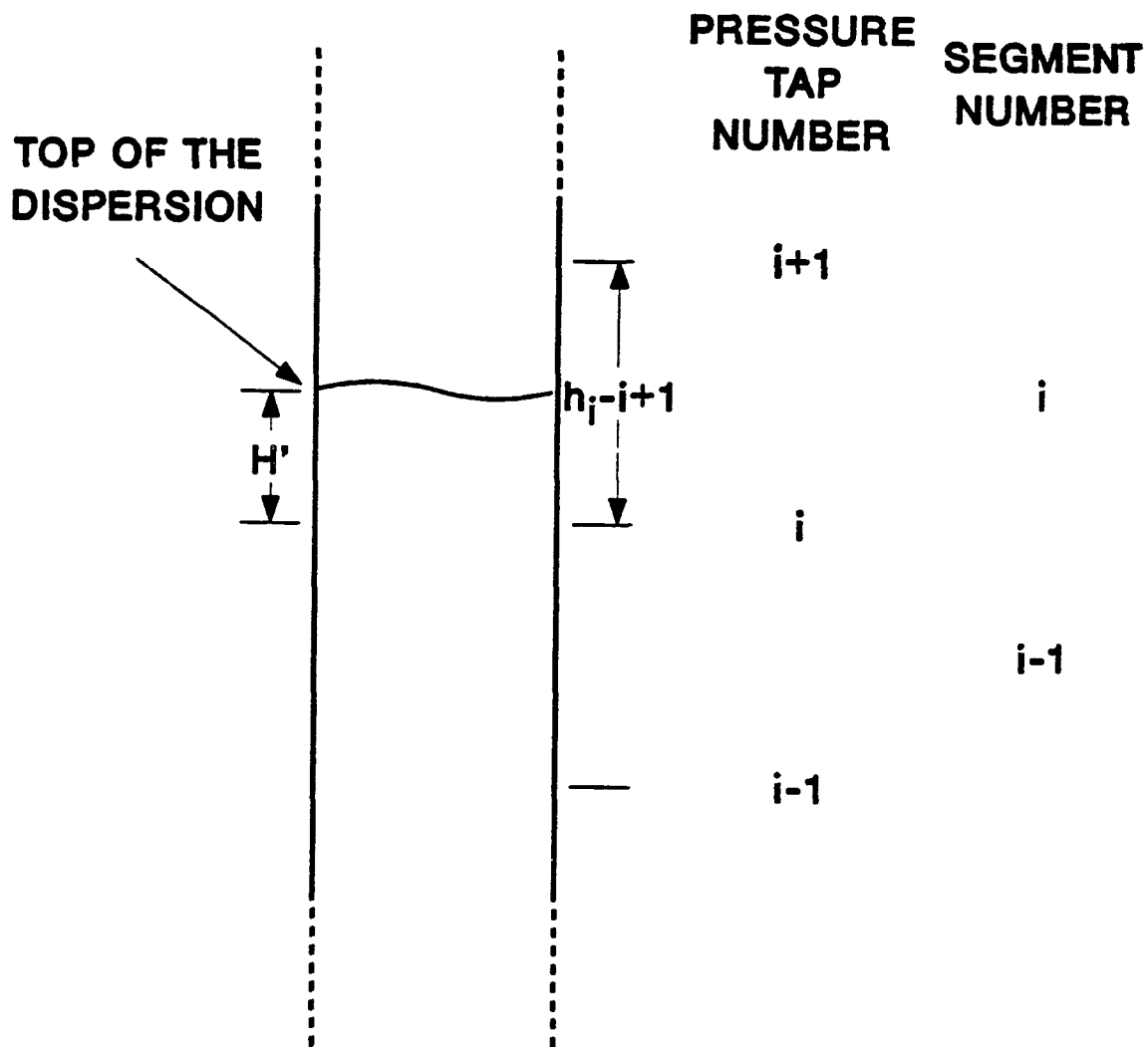
Figure B-1. Schematic diagram of the top of the dispersion with respect to pressure tap locations

275

same. However, when the axial hold-up increases with height, the use of Equation (B-5) is preferred, but this procedure may not provide an accurate estimate for $(s_d)_{i-(i+1)}$, since in this case $(s_d)_{i-(i+1)} < (s_d)_{(i-1)-i}$. This problem is particularly severe when foam occupies the upper portion of the column.

Once the height of the gas-liquid dispersion in the last segment is calculated from Equation (B-4), the total expanded height is obtained from

$$H = H_i + H' \tag{B-8}$$

where H_i is the distance from the distributor to the port i. Then the average hold-up for the entire column can be calculated as

$$\epsilon_g = \frac{H-H_s}{H} = 1 - \frac{H_s}{H} \tag{B-9}$$

The static height is given by

$$H_s = \frac{(\Delta P)_{2-7}}{s_\ell} + b + h_{o-2} \tag{B-10}$$

where b is the intercept of a straight line on a calibration diagram, the actual liquid height versus ΔP; h_{o-2} is the distance between the distributor and pressure tap #2 (see Figure V-39); $(\Delta P)_{2-7}$ is the measured pressure drop between taps #2 and #7 at zero gas velocity.

Thus, the errors in the determination of H_s and H' will both have an effect on the average gas hold-up.

An alternative procedure to estimate the expanded bed height, and thus the average gas hold-up is as follows. Plot the total pressure (in height of the liquid medium) as a function of height determined from the various $(\Delta P)_{i-j}$ measurements and fit a curve through these data points. The inter-

276

section of this curve with the abscissa ($\Delta P = 0$) gives the expanded bed height. The average gas hold-up is then calculated using Equation (B-9).

APPENDIX C

DEVELOPMENT OF EQUATIONS FOR DGD AND SAMPLE CALCULATIONS

1. Derivation of the Relationship Between Normalized Liquid Level and Time

The general equation for the dynamic hold-up, $\epsilon_g(t)$ in the discretized form is [Equation (V-8) in Section D.3]:

$$\epsilon_g(t) = \epsilon_{go} \sum_{i=1}^{k} f_i \left[1 - \frac{t u_{Bi}}{H} \right] \qquad t^*_{N-k+1} \geq t > t^*_{N-k} \qquad (C-1)$$

The following equations can be used to modify Equation (C-1):

$$\epsilon_g(t) = \frac{H - H_s}{H} \qquad (C-2)$$

$$\epsilon_{go} f_i = \epsilon_{goi} \qquad (C-3)$$

where H_s is the height of the ungassed liquid (static height). Equation (C-1) now becomes:

$$\frac{H - H_s}{H} = \sum_{i=1}^{k} \epsilon_{goi} - \frac{t}{H} \sum_{i=1}^{k} \epsilon_{goi} u_{Bi} \qquad (C-4)$$

multiplying both sides by H/H_o gives

$$\frac{H}{H_o} - \frac{H_s}{H_o} = \frac{H}{H_o} \sum_{i=1}^{k} \epsilon_{goi} - \frac{t}{H_o} \sum_{i=1}^{k} \epsilon_{goi} u_{Bi} \qquad (C-5)$$

Equation (C-5) yields, upon rearrangement:

$$\frac{H}{H_o} = \frac{H_s/H_o}{1 - \sum_{i=1}^{k} \epsilon_{goi}} - t \frac{\sum_{i=1}^{k} \epsilon_{goi} u_{Bi}}{H_o \left[1 - \sum_{i=1}^{k} \epsilon_{goi} \right]} \qquad t^*_{N-k+1} \geq t > t^*_{N-k} \qquad (C-6)$$

This is an equation of a straight line with the first term on the right hand side representing the intercept and the second term represents the

279

slope multiplied by time (t).

2. Derivation of the Expressions for ϵ_{goi} and u_{Bi}

From Equation (C-6) the intercept for the k-th straight line is given as:

$$b_k = \frac{H_s/H_o}{1 - \sum_{i=1}^{k} \epsilon_{goi}} \qquad \text{(C-7)}$$

This can be rearranged to give:

$$\sum_{i=1}^{k} \epsilon_{goi} = 1 - \frac{H_s}{H_o b_k} \qquad \text{(C-8)}$$

Further rearrangement gives the fractional gas hold-up corresponding to the k-th bubble class:

$$\epsilon_{gok} = 1 - \frac{H_s}{H_o b_k} - \sum_{i=1}^{k-1} \epsilon_{goi} \qquad \text{(C-9)}$$

Similar manipulation of the expression for intercept of the k-1'th straight line would result in the following expression:

$$\sum_{i=1}^{k-1} \epsilon_{goi} = 1 - \frac{H_s}{H_o b_{k-1}} \qquad \text{(C-10)}$$

Combination of Equations (C-9) and (C-10) will then result in the following expression for ϵ_{gok}:

$$\epsilon_{gok} = \frac{H_s}{H_o} \left[\frac{1}{b_{k-1}} - \frac{1}{b_k} \right] \qquad \text{(C-11)}$$

From Equation (C-6) the slope of the k-th straight line is:

$$s_k = - \frac{\sum\limits_{i=1}^{k} \epsilon_{goi} u_{Bi}}{H_o \left[1 - \sum\limits_{i=1}^{k} \epsilon_{goi} \right]} \qquad (C-12)$$

This equation can be rearranged to give:

$$\sum\limits_{i=1}^{k} \epsilon_{goi} u_{Bi} = s_k H_o \left[\sum\limits_{i=1}^{k} \epsilon_{goi} - 1 \right] \qquad (C-13)$$

Substitution of Equation (C-8) into Equation (C-13) results in:

$$\sum\limits_{i=1}^{k} \epsilon_{goi} u_{Bi} = - \frac{s_k H_s}{b_k} \qquad (C-14)$$

which upon further manipulation gives the expression for the rise velocity of bubbles belonging to the k-th class:

$$u_{Bk} = \left[- \frac{s_k H_s}{b_k} - \sum\limits_{i=1}^{k-1} \epsilon_{goi} u_{Bi} \right] \frac{1}{\epsilon_{gok}} \qquad (C-15)$$

Similar rearrangement of the expression for the slope of the k-1'th straight line yields

$$\sum\limits_{i=1}^{k-1} \epsilon_{goi} u_{Bi} = - \frac{s_{k-1} H_s}{b_{k-1}} \qquad (C-16)$$

Combination of Equations (C-11), (C-15) and (C-16) gives the following expression for u_{Bk}:

$$u_{Bk} = \frac{H_o \left[b_k s_{k-1} - b_{k-1} s_k \right]}{b_k - b_{k-1}} \qquad (C-17)$$

281

The general expressions for ϵ_{goi} and u_{Bi}, for $i = 1 \rightarrow N$ are

$$\epsilon_{goi} = \frac{H_s}{H_o} \left[\frac{1}{b_{i-1}} - \frac{1}{b_i} \right] \qquad (C-18)$$

$$u_{Bi} = \frac{H_o \left[b_i s_{i-1} - b_{i-1} s_i \right]}{b_i - b_{i-1}} \qquad (C-19)$$

In the above equations, b_o represents the normalized static height (i.e. $b_o = H_s/H_o$) and b_N represents the normalized expanded height at time t=0 (i.e. $b_N = H_o/H_o = 1$).

3. Equations for Bimodal and Trimodal Distributions

The equations for ϵ_{goi} and u_{Bi} developed above assumed N distinct bubble sizes. For the case of two bubble sizes the general equations (C-18 and C-19) reduce to the following:

$$\epsilon_{goS} = 1 - \frac{H_s}{b_1 H_o} \qquad (C-20)$$

$$u_{BS} = - \frac{H_s s_1}{b_1 - \dfrac{H_s}{H_o}} \qquad (C-21)$$

and

$$\epsilon_{goL} = \frac{H_s}{H_o} \left[\frac{1}{b_1} - 1 \right] \qquad (C-22)$$

$$u_{BL} = \frac{H_o \left[s_1 - b_1 s_2 \right]}{1 - b_1} \qquad (C-23)$$

where S and L indicate small and large bubbles.

282

For the case of three bubble sizes, i.e. small (S), medium (M) and large (L), the equations for small bubbles are the same as above (i.e. Equations (C-20) and (C-21)), the remaining equations are as follows:

$$\epsilon_{goM} = \frac{H_s}{H_o} \left[\frac{1}{b_1} - \frac{1}{b_2} \right] \qquad (C-24)$$

$$u_{BM} = \frac{H_o \left[b_2 s_1 - b_1 s_2 \right]}{b_2 - b_1} \qquad (C-25)$$

$$\epsilon_{goL} = \frac{H_s}{H_o} \left[\frac{1}{b_2} - 1 \right] \qquad (C-26)$$

$$u_{BL} = \frac{H_o \left[s_2 - b_2 s_3 \right]}{1 - b_2} \qquad (C-27)$$

The equations for the fraction of bubbles in a given class, the number of bubbles in a given class, and the Sauter mean diameter, are the same as those developed for N bubble classes (i.e. Equations (V-14), (V-25) and (V-27), respectively).

4. Example and Sample Calculations

Figure C-1 shows results for normalized liquid level (H/H_o) versus time elapsed (t) for FT-300 wax (Run 13-3). For this case, the data at $u_g = 0.01$ m/s can be fitted by two straight lines (bimodal distribution), while data at $u_g = 0.3$ and $u_g = 0.9$ m/s can be fitted to three straight lines (trimodal distribution). t_1^* and t_2^* indicate times corresponding to the two break points for the curve at $u_g = 0.09$ m/s. At time t_1^* all large bubbles have disengaged, and at time t_2^* all medium bubbles have disengaged from the liquid. The normalized liquid level data at 0.03 m/s show that medium size
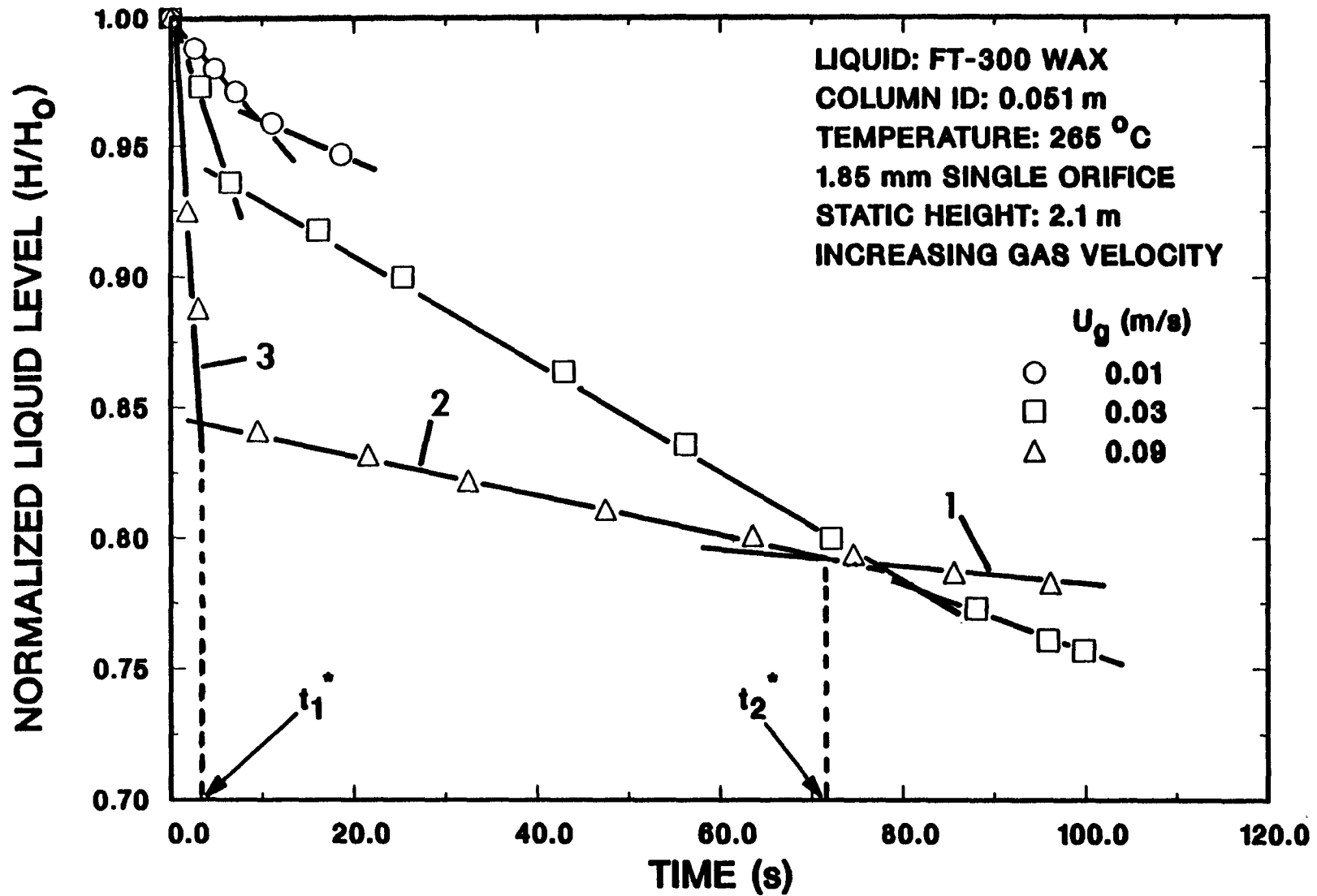
Figure C-1. Change in the normalized liquid level as a function of time and superficial gas velocity (Run 13-3)

bubbles disengaged over a longer period of time at this velocity compared to 0.01 and 0.09 m/s because foam was present at 0.03 m/s and the rate at which the level dropped (including foam) was much slower.

Figures C-2 and C-3 are examples of bubble size distribution curves obtained from DGD measurements during Run 13-3. The figures show the variation of bubble size (small, medium and large) with superficial gas velocity. The size of small bubbles has a maximum at u_g=0.01 m/s and is fairly constant thereafter. This is typical of all runs (including those with reactor waxes). The medium size bubbles also show a similar behavior for most runs. However, large sized bubbles did not show a fixed trend. Their diameter increased with u_g for most runs. This increase was more pronounced for runs conducted in the 0.051 m ID column, probably due to the rapidly growing slugs; the increase was very gradual in the 0.229 m ID column, indicating that large bubbles had approached their maximum value.

The following calculations illustrate the procedure used to estimate the hold-ups corresponding to the various bubble size classes and the Sauter mean diameter. H/H_o versus t data from Run 13-3 at a superficial gas velocity of 0.09 m/s are used in this example. The data are plotted on Figure C-1 and were fitted to three straight lines (i.e. a trimodal distribution).

a. The first step is to determine the slopes and intercepts of the three straight lines fitted to the data obtained at 0.09 m/s.

	Line 1	Line 2	Line 3
slope (s_i)	−0.0004	−0.0007	−0.0320
intercept (b_i)	0.8225	0.8460	0.9906
No. of points	4	14	5
R^2	0.9959	0.9945	0.9823
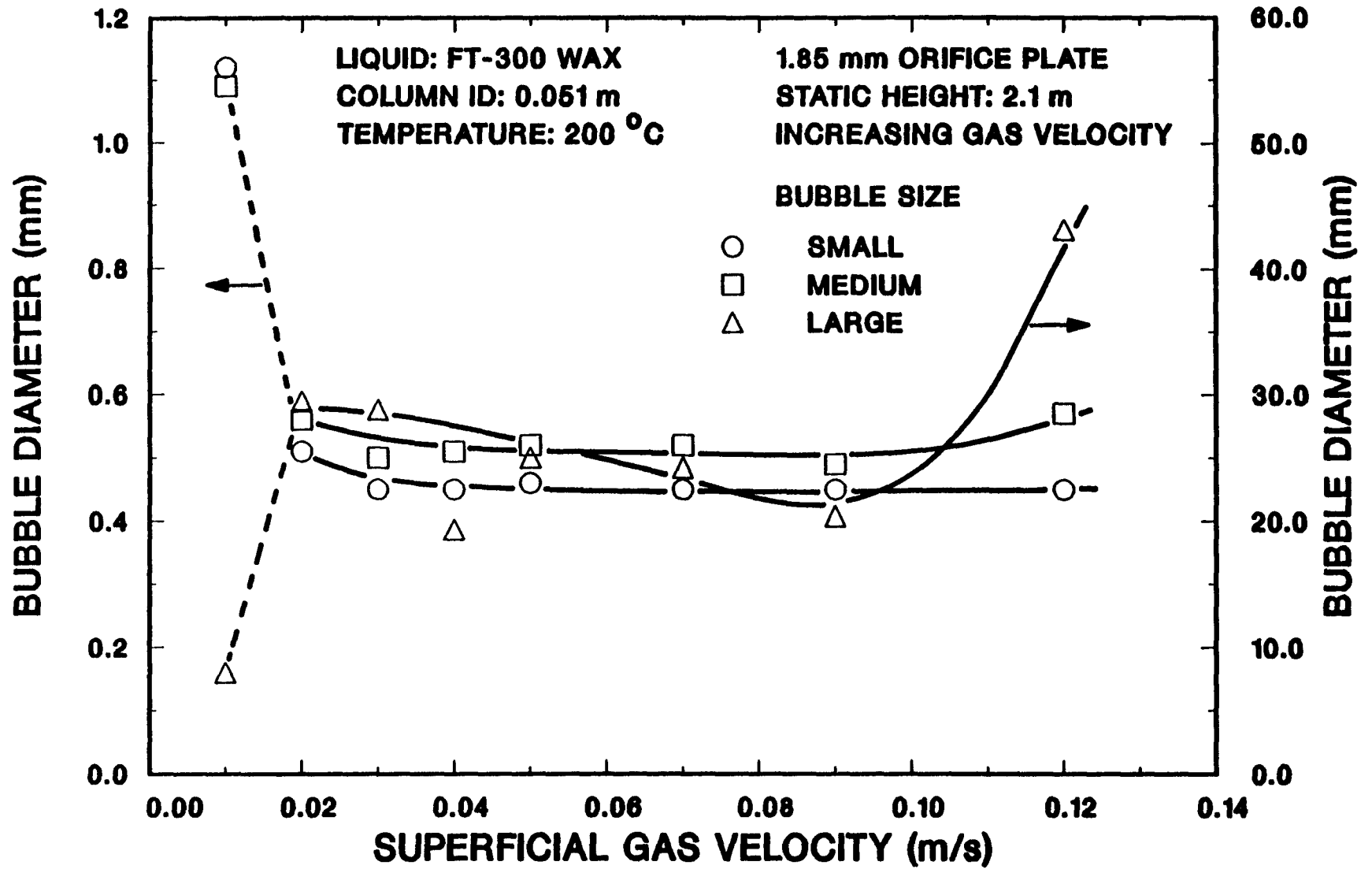
Figure C-2. Effect of superficial gas velocity on bubble sizes (Run 13-2)
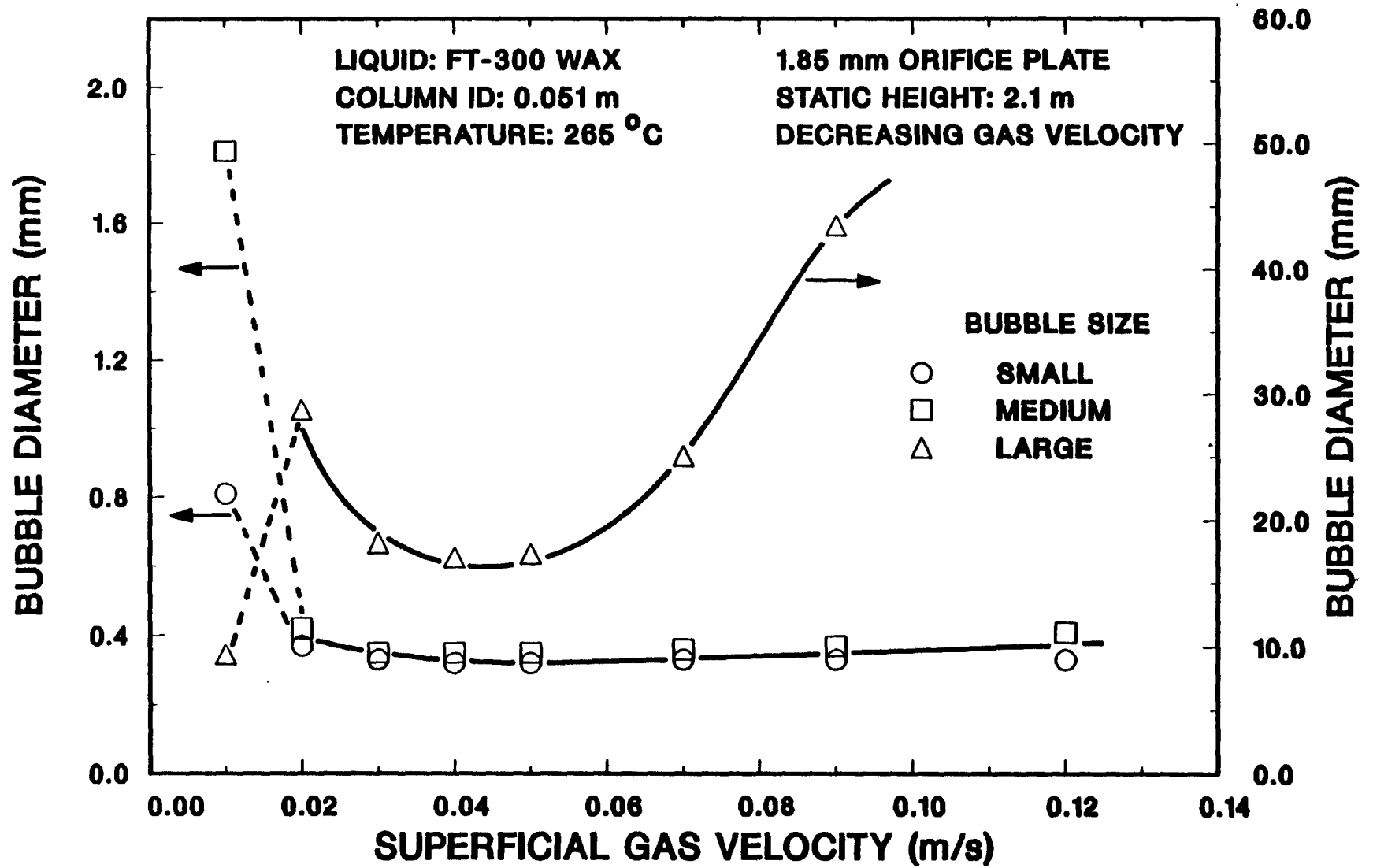
Figure C-3. Effect of superficial gas velocity on bubble sizes (Run 13-3)

Here, R^2 is the correlation coefficient and represents the goodness-of-fit of data to the straight line. A value of 1.0 would represent a perfect fit of data to the straight line. The values of R^2 for this case are close to 1.0 and imply a very good fit.

b. The values for ϵ_{goi} and u_{Bi} can now be estimated using Equations (C-20), (C-21), and (C-24) − (C-27). At 0.09 m/s, the static height (H_s) was 2.1 m and the expanded liquid height at time zero (H_o) was 2.718 m.

The fractional gas hold-up for small bubbles is calculated using Equation (C-20) as

$$\epsilon_{goS} = 1 - \frac{H_s}{b_1 H_o}$$

$$= 1 - \frac{2.1}{(0.8225)(2.718)}$$

$$= 0.0606 \ (\text{or } 6.06\%)$$

similarly, Equation (C-24) is used to calculate the fractional gas hold for medium size bubbles.

$$\epsilon_{goM} = \frac{H_s}{H_o}\left[\frac{1}{b_1} - \frac{1}{b_2}\right]$$

$$= \frac{2.1}{2.718}\left[\frac{1}{0.8225} - \frac{1}{0.8460}\right]$$

$$= 0.0261 \ (\text{or } 2.61\%)$$

288

The fractional gas hold-up for large bubbles is calculated using Equation (C-26) as

$$\epsilon_{goL} = \frac{H_s}{H_o} \left[\frac{1}{b_2} - 1 \right]$$

$$= \frac{2.1}{2.718} \left[\frac{1}{0.8460} - 1 \right]$$

$$= 0.1407 \ (14.07\%)$$

The rise velocity for the small bubbles is calculated using Equation (C-21) as

$$u_{BS} = - \frac{H_s s_1}{b_1 - \dfrac{H_s}{H_o}}$$

$$= - \frac{(2.1)(-0.0004)}{0.8225 - \dfrac{2.1}{2.718}}$$

$$= 0.0168 \ m/s$$

Equation (C-25) is used to calculate the rise velocity of medium size bubbles

$$u_{BM} = \frac{H_o \left[b_2 s_1 - b_1 s_2 \right]}{b_2 - b_1}$$

$$= \frac{2.718[(0.8460)(-0.0004) - (0.8225)(-0.0007)]}{0.8460 - 0.8225}$$

$$= 0.0275 \ m/s$$

and, Equation (C-27) gives the rise velocity of large bubbles

$$u_{BL} = \frac{H_o[s_2 - b_2 s_3]}{1 - b_2}$$

$$= \frac{2.718[-0.0007 - (0.8460)(-0.0320)]}{1 - 0.8460}$$

$$= 0.4654 \text{ m/s}$$

c. The volume fractions for the small, medium and large bubbles can be calculated using Equation V-14. The average gas hold-up at this velocity was 22.74 (or ϵ_{go} = 0.2274).

Thus,

$$f_i = \frac{\epsilon_{goi}}{\epsilon_{go}}$$

For small bubbles, the volume fraction is

$$f_S = \frac{0.0606}{0.2274} = 0.27$$

for medium size bubbles it is

$$f_M = \frac{0.0261}{0.2274} = 0.11$$

and, for large bubbles the volume fraction is

$$f_L = \frac{0.1407}{0.2274} = 0.62$$

d. The bubble sizes corresponding to the small, medium and large classes
    of bubbles can be estimated using the appropriate correlations.
    Figure V-65 shows the relation between bubble rise velicity and bubble
    diameter for FT-300 wax at 265°C. This plot can be used along with
    bubble rise velocities (u_{Bi}) estimated above to obtain the values for
    d_{Bi}.

    Abou-el-Hassan's (1983) correlation (segment 1 on Figure V-65) was
    used to obtain:

$$d_{BS} = 0.33 \text{ mm}$$

as the size of small bubbles, and

$$d_{BM} = 0.37 \text{ mm}$$

as the size of medium bubbles.

The correlation proposed by Clift, Weber and Grace (1978; segment 2 on
Figure V-65) was used to obtain the diameter of the large bubbles

$$d_{BL} = 43.45 \text{ mm}$$

e. Equation (V-27) is now used to estimate the Sauter mean bubble dia-
    meter for the bubble size distribution.

$$d_s = \frac{\epsilon_{go}}{\sum_{i=1}^{3} \epsilon_{goi}/d_{Bi}}$$

$$= \frac{0.2274}{\frac{0.0606}{0.33} + \frac{0.0261}{0.37} + \frac{0.1407}{43.45}}$$

$$= 0.88 \text{ mm}$$

f.   The number of bubbles of a given size is calculated using Equation (V-25). The column diameter (d_c) for this example is 0.051 m.

$$n_i = \frac{3\epsilon_{goi}d_c^2H_o}{2d_{Bi}^3}$$

The number of small bubbles is

$$n_S = \frac{(3)(0.0606)(0.051)^2(2.718)}{(2)(0.33 \times 10^{-3})^3}$$

$$= 1.788 \times 10^7$$

The number of medium size bubbles is

$$n_M = \frac{(3)(0.0261)(0.051)^2(2.718)}{(2)(0.37 \times 10^{-3})^3}$$

$$= 5.464 \times 10^6$$

and the number of large bubbles is

$$n_L = \frac{(3)(0.1407)(0.051)^2(2.718)}{(2)(43.45 \times 10^{-3})^3}$$

$$= 18$$

APPENDIX D

SUMMARY OF SELECTED DGD DATA

Table D-1. Summary of dynamic gas disengagement results for FT-300 wax.
(Run 13-3, 0.051 m ID column, 1.85 mm orifice plate distributor, 265°C)

u_g (m/s)	d_{BS} (mm)	d_{BM} (mm)	d_{BL} (mm)	ϵ_{go} (%)	f_S	f_M	f_L	d_s (mm)	H_o (m)	n_S	n_M	n_L
0.01	0.81	1.81	09.4	5.6	0.45	0.23	0.32	1.40	2.17	3.91×10^5	1.84×10^4	179
0.02	0.37	0.42	28.7	20.8	0.59	0.27	0.13	0.44	2.59	2.45×10^7	7.68×10^6	12
0.03	0.33	0.35	18.2	26.3	0.65	0.19	0.16	0.39	2.79	5.15×10^7	1.28×10^7	73
0.04	0.32	0.35	17.1	27.9	0.56	0.22	0.22	0.42	2.87	5.26×10^7	1.62×10^7	137
0.05	0.32	0.35	17.3	25.7	0.49	0.20	0.32	0.48	2.79	4.11×10^7	1.29×10^7	168
0.07	0.33	0.36	25.1	22.5	0.32	0.16	0.52	0.69	2.69	2.09×10^7	8.29×10^6	77
0.09	0.33	0.37	43.5	22.7	0.27	0.11	0.62	0.88	2.72	1.79×10^7	5.46×10^6	18
0.12	0.33	0.41	73.8	25.8	0.25	0.05	0.69	1.10	2.85	2.00×10^7	2.19×10^6	5

Table D-2. Summary of dynamic gas disengagement results for FT-300 wax.
(Run 13-2, 0.051 m ID column, 1.85 mm orifice plate distributor, 200°C)

u_g (m/s)	d_{BS} (mm)	d_{BM} (mm)	d_{BL} (mm)	ϵ_{go} (%)	f_S	f_M	f_L	d_s (mm)	H_o (m)	n_S	n_M	n_L
0.01	1.12	1.09	8.0	4.7	0.28	0.13	0.59	2.27	2.21	8.04×10^4	4.03×10^4	470
0.02	0.51	0.56	29.5	14.7	0.41	0.32	0.27	0.72	2.46	4.34×10^6	2.55×10^6	15
0.03	0.45	0.50	28.8	19.5	0.46	0.25	0.29	0.65	2.60	1.00×10^7	3.88×10^6	24
0.04	0.45	0.51	19.3	18.8	0.40	0.16	0.44	0.81	2.58	8.26×10^6	2.33×10^6	113
0.05	0.46	0.52	25.0	18.4	0.41	0.06	0.54	0.98	2.57	7.63×10^6	7.56×10^5	63
0.07	0.45	0.52	24.2	18.6	0.21	0.09	0.71	1.53	2.57	4.22×10^6	1.12×10^6	92
0.09	0.45	0.49	20.4	21.2	0.16	0.09	0.75	1.73	2.64	3.77×10^6	1.71×10^6	191
0.12	0.45	0.57	43.1	24.1	0.16	0.05	0.80	2.25	2.74	4.37×10^6	6.42×10^5	26

Table D-3. Summary of dynamic gas disengagement results for FT-300 wax.
(Run 6-2, 0.051 m ID column, 4 mm orifice plate distributor, 265°C)

u_g (m/s)	d_{BS} (mm)	d_{BM} (mm)	d_{BL} (mm)	ε_{go} (%)	f_S	f_M	f_L	d_s (mm)	H_o (m)	n_S	n_M	n_L
0.01	0.68	1.37	7.0	6.0	0.60	0.29	0.12	0.91	2.34	1.02×10^6	6.09×10^4	182
0.02	0.42	0.47	34.7	18.1	0.52	0.39	0.10	0.49	2.67	1.30×10^7	6.95×10^6	4
0.03	0.34	0.38	36.9	29.7	0.46	0.42	0.12	0.41	2.87	3.86×10^7	2.53×10^7	8
0.04	0.34	0.38	31.0	30.3	0.48	0.34	0.18	0.43	2.90	4.18×10^7	2.10×10^7	20
0.05	0.34	0.39	36.9	28.4	0.47	0.29	0.24	0.47	2.82	3.67×10^7	1.53×10^7	15
0.07	0.33	0.38	33.6	27.3	0.49	0.12	0.39	0.55	2.74	3.97×10^7	6.21×10^6	30
0.09	0.35	0.56	39.6	24.6	0.32	0.10	0.58	0.89	2.64	1.90×10^7	1.44×10^6	23
0.12	0.34	0.50	28.9	28.0	0.22	0.12	0.66	1.11	2.77	1.64×10^7	2.91×10^6	83

Table D-4. Summary of dynamic gas disengagement results for FT-300 wax.
(Run 2-8, 0.229 m ID column, 19 X 1.85 mm perforated plate distributor, 265°C)

u_g (m/s)	d_{BS} (mm)	d_{BM} (mm)	d_{BL} (mm)	ϵ_{go} (%)	f_S	f_M	f_L	d_s (mm)	H_o (m)	n_S	n_M	n_L
0.01	0.88	1.12	7.4	5.5	0.42	0.16	0.42	1.47	2.20	5.91×10^6	1.08×10^6	9606
0.02	0.39	0.51	58.2	17.4	0.53	0.37	0.11	0.49	2.50	3.04×10^8	9.47×10^7	19
0.03	0.33	0.44	62.7	19.8	0.65	0.19	0.16	0.42	2.57	7.21×10^8	9.14×10^7	25
0.04	0.31	0.38	51.6	16.9	0.33	0.34	0.33	0.51	2.46	3.67×10^8	2.01×10^8	79
0.05	0.31	0.38	52.6	17.3	0.34	0.23	0.43	0.59	2.46	3.85×10^8	1.38×10^8	99
0.07	0.31	0.36	45.7	18.9	0.31	0.18	0.51	0.66	2.52	3.90×10^8	1.46×10^8	199
0.09	0.31	0.35	42.1	19.8	0.31	0.15	0.54	0.69	2.54	4.05×10^8	1.43×10^8	285
0.12	0.31	0.53	57.8	22.8	0.39	0.08	0.52	0.70	2.64	6.26×10^8	2.62×10^7	129

Table D-5. Summary of dynamic gas disengagement results for Sasol's Arge reactor wax.
(Run 8-4, 0.051 m ID column, 1.85 mm orifice plate distributor, 265°C)

u_g (m/s)	d_{BS} (mm)	d_{BM} (mm)	d_{BL} (mm)	ϵ_{go} (%)	f_S	f_M	f_L	d_s (mm)	H_o (m)	n_S	n_M	n_L
0.01	0.41	1.14	23.2	4.7	0.31	0.26	0.43	1.01	2.19	1.75×10^6	6.93×10^4	14
0.02	0.40	0.59	20.5	7.6	0.21	0.22	0.57	1.08	2.26	2.20×10^6	7.03×10^5	44
0.03	0.36	0.55	29.1	10.0	0.18	0.21	0.62	1.12	2.32	3.44×10^6	1.11×10^6	22
0.04	0.38	0.55	33.7	12.0	0.15	0.16	0.69	1.40	2.35	3.05×10^6	1.06×10^6	20
0.05	0.35	0.55	23.7	13.3	0.12	0.15	0.73	1.53	2.38	3.48×10^6	1.11×10^6	67
0.07	0.34	0.50	53.2	16.7	0.10	0.11	0.78	1.84	2.47	4.16×10^6	1.45×10^6	8
0.09	0.33	0.55	31.5	19.2	0.12	0.08	0.81	1.93	2.53	6.12×10^6	8.53×10^5	49

Table D-6. Summary of dynamic gas disengagement results for Mobil's reactor wax.
(Run 9-3, 0.051 m ID column, 1.85 mm orifice plate distributor, 265°C)

u_g (m/s)	d_{BS} (mm)	d_{BM} (mm)	d_{BL} (mm)	ϵ_{go} (%)	f_S	f_M	f_L	d_s (mm)	H_o (m)	n_S	n_M	n_L
0.01	0.51	3.10	15.9	4.9	0.35	0.21	0.44	1.29	2.09	1.02×10^6	2.80×10^3	43
0.02	0.50	1.11	30.7	7.6	0.29	0.17	0.54	1.33	2.16	1.49×10^6	7.76×10^4	12
0.03	0.49	0.88	28.5	9.4	0.17	0.11	0.71	1.97	2.21	1.19×10^6	1.31×10^5	25
0.04	0.51	0.92	32.4	11.2	0.17	0.09	0.74	2.23	2.26	1.25×10^6	1.09×10^5	22
0.05	0.53	1.36	35.5	13.2	0.14	0.09	0.77	2.89	2.31	1.09×10^6	4.09×10^4	20
0.07	0.50	1.13	47.2	16.0	0.11	0.08	0.81	3.21	2.39	1.31×10^6	8.39×10^4	11
0.09	0.52	4.50	51.0	19.2	0.11	0.11	0.78	4.08	2.49	1.40×10^6	2.33×10^3	11
0.12	0.58	3.90	47.3	21.8	0.08	0.09	0.83	5.50	2.62	9.29×10^5	3.33×10^3	17

APPENDIX E

HOLD-UP MEASUREMENTS WITH COMPOSITES OF MOBIL REACTOR WAXES

The effect of liquid medium on average gas hold-up was studied using paraffin waxes, reactor waxes and distilled water. The results were presented and discussed in Section V-B.7. One of the reactor waxes used in these studies was a composite of reactor waxes produced from Mobil's runs CT-256-9, -11 and -12. Following these experiments, we planned to further investigate the hydrodynamics of Mobil reactor waxes produced from other runs in Mobil's Unit CT-256 with a two-fold objective. We wanted to better understand the behavior of reactor waxes produced under different conditions and at the same time have results which could be compared with results from Mobil's studies (Kuo et al., 1985) with similar reactor waxes. Two new composites (a composite of reactor waxes produced during runs CT-256-4 and -7, and a composite of reactor waxes produced during runs CT-256-5 and -8) were obtained from the Department of Energy for this purpose.

Experiments were performed in the 0.051 m ID glass column at 265°C and 200°C with the new waxes. The 1 mm and 1.85 mm orifice plates and the 40 μm SMP distributors were employed in these experiments. The effect of small quantities of non-coalescing impurities (1-5% of FT-200 waxes) in the coalescing reactor waxes was also investigated.

The major highlights from these studies are:

- Foam was not produced in any of the runs with the two composites and their behavior was qualitatively similar to that of composite from runs 9, 11 and 12.

- Composite of waxes from runs 4 and 7 showed a slight effect of temperature, with lower hold-ups obtained at 200°C compared to values at 265°C. For all distributors employed, this composite also gave slightly higher hold-ups than either the composite from runs 5 and 8,

or the composite from runs 9, 11 and 12.

- Hold-up values reported by Kuo et al., for similar waxes, are consistently higher than those obtained in the present study.

- When small quantities of FT-200 wax (between 1 and 5% by weight) were added to reactor waxes, hold-ups increased to levels comparable to those obtained in the Mobil study with reactor waxes. A similar increase in hold-up was observed when trace amounts of tap water were added to distilled water.

The effect of superficial gas velocity on hold-ups obtained from experiments conducted with the runs 4 and 7 composite are shown in Figure E-1. These results are qualitatively similar to those obtained using the composite from Mobil's runs 9, 11 and 12 (Figure V-32 in Section V-B.7). Foam was not observed in the runs made with the 1 and 1.85 mm orifice plate distributors. For the run conducted with the 40 μm SMP distributor, foam appeared initially at a gas velocity of 0.01 m/s but disappeared after approximately half hour on stream. The marginally lower gas hold-ups at 200 °C compared to values at 265°C could be attributed to the higher viscosity at 200°C. Results obtained from experiments conducted with the composite from runs 5 and 8 are shown in Figure E-2. Hold-ups from the runs with the different distributors, 1 and 1.85 mm orifice plate and 40 μm SMP, and different temperatures, 200°C and 265°C, are similar. For this composite, unlike with the other two composites, no foam was produced with the SMP distributor at u_g = 0.01 m/s, and hold-ups in the velocity range 0.01-0.04 m/s were lower than values with the other two composites.

Viscosities of Mobil waxes were shown in Table VI-1 (Section VI-A). Measurements made in our laboratory show that the viscosities for the
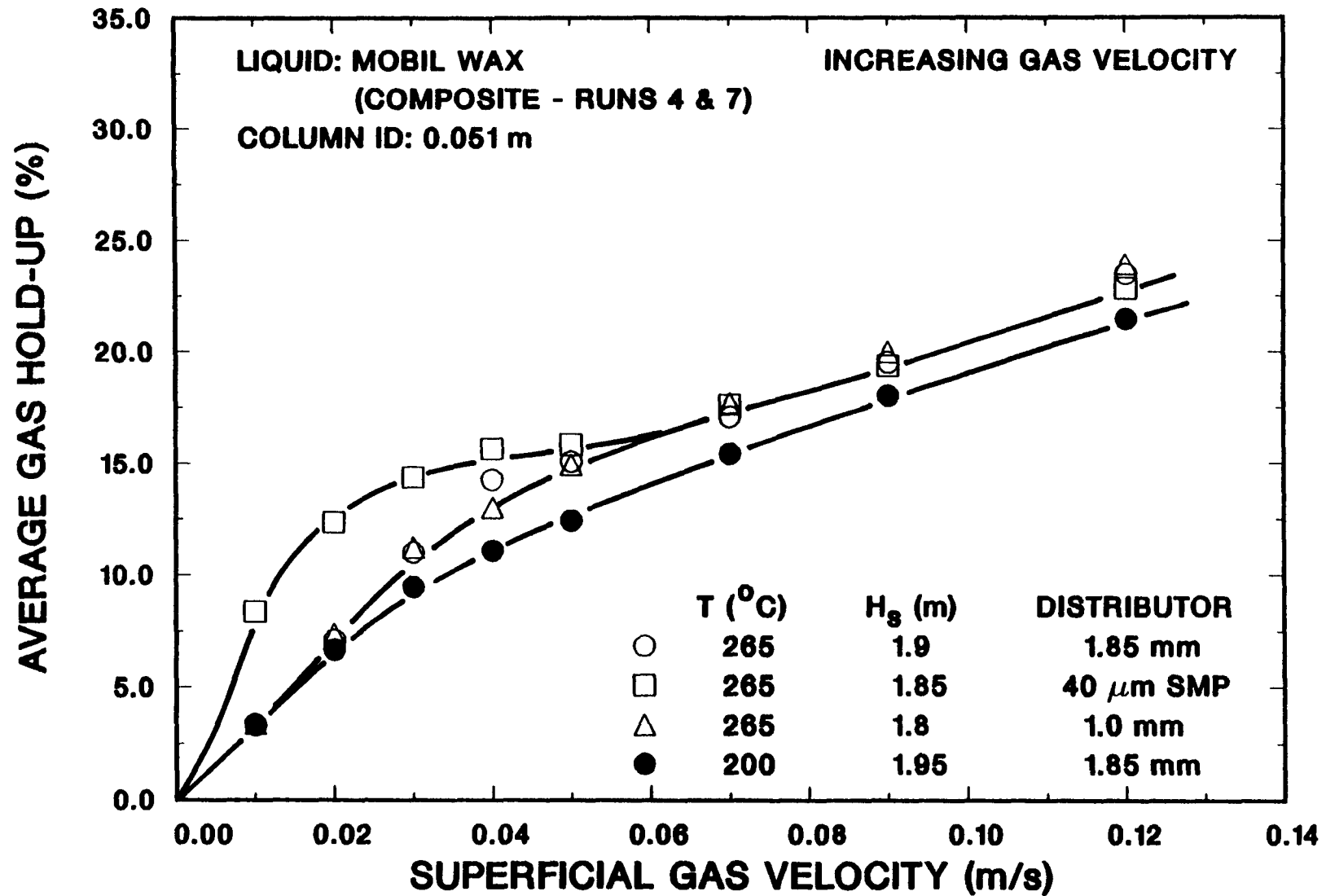
302

Figure E-1. Effect of superficial gas velocity, distributor type and temperature on gas hold-up (composite wax from Mobil runs CT-256-4 and -7; O - Run 21-1; ☐ - Run 21-2; △ - Run 21-3; ● - Run 21-4)
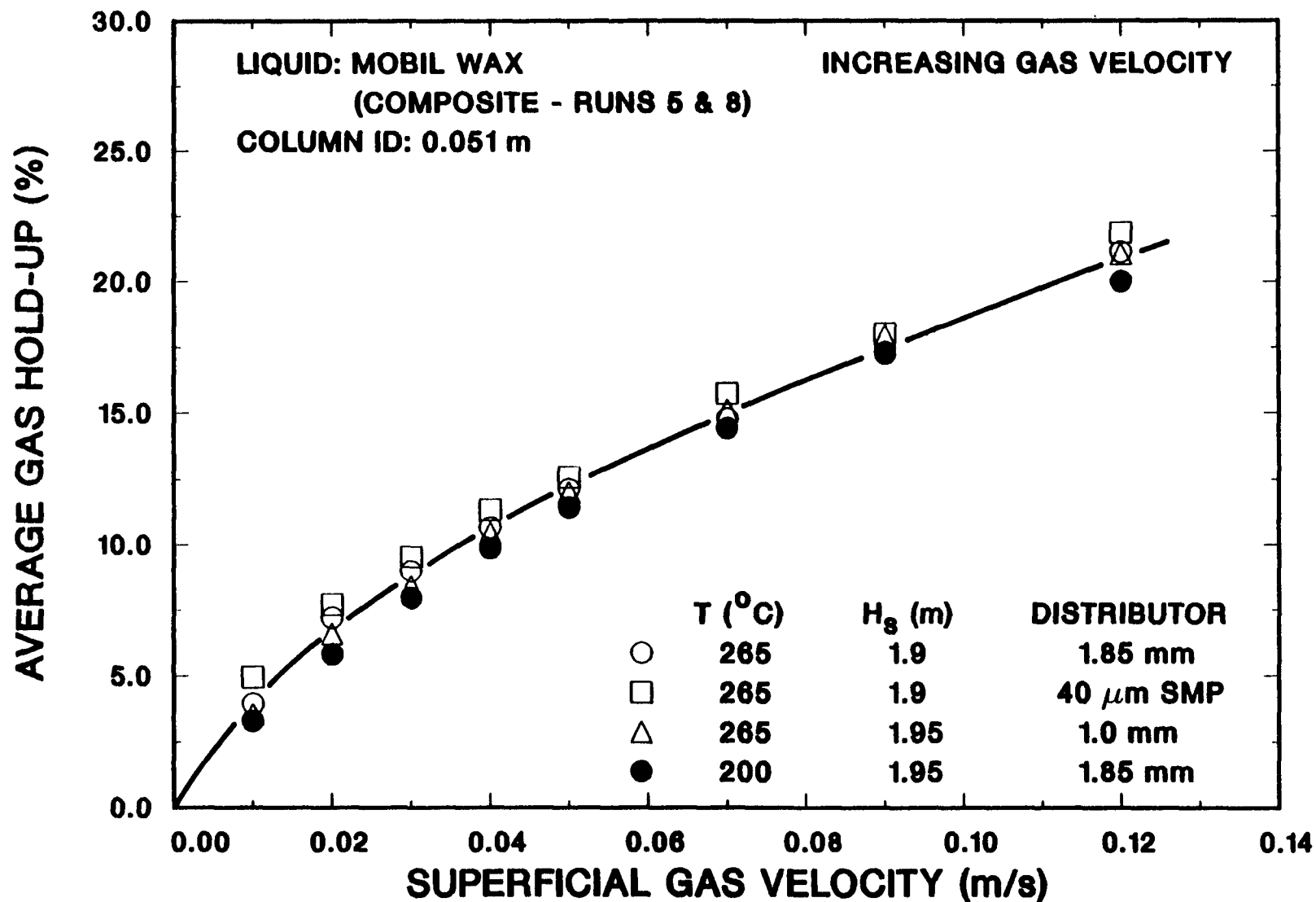
Figure E-2. Effect of superficial gas velocity, distributor type and temperature on gas hold-up (composite wax from Mobil runs CT-256-5 and -8; O - Run 22-3; □ - Run 22-1; △ - Run 22-2; ● - Run 22-4)

composite from runs 4 and 7 were lower than those for the composite from runs 5 and 8 in the temperature range used during these measurements (T ≤ 230°C). However, when viscosity of the composites were estimated at 265°C from data at lower temperatures, assuming Arrhenius type of dependency of viscosity with temperature, similar values were obtained for the two composites. This leads us to believe that the difference in behavior between the two composites, with the SMP distributor, is probably due to differences in the compositions of the two waxes.

Figure E-3 compares hold-up values obtained with the three Mobil wax composites when experiments were conducted at 265°C using the 1.85 mm orifice plate distributor. Earlier comparison of hold-ups obtained when different liquid media (including the composite from runs 9, 11 and 12) were used (Figure V-34, Section V-B.7) showed that, in the "slug-flow" regime, hold-ups with the different liquids were very similar. Results shown in Figure E-3 further support these findings. Hold-up values with the composite from runs 4 and 7 are consistently higher than values for the other two composites, however, the difference is not significant (between 2% - 3% absolute).

Hold-up values obtained by Kuo et al. (1985) from experiments conducted at 260°C with the run 7 wax and the run 8 wax using a 1 mm orifice plate distributor, are shown in Figure E-4. Also shown are hold-ups obtained from the present study, with the composite from runs 4 and 7, and the composite from runs 5 and 8, under similar conditions. Reactor waxes produced in runs 4 and 7 have similar physical properties (Table VI-1; Section VI-A) and their compositions are expected to be similar. The same is true for reactor waxes produced in runs 5 and 8. However, results
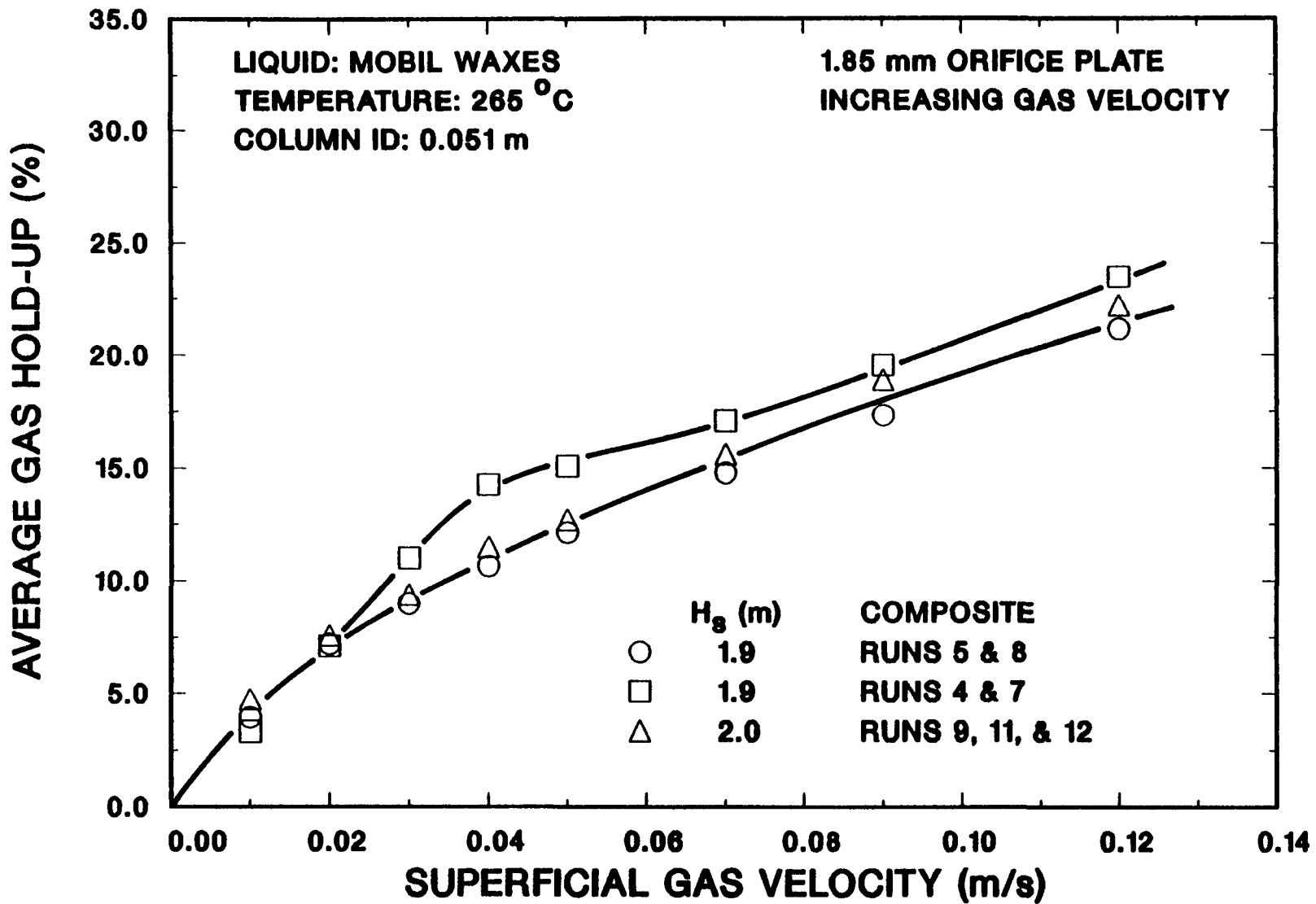
Figure E-3. Comparison of hold-ups obtained in studies with different Mobil wax composites (O - Run 22-3; ☐ - Run 21-1; △ - Run 9-3)
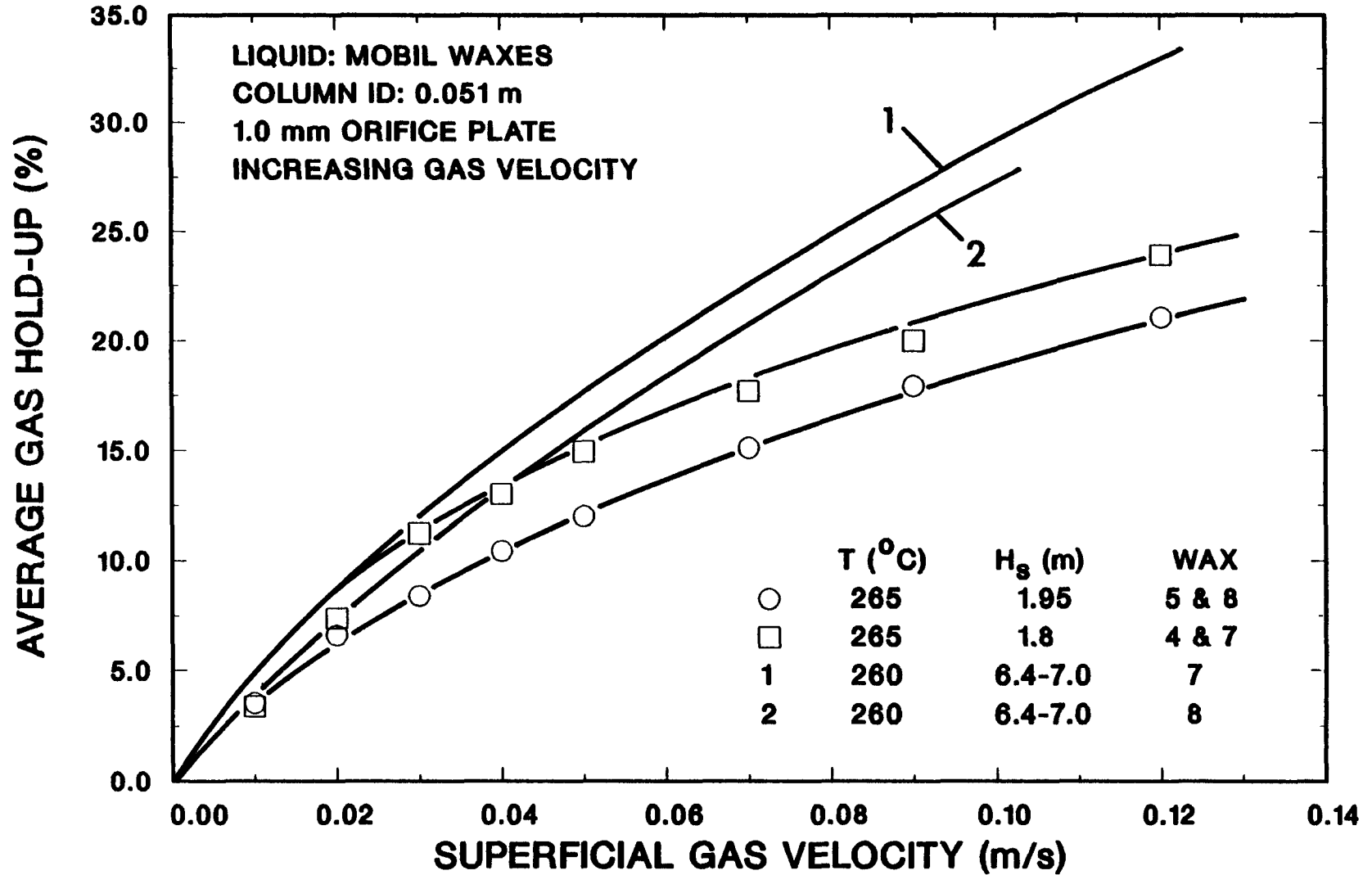
Figure E-4. Comparison of hold-ups obtained in present study with literature values (1,2 - Kuo et al., 1985; Symbols - present study; Wax type is indicated by run numbers in Mobil's Unit CT-256 during which wax was produced; O - Run 22-2; □ - Run 21-3)

presented in figure E-4 show that hold-ups obtained by Kuo et al. with the run 7 wax are significantly higher than those obtained by us with the composite from runs 4 and 7 for $u_g > 0.03$ m/s. Similarly, results obtained by them with the run 8 wax are higher than those obtained in the present study with the composite from runs 5 and 8 for $u_g > 0.02$ m/s. The only difference in the conditions employed in the two studies (Kuo et al. and the present study) is the difference in static heights. Kuo et al. used static heights in the range 6.4 - 7.0 m, whereas static heights in the range 1.8 - 2.0 m were used in our experiments. For coalescing media, such as reactor waxes, we do not expect taller beds to have higher hold-ups. This is because the small bubbles near the distributor would coalesce into fast rising large bubbles or slugs. These would lower the hold-up in the top-half of the column, implying lower hold-ups for taller columns. Evidence to support this is available from axial gas hold-up profiles obtained by Kuo et al. for experiments conducted using the run 7 reactor wax in the 0.051 m ID by 9.1 m tall column (Kuo et al., 1985). Their results show that for $u_g > 0.025$ m/s, gas hold-up decreased with height. This suggests that hold-ups in a taller column should be lower than those obtained in a shorter column. Thus the differences in static heights cannot be used to explain the discrepancies in hold-up values from the two studies.

The experiments by Mobil, with reactor waxes in tall columns, were done after conducting experiments with FT-200 wax (foaming system). Thus, small amounts of FT-200 left on the column wall might have contaminated the reactor waxes and affected the gas hold-up. This effect was investigated in our laboratory by adding small quantities (between 1% and 5%) of FT-200

308

to reactor waxes, and measuring hold-ups. Hold-ups, with a mixture of 3% by weight FT-200 and composite from runs 4 and 7, were significantly higher than hold-ups for the pure composite (Figure E-5), and were comparable with values reported by Kuo et al. for the run 7 wax. Similarly, when 5% by weight of FT-200 was added to the composite from runs 5 and 8, hold-ups were higher than those observed with the pure composite (Figure E-6), though somewhat lower than those reported by Kuo et al. for $u_g > 0.05$ m/s. These results show that small amounts of non-coalescing impurities present in a coalescing medium, can lead to a significant increase in gas hold-ups. Similar behavior was observed for runs conducted with distilled water. When experiments were done with distilled water, following runs with tap water in the same column, higher hold-up values were obtained compared to values from a run in a clean column (Figure E-7). This was caused by the small amounts of tap water remaining on the column wall. Hold-ups for the contaminated distilled water are between those for distilled water and tap water (Figure E-7).

The experiments with reactor waxes having non-coalescing impurities, and with contaminated distilled water show that, in order to get true gas hold-ups for coalescing media, special care needs to be taken to prevent non-coalescing impurities from entering into the system. Only small amounts of such impurities can lead to significantly higher hold-ups for the coalescing media.
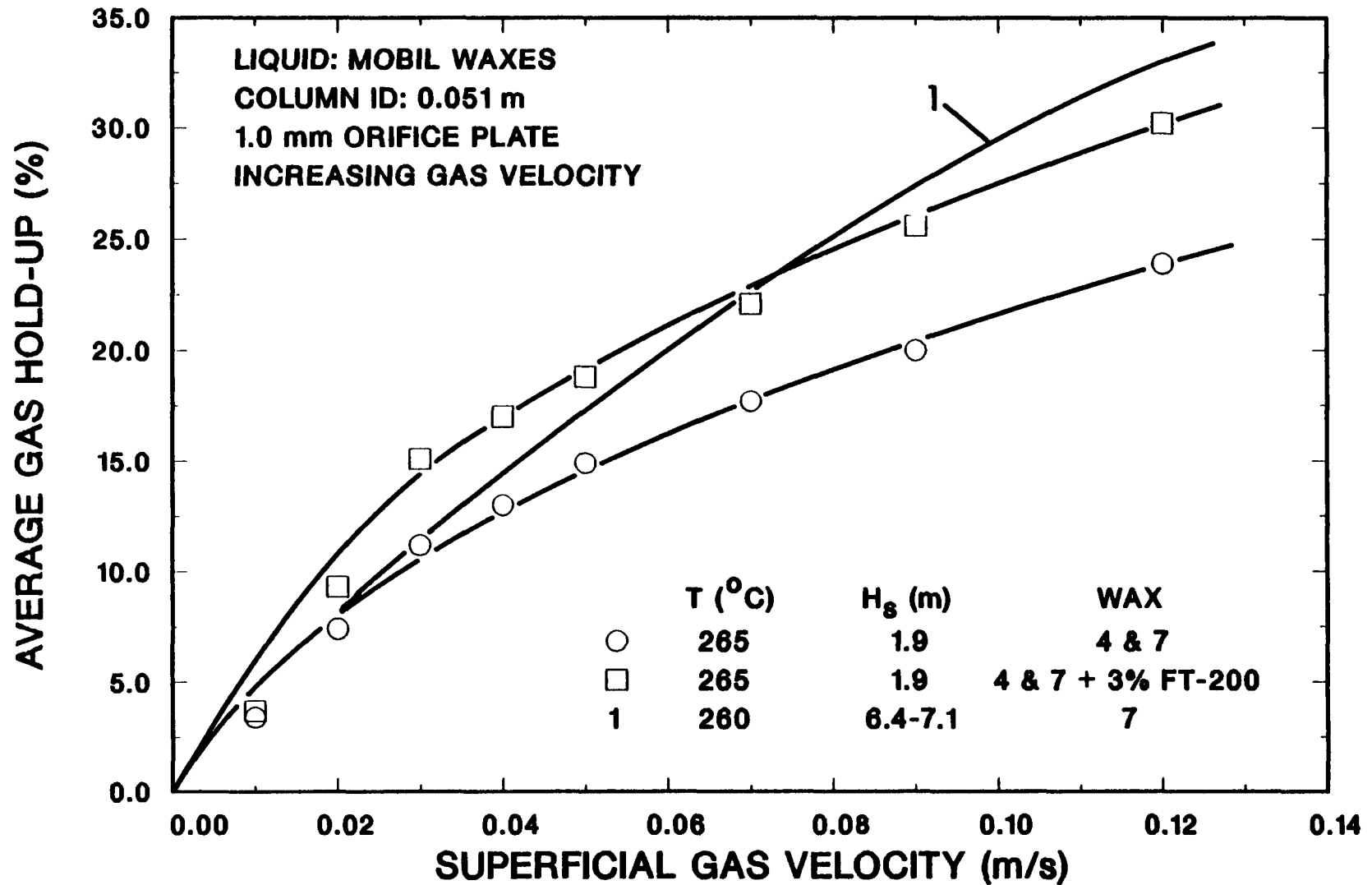
Figure E-5. Effect of small quantities of FT-200 on hold-up (1 - Kuo et al., 1985; Symbols - present study; Wax type is indicated by run numbers in Mobil's Unit CT-256 during which wax was produced; ○ - Run 21-3; □ - Run 23-3)
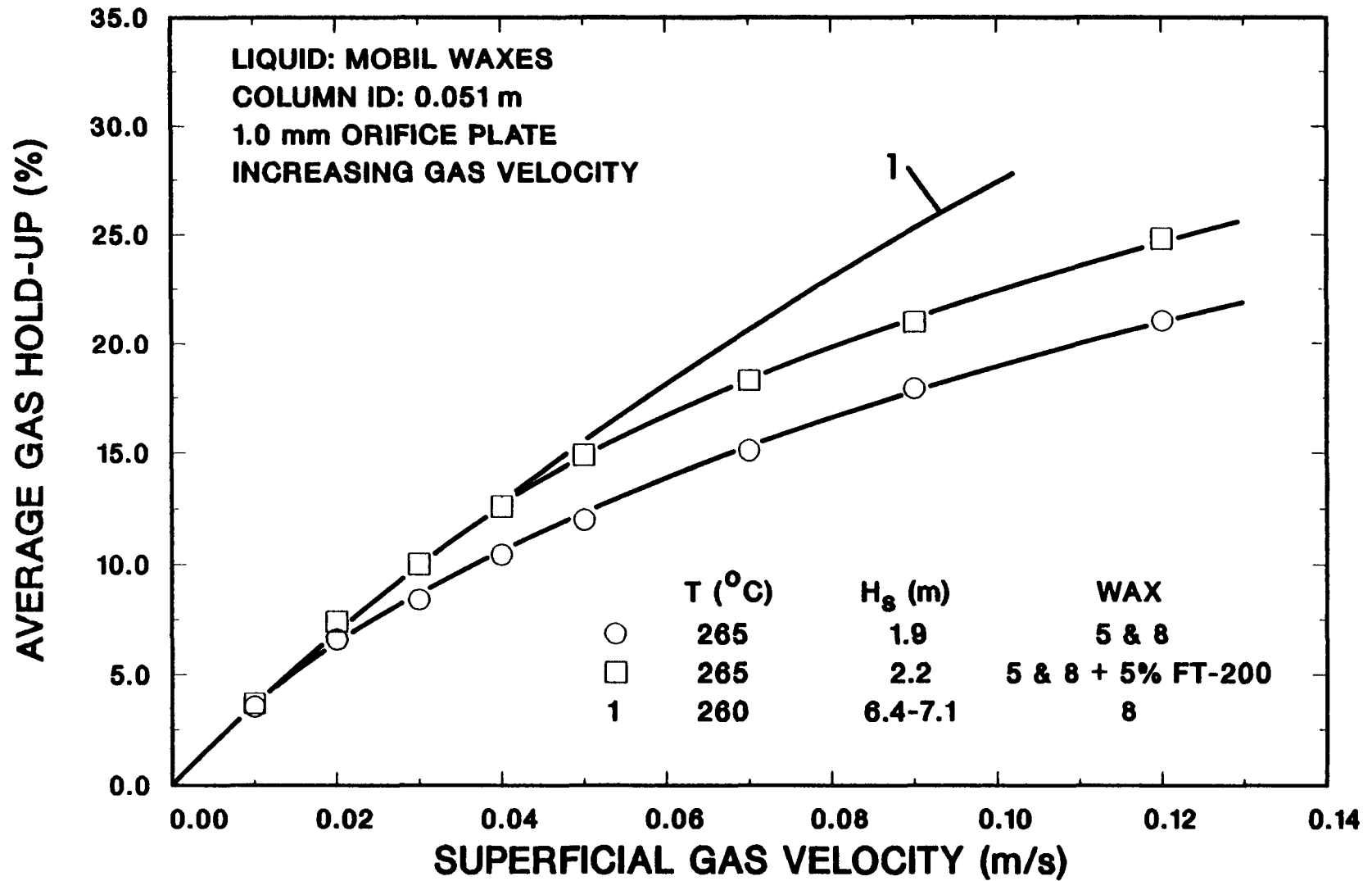
310

Figure E-6. Effect of small quantities of FT-200 on hold-up (1 - Kuo et al., 1985; Symbols - present study; Wax type is indicated by run numbers in Mobil's Unit CT-256 during which wax was produced; ○ - Run 22-2; □ - Run 24-3)
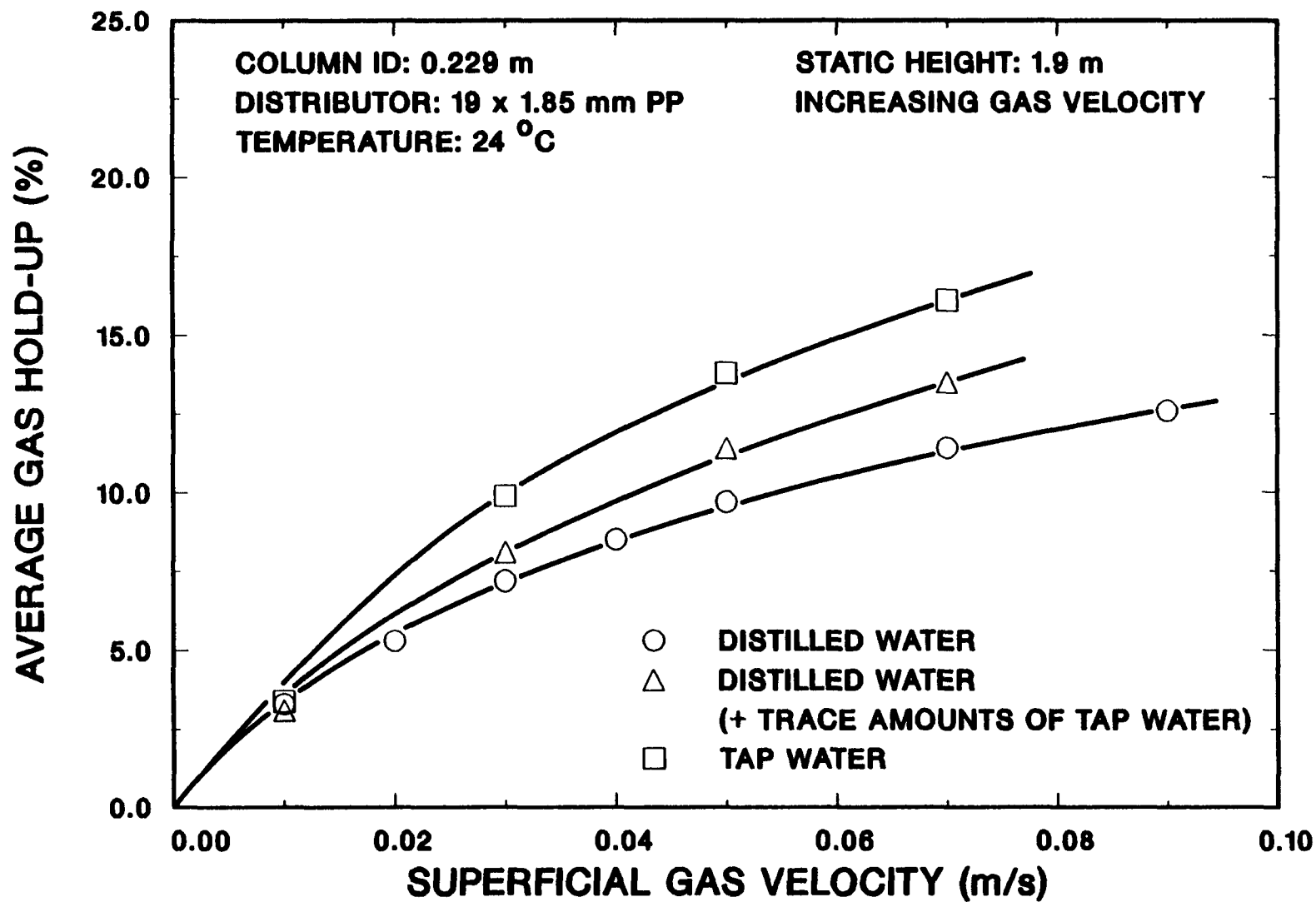
Figure E-7. Effect of contamination on hold-ups with distilled water